General Disclaimer

One or more of the Following Statements may affect this Document

- This document has been reproduced from the best copy furnished by the organizational source. It is being released in the interest of making available as much information as possible.
- This document may contain data, which exceeds the sheet parameters. It was furnished in this condition by the organizational source and is the best copy available.
- This document may contain tone-on-tone or color graphs, charts and/or pictures, which have been reproduced in black and white.
- This document is paginated as submitted by the original source.
- Portions of this document are not fully legible due to the historical nature of some of the material. However, it is the best reproduction available from the original submission.

Produced by the NASA Center for Aerospace Information (CASI)

NASA CR-132748

THE RECOVERY OF MICROWAVE SCATTERING PARAMETERS FROM SCATTEROMETRIC MEASUREMENTS WITH SPECIAL APPLICATION TO THE SEA

by J. P. Claassen and A. K. Fung

(NASA-CR-132748) THE RECOVERY OF MICROWAVE SCATTERING PARAMETERS FROM SCATTEROMETRIC MEASUREMENTS WITH SPECIAL APPLICATION TO THE SEA (Kansas Univ. Center for Research, Inc.) 207 p HC $7.75 CSCL 08J G3/48

N76-12626

Unclas 02980

DEC 1975
RECEIVED
NASA STI FACILITY
INPUT BRANCH

Prepared under Contract No. NAS1-10048 by
UNIVERSITY OF KANSAS CENTER FOR RESEARCH, INC.
Space Technology Center
2291 Irving Hill Drive - Campus West
Lawrence, KS 66045

for

NATIONAL AERONAUTICS AND SPACE ADMINISTRATION

1. Report No.	2. Government Accession No.	3. Recipient's Catalog No.
NASA CR-132748		

4. Title and Subtitle

THE RECOVERY OF MICROWAVE SCATTERING PARAMETERS FROM SCATTEROMETRIC MEASUREMENTS WITH SPECIAL APPLICATION TO THE SEA

5. Report Date

6. Performing Organization Code

7. Author(s)

J. P. Claassen and A. K. Fung

8. Performing Organization Report No.

TR186-13

9. Performing Organization Name and Address

University of Kansas Center for Research, Inc.
Space Technology Center
2291 Irving Hill Drive - Campus West
Lawrence, KS 66045

10. Work Unit No.

11. Contract or Grant No.

NAS1-10048

12. Sponsoring Agency Name and Address

National Aeronautics and Space Administration
Washington, DC 20546

13. Type of Report and Period Covered

Contractor Report

14. Sponsoring Agency Code

15. Supplementary Notes

16. Abstract When the average scattering properties of a non-coherent extensive scene with homogeneous statistics are measured, it is essential that an appropriate radar-scene interaction relation be employed to properly interpret the results. The interaction relationship hopefully will be sufficiently general to isolate various polarized scattering parameters and to predict the average return for an arbitrarily polarized antenna. The complete non-coherent radar equation is derived within this work and a measurement-inversion technique is developed to isolate all the scattering paramerers for a scene satisfying reciprocity. When the measurement technique is specialized to scenes having a scattering characteristic similar to the sea, antenna polarization specifications for accurate retrieval of the scattering parameters are established through simulations. The extrapolation of these results directly or indirectly through the use of the non-coherent radar equation can yield antenna polarization specifications for other scenes. The results serve as a guideline for designing meaningful and accurate scatterometer experiments.

It is specifically shown that for scenes satisfying reciprocity, one must admit three complex valued scattering coefficients in addition to the three well known real valued scattering coefficients The complex valued coefficients are associated with the cross-correlation scattering properties of the scene. As a result of the spatial integration to acquire an average return, the scattering coefficients must satisfy Schwarts' inequality. An immediate consequence of strict inequality for the complexed valued coefficients is that radar returns from non-coherent scenes must be partially polarized. The characteristics of the complex valued coefficients are demonstrated from scattering theories applicable to the sea.

The measurement-inversion technique is proposed with and without regard to the difference between antenna and surface polarizations. It is demonstrated that the distinction between polarizations in negligible for narrow beam antenna at all but small view angles. For small view angles one must, in general, employ the inversion based on surface polarizations if he wishes to compare his measurements with theory or that of other experimenters. Inversions based on antenna polarizations can; however, be performed at small incident angle if very small beamwidths are employed. In this case, nadir can only be probed in an asymptotic sense. This is also a necessary procedure when an anisotropic character is to be measured at small incident angles.

(continued)

17. Key Words (Suggested by Author(s))	18. Distribution Statement
Measurement theory Scattering coefficients Radar scatterometers	Unclassified - Unlimited STAR Category 48

19. Security Classif. (of this report)	20. Security Classif. (of this page)	21. No. of Pages	22. Price*
Unclassified	Unclassified		

*For sale by the National Technical Information Service, Springfield, Virginia 22161

16. Abstract (continued)

Within the simulations it is shown that there is little difficulty in recovering the dominant scattering coefficients with modest realizations of the polarization specifications. Retrieval of the weaker scattering parameters requires more careful observation of the polarization requirements. In the latter case, it is shown that more relaxed realizations of the polarization specifications can be tolerated for many of the measurements if the phase of the cross polarized leakage can be adjusted to an optimun value.

In general it is indicated that three real and three complex valued scattering coefficients can interact with the scatterometer antenna in an undesirable fashion when attempting recovery of any one coefficient. The measurement error arises either as a result of inadequate realizations of the specified antenna polarization or as a result of the inherent mis-match between antenna and surface polarizations for small angles.

FOREWORD

This report was prepared by the Remote Sensing Laboratory of the University of Kansas Space Technology Laboratories under Contract NAS1-10048. Under this contract the principal investigator is Dr. R. K. Moore and the project engineer is Dr. A. K. Fung.

This document covers a particular task in an on-going effort between NASA Langley Research Center and the University of Kansas to demonstrate the value of the microwave scatterometer as a remote sea wind sensor. Specifically the interaction between an arbitrarily polarized scatterometer antenna and a non-coherent distributive target is derived and applied to develop a measuring technique to recover <u>all</u> the scattering parameters. The results are helpful for specifying antenna polarization properties for accurate retrieval of the parameters not only for the sea but also for other distributive scenes.

TABLE OF CONTENTS

		Page
ABSTRACT		i
FORWARD		iii
LIST OF ILLUSTRATIONS		vi
GLOSSARY OF SYMBOLS		x
1.0	SUMMARY	1
2.0	INTRODUCTION	5
3.0	BACKGROUND	8
	3.1 Introduction	8
	3.2 The Reception of Monochromatic Waves and the Radar Equation	9
	3.2.1 Transmitted Fields	9
	3.2.2 Receiving Polarized Waves	10
	3.2.3 Monochromatic Reception and the Radar Equation	10
	3.3 The Non-Coherent Radar Equation	12
	3.4 The Reception of Quasi-Monochromatic, Partially Polarized Waves	13
	3.4.1 General	13
	3.4.2 Quasi-Monochromatic Partially Polarized Waves	14
4.0	DERIVATION OF THE SCATTEROMETER EQUATION	16
	4.1 Introduction	16
	4.2 Derivation	16
	4.3 The Scatterometer Equation Including the Distinction Between Antenna and Surface Polarizations	27
5.0	DISCUSSION	36
	5.1 Introduction	
	5.2 General	36
	5.2.1 The Scattering Coefficient	36
	5.2.2 Special Cases	40
	5.3 Characteristics of the Correlation Terms	41
	5.4 The Degree of Polarization of Radar Returns	50
	5.5 Visualization of the Polarization Properties of the Antenna and Scene	52
6.0	THE INVERSION OF SCATTEROMETER MEASUREMENTS FOR THE SCENE PARAMETERS	59
	6.1 Introduction	59
	6.2 Mathematical and Physical Aspects	59
	6.3 Desirable Antenna Properties	64
	6.4 The Inversion of Scatterometer Measurements	66

TABLE OF CONTENTS (CONTINUED)

		Page
7.0	PRACTICAL CONSIDERATIONS IN RETRIEVING THE SCATTERING COEFFICIENTS	73
7.1	Introduction	73
7.2	Description of the Scatterometer Simulation Program	74
7.3	Resolution Requirement	79
7.3.1	General	79
7.3.2	Polarization Decomposition of the Incident Beam	79
7.3.3	An Evaluation of the Delta Function Approximation	80
7.4	Antenna Requirements for the Accurate Recovery of the Scattering Coefficients	86
7.4.1	General	86
7.4.2	Error Characteristics	91
7.4.3	Alternatives	99
7.5	Evaluation of the Inversion Parameters	102
7.5.1	Introduction	102
7.5.2	Derivation of the Pattern Spectrum	102
7.5.3	Sampling Requirement	103
7.5.4	Illustration	105
8.0	CONCLUSIONS AND RECOMMENDATIONS	108
8.1	General	108
8.2	Final Remarks	112
REFERENCES		114
APPENDIX A –	Correlation and Cross-Correlation Products from Kirchhoff Theory	118
APPENDIX B –	The Scatterometer Equation Within the Context of a Scattering Theory	130
APPENDIX C –	Correlation and Cross-Correlation Scattering Properties of a Slightly Rough Surface	138
APPENDIX D –	Scatterometer Simulation Program (SCATSIM)	145
APPENDIX E –	Routine WHERE	194

LIST OF ILLUSTRATIONS

		Page
Figure 4.1	The Geometry of the Scatterometer Antenna-Scene Interaction.	17
Figure 4.2	Angular Coherency of Backscatter for a Circular Patch with Radius of One Meter and for a Frequence of 13.9 GHz.	21
Figure 4.3	Geometry of the Pattern Measurement Coordinate Systems.	28
Figure 4.4	Comparison of Antenna and Surface Coordinate Frames with the Surface Polarizations Defined with Respect to a General Line of Sight Vector.	29
Figure 5.1	Scattering Characteristics Based on Small Perturbation Theory.	43
Figure 5.2	Cross-Correlation Phase Property Based on Small Perturbation Theory.	44
Figure 5.3	The Scattering Characteristic of $<S_{vv}S^*_{hh}>$ Based on Kirchoff Theory.	47
Figure 5.4	Cross-Correlation Phase Property Based on Kirchhoff Theory.	48
Figure 5.5	The Degree of Polarization Behavior as Predicted from Small Perturbation Theory.	53
Figure 5.6	Surface Polarization Sphere.	54
Figure 5.7	Antenna Polarization Sphere.	56
Figure 5.8	Alternate Antenna Polarization Sphere.	57
Figure 6.1	Increased Resolution of the Kernel Function Caused by the Two-Way Sharpening of the Pattern.	63
Figure 6.2	Far Fields of a Paraboloid with a Dipole Feed.	65
Figure 6.3	Far Fields of a Paraboloid with a Balanced Feed.	67
Figure 7.1	Scattering Characteristics Employed in the Scatterometer Simulation Program.	78
Figure 7.2	Depolarization of the Incident Beam as Induced by the Difference Between Antenna and Surface Polarizations.	81
Figure 7.3	Accuracy of the Delta Function Approximation for the Approximate Inversion Model at $\theta = 0^\circ$.	82

		Page
Figure 7.4	Comparison of Antenna and Surface Polarizations at Nadir with Decomposition Diagram to Explain Cross Polarized Measurements.	84
Figure 7.5	Accuracy of the Delta Function Approximation for the Approximate Inversion Model at $\theta = 4^o$.	87
Figure 7.6	Accuracy of the Delta Function Approximation for the Exact Inversion Model at $\theta = 4^o$.	88
Figure 7.7	Accuracy of the Delta Function Approximation for the Approximate Inversion Model at $\theta = 8^o$.	89
Figure 7.8	Accuracy of the Delta Function Approximation for the Exact Inversion Model at $\theta = 8^o$.	90
Figure 7.9	Error Characteristics of $<\|S_{vv}\|^2>$ for Various Levels of Pattern Cross Polarization with Antenna Phase Condition $\beta_t = \beta_r = 0^o$.	92
Figure 7.10	Error Characteristics of $<\|S_{vv}\|^2>$ for Various Levels of Cross Polarization with an Antenna Phase Condition $\beta_t = \beta_r = 90^o$.	93
Figure 7.11	Error Characteristics for $<\|S_{hh}\|^2>$ at Various Levels of Pattern Cross Polarization for an Antenna Phase Condition $\beta_t = \beta_r = 0^o$.	95
Figure 7.12	Error Characteristics for $<\|S_{hh}\|^2>$ at Various Levels of Pattern Cross Polarization for an Antenna Phase Condition $\beta_t = \beta_r = 90^o$.	96
Figure 7.13	Error Characteristics for $<\|S_{vh}\|^2>$ at Various Levels of Pattern Cross Polarization for an Antenna Phase Condition $\beta_t = \beta_r = 0^o$.	97
Figure 7.14	Error Characteristics for $<\|S_{vh}\|^2>$ at Various Levels of Pattern Cross Polarization for an Antenna Phase Condition $\beta_t = \beta_r = 90^o$.	98
Figure 7.15	Error Characteristics for $<S_{vv}S^*_{hh}>$ as Dependent on Uncertainty in Pattern Balance and Phase.	100
Figure 7.16	Error Characteristics for the Cross Correlations $<S_{vv}S^*_{vh}>$ and $<S_{hv}S^*_{hh}>$ as a Function of Pattern Cross Polarization Level.	101

LIST OF ILLUSTRATIONS (CONTINUED)

		Page
Figure 7.17	The Domain of Integration in the Autocorrelation Integral.	104
Figure 7.18	Sampling Points for a Square Aperture 1.1 Meters by 1.1 Meters Operating at a Wavelength of 2.16 Centimeters.	106

LIST OF TABLES

		Page
Table 7.1	Power Composition Matrix for a Nadir Measurement	85
Table 7.2	Observation Matrix Based on Surface Polarizations	85

GLOSSARY OF SYMBOLS

A	= Area of radar illumination
C_s	= Coherence matrix for scattered field
$C_{t(r)}$	= Coherence matrix for transmit (receive) antenna
$\bar{E}_s$	$= e_{vs}\bar{i}_\theta + e_{hs}\bar{i}_\phi$, scattered field intensity in volts/meter per steradian
$\bar{E}_t$	$= e_{vt}\bar{i}_\theta + e_{ht}\bar{i}_\phi$, incident field intensity in volts/meter
$G_{t(r)}$	= Maximum directivity when transmitting (receiving)
$g_{v(h)}$	= Normalized vertically (horizontally) polarized pattern in the surface coordinate system
$g_{\theta(\phi)}$	= As above, however, in the antenna coordinate system
$\bar{I}$	= Antenna input current
Im	= Imaginary part operator
$\bar{i}_{\theta(\theta')}$	= Unit spherical polar vector in the surface (antenna) coordinate system
$\bar{i}_{\phi(\phi')}$	= Unit spherical azimuthal vector in the surface (antenna) coordinate system
k	= Propagation constant
L	= Complex effective height vector
M_s	= Mutual coherence matrix for the scattered field
M_r	= Mutual coherence matrix for the reception antenna
P	= Degree of polarization
R_r	= Antenna radiation resistance
R	= Radar range
Re	= Real part operator
β_{ij}	= Scattering operator for the j^{th} incident polarization and the i^{th} scattered polarization ($\beta'_{ij} R^2/A \cos\theta$)
β'_{ij}	= Scattering operator yielding resultant field (See β_{ij})

GLOSSARY OF SYMBOLS (continued)

$<S_{ij}S_{kl}>$ = $<\mathcal{S}_{ij}e_{jt}\mathcal{S}^*_{kl}e^*_{lt}>/e_{jt}e^*_{lt}$, scattering coefficient

t = Time

$< >$ = Time (spatial) average

T = Polarization rotation matrix

tr = Trace operator

(x,y,z) = Surface coordinate system

(x',y',z') = Antenna coordinate system

W_t = Transmit power

W = Receive power

Z_o = Free space impedance

β = Relative phase between the vertical and horizontal antenna polarizations defined with respect to the surface polarizations

β' = Relative phase between the vertical and horizontal antenna polarizations defined with respect to the antenna polarizations

θ_o = Incident angle

λ = Radar wavelength

μ_o = Free space permeability

ψ = Angle between antenna and surface polarizations

Ω = (θ,ϕ), line of sight

$d\Omega$ = $\sin\theta\, d\theta\, d\phi$

Ω_o = (θ_o,ϕ_o) antenna view angle

ω = Radian frequency

1.0 SUMMARY

The non-coherent radar equation is derived within the framework of a generalized reception theory. For scenes satisfying reciprocity, the resulting equation confirms a previously derived theory [6]; this result, however, was extended to account for the difference between antenna and surface polarizations. The present theory permits one to interpret the radar return and its reception within the context of scattering and coherence theories (see Section 5.2). Under the reciprocity assumption it is shown that in addition to the three commonly known real valued scattering coefficients there are three complex valued coefficients (without reciprocity there are four real and six complex valued coefficients). As a result of the new coefficients, the definition of a scattering coefficient had to be extended. Specifically a descriptive definition was suggested, viz.,

$$<S_{ij}S^*_{kl}> = \frac{\overline{<\mathcal{S}'_{ij}e_{jt}\mathcal{S}'^*_{kl}e^*_{lt}>}\ R^2}{e_{jt}e^*_{lt}\ A\cos\theta_o} \qquad (1\text{-}1)$$

where,

$\mathcal{S}'_{ij}e_{jt}$ = scattered field component

$\mathcal{S}_{ij}$ = linear polarized scattering operator

e_{jt} = incident field component

R = range to the illuminated area

A = incremental area of illumination

θ_o = incident angle

The subscripts denote the polarization states of the incident and scattered fields, either vertical v or horizontal h. The above definition encompasses the old as well as the new scattering coefficients. In the new notation $<S_{vv}S^*_{vv}>$ and $<S_{hh}S^*_{hh}>$ denote the polarized coefficients, $<S_{vh}S^*_{vh}>$ is the cross polarized coefficient, and $<S_{vv}S^*_{hv}>$ $<S_{vv}S^*_{hv}>$, and $<S_{vv}S^*_{hh}>$ are the new complexed valued coefficients. Other scattering coefficients participate in the scattering process as implied by Equation (1-1) above; however, when reciprocity is satisfied the above set is sufficient (See Equations (4-26) and (4-29).)

The complex valued coefficients account for the relative phase induced between the vertically and horizontally polarized components by the scattering surface. The phase characteristic of these scattering coefficients interact with the relative phase pro-

perties of the transmission and reception antennas to contribute an observed power composed of real and complex valued scattering coefficients. This interaction occurs within the coherent radar equation also; however the interaction must be interpreted differently for the non-coherent case. As a result of the spatial integration to acquire an average return, the complex valued coefficient must, in general satisfy Schwartz' inequality

$$|\langle S_{ij} S_{kl} \rangle|^2 \leq \langle |S_{ij}|^2 \rangle \langle |S_{kl}|^2 \rangle$$

For the coherent case, equality is always assured. However, for the non-coherent case strict inequality can occur. As a result of the strict inequality, one can attribute a partially polarized character to non-coherent radar returns (See Section 5.4). Also as a result of the inequality, techniques for measuring the scattering matrix for coherent targets cannot be employed for non-coherent targets. To illustrate the character of these scattering coefficients, several scattering theories applicable to sea returns were examined (See Section 5.3).

On the basis of the above theory a measurement and inversion technique was developed to measure all six coefficients (nine parameters when the real and imaginary parts are considered). The technique is based on intensity measurements by narrow beam radar scatterometers (See Section 6.4). Inversions are proposed with and without regard to the distinction between antenna and surface polarizations (See Section 6.4 and Section 7.2, respectively). It is demonstrated that the distinction between polarizations is negligible for narrow beam antennas at all but small view angles (See Sections 5.5 and 7.3). For small view angles, inversions based on surface polarizations are more accurate, in general, if the measurements are to be compared with theory or with other experimenters. For example, a 50% error occurs at nadir in inverting for $\langle |S_{vh}|^2 \rangle$ (defined with respect to the surface polarizations) when the inversion technique is based on antenna polarizations. Comparison of the inversions with and without regard to the distinction are shown in Figures (7.3) through (7.8). Inversions based on antenna polarizations can, however, be performed at small view angles if very small beamwidths are employed. In this case nadir can only be probed in an asymptotic sense. The degree to which one can approach nadir and yet meet the constraint that the antenna polarizations across the main beam approximately match those of the surface is dependent on beamwidth. Figure (7.2) parametrically shows the beamwidth requirement as a function of view angle to minimize unwanted orthogonally polarized content in the measurement.

This latter technique is preferred in as much as the measurements may be restricted to a partial set of coefficients whereas when inversions are performed with respect to the surface polarizations the entire set of measurements must be performed. It is also advantageous to use inversions based on antenna polarizations and small beamwidth antennas when an anisotropic characteristic is to be measured at small view angles.

Computer simulations were conducted to determine the effect of deviations from the ideal antenna polarizations (required by the measurement technique) on the accurate recovering of all nine scattering parameters. The deviations, for example, can be introduced by the mis-match between surface and antenna polarizations presuming the scattering parameters are to be reported with respect to the surface polarizations. Also, deviations obviously occur because ideal antenna polarization speciifications cannot be realized by practical antennas. Within these simulations a scattering characteristic similar to that of the sea was employed as illustrated in Figure (7.1). All simulations were conducted with the assumption that the relative phase between the cross-polarizations was stationary across the main beam.

The simulations indicated that there is little difficulty in recovering the three dominant scattering coefficients with off-the shelf antennas as illustrated by Figures (7.9) through (7.12) and Figure (7.15). Some difficulty can be anticipated when $<|S_{hh}|^2>$ is more than 10 dB beneath $<|S_{vv}|^2>$ as illustrated by Figures (7.11) and (7.12). In this case the cross polarized level must be better than 20 dB below the dominant (h) polarization. On the other hand, the antenna polarization requirement must be more carefully observed when retrieving the six weak scattering parameters as illustrated by Figures (7.13) through (7.16). In some cases an adjustment in the relative phase of the cross polarization (if possible) can relax the antenna requirement. When the relative phase cannot be controlled in the case of cross polarized measurements, a rule of thumb for the quality of the antenna was established. If the measurement is to be performed with a 0.5 dB accuracy and $<|S_{vh}|^2>$ is X dB beneath the geometric mean of $<|S_{vv}|^2>$ and $<|S_{hh}|^2>$, then the one-way cross polarized pattern must be X + 16 dB beneath the dominant.

When the dynamic range of the scattering coefficients is large, it is clear from the simulation studies that the experimenter must carefully design his antenna to accurately retrieve the weaker coefficients. Certain types of antennas which have potential in achieving the ideal polarization states are suggested in

Chapter 6. The antenna specifications for observations over the sea or scenes having similar scattering characteristics can be based on the results reported in Chapter 7. However, for scenes having an entirely different characteristic, it is advisable to conduct simulations similar to those reported here. The simulation program, documented in Chapter 7 and Appendix D, may be easily modified for this purpose. These observations as well as others serve as a guide for designing meaningful and accurate scatterometer* experiments.

* The term scatterometer was introduced by R. K. Moore of the University of Kansas. A scatterometer is a radar designed to accurately measure the scattering properties of non-coherent scenes. The term scatterometer and non-coherent radar will be used interchangeably.

2.0 INTRODUCTION

Various research programs have been proposed or are in progress to demonstrate the potential of monitoring, on a global basis, important geological, environmental, hydrological, oceanographic, meteoroloical, and agrarian parameters. The usefulness of remotely sensing certain parameters has been repeatedly demonstrated with optical and infrared sensors. More recently however, satellite and microwave technologies have developed to a point where microwave sensors are also suitable candidates as remote sensing devices. The microwave radiometer and radar scatterometer are prime candidate sensors.

In remote sensing technology it is common knowledge that the retrieval of the remotely sensed parameters often entails compensation of the measurements for sensor and atmospheric effects. The antenna is one element of the sensor system that requires special consideration. An understanding of the antenna-scene interaction is essential to designing meaningful experiments and for specifying the antenna with which the experiments are to be conducted.

The radio astronomers, for example, have developed a rigorous theory involving the complex visiblity function to describe the interaction of a radiometer antenna with a small celestial scene [1]. Measurement techniques were based on the theory to derive complete emission properties of the scene. Recently Claassen and Fung [2] and Peake [3] have reported radiometer interaction relationships for nominally flat scenes having a simple partially polarized emission property. A measurement technique based on the relationship was developed by Claassen and Fung. Grody [4] has illustrated how the difference between antenna and surface polarizations impact radiometer experiments. To date little has been done to develop and use a comprehensive radar scatterometer antenna-scene interaction relationship for non-coherent targets. Most efforts have treated only the spatial extent of the antenna pattern and have avoided general antenna and scene polarization properties [5]. An exception occurs in the theory developed by Williams, et al. [6]. Their characterization of the scene parameters was based on the coherent radar equation and no measurement technique was reported.

In this study a complete non-coherent radar equation is derived and interpreted. The resulting expressions are valid for an arbitrary antenna. The result is also extended to consider the differences between antenna and surface polarizations. The distinction

is important when measurements are to be compared with theoretical predictions. It is shown that six differential scattering coefficients are required to describe the antenna-scene interaction when reciprocity applies. Three of the six coefficients are complex valued. The coefficients are interpreted within the context of scattering and coherence theories. A retrieval technique based on intensity measurements is proposed to measure all the scattering coefficients. Computer simulations, based on the technique and a scattering characteristic similar to that of the sea, were conducted. The results of the simulation were employed (1) to validate an approximation used in the inversion, (2) to demonstrate antenna requirements for accurate retrieval of the scattering coefficients, and (3) to evaluate whether the distinction between antenna and surface polarizations is important.

The development of material in the subsequent chapters is accumulative. Chapter 3 develops the background theory relevant to the derivation and understanding of the complete non-coherent radar equation. An adequate number of references are cited so that the reader can fill in background more deeply if he so desires. The derivation of the non-coherent radar equation is presented in Chapter 4. In the latter section of this chapter the equation is altered to account for the difference between antenna and surface polarizations. Chapter 4 is strongly supported by the contents of Appendix A and B. Chapter 5 is devoted to developing an understanding of the non-coherent radar equation and the polarization properties of radar returns. Certain scattering theories described in Appendices A and C are visited to illustrate the behavior of the complex valued coefficients. The difference between antenna and surface polarizations is also illustrated. The measurement and inversion technique is presented in Chapter 6. The mathematical aspects of the inversion are treated in general and then specialized to the radar problem. Certain antenna properties which simplify the inversion are described. Antenna types capable of realizing these properties are suggested. The measurement and inversion technique is evaluated within Chapter 7. A computer program which simulates the measurement and retrieval of all nine scattering parameters is described briefly. Full documentation of the scatterometer simulation program is provided in Appendix D. The results of the simulation are employed to illustrate antenna polarization requirements to measure all nine scattering parameters. Other practical aspects in making radar scatterometer measurements are also discussed. The measurement of the pattern amplitudes is specifically treated. Appendix E describes a computer program which specifies the points

at which a pattern must be measured. The conclusions and recommendations are presented in Chapter 8. A summary of all significant results is presented in Chapter 1. It is advisable to read the summary before entering the technical chapters.

3.0 BACKGROUND

3.1 Introduction

The theory and measurement of radar cross sections have been well developed for discrete coherent targets. An excellent review on the measurement of radar cross sections is found in a special issue of the Proceedings of the IEEE [7]. The theory of measuring non-coherent radar cross sections, except for the isolated works of Williams, et al. [6] and to some degree Hagfors [8], is largely lacking. Williams, et al. simply extended the theory for coherent targets to a non-coherent scene. In doing so, they over-looked some subtle distinctions between coherent and non-coherent theories as shown in Chapter 5. No measurement technique was presented. Hagfors, on the other hand, related Stoke's parameters for the incident wave to Stoke's parameters for the scattered wave in terms of the Mueller matrix [9]. In general, there are sixteen parameters in the Mueller matrix. However, as shown by Hagfors, targets exhibiting reciprocity and circular symmetry can be characterized by five independent entries in the Mueller matrix. Hagfors related his measurements to some of the five independent entries but no attempt was made to isolate all five entries. By using "Gedanken Experimente" as Hagfors did, one can show that for a flat scene there are nine independent entries. At nadir there can conceivably be only five if the scene is cylindrical symmetric (isotropic). The fact that there are nine independent entries in the Mueller matrix for flat scenes implies that there should be nine scattering parameters. To date only three scattering coefficients have been reported by the earth resources community [10] [11] [12].

In preparing the background for this effort the author chooses to avoid the use of Stoke's parameters and Mueller matrices since the earth resource community is, for the large part, unfamiliar with them. Instead polarization coherency matrices, an entirely equivalent representation for the polarization state of the transverse wave, are employed. The relationship between the entries in the coherency matrix and the standard differential scattering coefficients are clearer. To properly introduce the more general reception theory in terms of coherency matrices, the background for the reception of (polarized) monochromatic waves is first established. It is then employed to derive the coherent radar equation. In doing so the importance of reception theory in understanding the radar equation is clarified.

3.2 The Reception of Monochromatic Waves and the Radar Equation

3.2 Transmitted Fields

Schelkunoff has shown that the far field of any antenna has a dipole field characteristic [13], viz.,

$$\vec{E}(\theta,\phi) = \frac{-jZ_0\vec{N}(\theta,\phi)e^{-jkr}}{2\lambda r} \tag{3-1}$$

where

$\vec{N}$ = radiation vector

Z_o = intrinsic impedance of the medium

λ = wave length

r = distance to the far field point

k = propagation constant

and where the time factor $e^{j\omega t}$ is suppressed. The radiation vector $\vec{N}$, in general, has complex components and induces a relative phase between the far field exponents. As a consequence, the far field has an arbitrary elliptical polarization. Now since $\vec{N}$ is proportional to the antenna input current I, Sinclair [14] proposed that a complex effective height vector $\vec{L}$ be introduced so that

$$\vec{L}(\theta,\phi) = \vec{N}(\theta,\phi)/I \tag{3-2}$$

The far field can therefore be expressed as

$$\vec{E} = \frac{-j\omega\mu_o I\vec{L}e^{-jkr}}{4\pi r} \tag{3-3}$$

where

ω = radian frequency

μ_o = permeability of free space

In general, $\vec{L}$ may have both θ and ϕ components in a spherical coordinate system and both may be complex. Specifically to emphasize this property, we may write $\vec{L}$ in normalized form

$$\vec{L} = |\vec{L}|\ (\cos\delta\bar{i}_\theta + \sin\delta e^{j\beta}\bar{i}_\phi) \tag{3-4}$$

or more compactly as

$$\vec{L} = |\vec{L}| \ (1_v \vec{i}_\theta + 1_h \vec{i}_\phi) \tag{3-5}$$

δ reflects the orientation of a linear polarization when $\beta = 0$ and when $\beta \neq 0$, β is the relative phase between the components. With a little effort δ and β can be related to the axial ratio and orientation of a polarization ellipse [15].

3.2.2 Receiving Polarized Waves

Suppose the above antenna is used to receive a plane wave described by

$$\vec{E} = (E_v \vec{i}_\theta + E_h \vec{i}_\phi) e^{-j\vec{k}\cdot\vec{r}} \tag{3-6}$$

where $\vec{k}$ is the propagation vector. E_v and E_h are the vertically and horizontally polarized amplitudes, respectively. Then it can be shown by the reciprocity theorem [16] that the open circuit vdtage induced into the terminals of an antenna having effective height $\vec{L}$ is given by [14]

$$V = \vec{E}\cdot\vec{L} \tag{3-7}$$

The power available at the antenna terminals under matched conditions is given by

$$P = |\vec{E}\cdot\vec{L}|^2 \ /8R_r \tag{3-8}$$

where R_r is the radiation resistance of the antenna.

3.2.3 Monochromatic Reception and the Radar Equation

It has been shown by Sinclair [17] and by Kennaugh[18] that a radar target can act as a polarization transformer. Sinclair expresses the transformation by a scattering matrix which can be incorporated in the radar equation. The scattering matrix is defined by

$$S = \begin{bmatrix} \sqrt{\sigma_{vv}}e^{j\rho_{vv}} & \sqrt{\sigma_{vh}}e^{j\rho_{vh}} \\ \sqrt{\sigma_{hv}}e^{j\rho_{hv}} & \sqrt{\sigma_{hh}}e^{j\rho_{hh}} \end{bmatrix} \tag{3-9}$$

where

σ_{pq} = radar cross section for a q linearly polarized incident wave and a p reflected wave

ρ_{pq} = phase center for each component of the reflected wave

p,q = v or h

If the incident field is denoted as

$$\vec{E}_t = (e_{vt}\vec{1}_\theta + e_{ht}\vec{1}_\phi)e^{-jkr} \tag{3-10}$$

or

$$\vec{E}_t = \frac{-j\omega\mu_o I_t \vec{L}_t e^{-jkr}}{4\pi\ r} \tag{3-11}$$

then the scattered field $\vec{E}_s$ in component form is given by*

$$\begin{bmatrix} e_{vs} \\ e_{hs} \end{bmatrix} = 1/(\sqrt{4\pi}\ r)\ S \begin{bmatrix} e_{vt} \\ e_{ht} \end{bmatrix} \tag{3-12}$$

If $\vec{L}_r$ denotes the complex effective height vector of the receiving antenna co-located with the transmit antenna, then the power received under matched conditions is given by

$$P = |\vec{E}_s \cdot \vec{L}_r|^2/8R_r \tag{3-13}$$

or

$$P = \frac{(\omega\mu_o I_t)^2 |L_t|^2 |L_r|^2 |1_t S 1_r|^2}{8(4\pi)\ r^4 R_r} \tag{3-14}$$

where

$$\vec{L}_{t,r} = |\vec{L}_{t,r}| \quad (1_{vt;r}\vec{1}_\theta + 1_{ht,r}\vec{1}_\phi) \tag{3-15}$$

$$1_t = \begin{bmatrix} 1_{vt} \\ 1_{ht} \end{bmatrix}$$

---

*Matrix notation for transverse wave components is frequently used throughout.

$$\hat{1}_r = \begin{bmatrix} \hat{1}_{vr} \\ \hat{1}_{hr} \end{bmatrix} \qquad (3\text{-}15)$$

Now it is well known [18] that the antenna gain is given by

$$G_{t,r} = \frac{4\pi \, |\vec{L}_{t,r}(\theta,\phi)|^2}{\int |\vec{L}_{t,r}|^2 d\Omega} \qquad (3\text{-}16)$$

and the radiation resistance by

$$R_{t,r} = Z_0/(4\lambda^2) \int |L_{t,r}|^2 d\Omega \qquad (3\text{-}17)$$

As a result, the received power can be written in more familiar form

$$W_r = \frac{\lambda^2 G_t(\theta,\phi) \; G_r(\theta,\phi) W_t \sigma}{(4\pi)^3 r^4} \qquad (3\text{-}18)$$

where the radar cross-section has been identified as

$$\sigma = |\hat{1}_r S \hat{1}_t|^2 \qquad (3\text{-}19)$$

The above expression for the radar cross section reduces to the linear polarized cases when both $\hat{1}_t$ and $\hat{1}_r$ contain a single non-zero component. For the coherent target the above formulation completely describes the interaction between three apertures, the transmitting and receiving antennas and the target*.

Methods for measuring the elements of the scattering matrix have been reviewed by Huynen [21]. Methods of measuring radar cross sections σ have been reviewed by Blacksmith, et al. [22] and by Kell and Ross [23].

3.3 The Non-Coherent Radar Equation

Radar returns for a non-coherent scene have been defined in terms of a differential scattering coefficient σ^o rather than a scattering cross section σ. σ^o is unitless

*It has been shown that the target actually acts like two coupled apertures [20].

and expresses the equivalent average radar cross section per unit area. Moore [5] has shown from elementary considerations that when σ^o is employed the average return is given by

$$W_r = W_t/(4\pi)^3 \int G_t G_r \sigma^o/r^4 \, dA \tag{3-20}$$

where the integration is performed over the illuminated area. For linear polarizations the differential scattering coefficients have been defined in analogy to σ for the coherent case [5] [24]

$$\sigma^o_{qp} = \frac{4\pi r^2 \langle |E_{sq}|^2 \rangle}{A \, |E_{ip}|^2} \tag{3-21}$$

where

A = illuminated area

r = distance between the illuminated area and the point of observation

E_{sq} = scattered field intensity

E_{ip} = incident field intensity

p,q = v or h

Williams et al. [6] have shown that radar returns cannot be characterized by linear polarized scattering coefficients for an arbitrary antenna polarization and an arbitrary scene. They offer an expression for the differential power contribution by a small patch of the scene. Their formulation, however, is entirely identical to the radar equation for coherent targets, i.e., the effects of spatial averaging have not been considered.

3.4 The Reception of Quasi-Monochromatic, Partially Polarized Waves

3.4.1 General

The treatment of radar returns for non-coherent scenes to date has relied on intuitive extensions of (polarized) monochromatic theory. Yet when one contemplates how the measurement of the non-coherent scattering coefficients is actually performed, one is acutely aware that the measurement involves estimating the mean of a fading signal having a certain doppler bandwidth. The resulting returns are, as a

consequence, quasi-monochromatic rather than monochromatic. Furthermore, it is presumptive to anticipate that average returns from a randomly rough target are completely polarized*. Indeed one should anticipate that the actual return will be a mixture of randomly polarized and polarized waves, i.e., will be partially polarized. Hence, any derivation of the non-coherent radar equation should include this possibility.

Ko [15] has developed a comprehensive reception theory for quasi-monochromatic partially polarized waves. This theory is reviewed below and will be employed in the succeeding chapter. Important to this theory are the notions of an analytic signal as defined by Gabor [26] and the polarization coherence matrix as originated by Wiener [27] and Perrin [28] and later developed by Wolf [29]. An excellent discussion of both topics appears in a text by Born and Wolf [30].

3.4.2 Quasi-Monochromatic Partially Polarized Waves

Wolf [29] has shown that a quasi-monochromatic wave whose bandwidth is small in comparison to the mean angular frequency $\overline{\omega}$ can be represented in analytic signal form of the type

$$\overline{E}(r,\theta,\phi,t) = e_v(r,\theta,\phi,t)\overline{i}_\theta + e_h(r,\theta,\phi,t)\overline{i}_\phi \tag{3-22}$$

where

$$e_v = a_v(r,\theta,\phi,t)e^{j(\overline{\omega}t-kr+\alpha_v(\theta,\phi,t))} \tag{3-23}$$

$$e_h = a_h(r,\Theta,\Phi,t)e^{j(\overline{\omega}t-kr+\alpha_h(\theta,\phi,t))}$$

The actual signal may be isolated by taking the real part of the above expression. The elements of this analytic signal have properties such that $a_{v,h}(r,t) \geq 0$ and $\alpha_{v,h}(\overline{r},t)$ is real. The correlation of the Θ and $\emptyset$ components determines the state of polarization of the wave. Wolf [29] defines the correlation by the complex factor

$$\mu_{vh} = \frac{< e_v e_h^* >}{\sqrt{<|e_v|^2><|e_h|^2>}} \tag{3-24}$$

*Monochromatic waves are completely polarized.

Where the angular bracket < > represents a time average. By Schwartz' inequality, $|\mu_{vh}| \leq 1$. The absolute value of μ_{vh} is a measure of the degree of correlation between v and h components while the phase angle of μ_{vh} reflects the relative phase between the two components. If $|\mu_{vh}| = 1$, the wave is said to be completely polarized. If $|\mu_{vh}| = 0$ and if $\langle |e_v|^2 \rangle = \langle |e_h|^2 \rangle$, then the wave is randomly polarized. The wave is said to be partially polarized when $|\mu_{vh}|$ is between zero and one. The state of polarization may be completely characterized by a coherency matrix

$$C = \begin{bmatrix} \langle e_v e_v^* \rangle & \langle e_v e_h^* \rangle \\ \langle e_h e_v^* \rangle & \langle e_h e_h^* \rangle \end{bmatrix} \tag{3-25}$$

as shown by Wolf [29] (See also Born and Wolf [30]).

Following Ko [25] and Collin [9] we may now suppose that a quasi-monochromatic partially polarized wave with coherency matrix C is incident on an antenna with effective height $\underline{L}$. If the bandwidth of the wave or receiver is sufficiently narrow, then the open circuit voltage in analytic signal form is given by

$$V = \vec{E} \cdot \vec{L}(\theta, \phi, \bar{\omega}) \tag{3-26}$$

where $\bar{\omega}$ is the mean frequency of the wave. If a coherency matrix is introduced for the antenna

$$C_r = \begin{bmatrix} l_v l_v^* & l_v l_h^* \\ l_h l_v^* & l_h l_h^* \end{bmatrix} \tag{3-27}$$

where $|l_v|^2 + |l_h|^2 = 1$, then as shown by Ko [25], the power observed at the antenna terminals under matched conditions is given by

$$W(\theta, \phi) = \frac{\lambda^2 G(\theta, \phi)}{4\pi Z_0} \operatorname{tr} C_r C^{\dagger} \tag{3-28}$$

where tr is the trace operator and $\dagger$ is the transpose operator. The coherency matrix for the impinging wave is the transpose of that defined by Ko. All coherency matrices employed within this work are defined with respect to a coordinate system located at the observing antenna. Further interpretation of this expression is deferred until Chapter 5 where a similar expression is discussed in the context of the scatterometer equation.

4.0 DERIVATION OF THE SCATTEROMETER EQUATION

4.1 Introduction

A generalized reception theory [9] [25] and notions from scattering theory are combined to derive the complete scatterometer equation for a scatterometer antenna having a specified but otherwise arbitrary transmit and receive property. The radar return is treated as a quasi-monochromatic-partially-polarized wave. The quasi-monochromatic character is induced into the return signal as the antenna linearily scans the scene. The scan is, of course, important in achieving a spatial average. The partially polarized assumption as well as the quasi-monochromatic characters permits one to derive the scatterometer equation elegantly within the framework of the generalized reception theory. Intuitively, it is reasonable to assume that scatterometer returns are partially polarized since a spatial average constitutes the return. This interpretation will be illustrated in Section 5.4.

The scatterometer equation is initially derived assuming that the scatterometer antenna transmission and reception properties are defined in terms of the surface polarizations. In the last section of the chapter the distinction between antenna polarizations and surface polarizations is introduced and the impact of this distinction on the scatterometer equation is shown.

4.2 Derivation

To determine the average power return from a homogeneous randomly extensive target, we suppose that a narrow beam scatterometer linearily scans across the scene with its antenna pointed in direction $\Omega_o = (\theta_o, \phi_o)$. If the scene has an anisotropic character it is important that ϕ_o be maintained constant during the scan (see Figure 4.1). The incident (transmitted) field E_t may be related to the antenna complex effective height vector L_t, a reception property, in the standard way [25]*

$$E_t = \begin{bmatrix} e_{vt} \\ e_{ht} \end{bmatrix} = \frac{-j\omega\mu_o i_t L_t e^{j(\omega t - kr(t))}}{4\pi r} \qquad (4\text{-}1)$$

* Reception and scattering relationships in the far field adapt well to the matrix notation. Capital letters will denote matrices and lower case letters will denote their elements.

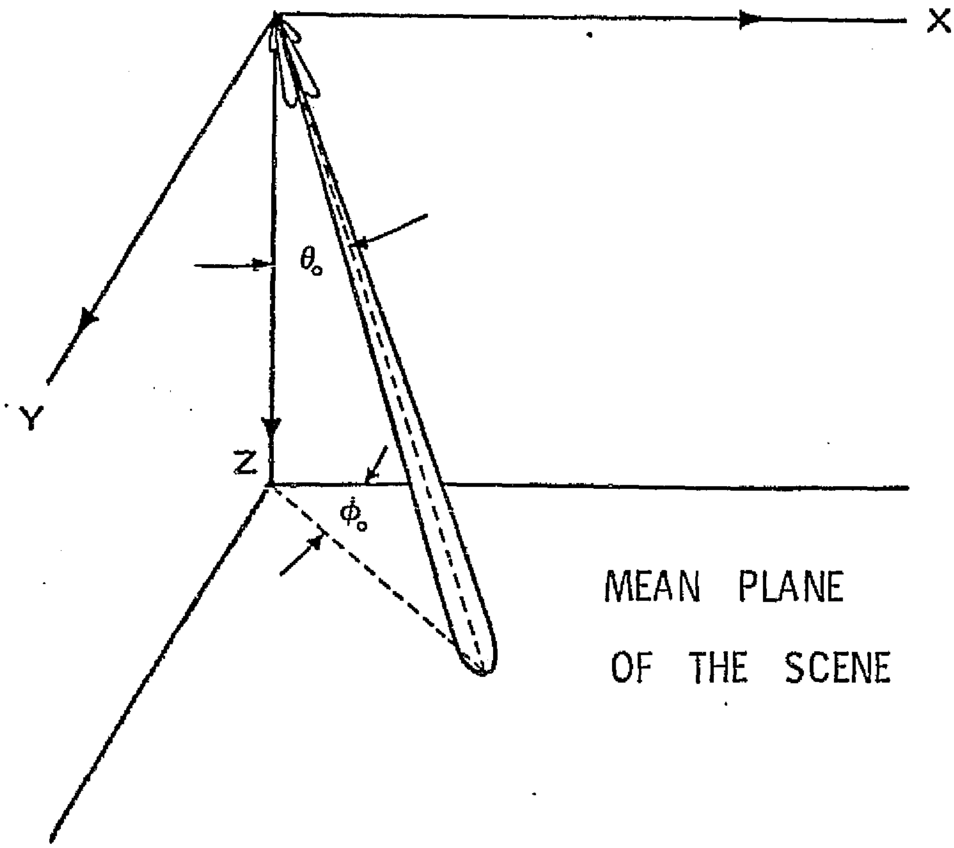

FIGURE 4.1 The Geometry of the Scatterometer Antenna-Scene Interaction

where e_{vt} is the vertically polarized component, e_{ht} is the horizontally polarized component and

$$L_t = \begin{bmatrix} l_{vt} \\ l_{ht} \end{bmatrix} \tag{4-2}$$

The subscript v and h are employed to denote the vector components aligning with the spherical polarized unit vectors $\bar{i}_\theta$ and $\bar{i}_\phi$, respectively, associated with the surface coordinate system of Figure 4.1. The backscattered field arriving with direction (θ, ϕ) from a differential patch of the surface will be denoted

$$E_s(\theta, \phi, t) = \begin{bmatrix} e_{vs} \\ e_{hs} \end{bmatrix} \tag{4-3}$$

Only transverse components for each line of sight (θ, ϕ) are admitted in the matrix. The field has the units of volts/meter per steradian. Each component of E_s must be regarded as an analytic signal since the relative motion between the antenna and the rough scene induces a time varying response for each line of sight.

Now the antenna does not respond to the resultant field at the point of observation. Rather, if L_R denotes the complex effective height vector during reception, the antenna integrates the field components arriving with different directions so that the open circuit voltage appearing at the antenna terminals is given by

$$V_r(\Omega_o) = \int E_s^\dagger(\Omega) L_r(\Omega, \Omega_o) d\Omega \tag{4-4}$$

where Ω_o, as the reader will recall, denotes the look direction and where the symbol $\dagger$ denotes the transpose operator. For narrow beam scatterometers the integration may be limited to the main beam and under worst circumstances to the first side lobes. The average power observed at the terminals of the antenna under matched conditions is given by

$$W(\Omega_o) = \frac{\langle |V(\Omega_o)|^2 \rangle}{8R_r}. \tag{4-5}$$

where R_r is the radiation resistance during reception (r) and $\langle\ \rangle$ denotes a time average or equivalently a spatial average since the scatterometer is scanning across the scene.

Expanded, the received power is given by

$$W(\Omega_o) = \frac{1}{8R_r} \iint \langle E_s^{\dagger}(\Omega) L_r(\Omega,\Omega_o) \; E_s^{\dagger *}(\Omega') \; L_r^{*}(\Omega',\Omega_o) \rangle d\Omega d\Omega' \tag{4-6}$$

Define a mutual (polarization) coherence matrix for the scattered fields as

$$M_s(\Omega,\Omega') = \begin{bmatrix} \langle e_{vs}(\Omega) e_{vs}^{*}(\Omega') \rangle & \langle e_{vs}(\Omega) e_{hs}^{*}(\Omega') \rangle \\ \langle e_{hs}(\Omega) e_{vs}^{*}(\Omega') \rangle & \langle e_{hs}(\Omega) e_{hs}^{*}(\Omega') \rangle \end{bmatrix} \tag{4-7}$$

Similarly a mutual coherence matrix can be defined for the receiving antenna

$$M_r = \begin{bmatrix} l_{vr}(\Omega,\Omega_o) l_{vr}^{*}(\Omega',\Omega_o) & l_{vr}(\Omega,\Omega_o) l_{hr}^{*}(\Omega',\Omega_o) \\ l_{hr}(\Omega,\Omega_o) l_{vr}^{*}(\Omega',\Omega_o) & l_{hr}(\Omega,\Omega_o) l_{hr}^{*}(\Omega',\Omega_o) \end{bmatrix} \tag{4-8}$$

Then the average return can be written in compact form

$$W_{tr}(\Omega_o) = \frac{1}{8R_r} \iint \mathrm{tr} \; M_r M_s^{\dagger} \; d\Omega \; d\Omega' \tag{4-9}$$

where tr denotes the trace operator.

For a random scene it is reasonable to assume that the scattered fields are angularly non-coherent, i.e.,

$$\langle e_{is}(\Omega) \; e_{js}^{*}(\Omega') \rangle = \langle e_{is}(\Omega) e_{js}^{*}(\Omega) \rangle \; \delta(\Omega-\Omega') \tag{4-10}$$

The pragmatic aspect of this assumption is established in Appendix A. There it is shown that for a finitely conducting-smoothly undulating surface the degree of coherency (correlation) defined by

$$D_{ij} = \langle e_{is}(\Omega) \; e_{js}^{*}(\Omega') \rangle \; / \; \langle e_{is}(\Omega) \, e_{js}^{*}(\Omega) \rangle \tag{4-11}$$

is given by

$$D_{ij} \equiv 2 \exp(-k^2 \sin^2\theta\, \sigma^2 \Delta^2\theta/2)\ \mathrm{Jinc}(k \cos\theta R_o \Delta\theta) \tag{4-12}$$

where

σ^2 = surface height variance

k = $2\pi/\lambda$

θ = incident angle

$\Delta\theta$ = small angular deviation from θ

R_o = radius of the illuminated area

i,j = v or h

The delta function type character of the angular coherency D_{ij} is illustrated in Figure 4.2 for a patch of rough surface having a radius of one meter and illuminated at 13.9 GHz. A close examination of D_{ij} reveals that, in general, the size of the illuminated area rather than the surface roughness dominates the correlation property at all angles of incidence except for the very large incident angles. The above result is based on plane wave illumination. The degree of coherency is thought to have a stronger delta function character in the case of spherical wave illumination since returns arriving from different directions arise from different patches of the scene whose statistical characteristics are poorly correlated. A discussion of this latter point within the context of a scattering theory appears in Appendix B.

Under the above assumption the return power reduces to

$$W_{tr}(\Omega_o) = \frac{1}{8R_r} \int \mathrm{tr}\ C_r C_s^{\dagger}\ d\Omega \tag{4-13}$$

where

$$\begin{aligned} C_r &= M_r(\Omega,\Omega,\Omega_o) \\ C_s &= M_s(\Omega,\Omega) \end{aligned} \tag{4-14}$$

are the coherency matrices for the receiving antenna and the scattered fields, respectively. As a result of the integration the units of the elements within C_s become $(v/m)^2$ per steradian. The change in units is clarified in Appendix B.

Now also under the non-coherent assumption, it is permissible to introduce the

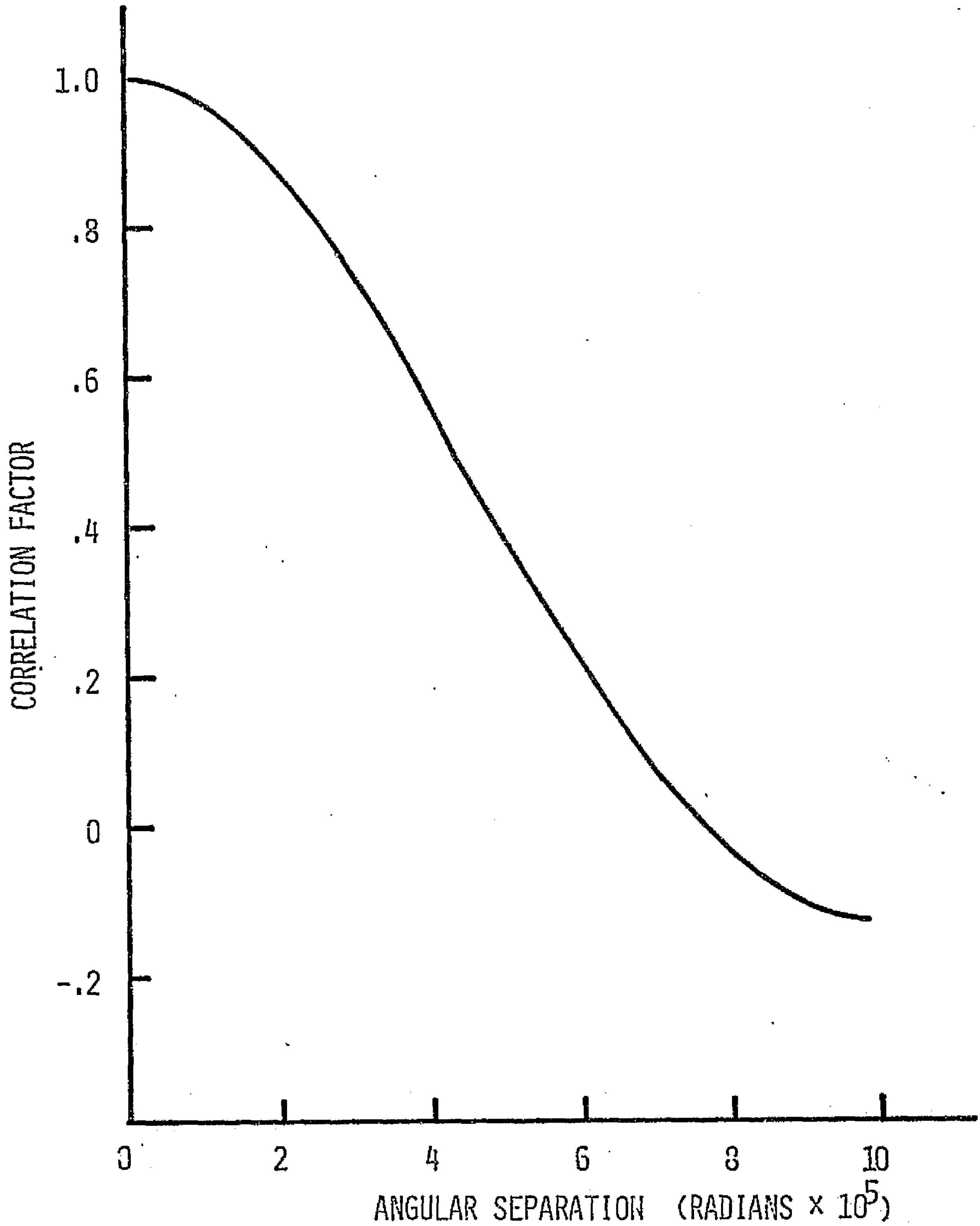

FIGURE 4.2 ANGULAR COHERENCY OF BACKSCATTER FOR A CIRCULAR PATCH WITH RADIUS OF ONE METER AND FOR A FREQUENCY OF 13.9 GHz

notion of a matrix of differential scattering operators so that for each arrival direction the backscattered field (coming from a differential patch of the surface) is related to the incident field in the following way

$$E_s = \begin{bmatrix} \mathcal{S}_{vv} & \mathcal{S}_{vh} \\ \mathcal{S}_{hv} & \mathcal{S}_{hh} \end{bmatrix} E_t \qquad (4\text{-}15)$$

The second subscript indicates the polarization of the incident field and the first subscript denotes the polarization of the resulting backscattered field. The objective for introducing this operator is that it identifies the scattered field components for each component of the incident field. With the introduction of this matrix the coherence matrix associated with the scattered field may be written as

$$\begin{aligned}
[C_s]_{vv} &= \langle \mathcal{S}_{vv}\mathcal{S}^*_{vv} e_{vt} e^*_{vt}\rangle + 2\mathrm{Re}\langle \mathcal{S}_{vv}\mathcal{S}^*_{vh} e_{vt} e^*_{ht}\rangle + \\
&\quad \langle \mathcal{S}_{vh}\mathcal{S}^*_{vh} e_{ht} e^*_{ht}\rangle \\
[C_s]_{vh} &= \langle \mathcal{S}_{vv}\mathcal{S}^*_{hv} e_{vt} e^*_{vt}\rangle + \langle \mathcal{S}_{vv}\mathcal{S}^*_{hh} e_{vt} e^*_{ht}\rangle + \langle \mathcal{S}_{vh}\mathcal{S}^*_{hv} e_{ht} e^*_{vt}\rangle \\
&\quad + \langle \mathcal{S}_{vh}\mathcal{S}^*_{hh} e_{ht} e^*_{ht}\rangle \qquad (4\text{-}16) \\
[C_s]_{hh} &= \langle \mathcal{S}_{hv}\mathcal{S}^*_{vh} e_{vt} e^*_{vt}\rangle + 2\mathrm{Re}\langle \mathcal{S}_{hv}\mathcal{S}^*_{hh} e_{vt} e^*_{ht}\rangle + \\
&\quad \langle \mathcal{S}_{hh}\mathcal{S}^*_{hh} e_{ht} e^*_{ht}\rangle \\
[C_s]_{hv} &= [C_s]^*_{vh}
\end{aligned}$$

The action of the scattering operators on the incident fields is clearly evident in the above expression.

If the incident wave were a plane wave, it is natural to define a scattering coefficient as

$$\langle S_{ij} S^*_{kl}\rangle = \langle \mathcal{S}_{ij} e_{jt} \mathcal{S}^*_{kl} e^*_{lt}\rangle / e_{it} e^*_{lt} \qquad (4\text{-}17)$$

If the above definition is employed for a spherical wave, the scattering operator will have to contend with a quadratic phase factor in the incident wave and with a varying intensity across the surface. The resulting scattering coefficient would depend on the geometry of the antenna pattern. However, under the non-coherent assumption the incident wave may be considered locally plane on each patch of the surface and the scattering action is then interpreted in accordance with the plane wave definition for the scattering coefficient. In particular, the expectations in C_s may be written as

$$<\mathcal{S}_{ij} e_{jt} \mathcal{S}^*_{kl} e^*_{lt}> \quad = \quad \left[\frac{\omega\mu_o i_t}{4\pi r}\right]^2 \quad <S_{ij} S^*_{kl}> l_{jt} l^*_{lt} \qquad (4\text{-}18)$$

where Equation (4-1) has been employed. The scattering coefficient is now allowed to vary with $(\theta,\emptyset)$ across the illuminated area. The integrand of the equation can now equation can now be written as

$$\begin{aligned} \mathrm{tr}\ C_r\ C_s^\dagger = \frac{(\omega\ \mu_o i_t)^2}{(4\pi r)^2} \Big\{ & |l_{vr}|^2 \ \Big[<|S_{vv}|^2>\ |l_{vt}|^2 + 2\mathrm{Re} \\ & <S_{vv} S^*_{vh}> l_{vt} l^*_{ht} + <|S_{vh}|^2> |l_{ht}|^2\Big] + 2\mathrm{Re} \\ & l_{vr} l^*_{hr} \Big[<S_{vv} S^*_{hv}>\ |l_{vt}|^2 + <S_{vv} S^*_{hh}> l_{vt} l^*_{ht} + \\ & <S_{vh} S^*_{hh}> |l_{ht}|^2\Big] + |l_{hr}|^2 \Big[<|S_{hv}|^2> |l_{vt}|^2 + \\ & 2\mathrm{Re} <S_{hv} S^*_{hh}>\ l_{vt} l^*_{ht} + <|S_{hh}|^2> |l_{ht}|^2\Big]\Big\} \end{aligned} \qquad (4\text{-}19)$$

As a result of the non-coherent assumption and the introduction of the scattering coefficients, the transmit antenna pattern parameters have been divorsed from the composite scattering operators. The reader will observe that the scattering coefficient employed

here has the units of m^2/m^2 per steradian. This definition is natural to this derivation and is a direct consequence of the integrating action of the antenna about its observation point (Equation (4-4)). Further discussion of the scattering coefficients is deferred until Section 5.2. The above steps in the derivation are clarified in the context of a simple scattering theory in Appendix B. As illustrated there, the above theory can be expressed as a continuum limit of an incremental theory which treats the backscatter on a patch by patch basis. Each patch is associated with an arrival direction.

Now the following identifications are helpful in re-formulating the results in more common terminology:

$$g_{pi}(\theta,\phi) = \frac{|l_{pi}|^2}{\max\limits_{\Theta,\phi}\left\{|l_{vi}|^2 + |l_{hi}|^2\right\}} \tag{4-20}$$

$$\beta_i(\theta,\phi) = \tan^{-1}\left(\mathrm{Im}\ l_{vi}l^*_{hi}/\mathrm{Re}\ l_{vi}l^*_{hi}\right) \tag{4-21}$$

$$G'_i(\theta,\phi) = \frac{4\pi\left(|l_{vi}|^2 + |l_{hi}|^2\right)}{\int\left[|l_{vi}|^2 + |l_{hi}|^2\right] d\Omega} \tag{4-22}$$

$$G_i = \max_{\theta,\phi}\left\{G'_i(\theta,\phi)\right\} \tag{4-23}$$

$$i_t^2 = 2W_t/R_t \tag{4-24}$$

$$R_t = (Z_o/\ 4\lambda^2)\int\left[|l_{vi}|^2 + |l_{hi}|^2\right] d\Omega \tag{4-25}$$

where $i = t$ (transmit) or r (receive) and $p = v$ or h polarization. Descriptively, during transmission g_{vt} is the normalized gain of the vertically polarized pattern whereas g_{ht} is the accompanying horizontally polarized pattern. The relative phase between these two polarizations is denoted as β_t. In general all three are functions of the pattern coordinates. G'_t is the gain under a matched polarization condition and G_t is the maximum gain (presumably on boresight). W_t is the transmitted power and R_t is the radiation resistance when the antenna is transmitting. Similar explanations apply to the reception parameters. They are identified with a subscript r. With the introduction of the above pattern parameters, the scatterometer equation can be written as.

$$W(\Omega_o) = (\lambda/4\pi)^2 \, G_t G_r W_t \int I_{tr}/r^2 \, d\Omega \qquad (4\text{-}26)$$

where

$$\begin{aligned} I_{tr} = \; & g_{vr}\left(g_{vt}\langle|S_{vv}|^2\rangle + 2\sqrt{g_{vt}g_{ht}}\, \mathrm{Re}\langle S_{vv}S_{vh}^*\rangle e^{j\beta_t}\right) + \\ & 2\sqrt{g_{vr}g_{hr}}\left[g_{vt}\mathrm{Re}\langle S_{vv}S_{hv}^*\rangle e^{j\beta_r} + g_{ht}\mathrm{Re}\langle S_{vh}S_{hh}^*\rangle e^{j\beta_r}\right. \\ & \left. + \left(\sqrt{g_{vt}g_{ht}}\, \mathrm{Re}(\langle S_{vv}S_{hh}^*\rangle e^{j(\beta_t+\beta_r)} + \langle S_{vh}S_{hv}^*\rangle e^{j(\beta_t-\beta_r)}\right)\right] \\ & + g_{hr}\left(\langle|S_{hh}|^2\rangle g_{ht} + 2\sqrt{g_{vt}g_{ht}}\, \mathrm{Re}\langle S_{hv}S_{hh}^*\rangle e^{j\beta_t}\right) \\ & + g_{vr}g_{ht}\langle|S_{vh}|^2\rangle + g_{hr}g_{vt}\langle|S_{hv}|^2\rangle \end{aligned} \qquad (4\text{-}27)$$

It is interesting to note at this point that there are ten scattering coefficients. Additional simplification occurs when reciprocity applies. Under this assumption

$$S_{vh} = S_{hv} \qquad (4\text{-}28)$$

since field reciprocity implies that the operators must be identical. When the above property is applied to the definition of a scattering coefficient

$$I_{tr} = g_{vr}g_{vt}\langle|S_{vv}|^2\rangle + 2\mathrm{Re}(g_{vr}\sqrt{g_{vt}g_{ht}}\,e^{j\beta_t} + g_{vt}\sqrt{g_{vr}g_{hr}}\,e^{j\beta_r})\langle S_{vv}S_{vh}^*\rangle + 2\mathrm{Re}(g_{hr}\sqrt{g_{vt}g_{ht}}\cdot e^{j\beta_t} + g_{ht}\sqrt{g_{vr}g_{hr}}\,e^{j\beta_r})\langle S_{vh}S_{hh}^*\rangle + 2\sqrt{g_{vr}g_{hr}}\cdot\sqrt{g_{vt}g_{ht}}\,\mathrm{Re}\langle S_{vv}S_{hh}^*\rangle e^{j(\beta_t+\beta_r)} + (g_{vr}g_{ht} + g_{hr}g_{vt} + 2\sqrt{g_{vr}g_{hr}g_{vt}g_{ht}}\,\mathrm{Re}\ e^{j(\beta_t-\beta_r)})\langle|S_{vh}|^2\rangle + g_{hr}g_{ht}\langle|S_{hh}|^2\rangle \quad (4\text{-}29)$$

When reciprocity applies the number of coefficients reduces to six.

The above result is the complete non-coherent radar equation under the reciprocity assumption. Although the equation was derived from the viewpoint of polarizations ascribable to the surface, the same equation would have resulted had the antenna and surface polarization states been defined with respect to the antenna. In the latter case the scattering coefficients would not be comparable with those defined by the theorist who derives scattering coefficients with respect to the surface polarizations. In addition, the scattering coefficients for an arbitrarily line of sight would, in general, be a function of antenna view angle also. Pragmatically,the antenna polarizations are referenced to a coordinate system rigidly bound to the physical antenna. The antenna polarization vectors, consequently, move with the antenna as it changes view angle. The surface polarization vectors on the otherhand, remain rigidly oriented with respect to the surface. The transformation between the two polarizations description is derived in the succeeding section. The distinction between antenna and surface polarizations on the scatterometer equation is treated simply by transforming the transmission and reception coherency matrices, C_t and C_r, from the antenna coordinate system in which they were measured to the surface coordinate system in which the surface polarizations are naturally defined.

4.3 The Scatterometer Equation Including the Distinction Between Antenna and Surface Polarizations

Suppose that the antenna patterns, both polarized and cross-polarized patterns, are measured with the scatterometer antenna mounted on an azimuth-over-elevation positioner. To describe the antenna polarizations measured from such an antenna positioner, afix a primed coordinate system rigidly to the antenna. Let the x' axis denote the boresight axis and let the z' axis be oriented in a direction coinciding with the vertical polarization sense (with respect to the antenna) for an observer on the boresight axis. Then the antenna polarizations, vertical and horizontal, will coincide with the spherical polar unit vectors $\bar{1}_{\theta'}$ and $\bar{1}_{\phi'}$, respectively, of the afixed coordinate system. The antenna coordinate system is illustrated with respect to the pattern measuring antennas in Figure 4.3. Patterns are "cut" by incrementing the positioner in elevation when the y' and y" axis coincide and then rotating the positioner about the z' axis. The measuring antennas are located on the x" axis of the range coordinates (x",y",z").

Within the antenna coordinate system the transmitted fields will be denoted by $e_{\theta' t}$ and $e_{\phi' t}$ and the complex effective reception heights by $l_{\theta' r}$ and $l_{\phi' r}$*. Both pairs of parameters are, in general, complex (to convey the relative phase between members within the pairs) and vary with θ' and ϕ'.

Now locate the antenna (primed) coordinate system so that its origin coincides with the origin of the surface coordinate system (Figure 4.1). Without loss in generality it is assumed that the antenna scans linearily in the x direction of the surface coordinate system and that observations are conducted in the x - z plane. The antenna is so oriented that its vertical polarization sense coincides with the surface vertical polarization sense at the intersection of the boresight point with the surface. Within the xz plane the antenna is pointed at an angle θ_o with respect to the local vertical (z axis). The geometry of the two coordinate systems relative to one another is shown in Figure 4.4.

To develop the relationship between the antenna and surface coordinates consider any line of sight vector $\bar{1}_r$ which emanates from the common origin and whose extension intersects the surface (See Figure 4.4). By definition, the antenna polarization pair $(\bar{1}_{\theta}', \bar{1}_{\phi}')$ and the surface polarization pair $(\bar{1}_{\theta}, \bar{1}_{\phi})$ are both perpendicular to $\bar{1}_r$. It follows that the polarization pairs at every line of sight are related by a simple rotation,

* Not normalized as in Chapter 3.

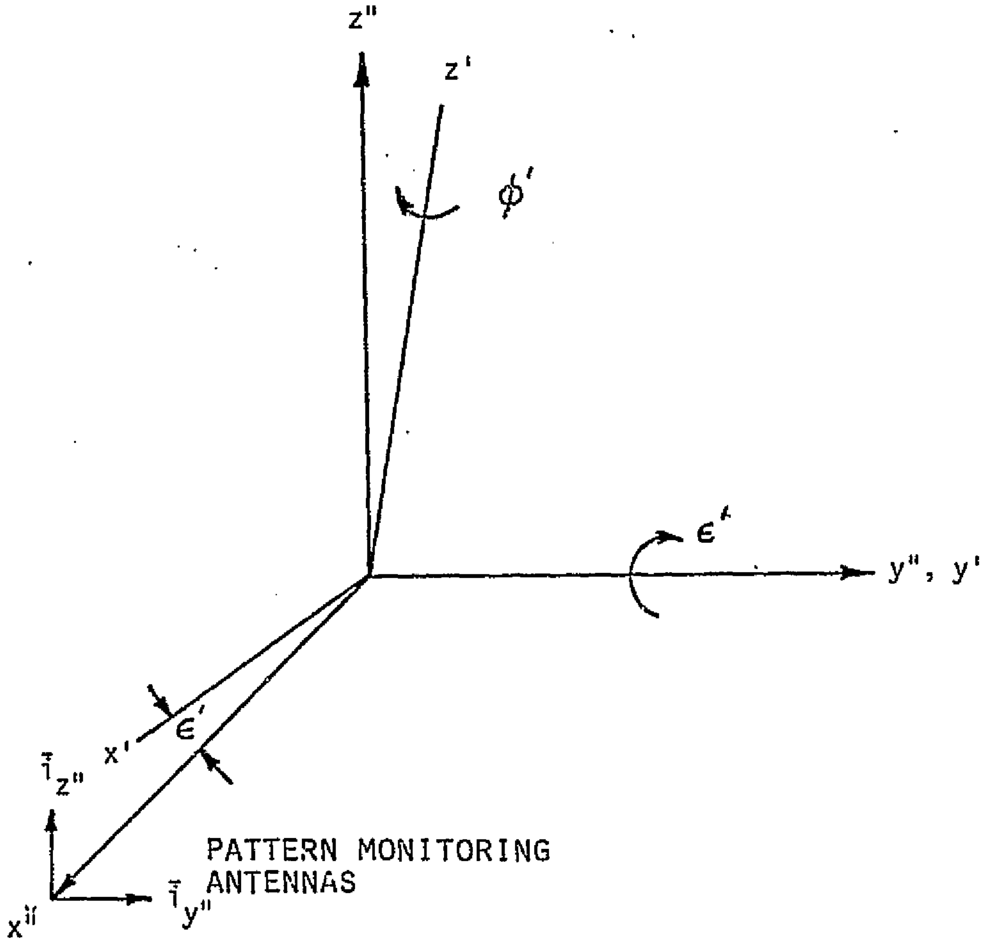

FIGURE 4.3 GEOMETRY OF THE PATTERN MEASUREMENT COORDINATE SYSTEM

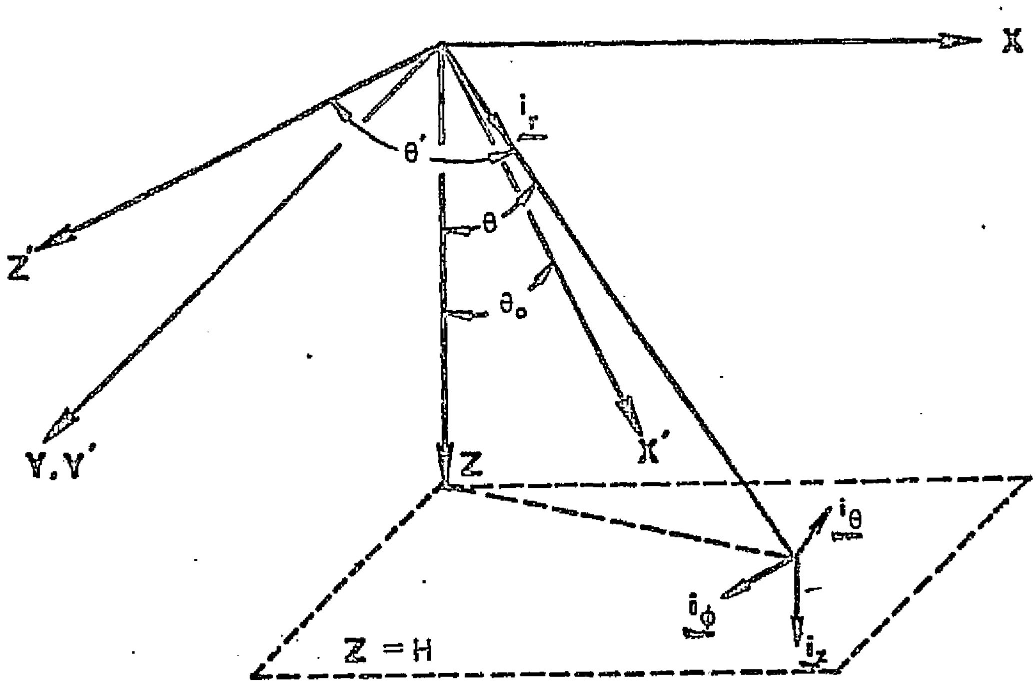

HORIZONTAL POLARIZATION

$$\bar{i}_\phi = \frac{\bar{i}_z \times \bar{i}_r}{|\bar{i}_z \times \bar{i}_r|}$$

VERTICAL POLARIZATION

$$\bar{i}_\theta = \bar{i}_\phi \times \bar{i}_r$$

FIGURE 4.4 COMPARISON OF ANTENNA AND SURFACE COORDINATE FRAMES WITH THE SURFACE POLARIZATIONS DEFINED WITH RESPECT TO A GENERAL LINE OF SIGHT VECTOR

say ψ. Define ψ, so that*

$$\bar{i}_\theta \cdot \bar{i}_{\theta'} = \bar{i}_\phi \cdot \bar{i}_{\phi'} = \cos\psi \tag{4-30}$$

and

$$\bar{i}_\theta \cdot \bar{i}_{\phi'} = -\bar{i}_\phi \cdot \bar{i}_{\theta'} = \sin\psi \tag{4-31}$$

By noting the transformation between the coordinate systems, the reader can easily show that

$$\cos\psi = \cos\phi \cos\phi' + \sin\phi \sin\phi' \sin\theta_0 \tag{4-32}$$

and

$$\sin\psi = \cos\theta\ (\sin\phi \cos\phi' - \cos\phi \sin\phi' \sin\theta_0) + \sin\theta \cos\theta_0 \sin\phi \tag{4-33}$$

where ϕ' is the spherical azimuthal angle in the primed coordinate system. Now ϕ' can be eliminated by observing that

$$\tan\phi' = (\bar{i}_r \cdot \bar{i}_{y'}) / (\bar{i}_r \cdot \bar{i}_{x'}) \tag{4-34}$$

to get

$$\phi' = \tan^{-1}\left[\frac{\sin\theta \sin\phi}{\cos\theta \cos\theta_0 + \sin\theta \sin\theta_0 \cos\phi}\right] \tag{4-35}$$

Finally from the above we have established the transform T between the antenna and surface polarizations, viz.,

$$\begin{pmatrix}\bar{i}_\theta \\ \bar{i}_\phi\end{pmatrix} = T \begin{pmatrix}\bar{i}_{\theta'} \\ \bar{i}_{\phi'}\end{pmatrix} \tag{4-36}$$

where

$$T = \begin{bmatrix}\cos\psi & \sin\psi \\ -\sin\psi & \cos\psi\end{bmatrix} \tag{4-37}$$

---

* Note: An alternate method of mounting the antenna could have resulted in defining ψ so that $\cos\psi = \bar{i}_\theta \cdot \bar{i}_{\phi'}$, etc. The difference between the two is discussed in Chapter 5.

The entries in T are provided by Equations (4-32) and (4-33) with the assist of Equation (4-35). When the antenna pattern is finally introduced the following relationship

$$\cos\theta' = \vec{i}_r \cdot \vec{i}_{z'} \tag{4-38}$$

or

$$\cos\theta' = \cos\theta\sin\theta_o - \sin\theta\cos\theta_o\cos\phi \tag{4-39}$$

in addition to Equation (4-35) will be helpful in identifying the pattern coordinates when the surface coordinates are given.

Now from the preceding derivation (Equation (4-13)), we had

$$W_{tr} = \frac{1}{8R_r} \iint tr\ C_r\ C_s^{\dagger}\ d\Omega \tag{4-40}$$

where

$$C_s = \langle \mathcal{S}\ C_t\ \mathcal{S}^{t*} \rangle \tag{4-41}$$

$$C_r = \begin{bmatrix} |1_{vr}|^2 & 1_{vr}\ 1_{hr}^* \\ 1_{hr}\ 1_{vr}^* & |1_{hr}|^2 \end{bmatrix} \tag{4-42}$$

$$C_t = \begin{bmatrix} |e_{vt}|^2 & e_{vt}\ e_{ht}^* \\ e_{ht}\ e_{vt}^* & |e_{ht}|^2 \end{bmatrix} \tag{4-43}$$

The above coherency matrices are written in terms of the surface polarizations since the scattering operators are defined on the basis of these polarizations. When the antenna transmission and reception properties are, however, defined within another coordinate system (the primed coordinate system), these properties must be

appropriately transformed. It is easily shown that if C'_r and C'_t are the coherency matrices in the primed coordinate system, then in the surface coordinate system

$$C_r = T\, C'_r\, T^{\dagger} \tag{4-44}$$

and

$$C_t = T\, C'_t\, T^{\dagger} \tag{4-45}$$

From the above expressions the following identities can be established

$$|1_{vr}|^2 = \cos^2\psi\, |1'_{vr}|^2 + \sin 2\psi \,\mathrm{Re}\, 1'_{vr}\, 1'^{*}_{hr} + \sin^2\psi\, |1'_{hr}|^2$$

$$1_{vr}\, 1^{*}_{hr} = \left[|1'_{hr}|^2 - |1'_{vr}|^2 \right] \sin\psi \cos\psi + \cos^2\psi\; 1'_{vr} 1'^{*}_{hr} - \sin^2\psi\; 1'^{*}_{hr}\, 1'_{vr}$$

$$1^{*}_{hr}\, 1_{vh} = \left[1_{vr}\, 1^{*}_{hr} \right]^{*} \tag{4-46}$$

$$|1_{hr}|^2 = \sin^2\psi\, |1'_{vr}|^2 - \sin 2\psi \,\mathrm{Re}\, 1_{vr}\, 1'^{*}_{hr} + \cos^2\psi\, |1'_{hr}|^2$$

A similar expression can be established for the elements of C_t. It is noted that the coherency matrices reduce to those in the surface coordinate system when $\psi = 0$.

Now let $g_{\theta' t}$, $g_{\phi' t}$, β'_t describe the antenna during transmission and $g_{\theta' r}$, $g_{\phi' r}$ and β'_r during reception. When the transformed coherency matrices are incorporated into the scatterometer equation and relationships of the type as shown in Equations (4-20) through (4-25) are noted in the antenna coordinate system, the scatterometer equation can be written as

$$W_{tr}(\theta_o) = \frac{\lambda^2 G_t G_r W_t}{(4\pi)^2} \int \frac{I_{tr}}{r^2}\, d\Omega \tag{4-47}$$

provided that the following identities are understood

$$g_{vp} = g_{\theta' p} \cos^2\psi + \sqrt{g_{\theta' p}\, g_{\phi' p}}\, \sin 2\psi \cos\beta'_p + g_{\phi' p} \sin^2\psi$$

$$g_{hp} = g_{\theta' p} \sin^2\psi - \sqrt{g_{\theta' p}\, g_{\phi' p}}\, \sin 2\psi \cos\beta'_p + g_{\phi' p} \cos^2\psi$$

$$\beta_p = \tan^{-1} \frac{\sqrt{g_{\theta' p} g_{\phi' p}} \sin\beta_p'}{(g_{\theta' p} - g_{\phi' p})\sin\psi\cos\psi + \sqrt{g_{\theta' p} g_{\phi' p}} \cos\beta_p'(\cos^2\psi - \sin^2\psi)} \quad (4\text{-}48)$$

where p = t or r. The latter identities indicate how the common antenna parameters transform. It is noted that β_p, g_{vp} or g_{hp} is each dependent on all three antenna parameters, β'_p, $g'_{\theta p}$ and $g'_{\phi p}$. To appreciate the additional complexity in the scatterometer equation resulting from the transformation expand the integrand in the form

$$\begin{aligned} I_{tr} &= I_1 < |s_{vv}|^2 > + I_2 < |s_{hh}|^2 > + I_3 < |s_{vh}|^2 > \\ &+ 2\ I_4 \text{ Re} < s_{vv}\ s^*_{hh} > - 2\ I_5 \text{ Im} < s_{vv}\ s^*_{hh} > \\ &+ 2\ I_6 \text{ Re} < s_{vv}\ s^*_{hv} > - 2\ I_7 \text{ Im} < s_{vv}\ s^*_{hv} > \\ &+ 2\ I_8 \text{ Re} < s_{vh}\ s^*_{hh} > - 2\ I_9 \text{ Im} < s_{vh}\ s^*_{hh} > \end{aligned} \quad (4\text{-}49)$$

Then it will be noted that

$$I_1 = \left[g_{\theta' r} \cos^2\psi + \sqrt{g_{\theta' r}\, g_{\phi' r}} \sin 2\psi \cos\beta_r' + g_{\phi' r} \sin^2\psi\right] \cdot$$
$$\left[g_{\theta' t} \cos^2\psi + \sqrt{g_{\theta' t}\, g_{\phi' t}} \sin 2\psi \cos\beta_t' + g_{\phi' t} \sin^2\psi\right] \quad (4\text{-}50a)$$

$$I_2 = \left[g_{\theta' r} \sin^2\psi - \sqrt{g_{\theta' r}\, g_{\phi' r}} \sin 2\psi \cos\beta_r' + g_{\phi' r} \cos^2\psi\right] \cdot \quad (4\text{-}50b)$$
$$\left[g_{\theta' t} \sin^2\psi - \sqrt{g_{\theta' t}\, g_{\phi' r}} \sin 2\psi \cos\beta_t' + g_{\phi' t} \cos^2\psi\right]$$

$$I_3 = \left[g_{\theta' r} \sin^2\psi - \sqrt{g_{\theta' r}\, g_{\phi' r}} \sin 2\psi \cos\beta_r' + g_{\phi' r} \cos^2\psi\right] \cdot$$
$$\left[g_{\theta' t} \cos^2\psi + \sqrt{g_{\theta' t}\, g_{\phi' t}} \sin 2\psi \cos\beta_t' + g_{\phi' t} \sin^2\psi\right] + \quad (4\text{-}50c)$$

$$\left[g_{\theta' r} \cos^2\psi + \sqrt{g_{\theta' r}\, g_{\phi' r}} \sin 2\psi \cos\beta_r' + g_{\varphi' r} \sin^2\psi\right] \cdot$$
$$\left[g_{\theta' t} \sin^2\psi - \sqrt{g_{\theta' t}\, g_{\phi' t}} \sin 2\psi \cos\beta_t' + g_{\phi' r} \cos^2\psi\right] +$$

$$2\left[\left(g_{\phi'r}-g_{\theta'r}\right)\sin\psi\cos\psi+\sqrt{g_{\theta'r}\,g_{\phi't}}\cos 2\psi\cos\beta_r'\right]\cdot$$
$$\left[\left(g_{\phi't}-g_{\theta't}\right)\sin\psi\cos\psi+\sqrt{g_{\theta't}\,g_{\phi't}}\cos 2\psi\cos\beta_t'\right]+$$
$$2\sqrt{g_{\theta't}\,g_{\phi't}}\sqrt{g_{\theta'r}\,g_{\phi'r}}\sin\beta_t'\sin\beta_r'$$

$$I_4=2\left[\left(g_{\phi'r}-g_{\theta'r}\right)\sin\psi\cos\psi+\sqrt{g_{\theta'r}\,g_{\phi'r}}\cos 2\psi\cos\beta_r'\right]\cdot$$
$$\left[\left(g_{\phi't}-g_{\theta't}\right)\sin\psi\cos\psi+\sqrt{g_{\theta't}\,g_{\phi't}}\cos 2\psi\cos\beta_t'\right]-\tag{4-50d}$$
$$\sqrt{g_{\theta't}\,g_{\phi'r}}\sqrt{g_{\theta't}\,g_{\phi't}}\sin\beta_t'\sin\beta_r'$$

$$I_5=\left[\left(g_{\phi'r}-g_{\theta'r}\right)\sin\psi\cos\psi+\sqrt{g_{\theta'r}\,g_{\phi'r}}\cos 2\psi\cos\beta_r'\right]\cdot$$
$$\sqrt{g_{\theta't}\,g_{\phi't}}\sin\beta_t'+\left[\left(g_{\phi't}-g_{\theta'r}\right)\sin\psi\cos\psi+\right.\tag{4-50e}$$
$$\left.\sqrt{g_{\theta't}\,g_{\phi't}}\cos 2\psi\cos\beta_t'\right]\quad\sqrt{g_{\theta'r}\,g_{\phi'r}}\sin\beta_r'$$

$$I_6=\left[g_{\theta'r}\cos^2\psi+\sqrt{g_{\theta'r}\,g_{\phi'r}}\sin 2\psi\cos\beta_r'+g_{\phi'r}\sin^2\psi\right]\cdot$$
$$\left[\left(g_{\phi't}-g_{\theta't}\right)\sin\psi\cos\psi+\sqrt{g_{\theta't}\,g_{\phi't}}\cos 2\psi\cos\beta_t'\right]+$$
$$\left[g_{\theta't}\cos^2\psi+\sqrt{g_{\theta't}\,g_{\phi't}}\sin 2\psi\cos\beta_t'+g_{\phi'r}\sin^2\psi\right]\cdot$$
$$\left[\left(g_{\phi'r}-g_{\theta'r}\right)\sin\psi\cos\psi+\sqrt{g_{\theta'r}\,g_{\phi'r}}\cos 2\psi\cos\beta_r'\right]\tag{4-50f}$$

$$I_7=\left[g_{\theta'r}\cos^2\psi+\sqrt{g_{\theta'r}\,g_{\phi'r}}\sin 2\psi\cos\beta_r'+g_{\phi'r}\sin^2\psi\right]\cdot$$
$$\sqrt{g_{\theta't}\,g_{\phi't}}\sin\beta_t'+\left[g_{\theta't}\cos^2\psi+\sqrt{g_{\theta't}\,g_{\phi't}}\sin 2\psi\cos\beta_t'\right.$$
$$\left.g_{\phi't}\sin^2\psi\right]\sqrt{g_{\theta'r}\,g_{\phi'r}}\sin\beta_r'\tag{4-50g}$$

$$I_8 = \left[g_{\theta' t} \sin^2 \psi - \sqrt{g_{\theta' t}\, g_{\phi' t}} \sin 2\psi \cos \beta_t' + g_{\phi' t} \cos^2 \psi \right] \cdot$$

$$\left[(g_{\phi' r} - g_{\theta' r}) \sin \psi \cos \psi + \sqrt{g_{\theta' r}\, g_{\phi' r}} \cos 2\psi \cos \beta_r' \right] +$$

$$\left[g_{\theta' r} \sin^2 \psi - \sqrt{g_{\theta' r}\, g_{\phi' r}} \sin 2\psi \cos \beta_r' + g_{\phi' r} \cos^2 \psi \right] \cdot$$

$$\left[(g_{\phi' t} - g_{\theta' t}) \sin \psi \cos \psi + \sqrt{g_{\theta' t}\, g_{\phi' t}} \cos 2\psi \cos \beta_t' \right] \qquad (4\text{-}50h)$$

$$I_9 = \left[g_{\theta' t} \sin^2 \psi - \sqrt{g_{\theta' t}\, g_{\phi' t}} \sin 2\psi \cos \beta_t' + g_{\phi' t} \cos^2 \psi \right] \cdot$$

$$\sqrt{g_{\theta' r}\, g_{\phi' r}} \sin \beta_r' + \left[g_{\theta' r} \sin^2 \psi - \sqrt{g_{\theta' r}\, g_{\phi' r}} \sin 2\psi \cos \beta_r' + \right.$$

$$\left. g_{\phi' r} \cos^2 \psi \right] \cdot \sqrt{g_{\theta' t}\, g_{\phi' t}} \sin \beta_t' \qquad (4\text{-}50i)$$

When accurate measurements of the scattering coefficients, say the complete set of nine parameters is desired, one must contend with inverting a system of integral equations of the type derived above. The scattering coefficients are rigorously defined in terms of the surface polarization, a definition universally employed by the scattering theorist. If comparisons with theory are necessary then the antenna properties must be transformed to conform with this definition. To date measurements have been reported without the recognition that Equations (4-47) through (4-50) governor the interaction between the scatterometer antenna and the scene. Yet reasonable agreement between measurements from targets with known statistics and theory have been reported [10] [31] for the polarized scattering coefficients. This indicates that the complexity of I_1 through I_9 may be avoidable under some circumstances. To resolve this problem and related ones, the polarization coordinate systems will be compared and the character of the scatterometer equation will also be examined in depth in succeeding chapters. Once the character of the scatterometer equation is established, a measurement technique to recover all six scatting coefficients is specified. Computer simulations based on the specified technique are then conducted to determine antenna requirements for accurate measurements.

5.0 DISCUSSION OF THE SCATTEROMETER EQUATION

5.1 Introduction

This chapter is devoted to developing an understanding of the scatterometer equation. The character of the scattering coefficients is established by reference to previous definitions, both coherent and non-coherent. It is shown that the non-coherent definition appearing in the literature must be extended to include new kinds of coefficients. The composition of the average return is examined from the standpoint of coherence theory and the complete set of scattering coefficients. The importance of the phase characteristic of the wave and the receiving antenna in governing the observed power is described. It is also shown that certain properties of the coherent scattering coefficients cannot be extrapolated to the non-coherent case. Well known theories applicable to the sea are also employed to illustrate the behavior of the scattering coefficients having a cross-correlation property. Other possibilities for the cross-correlation coefficients are also treated intuitively.

Within this chapter it is also shown that this formulation of the scatterometer equation admits partially polarized returns. A previous formulation [6] failed in this respect. The degree of polarization of the average sea return is specifically illustrated using a simple scattering theory.

Finally the distinction between surface and antenna polarizations is illustrated. Certain aspects of this distinction are qualitaively applied to specifying antenna requirements.

5.2 General

5.2.1 The Scattering Coefficient

The scattering coefficients within the scatterometer equation may be partially identified with the differential scattering coefficients defined by Peake [24]. As the reader may recall, Peake defines

$$\gamma_{ij} = \frac{4\pi r^2 \langle|e_{is}|^2\rangle}{A\cos\theta_0 |e_{jt}|^2} \tag{5-1}$$

where $|e_{jt}|^2$ is the polarized incident intensity, $\langle|e_{is}|^2\rangle$ is the i polarized backscatter intensity in volts^2/m^2, θ is the incident angle and A is the illuminated area. The scattering coefficient employed in this formulation is simply related to γ_{ij} in the

following way

$$<|S_{ij}|^2> = \gamma_{ij}/4\pi \qquad (5\text{-}2)$$

The difference by 4π occurs since the scattered intensities were defined in terms of inverse steradians. It is clear that, in view of the three addition coefficients, it is more appropriate to define the coefficients in terms of the scattering operators

$$<S_{ij}S^*_{kl}> = <\mathcal{S}'_{ij}\mathcal{S}^{*\prime}_{kl}e_{jt}e^*_{lt}> R^2 / e_{jt}e^*_{lt}\ \Delta A\cos\theta_o \qquad (5\text{-}3a)$$

where $\mathcal{S}'_{ij}\ E_{jt}$ yields a scattered field with units volts/meter. The operators in the derivation are related to those in the definition in the following way

$$\mathcal{S}_{ij}\mathcal{S}^*_{kl} = \mathcal{S}'_{ij}\mathcal{S}^{*\prime}_{kl}\ R^2 /\Delta A \cos\theta_o \qquad (5\text{-}3b)$$

To understand the function of these cross-correlation coefficients one must examine the coherence matrix for the scattered wave. Under the non-coherence and reciprocity assumptions the elements of C_s are given by

$$[C_s]_{vv} = <|S_{vv}|^2>|e_{vt}|^2 + 2\mathrm{Re}<S_{vv}S^*_{vh}>e_{vt}e^*_{ht} + <|S_{vh}|^2>|e_{ht}|^2$$

$$[C_s]_{vh} = <S_{vv}S^*_{hv}>|e_{vt}|^2 + <S_{vv}S^*_{hh}>e_{vt}e^*_{ht} + <|S_{vh}|^2>e_{ht}e^*_{vt} + <S_{vh}S^*_{hh}>|e_{ht}|^2$$

$$[C_s]_{hv} = [C_s]^*_{vh} \qquad (5\text{-}4)$$

$$[C_s]_{hh} = <|S_{vh}|^2>|e_{vt}|^2 + 2\mathrm{Re}<S_{hv}S^*_{hh}>e_{vt}e^*_{ht} + <|S_{hh}|^2>|e_{ht}|^2$$

The power in the scattered wave is carried in the trace of C_s whereas the relative phase between the orthogonal components in an average sense is carried in the off diagonal elements. From the structure of the coherence matrix it is evident that the cross-correlation coefficients can be complex valued. The cross-correlation coefficients therefore alter the phase property of the scattered wave. Some of the relative phase is attributable to the incident wave and some to the surface, eg., $e_{vt} e_{ht*}$ and $<S_{vv}S_{hh*}>$, respectively. The cross-correlation terms also appear in the diagonal terms and consequently contribute to the total power available in the scattered wave when both polarizations appear in the incident wave.

During reception the coherency matrix of the antenna interacts with the coherency matrix for the wave. The interaction is completely described by taking the trace of $C_r C_s^\dagger$. The trace is given by

$$\mathrm{tr}\ C_r C_s^\dagger = |l_{vr}|^2 [C_s]_{vv} + l_{vr} l_{hr}^* [C_s]_{vh} + l_{hr} l_{vr}^* [C_s]_{hv} + |l_{hr}|^2 [C_s]_{hh} \tag{5-5}$$

(The expanded version of the trace is given in Equation (4-19) of Chapter 4). The phase interaction between the scattered wave and the antenna is described by the middle terms in the trace expression. These terms are complex conjugate pairs and consequently make a real contribution to the observed power.

To show that the phase properties of the antenna and the wave are important to the observed return it must be recalled that in the case of polarized waves, the antenna polarization states must be matched to the polarization state of the wave to observe maximum power [14]. This requirement in terms of coherency matrices implies that

$$C_r/\mathrm{tr}C_r = C_s^*/\mathrm{tr}\ C_s \tag{5-6}$$

Under the polarized assumption C_s takes the form

$$C_s/\mathrm{tr}C_s = \begin{bmatrix} a & c \\ c^* & b \end{bmatrix} \tag{5-7}$$

where $a + b = 1$, $c = \sqrt{ab}\,e^{j\alpha}$, and α is the relative phase between the v and h components. The observed power will be proportional to $(a+b)^2\ \mathrm{tr}C_r\ \mathrm{tr}\ C_s$ or

$\mathrm{tr}\, C_r \mathrm{tr}\, C_s$. If the reception matrix had been given by

$$C_r = \begin{bmatrix} b & -c^* \\ -c & a \end{bmatrix} \qquad (5\text{-}8)$$

no power would be observed at the antenna terminals as can be easily demonstrated. In this case the antenna polarization state is said to be orthogonal to the polarization state of the arriving wave.

If the wave is partially polarized Ko [25] has shown that the observed power may vary from a minimum of $\lambda^2 G_r(1-P)\, \mathrm{tr}\, C_s / 8 Z_o$ to a maximum of $\lambda^2 G_r(1+P)\, \mathrm{tr}\, C_s / 8 Z_o$. where P is the degree of polarization (See Section 4 of this chapter). To understand this result it must be noted that a partially polarized wave can be uniquely decomposed into a sum of a randomly polarized wave and a completely polarized wave [30] . As a consequence for an arbitrarily polarized backscattered wave, the decomposition can be written as

$$C_s = \mathrm{tr}\left[C_s\right]\left\{(1-P)\begin{bmatrix} 1/2 & 0 \\ 0 & 1/2 \end{bmatrix} + P\begin{bmatrix} \rho_{vv} & \rho_{vh} \\ \rho_{hv} & \rho_{hh} \end{bmatrix}\right\} \qquad (5\text{-}9)$$

where P is defined in Equation (5-30) and

$$\rho_{vv} = \frac{1}{P\ \mathrm{tr}\left[C_s\right]}\left[\left[C_s\right]_{vv} - 1/2(1-P)\right]$$

$$\rho_{vh} = \frac{\left[C_s\right]_{vh}}{P\ \mathrm{tr}\left[C_s\right]} \qquad (5\text{-}10)$$

$$\rho_{hv} = \rho^*_{vh}$$

$$\rho_{hh} = \frac{1}{P\ \mathrm{tr}\left[C_s\right]}\left[\left[C_s\right]_{hh} - 1/2(1-P)\right]$$

The first term is the randomly polarized component and the second is the completely polarized component. If the receiving antenna is orthogonal to the completely polarized part, then only the randomly polarized component is observed at the antenna terminals. If the antenna is matched to the completely polarized part maximum power is observed.

The extremes in the observable power are a positive indication of the importance of the phase interaction of the antenna and the wave. The cross-correlation scattering coefficients and the cross-polarized scattering coefficient can be effective in altering the phase property of the return.

The cross-correlation terms have their analogues in scattering theory for coherent targets [21]. In the theory for discrete targets the complex scattering matrix is commonly employed to define scattering properties. The elements of this matrix have the property that

$$|S_{ii}S_{jk}^*| = |S_{ii}||S_{jk}| \tag{5-11}$$

However for a statistical target this property is not necessarily true. Since the scattering coefficients can be considered as a inner product of the form

$$\langle S_{ii}S_{jk}^*\rangle = \langle \mathcal{S}_{ii}e_{it}\,\mathcal{S}_{jk}^*\bar{e}_{kt}^*\rangle \tag{5-12}$$

where $e_{it}e_{kt}^* = 1$, it is concluded by Schwartz' inequality that

$$|\langle S_{ii}S_{jk}^*\rangle| \leq \sqrt{\langle|S_{ii}|^2\rangle\langle|S_{jk}|^2\rangle} \tag{5-13}$$

As a consequence the magnitudes of the scattering coefficients may not be simply related as suggested by William, et al. [6]. The inequality is an admission that the amplitudes or phase centers between scattered field components can be correlated.

One can identify two scattering parameters with each complex valued scattering coefficient, viz., its real and imaginary parts. As a result one may attribute nine scattering parameters to Equation (4-29) where reciprocity has been applied. Similarly from Equation (4-27) where reciprocity has not been applied, sixteen scattering parameters can be identified. These observations are in agreement with the "Gedanken Experimente" cited in Chapter 3.

5.2 2 Special Cases

An examination of the scatterometer equation indicates that the equation under appropriate conditions reduces to the classical cases. For example, when vertically polarized measurements are conducted, i.e., $g_{ht} = g_{hr} = 0$, the integrand factor I_{tr} of the scatterometer equation becomes

$$I_{tr} = g_{vr}g_{vt}\langle|S_{vv}|^2\rangle \tag{5-14}$$

Similarly when horizontally polarized measurements are conducted, i.e., $g_{vt} = g_{vr} = 0$,

$$I_{tr} = g_{hr} g_{ht} <|S_{hh}|^2> \tag{5-15}$$

and when cross-polarized measurements are conducted, i.e., $g_{ht} = g_{vr} = 0$,

$$I_{tr} = g_{vt} g_{hr} <|S_{vh}|^2> \tag{5-16}$$

It should be noted that the reductions result from highly idealized representations of practical antennas. Invariably antennas have cross polarized leakage; and when leakage is present other scattering coefficients, both auto-correlation and cross-correlation types, will be excited. As shown in the last section of Chapter 4, even if the leakage is not present, the difference between antenna and surface polarizations can introduce, in effect, cross-polarized components in the incident wave and in the reception antenna. The impact of undesirable antenna properties and polarization mis-match on the measurement of isolated scattering parameters will be treated in Chapter 7.

An understanding of the cross-correlation coefficients from theories applicable to sea returns is developed in the succeeding section.

5.3 Characteristics of the Correlation Terms

Several scattering theories are examined to disclose the character of the cross-correlation terms in the scatterometer equation. Approximate backscatter solutions to the small perturbation theory [32] [33] [34] [35] and the Kirchhoff theory [36] [37] are specifically examined. These theories with some slight alterations are thought to apply to ocean backscatter and have shown reasonable agreement with measured results. The selection of these theories by no means exhausts the possibilities. Physically intuitive arguments are given at the end of this section to further enhance our understanding.

When returns are considered from a surface having a small roughness, satisfying $k^2\sigma^2\cos^2\theta \leq 1$, where σ is the rms surface height and k is the wave number, it can be shown that (see Appendix C)*

$$<S_{vv}S_{hh}^*> = \frac{k^4}{\pi^2} \cos^3\theta \mathcal{R}_v R_h W(2k \sin\theta, 0) \tag{5-17}$$

* The reader should be aware that in constructing the scattering coefficients from scattering theory and identifying them with measured coefficients involves an ergodic assumption, i.e., an ensemble average is equated with a spatial average.

In the above equation

$$\mathcal{R}_v = \frac{(\epsilon_r - 1)[\epsilon_r(1+\sin^2\theta) - \sin^2\theta]}{(\epsilon_r \cos\theta + \sqrt{\epsilon_r - \sin^2\theta})^2} \tag{5-18}$$

$$R_h = \frac{\cos\theta - \sqrt{\epsilon_r - \sin^2\theta}}{\cos\theta + \sqrt{\epsilon_r - \sin^2\theta}} \tag{5-19}$$

Comparison of the magnitude of this term with the polarized scattering coefficients shows that

$$|<S_{vv}S_{hh}^*>| = \sqrt{<|S_{vv}|^2><|S_{hh}|^2>} \tag{5-20}$$

The equality is true at least to the order to which these solutions are valid. The magnitude of this term is illustrated in Figure 5.1 wherein it is also compared with the polarized coefficients. The computations were based on a slightly rough sea. The phase of the cross correlation, defined by

$$\Phi = \tan^{-1}(\mathrm{Im}<S_{vv}S_{hh}^*>/\ \mathrm{Re}<S_{vv}S_{hh}^*>) \tag{5-21}$$

was computed and is shown in Figure 5.2 for three different water temperatures. The sea water temperature alters the complex dielectric constant of the surface and consequently influences $\mathcal{R}_v$ and R_h. It is observed from the graph that the imaginary part of $<S_{vv}S_{hh}^*>$ is small in comparison to its real part and only tends to become significant at the larger angles when compared with the real part.

An examination of the integrand of the scatterometer equation (4-29) indicates that the above cross-correlation term can make a significant contribution to a radar return when like and cross antenna polarizations are present during transmission and reception.

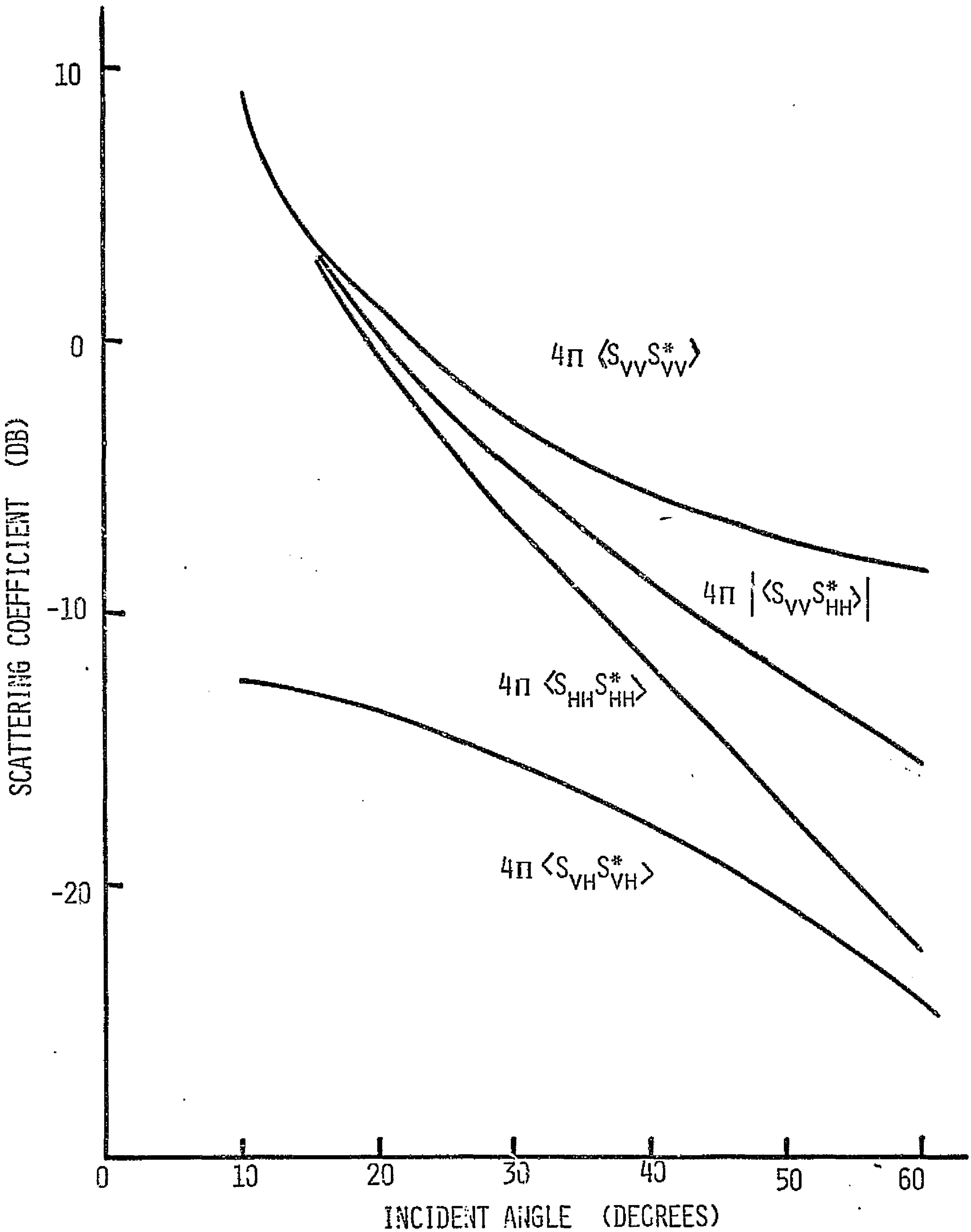

FIGURE 5.1 SCATTERING CHARACTERISTICS BASED ON SMALL PERTURBATION THEORY

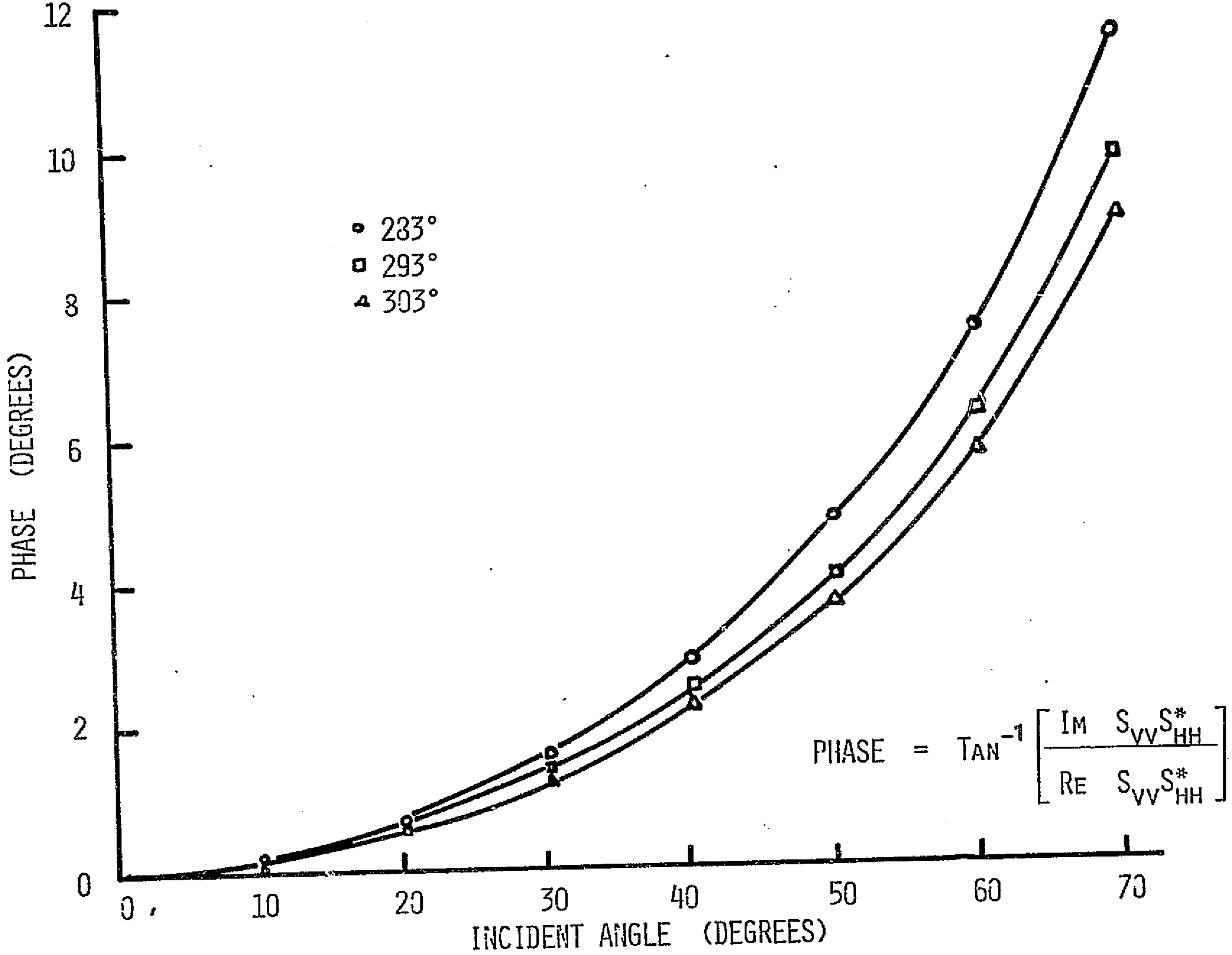

FIGURE 5.2 CROSS-CORRELATION PHASE PROPERTY BASED ON SMALL PERTURBATION THEORY

The contribution can be positive or negative depending upon the value of $(\beta_t + \beta_r)$ and can be comparable to the sum of the contributions arising from the polarized scattering coefficients. To illustrate the above statement it is sufficient to observe that the polarized contributions are proportional to $g_{vt} g_{vr} \langle |S_{vv}|^2 \rangle$ and $g_{ht} g_{hr} \langle |S_{hh}|^2 \rangle$. On the other-hand, if the imaginary part of $\langle S_{vv} S_{hh}^* \rangle$ is small so that $\langle S_{vv} S_{hh}^* \rangle \cong \sqrt{\langle |S_{vv}|^2 \rangle \cdot \langle |S_{hh}|^2 \rangle}$ then the contribution by the cross-correlation coefficient is given by

$$2\sqrt{g_{vt} g_{vr} g_{ht} g_{hr}} \sqrt{\langle |S_{vv}|^2 \rangle \langle |S_{hh}|^2 \rangle} \; \mathrm{Re} \;\; e^{j(\beta_r + \beta_t)}$$

If right circular polarization* is transmitted and received, then $\cos(\beta_t + \beta_r) = -1$ and $g_{vt} = g_{ht} = g_{vr} = g_{hr}$. It is apparent that when $\langle |S_{vv}|^2 \rangle \cong \langle |S_{hh}|^2 \rangle$, the magnitude of the cross-correlation contribution is identical to the sum of the polarized terms. The sign of the contribution is, in this case, negative. However, had the wave been received with a LC polarized antenna, the sign of the contribution would have been positive. The contribution by this scattering coefficient can also be very effective when attempting measurement of a weak scattering coefficient such as $\langle |S_{vh}|^2 \rangle$ with a "linearily" polarized antenna having some cross polarized leakage. This will be illustrated in Chapter 7.

When the cross-correlation terms of the type $\langle S_{vv} S_{vh}^* \rangle$ and $\langle S_{hv} S_{hh}^* \rangle$ are examined in the context of small perturbation theory, it is easily shown that these coefficients vanish at the lowest order where $\langle |S_{vv}|^2 \rangle$, $\langle |S_{hh}|^2 \rangle$ and $\langle |S_{vh}|^2 \rangle$ are non-zero (see Appendix C)**. The lack of correlation is physically reasonable since it is believed that the cross-polarized fields result from multiple scatter. When higher order solutions are included these cross-correlation terms will not vanish; however, their magnitudes will be extremely small.

The above theory is thought to apply with some modification to the sea for angles of observation between 30 and 80 degrees [37]. At smaller angles Kirchhoff theory [37] has predicted sea returns reasonably well. When the theory reported by Fung [36] is employed to explain near vertical returns it can be shown that (see Appendix A) for an isotropic stationary gaussian surface

$$\langle S_{vv} S_{hh}^* \rangle = \frac{R_1 \, R_2 \exp\left(- \tan^2\theta \, / \, 2m^2 \right)}{8\pi \, m^2 \cos^3\theta} \tag{5-22}$$

* Circular polarization is defined with respect to the antenna; but for narrow beams and sufficiently large angles, the circular polarization state transforms to the surface without significant alteration. This will be clarified at the end of this chapter and within Chapter 7.

** Recall $\langle |S_{vv}|^2 \rangle$ and $\langle |S_{hh}|^2 \rangle$ are first order solutions and $\langle |S_{vh}|^2 \rangle$ is a second order solution.

where

$$R_1 = R_v \left[\cos\theta + \sin\theta + T_v \cos\theta\right] \tag{5-23}$$

$$R_2 = R_h \left[\cos\theta + \sin\theta + T_h \cos\theta\right] \tag{5-24}$$

$$T_v = \frac{2\epsilon_r \sin\theta}{\sqrt{\epsilon_r - \sin^2\theta}\,(\epsilon_r \cos^2\theta - \sin^2\theta)} \tag{5-26}$$

$$T_h = \frac{-2 \sin\theta}{\sqrt{\epsilon_r - \sin^2\theta}} \tag{5-27}$$

Comparison of the magnitude of this cross-correlation terms with the magnitudes of the polarized scattering coefficients again shows that (Appendix A)

$$|\langle S_{vv} S_{hh}^* \rangle| = \sqrt{\langle |S_{vv}|^2 \rangle \langle |S_{hh}|^2 \rangle} \tag{5-28}$$

The equality is valid to at least first order in corrections to the reflection coefficient for the local slope. The magnitude and phase of the above result is illustrated in Figures 5.3 and 5.4, respectively, for an isotropically rough sea surface having a moderate rms surface slope. It is noted that the phase property may be attributed to the linear corrections of the reflection coefficients for the local slope. The resulting reflection coefficients compare favorably with that for normal incidence.

When cross-correlations involving S_{vh} or S_{hv} are considered within the Kirchhoff approximation little can be said regarding their character. A typical cross-correlation

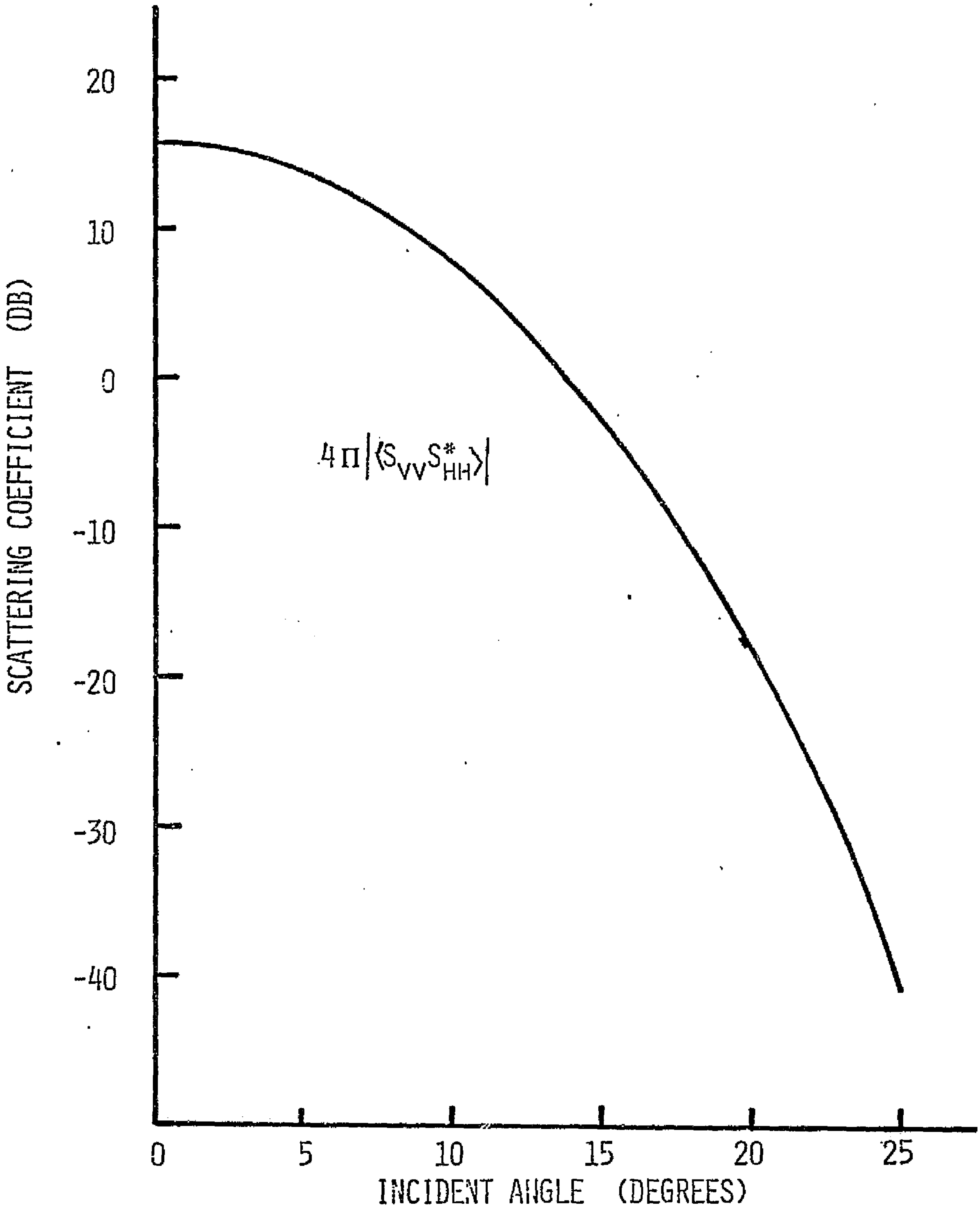

FIGURE 5.3 THE SCATTERING CHARACTERISTIC OF $|\langle S_{VV}S^*_{HH}\rangle|$ BASED ON KIRCHHOFF THEORY

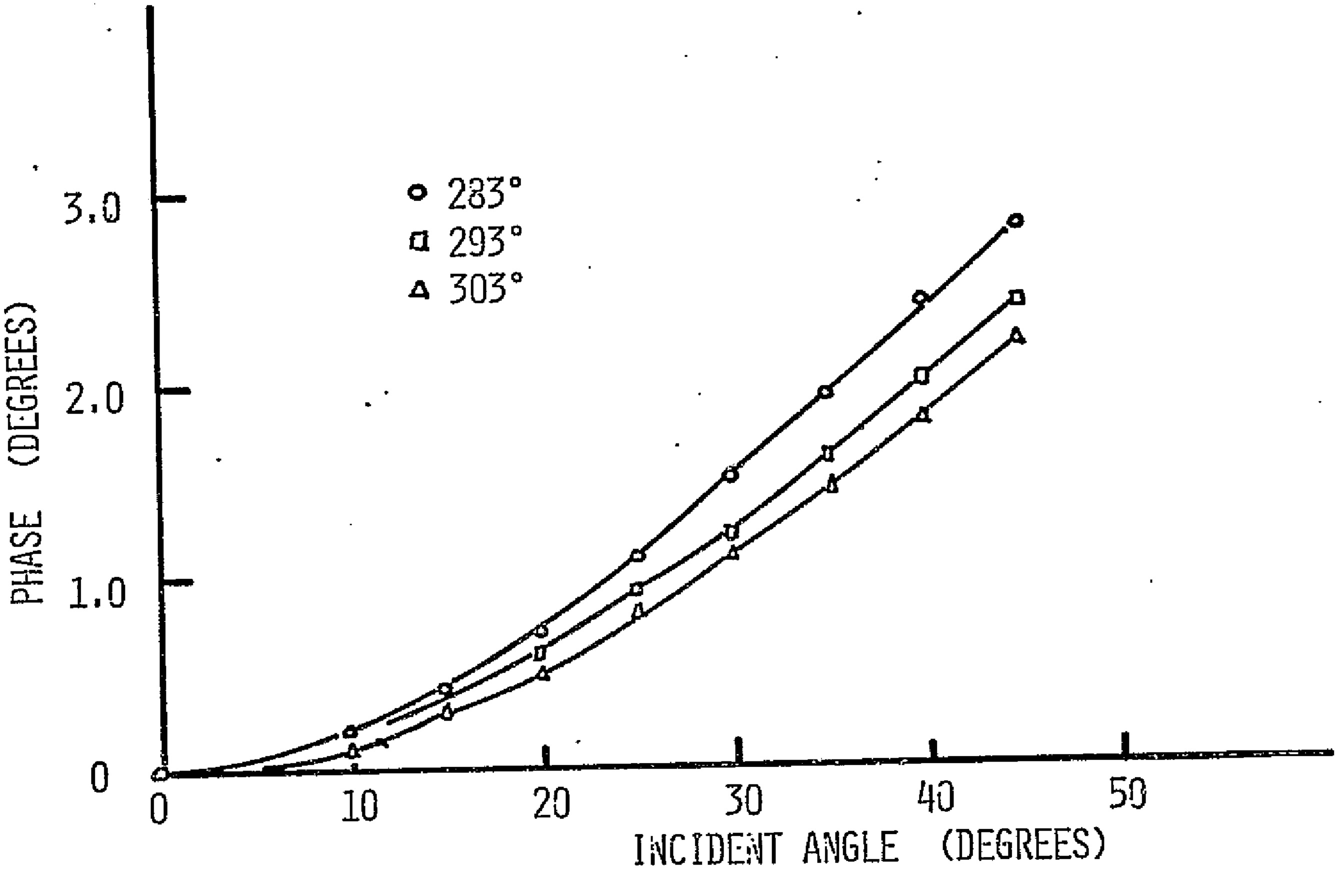

FIGURE 5.4 CROSS-CORRELATION PHASE PROPERTY BASED ON KIRCHHOFF THEORY

between field components is given by

$$<E_{vv}E_{vh}^*> = 4\,|K|^2\,R_v\,(\theta)\left[\cos\theta + (\,\sin\theta + T_v\,\cos\theta\,)\,\tan\theta\right]$$

$$\iiiint < \frac{Z_x\,(\,R_v + R_h\,)\,(\,\cos\theta\,Z_y - \sin\theta\,)}{Z_x^{\,2} + (\,\sin\theta - \cos\theta\,Z_y\,)^2}\, e^{-j2\bar{k}\cdot(\bar{r}_1 - \bar{r}_2)} > dx_1dy_1dx_2dy_2 \tag{5-29}$$

where integration by parts has simplified E_{vv} and the reflection coefficient R_v has been linearily approximated. Since the expectation involves higher order slope terms it is anticipated that the correlation will be weak. The stationary phase technique for solving the integral, for example, would cause the integrand to vanish.

On the basis of the above simple scattering theories, it is clear that the cross-correlation coefficient $<S_{vv}\,S_{hh}^*>$ can contribute to a radar return when both like and cross polarizations are present during transmission and reception. The theory for the slightly rough surface indicates that the phase of the correlation product is dependent on the relative phase between the so-called Rice reflection coefficients. The phase factor is somewhat significant at the larger angles. Correlation products containing S_{vh} or S_{hv} vanish for the slightly rough surface and appear to be negligible for Kirchhoff type surfaces also. These two theories by no means exhaust the possibilities.

Consider, for example, radar returns from a strongly de-polarizing scene such as a tenuous vegetated terrain in which the depolarization is attributable to linear re-radiation. Intuitively, one would expect sizeable contributions from the cross-correlation products containing S_{vh} or S_{hv}. The correlation contributions will likely arise from a single scatter process, particularly at the canopy. The contributions, as an examination of C_s shows, will arise if like and cross antenna polarizations are present during transmission or reception or both. When $<|S_{vh}|^2>$ is somewhat less than $<|S_{vv}|^2>$ and $<|S_{hh}|^2>$ and one attempts retrieval of $<|S_{vh}|^2>$ with a "linearily" polarized antenna possessing a cross leakage pattern one can anticipate contamination not only by $<|S_{vv}|^2>$, $<|S_{hh}|^2>$ and $<S_{vv}\,S_{hh}^*>$ but also by $<S_{vv}\,S_{hv}^*>$ and $<S_{vh}\,S_{hh}^*>$.

5.4 The Degree of Polarization of Radar Returns

Another important aspect of the scatterometer equation derived here is that the backscattered fields can be considered partially polarized. The partially polarized character is induced by measuring average returns from a non-coherent scene. This permits us to consider a statistical coherency matrix as a suitable representation for the return. It is well known that the degree of polarization of a wave is given by [30]

$$P = \sqrt{1 - \frac{4\,\|C_s\|}{(\mathrm{tr}\ C_s)^2}} \tag{5-30}$$

where C_s is the coherency matrix of the wave and $\|C_s\|$ denotes its determinant. If $P = 1$ the wave is said to be completely polarized. This occurs if and only if $\|C_s\| = 0$. To show that the present formulation admits partially polarized waves (possibly randomly polarized, $P = 0$), it is sufficient to show that $\|C_s\| \neq 0$. Now C_s is given in Equation (4-16) and with a little tedious effort one can show

$$\begin{aligned}
\|C_s\| = {} & |e_v|^4 \left[<|S_{vv}|^2> <|S_{hv}|^2> - |<S_{vv}S_{hv}^*>|^2 \right] + |e_v|\,|e_h|^2 \left[<|S_{vv}|^2> \right. \\
& \left. <|S_{hh}|^2> - |<S_{vv}S_{hh}^*>|^2 \right] + |e_h|^4 \left[<|S_{hh}|^2> <|S_{hv}|^2> - |<S_{hv}S_{hh}^*>|^2 \right] \\
& + 2|e_v|^2 \, \mathrm{Re}\, e_v e_h^* \left[<|S_{vv}|^2> <S_{hv}S_{hh}^*> - <S_{vv}S_{hh}^*> <S_{vv}^*S_{hv}> \right] + 2\mathrm{Re} \\
& (e_v e_h^*)^2 \left[<S_{vv}S_{vh}^*> <S_{hv}S_{hh}^*> - <S_{vv}S_{hh}^*> <|S_{hv}|^2> \right] + 2|e_h|^2 \mathrm{Re} \\
& <e_v e_h^*> \left[<S_{vv}S_{vh}^*> <|S_{hh}|^2> - <S_{vv}S_{hh}^*> <S_{vh}^*S_{hh}> \right]
\end{aligned} \tag{5-31}$$

where the subscript t has been dropped. If the determinant is to vanish independent of the transmitted fields then each difference term in the above expression must vanish.

A non-statistical target having a scattering matrix

$$S = \begin{bmatrix} |S_{vv}|e^{j\alpha} & |S_{vh}|e^{j\delta} \\ |S_{vh}|e^{j\delta} & |S_{hh}|e^{j\beta} \end{bmatrix} \tag{5-32}$$

will obviously meet the requirement. However, the general result indicates that the backscattered wave is partially polarized as the examples below illustrate.

For the case where terms of the type $\langle S_{vv} S_{vh}^* \rangle$ are assumed negligibly small, as we suspect they are over the sea, we have

$$\begin{aligned} \|C_s\| = {} & |e_v|^4 \langle|S_{vv}|^2\rangle\langle|S_{hv}|^2\rangle + |e_v|^2 |e_h|^2 \left[\langle|S_{vv}|^2\rangle\langle|S_{hh}|^2\rangle - |\langle S_{vv}S_{hh}^*\rangle|^2\right] \\ & + |e_h|^4 \langle|S_{hh}|^2\rangle\langle|S_{hv}|^2\rangle - 2\mathrm{Re}\,(e_v e_h^*)^2 \langle S_{vv}S_{hh}^*\rangle\langle|S_{hv}|^2\rangle \end{aligned} \tag{5-33}$$

At moderate to large incident angles over the ocean it is anticipated that the above term can be significantly different from zero. Specifically if a horizontally polarized wave is transmitted, we have

$$\|C_s\| = |e_h|^4 \langle|S_{hh}|^2\rangle\langle|S_{hv}|^2\rangle \tag{5-34}$$

The corresponding degree of polarization is given by

$$P_h = \frac{\langle|S_{hh}|^2\rangle - \langle|S_{vh}|^2\rangle}{\langle|S_{hh}|^2\rangle + \langle|S_{vh}|^2\rangle} \tag{5-35}$$

Similarly when a vertically polarized wave is transmitted, the degree of polarization is given by

$$P_v = \frac{\langle|S_{vv}|^2\rangle - \langle|S_{vh}|^2\rangle}{\langle|S_{vv}|^2\rangle + \langle|S_{vh}|^2\rangle} \tag{5-36}$$

If a circularly polarized wave is transmitted, then

$$\|C_s\| = <|S_{hv}|^2> \left[<|S_{vv}|^2> + <|S_{hh}|^2> + 2R_e<S_{vv}S_{hh}^*>\right] + <|S_{vv}|^2><|S_{hh}|^2> - |<S_{vv}S_{hh}^*>|^2 \tag{5-37}$$

and the degree of polarization is given by Equation (5-30).

The above cases were evaluated as a function of incident angle for the scattering characteristic of Figures 5.1 and 5.2. The results are shown in Figure 5.5. It is apparent that the partially polarized character is an important factor when the non-coherent scatterometer equation is appropriately interpreted.

5.5 Visualization of the Polarization Properties of the Antenna and Scene

Within the latter section of Chapter 4 the scatterometer equation accounting for the difference between antenna and surface polarizations was derived. It was shown that the polarization mis-alignment could be characterized by a simple rotation of either orthogonal polarization pair through an angle ψ. To show this mis-alignment character, rather than study the functional behavior of ψ on (θ, ϕ), it is more convenient to fall back on the properties of the spherical polar vectors $\bar{i}_\theta$ and $\bar{i}_\phi$.

Regardless of whether one considers the antenna or surface coordinate system, the projection of the polar vector $\bar{i}_\theta$ and the azimuthal vector $\bar{i}_\phi$ on any sphere whose center is located at the point of observation can be depicted,respectively, by longitudes and latitudes on that sphere. For any line of sight emanating from the origin of the sphere the longitude and latitude lines intersecting the line of sight on the sphere will correspond to the orientation of vertical and horizontal polarization, respectively, for that line of sight. We can therefore employ spheres marked with longitudes and latitudes to visualize the antenna or the surface polarizations.

To compare the alignment between antenna and surface polarizations choose the radii of both polarization spheres so that the spheres are tangent to the scattering surface at the sub-observational point as illustrated in Figures 5.6 and 5.7. A pole of the surface polarization sphere will be afixed to the sub-observational point. This polar axis will correspond to the z axis of Figure 4.4 The xy plane coincides with the equatorial plane and is parallel the surface. The antenna boresight axis lies in the xz plane and points at an angle of θ_o with respect to the z axis (Figure 5.6). Now, on the otherhand, the equatorial plane of the antenna polarization sphere coincides with the

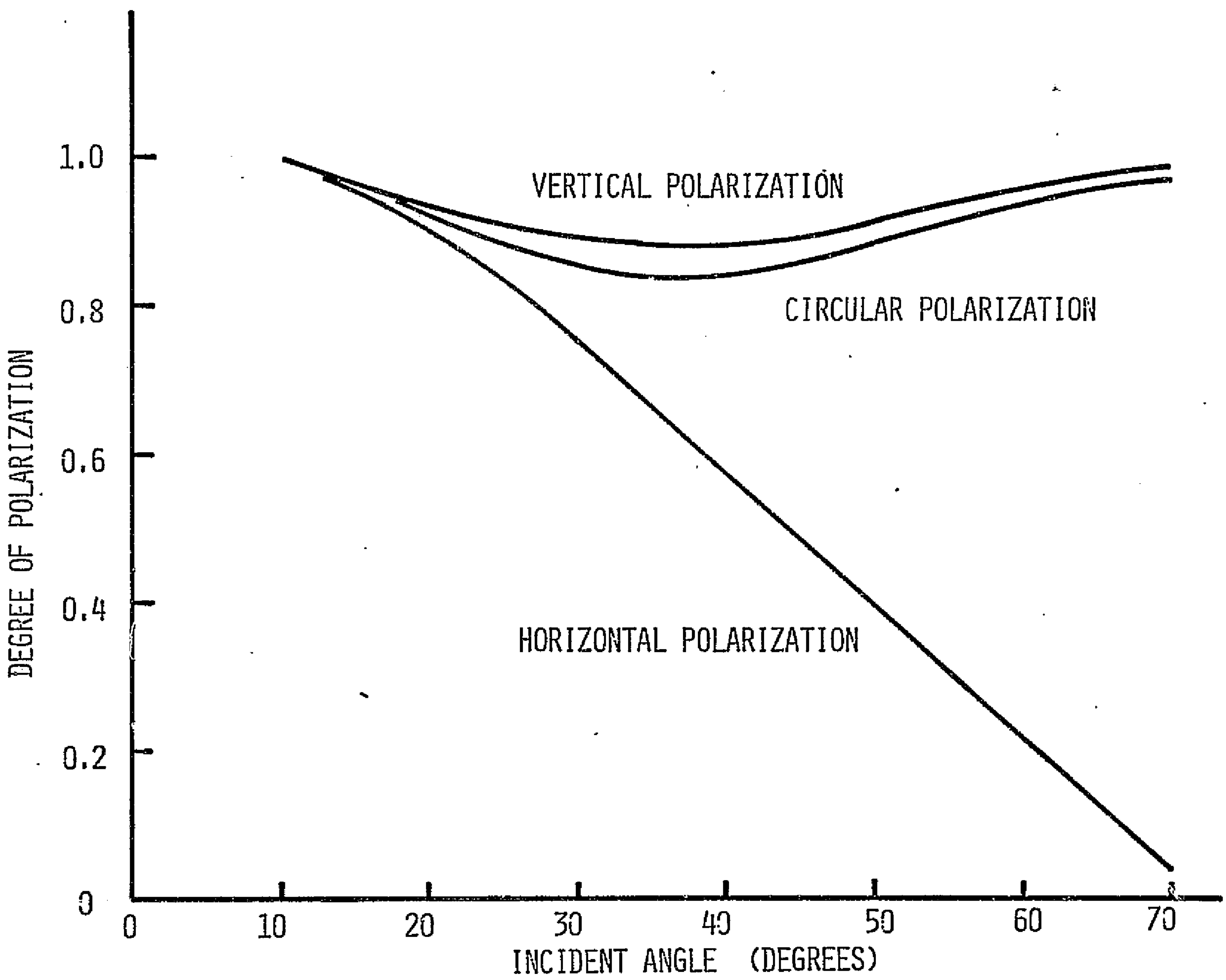

FIGURE 5.5 THE DEGREE OF POLARIZATION BEHAVIOR AS PREDICTED FROM SMALL PERTURBATION THEORY

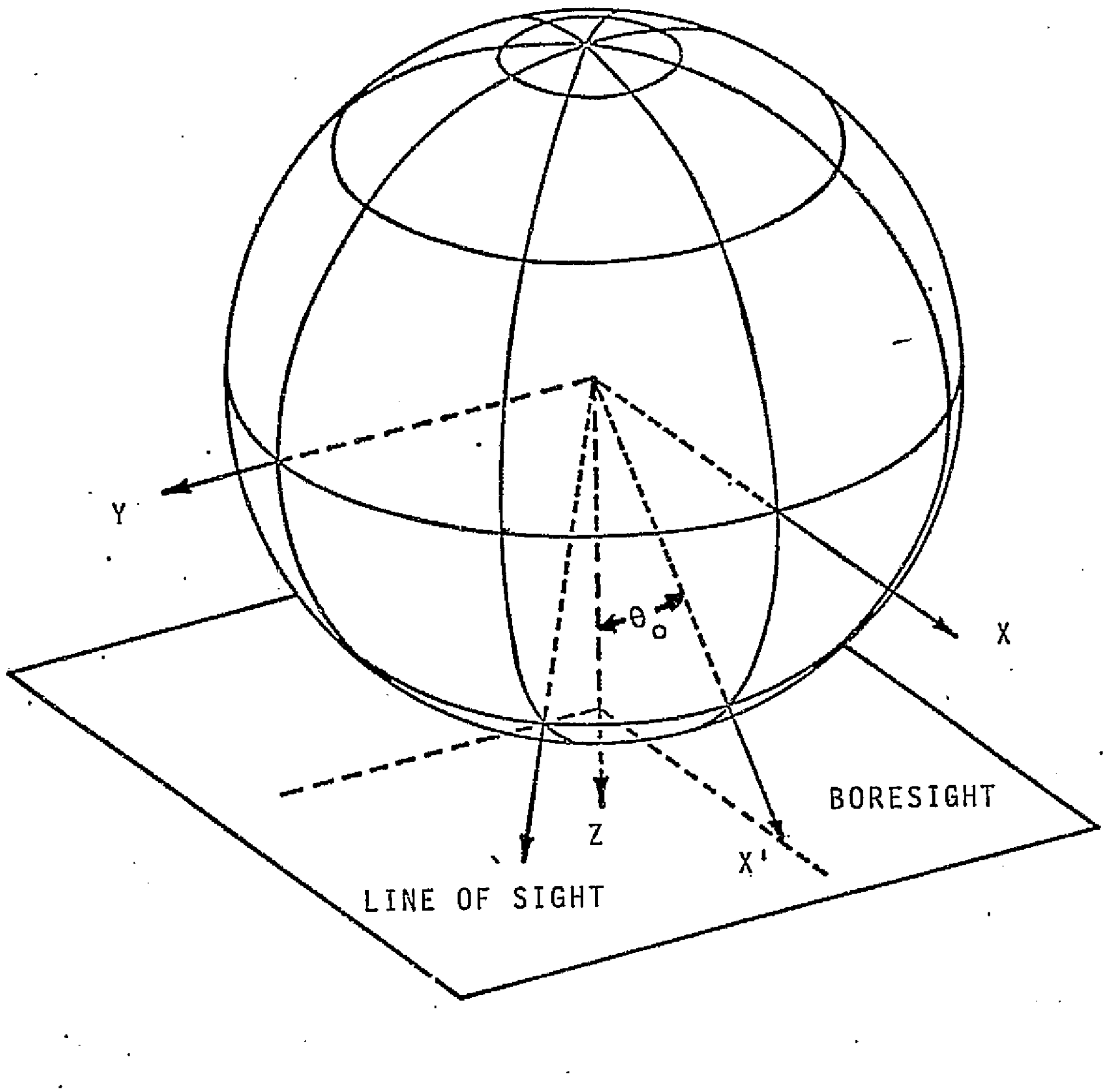

FIGURE 5.6 SURFACE POLARIZATION SPHERE

plane containing the boresight and the y axis. This plane corresponds to the x' y' plane in the antenna coordinate frame (Figure 5.7). The polar axis of antenna polarization sphere aligns with the z' coordinate. Comparison of the orientations of the latitudes and longitudes for any common line of sight will indicate the polarization mis-alignment property (Compare Figures 5.6 and 5.7). Within the plane of observation (the xz or x'z' plane) regardless of view angles the polarizations coincide. For any other line of sight there will be a difference in alignment. The mis-alignment is greatest in the polar regions of the antenna or surface polarization spheres. When the antenna is pointed toward the horizon the alignment is everywhere perfect (one must mentally rotate the sphere in Figure 5.7 so that the x' axis points to the horizon). When the antenna is pointed at the sub-observational point, the misalignment is severe everywhere in the vicinity of the sub-observational point. Within the nadir region the scattering coefficients defined with respect to the surface as compared to those one may define with respect to the antenna differ radically. For example, if a significant anisotropic scattering behavior occurs at nadir, any finite beam scatterometer would tend to integrate this behavior. The measurement, as a consequence, would be difficult to refer to the surface polarizations. The surface polarization character at nadir indicates that infinitesimal beamwidths must be used if the nadir region is to be probed and if scattering coefficients defined with respect to the surface are to be reported. This is clearly true if there is a difference in $<|S_{vv}|^2>$ and $<|S_{hh}|^2>$ scattering properties as viewed with respect to the surface.

As pointed out in Section 4.3, there is an alternate method of mounting the antenna which will produce a different polarization character. Suppose the antenna had been mounted so that its horizontal polarization vector ($\bar{i}_{\phi'}$) on the boresight axis (x') aligned with the surface vertical polarization at that line of sight. The polar axis of the antenna polarization sphere (z') would coincide with the -y axis of the surface coordinate system. The corresponding polarization sphere is illustrated in Figure 5.8. Comparison of the polarization property with that of the surface indicates that the mis-alignment is invariant with view angle and the polarizations do not align globally for any view angle. The polarizations continue to align in the plane of observation; however, the same mis-alignment in the nadir region remains a problem.

Regardless of the mounting position it is evident that for non-zero beamwidth antennas the discrepancy between antenna and surface polarizations prevails in the

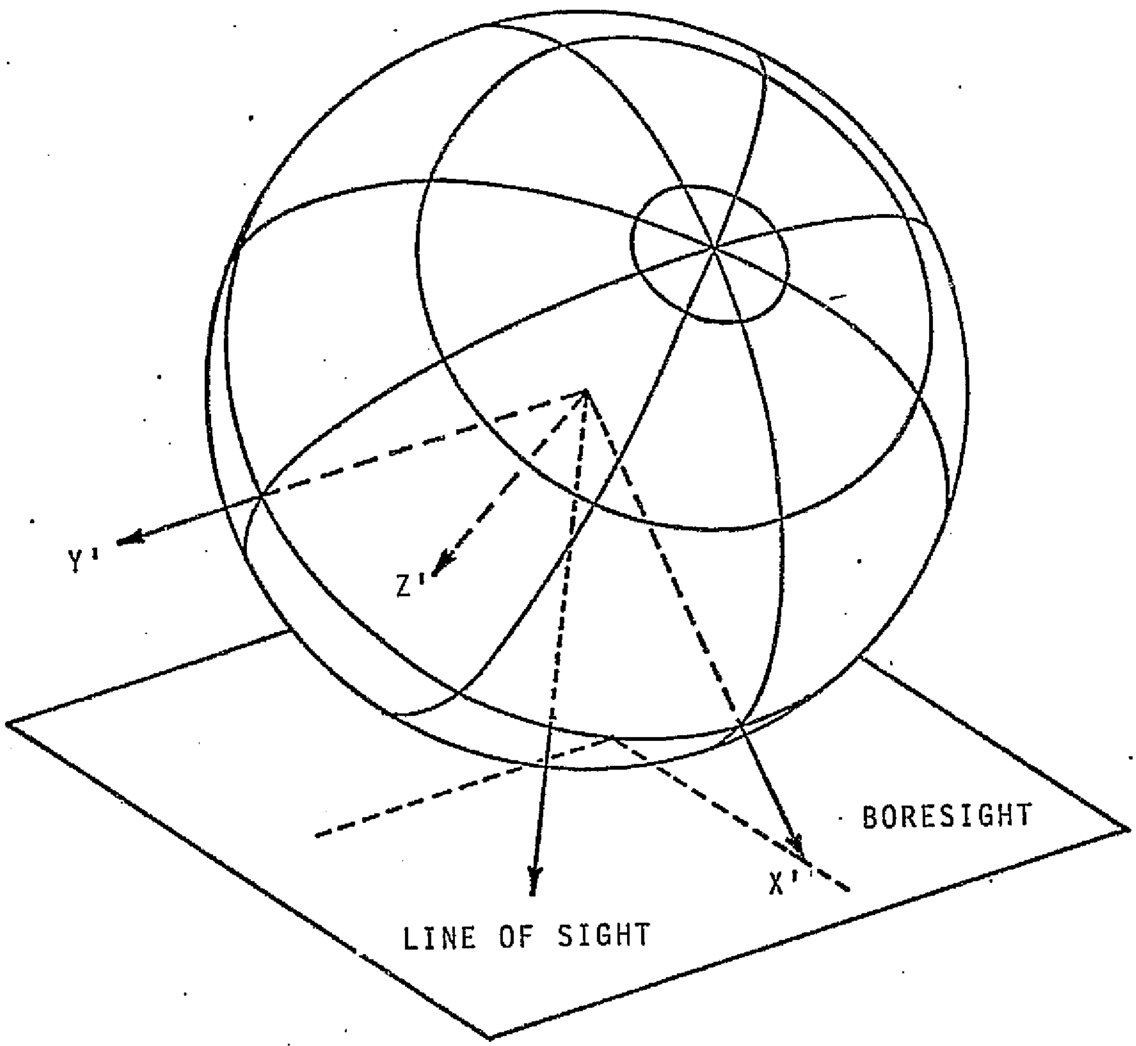

FIGURE 5.7 ANTENNA POLARIZATION SPHERE

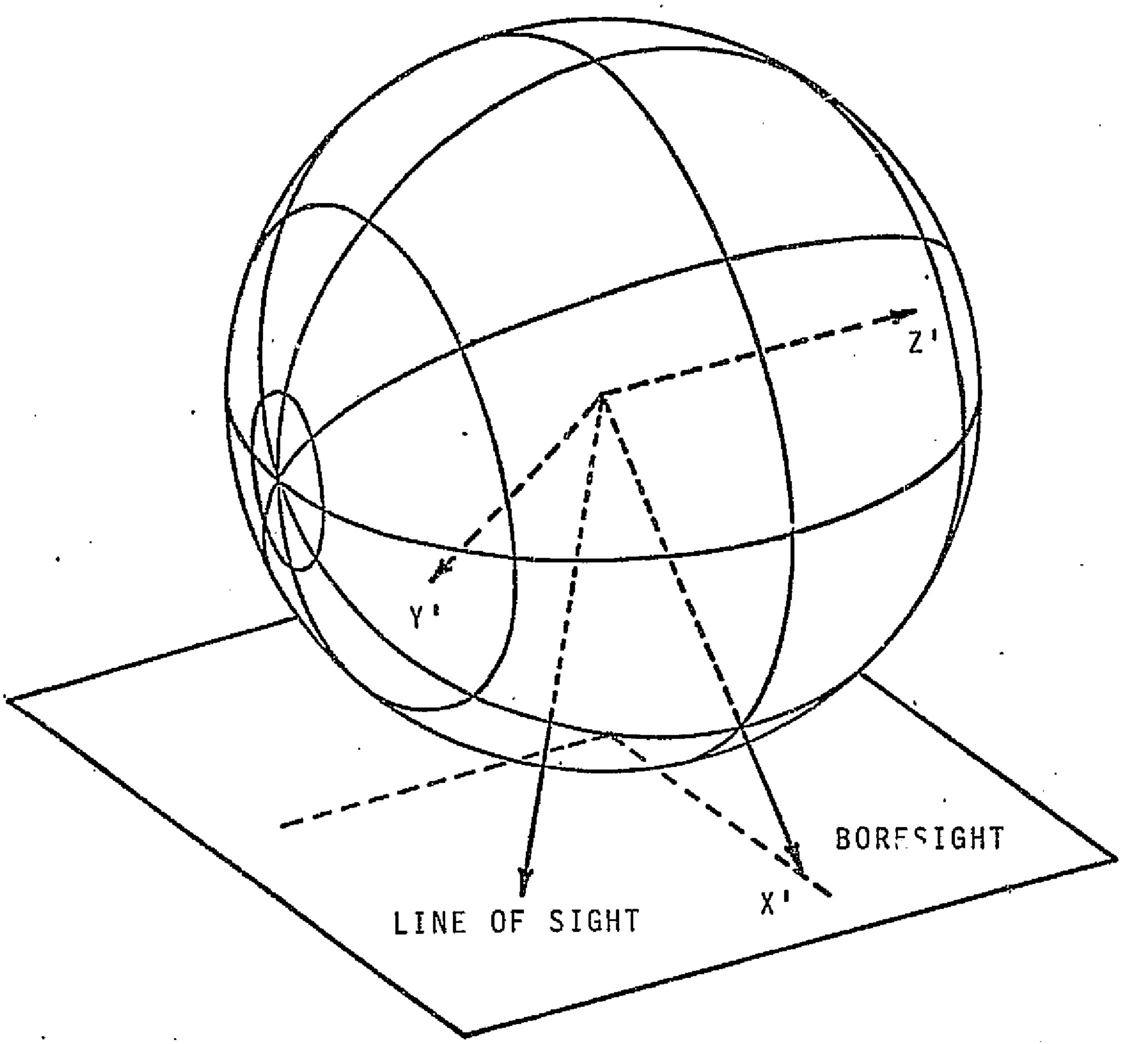

FIGURE 5.8 ALTERNATE ANTENNA POLARIZATION SPHERE

nadir region. It is clear that nadir is a forbidden region when one views it from the point of surface polarizations. At all but small view angles the polarization discrepancy over the main beam of narrow beamwidth antennas is generally small (how small will be shown in Chapter 7). At these angles as the beamwidth becomes narrower for a linearily polarized antenna, the percent antenna power occurring in the orthogonal surface polarization becomes smaller. As one approaches nadir the beamwidth must become increasingly narrower for the same degree of mis-alignment.

6.0 THE INVERSION OF SCATTEROMETER MEASUREMENTS FOR THE SCENE PARAMETERS

6.1 Introduction

The recovery of the scene scattering parameters entails an appropriate set of measurements and the inversion of a corresponding system of scatterometer equations of the type derived in Chapter 4. Within this chapter a measurement and an inversion technique is derived to recover a complete set of scattering coefficients. The technique is also specialized to the case where the scattered fields may be regarded as completely polarized. To assure that the technique is both as simple and as accurate as possible, certain antenna properties are specified. The consequences of not employing a suitably chosen antenna is illustrated in Chaper 7. The mathematical and physical aspects of inverting scatterometer measurements are treated in the following sections. Certain antenna properties which are helpful in approximating the measurements by a system of algebraic equations are identified. In this chapter the distinction between surface and antenna polarization is appropriately discarded to simplify the presentation. The consequence of this action is treated in Chapter 7.

6.2 Mathematical and Physical Aspects

The inversion of scatterometer measurements falls into the same mathematical category as do many remote sensing problems. Typically, the observational relationship reduces to solving a Fredholm integral equation of the first kind, viz.,

$$g(y) = \int K(y,x)\, f(x)dx \tag{6-1}$$

where $K(y,x)$ is usually a continuous function over a rectangular domain attributable to a sensor, $f(x)$ is the unknown sensor stimulus and $g(y)$ is the observed sensor response. The scatterometer equation is a generalization of the above expression. Since there are nine unknown scattering parameters, it is clear that there must be at least nine different kinds of measurements to retrieve all the parameters. If each kind of measurement is identified by a subscript i and if the scattering parameters are denoted by $\xi_j(\Omega)$ where $\Omega = (\theta, \phi)$, then the system of measurements can be written as

$$W_i(\Omega_o) = \left(\frac{\lambda}{4\pi}\right)^2 G_t G_r W_t \int \sum_{j=1}^{9} K_{ij}(\Omega,\Omega_o)\,\xi_j(\Omega)\,d\Omega$$

$$i = 1,2,\ldots,9 \qquad (6\text{-}2)$$

where

$$K_{i1} = (g_{vr}g_{vt})_i/r^2$$

$$K_{i2} = (g_{hr}g_{ht})_i/r^2$$

$$K_{i3} = (g_{vt}g_{hr}+g_{vr}g_{ht}+2\sqrt{g_{vt}g_{ht}g_{vr}g_{hr}}\cos(\beta_t-\beta_r))_i/r^2$$

$$K_{i4} = 2(\sqrt{g_{vt}g_{ht}g_{vr}g_{hr}}\cos(\beta_t+\beta_r))_i/r^2$$

$$K_{i5} = -2(\sqrt{g_{vt}g_{ht}g_{vr}g_{hr}}\cos(\beta_t+\beta_r))_i/r^2$$

$$K_{i6} = 2(g_{vr}\sqrt{g_{vt}g_{ht}}\cos\beta_t+g_{vt}\sqrt{g_{vr}g_{hr}}\cos\beta_r)_i/r^2$$

$$K_{i7} = -2(g_{vr}\sqrt{g_{vt}g_{ht}}\cos\beta_t+g_{vt}\sqrt{g_{vr}g_{hr}}\cos\beta_r)_i/r^2$$

$$K_{i8} = 2(g_{hr}\sqrt{g_{vt}g_{ht}}\cos\beta_t+g_{ht}\sqrt{g_{vr}g_{hr}}\cos\beta_r)_i/r^2$$

$$K_{i9} = -2(g_{hr}\sqrt{g_{vt}g_{ht}}\cos\beta_t+g_{ht}\sqrt{g_{vr}g_{hr}}\cos\beta_r)_i/r^2$$

$$(6\text{-}3)$$

are the kernel functions with respect to an integration on a sphere and where

$$\xi_1 = \langle |S_{vv}|^2 \rangle$$

$$\xi_2 = \langle |S_{hh}|^2 \rangle$$

$$\xi_3 = \langle |S_{vh}|^2 \rangle$$

$$\xi_4 = \mathrm{Re}\ \langle S_{vv} S^*_{hh} \rangle$$

$$\xi_5 = \mathrm{Im}\ \langle S_{vv} S^*_{hh} \rangle$$

$$\xi_6 = \mathrm{Re}\ \langle S_{vv} S^*_{vh} \rangle$$

$$\xi_7 = \mathrm{Im}\ \langle S_{vv} S^*_{vh} \rangle$$

$$\xi_8 = \mathrm{Re}\ \langle S_{vh} S^*_{hh} \rangle$$

$$\xi_9 = \mathrm{Im}\ \langle S_{vh} S^*_{hh} \rangle \tag{6-4}$$

are the unknown scattering parameters. The parameters leading the integral are constants.

For each i one must specify receive and transmit antenna polarization states and patterns such that the resulting system of equations can be solved approximately. There are undoubtedly many such specifications. However, there are certain physical considerations which make the search for the appropriate kernel function (antenna polarizations) simpler.

It has been shown, for example, that in the measurement of a auto-correlation coefficient, the kernel function can be approximated by a delta function if the antenna beam is sufficiently narrow to resolve the angular behavior of the coefficient [38]. The method assumes that the scattering parameter is constant across the significant portion of the kernel function. The unknown parameter is withdrawn from the integral and the resulting integral expression evaluated. The solution then becomes algebraic. This, in effect, is equivalent to assuming that the kernel is a delta function with a weight corresponding to the evaluation of the integral expression. The method is feasible since the kernel function is sharpened by a product of pattern terms as indicated in Equation 6-2. The two-way sharpening effect is illustrated in Figure 6.1 where both g and g^2 are plotted. It should be noted that the ordinate scale has been transformed logarithmically to dB. The kernel function is consequently significant only over a very small domain of $\{(\theta,\phi), \theta \angle \pi, 0 \angle \phi \leq 2\pi\}$.

It would be helpful if the delta function approximation could also be used to recover the cross-correlation scattering paramete . An examination of Equations 6-2 and 6-3 indicates that the two-way sharpening effect is present in the gain functions. However, there is no guarantee that β_t and β_r will remain constant across the significant domain of the gain functions. Generally the antenna phase factors are functions of (θ, ϕ). On the other hand, if these factors are stationary on the main beam, then the delta function approximation can be employed for these parameters also (see Equation 6-6). The ability to realize the stationary condition is treated in the subsequent section.

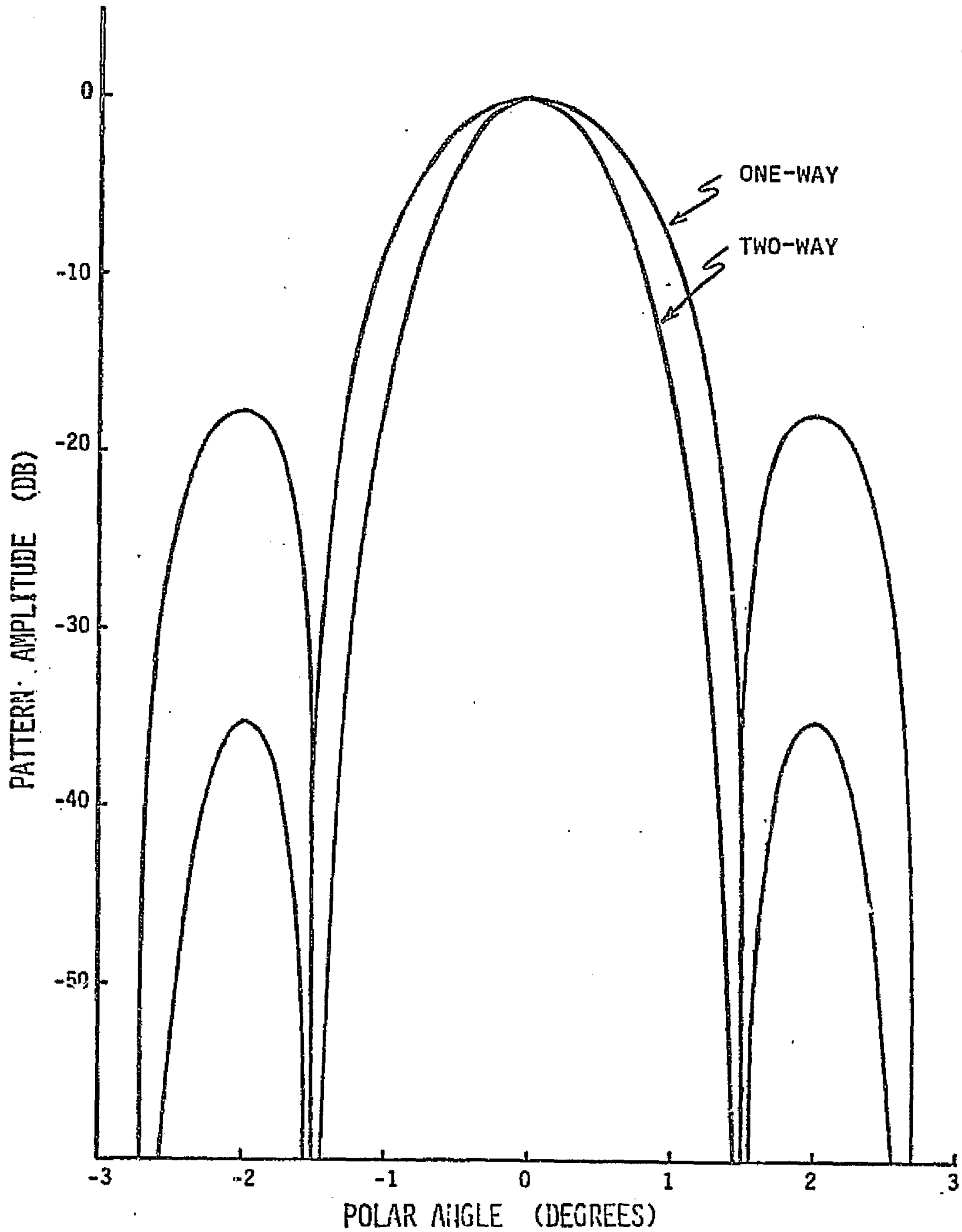

FIGURE 6.1 INCREASED RESOLUTION OF THE KERNEL FUNCTION CAUSED BY THE TWO-WAY SHARPENING OF THE PATTERN

6.3 Desirable Antenna Properties

If the delta function approximation is to be employed, then it is desirable to have the relative phase β_r and β_t constant across the main beam (See Equation (4-29)). This objective is equivalent to requiring that the gain and polarization be stationary across the main beam. Chu and Kouyoumjian [39] have derived the conditions under which stationary gain and polarizations can be achieved. Coincident stationarity, they state, can be realized by any planar aperture distribution which is symmetric with respect to two orthogonal axes in the aperture plane. An aperture is planar only if the excitation lies in the aperture plane and not orthogonal to it.

For some center fed paraboloids the above requirement can be met; however not all feeds result in a planar distribution even though the symmetry property is observed. This is illustrated for the case of a dipole feed. Although the distribution in the aperture plane is symmetric, it contains excitation components orthogonal to the plane. The orthogonal components are induced by the depolarization property of the paraboloid. The far field of such a dish is illustrated in Figure 6.2. The computation was based on a -10 dB taper, a f/D* ratio of 0.36 and a wavelength of 2.16 cm.

The introduction of variable cross polarized content can clearly destroy the stationary polarization requirement. Admittedly the cross-polarized content in the illustrated case is small; however, as will be shown later in Section 7.4, retrieval of the cross-polarized scattering coefficient can be affected by weak cross polarized pattern levels. Furthermore, dipole fed paraboloids with smaller f/D ratios will have a larger cross polarized level than illustrated here [44].

Recently, corrugated horns [40] [41] and dual mode horns [42] [43] with circularly symmetric patterns have been recognized as capable of eliminating cross-polarization in center fed paraboloids. The feed pattern of these horns are said to be balanced. Mathematically their radiation takes the form

$$\bar{E}_f = F(\theta', \phi') \left[\begin{pmatrix} \cos\phi' \\ \sin\phi' \end{pmatrix} \bar{\iota}_{\theta'} \mp \begin{pmatrix} \sin\phi' \\ \cos\phi' \end{pmatrix} \bar{\iota}_{\phi'} \right] \frac{\exp(-ik\rho')}{\rho'} \quad (6\text{-}5)$$

where the z' axis is directed along the axis of the paraboloid. Chu and Turrin [59] have shown that center fed paraboloids with balanced illumination exhibit no cross-polarized content in the aperture plane. The far-fields of the above described para-

* focal length ÷ paraboloid diameter

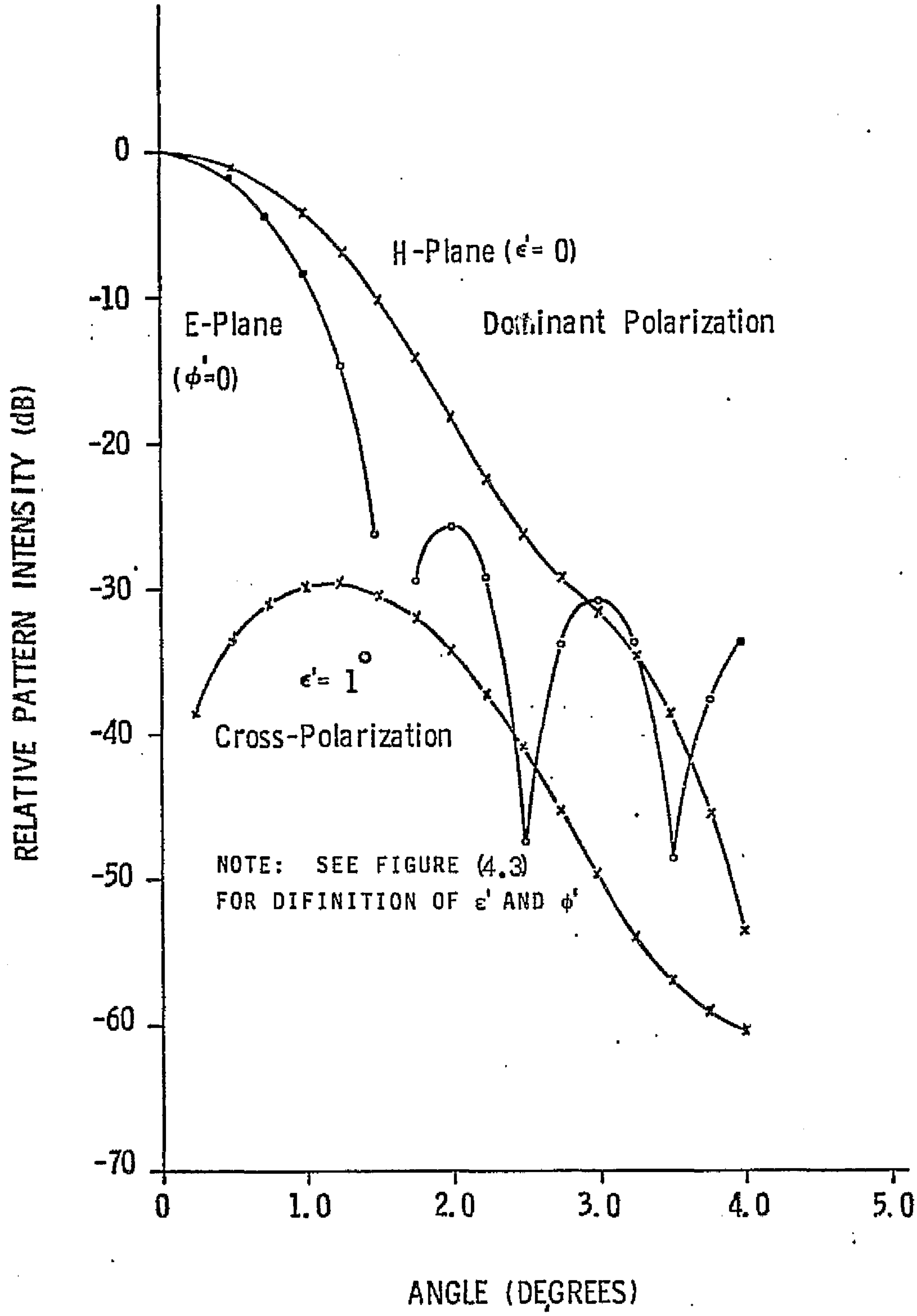

FIGURE 6.2 FAR FIELDS OF A PARABOLOID WITH A DIPOLE FEED

boloid with a balanced feed was computed and are shown in Figure 6.3. The cross-polarized field was totally absent in the numerical computations.

Balanced fed paraboloids are suitable candidates for scatterometry work when a complete set of scene parameters are desired. Since support struts and aperture blockage, in general, introduce cross-polarized radiation it is important to minimize blockage in addition to choosing an appropriate feed. The Cutler type feed with balance radiation may be a suitable approach.

Alternatively, an array of broadly directional radiators is also a suitable candidate. If the interaction between elements is weak, then the pattern of the array is the product of the array factor and the pattern of one of the elements. The polarization property in the main lobe will be dictated by the polarization property of the central segment of the elementary pattern. The polarization will generally be stationary across a small segment of the elementary pattern; and, therefore, the array polarization will also be stationary there.

6.4 The Inversion of Scatterometer Measurements

When a narrow beam scatterometer antenna with a coincident stationary gain and polarization property is employed, the scatterometer equation may be approximated by*

$$W_{tr}(\Omega_0) = K\Big\{ I_1 \langle |S_{vv}|^2 \rangle + I_2 \langle |S_{hh}|^2 \rangle + [\, I_3 + 2I_4 \cos(\beta_r - \beta_t)\,] \langle |S_{vh}|^2 \rangle +$$

$$2I_4 \,\mathrm{Re}\,[\, e^{i(\beta_t + \beta_r)} \langle S_{vv} S_{hh}^* \rangle] + 2\mathrm{Re}[\, I_5 e^{j\beta_t} + I_6\, e^{j\beta_r}\,] \langle S_{vv} S_{hv}^* \rangle +$$

$$2\mathrm{Re}[\, I_7\, e^{j\beta_t} + I_8\, e^{j\beta_r}\,] \langle S_{vh} S_{hh}^* \rangle \Big\} \qquad (6\text{-}6)$$

where

* The degree of accuracy will be demonstrated in Chapter 7.

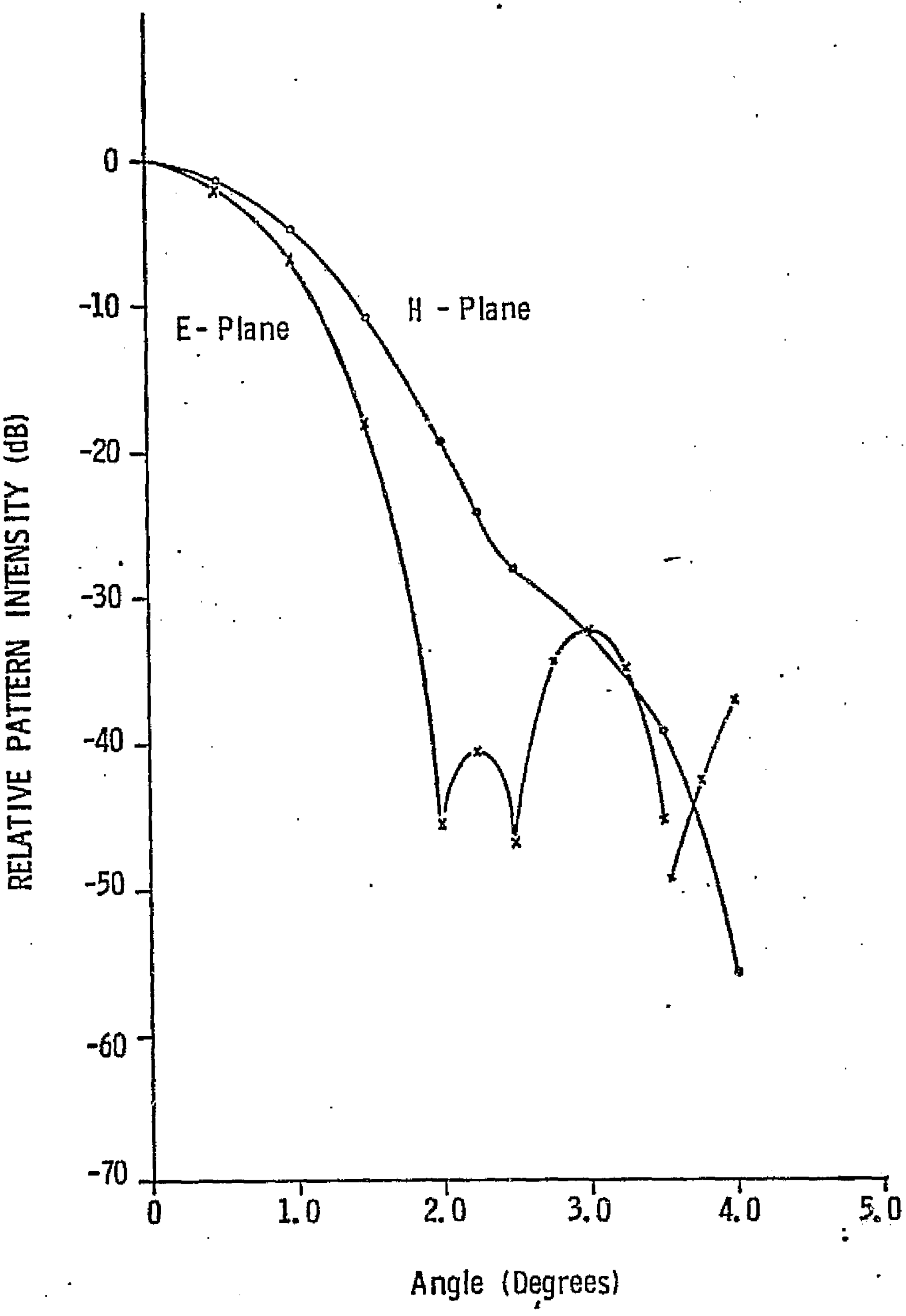

FIGURE 6.3 FAR FIELDS OF A PARABOLOID WITH A BALANCED FEED

$$I_1 = \iint g_{vt} g_{vr} \cos^2\theta \, d\Omega$$

$$I_2 = \iint g_{ht} g_{hr} \cos^2\theta \, d\Omega$$

$$I_3 = \iint (g_{ht} g_{vr} + g_{vt} g_{hr}) \cos^2\theta \, d\Omega$$

$$I_4 = \iint \sqrt{g_{vt} g_{ht}} \sqrt{g_{vr} g_{hr}} \cos^2\theta \, d\Omega$$

$$I_5 = \iint \sqrt{g_{vt} g_{ht}} \, g_{vr} \cos^2\theta \, d\Omega \qquad (6\text{-}7)$$

$$I_6 = \iint g_{vt} \sqrt{g_{vr} g_{hr}} \cos^2\theta \, d\Omega$$

$$I_7 = \iint \sqrt{g_{vt} g_{ht}} \, g_{hr} \cos^2\theta \, d\Omega$$

$$I_8 = \iint g_{ht} \sqrt{g_{vr} g_{hr}} \cos^2\theta \, d\Omega$$

$$K = \lambda^2 W_t G_t G_r / (4\pi z)^2 \qquad (6\text{-}8)$$

It has been assumed that observations are conducted over a planar earth so that $r = z/\cos\theta$. It has also been assumed that the kernel function has sufficient resolution that the scattering coefficient may be considered constant in the domain where the kernel function is significant. Now suppose that the scatterometer is equipped with a dual linearily polarized feed or if necessary two antenna with orthogonal linear polarizations to assure good isolation. The amplitude and phase of each feed channel is assumed controllable. Then as will be shown below, a series of fifteen intensity measurements with different polarization combinations is capable of extracting a complete set of nine scattering parameters, viz.,

$<|S_{vv}|^2>$, $<|S_{hh}|^2>$, $<|S_{vh}|^2>$, $Re <S_{vv}S_{hh}^*>$, $Im <S_{vv}S_{hh}^*>$, $Re <S_{vv}S_{hv}^*>$, $Im <S_{vv}S_{hv}^*>$, $Re <S_{vh}S_{hh}^*>$, and $Im <S_{vh}S_{hh}^*>$. A pair of measurements is required to isolate the real or imaginary part of the complex valued coefficients. The transmit-receive polarization states are indicated for each measurement:

1) VV $\quad (g_{vt} = g_{vr} = g,\ g_{ht} = g_{hr} = 0)$

$$W_{tr} = KI <|S_{vv}|^2> \tag{6-9a}$$

2) H-H $\quad (g_{vt} = g_{vr} = 0,\ g_{ht} = g_{hr} = g)$

$$W_{tr} = KI <|S_{hh}|^2> \tag{6-9b}$$

3) V-H $\quad (g_{vt} = g_{hr} = g,\ g_{ht} = g_{vr} = 0)$

$$W_{tr} = KI <|S_{vh}|^2> \tag{6-9c}$$

4a) LC-RC $\quad (g_{vt} = g_{ht} = g_{vr} = g_{hr} = \frac{1}{2} g,\ \beta_t = -90°,\ \beta_r = 90°)$

$$W_{tr} = KI \left[\frac{1}{4} <|S_{vv}|^2> + \frac{1}{4} <|S_{hh}|^2> + \frac{1}{2} Re <S_{vv}S_{hh}^*>\right] \tag{6-9d}$$

4b) Cross-Linear $(g_{vt} = g_{ht} = g_{vr} = g_{hr} = \frac{1}{2} g,\ \beta_t = 0,\ \beta_r = 180°)$

$$W_{tr} = KI \left[\frac{1}{4} <|S_{vv}|^2> + \frac{1}{4} <|S_{hh}|^2> - \frac{1}{2} Re <S_{vv}S_{hh}^*>\right] \tag{6-9e}$$

5a) Elliptical ($g_{vt} = g_{ht} = g_{vr} = g_{hr} = \frac{1}{2} g$, $\beta_t = -45°$, $\beta_r = 135°$)

$$W_{tr} = KI \left[\frac{1}{4} <|S_{vv}|^2> + \frac{1}{4} <|S_{hh}|^2> + \frac{1}{2} \mathrm{Im} <S_{vv} S_{hh}^*> \right] \tag{6-9f}$$

5c) Elliptical ($g_{vt} = g_{ht} = g_{vr} = g_{hr} = \frac{1}{2} g$, $\beta_t = 45°$, $\beta_r = -135°$)

$$W_{tr} = KI \left[\frac{1}{4} <|S_{vv}|^2> + \frac{1}{4} <|S_{hh}|^2> - \frac{1}{2} \mathrm{Im} <S_{vv} S_{hh}^*> \right] \tag{6-9g}$$

6a) V- Diagonal Linear ($g_{vt} = g$, $g_{ht} = 0$, $g_{vr} = g_{hr} = \frac{1}{2} g$, $\beta_r = 0$)

$$W_{tr} = KI \left[\frac{1}{2} <|S_{vv}|^2> + \frac{1}{2} <|S_{vh}|^2> + \mathrm{Re} <S_{vv} S_{hv}^*> \right] \tag{6-9h}$$

6b) V- Diagonal Linear ($g_{vt} = g$, $g_{ht} = 0$, $g_{vr} = g_{hr} = \frac{1}{2} g$, $\beta_r = 180°$)

$$W_{tr} = KI \left[\frac{1}{2} <|S_{vv}|^2> + \frac{1}{2} <|S_{vh}|^2> - \mathrm{Re} <S_{vv} S_{hv}^*> \right] \tag{6-9i}$$

7a) V-RC ($g_{vt} = g$, $g_{ht} = 0$, $g_{vr} = g_{hr} = \frac{1}{2} g$, $\beta_r = 90°$)

$$W_{tr} = KI \left[\frac{1}{2} <|S_{vv}|^2> + \frac{1}{2} <|S_{vh}|^2> + \mathrm{Im} <S_{vv} S_{hv}^*> \right] \tag{6-9j}$$

7b) V-LC ($g_{vt} = g$, $g_{ht} = 0$, $g_{vr} = g_{hr} = \frac{1}{2} g$, $\beta_r = -90°$)

$$W_{tr} = KI \left[\frac{1}{2} <|S_{vv}|^2> + \frac{1}{2} <|S_{vh}|^2> - \mathrm{Im} <S_{vv} S_{hv}^*> \right] \tag{6-9k}$$

8a) H- Diagonal Linear ($g_{vt} = 0$, $g_{ht} = g$, $g_{vr} = g_{hr} = \frac{1}{2} g$, $\beta_r = 0$)

$$W_{tr} = KI \left[\frac{1}{2} <|S_{hh}|^2> + \frac{1}{2} <|S_{vh}|^2> + \mathrm{Re} <S_{vh} S_{hh}^*> \right] \tag{6-9l}$$

8b) H- Diagonal Linear ($g_{vt} = 0$, $g_{ht} = g$, $g_{vr} = g_{hr} = \frac{1}{2} g$, $\beta_r = 180°$)

$$W_{tr} = KI \left[\frac{1}{2} <|S_{hh}|^2> + \frac{1}{2} <|S_{vh}|^2> - \mathrm{Re} <S_{vh} S_{hh}^*> \right] \tag{6-9m}$$

9a) H-RC $\quad (g_{vt} = 0,\ g_{ht} = g,\ g_{vr} = g_{hr} = \frac{1}{2} g,\ \beta_r = 90^\circ)$

$$W_{tr} = KI \left[\frac{1}{2} < |S_{hh}|^2 > + \frac{1}{2} < |S_{vh}|^2 > + \operatorname{Im} < S_{vh} S_{hh}^* > \right] \qquad (6\text{-}9n)$$

9b) H-LC $\quad (g_{vt} = 0,\ g_{ht} = g,\ g_{vr} = g_{hr} = \frac{1}{2} g,\ \beta_r = -90^\circ)$

$$W_{tr} = KI \left[\frac{1}{2} < |S_{hh}|^2 > + \frac{1}{2} < |S_{vh}|^2 > - \operatorname{Im} < S_{vh} S_{hh}^* > \right] \qquad (6\text{-}9o)$$

where

$$I = \iint g^2 \cos^2\theta \, d\Omega \qquad (6\text{-}10)$$

The transmit and receive polarizations may be interchanged without affecting the above equations. The above set of equations assumes that the scattering coefficients are defined with respect to the antenna frame. As will be shown for narrow beam antenna, the above polarization states will retrieve scattering coefficients defined with respect to the surface at all but very small incident angles. The above polarization states may be incorporated in the equations which distinguish surface and antenna polarizations to develop an inversion technique based on the distinction. These equations are developed in the succeeding chapter.

From the above set of equations it is noted that $<|S_{vv}|^2>$, $<|S_{hh}|^2>$ and $<|S_{vh}|^2>$ are each derived from a single measurement i.e. measurements (1), (2), and (3), respectively. The remaining parameters are isolated by differencing pairs of equations. It is clear that if a complete set of scattering parameters is desired, the measurement set is over-specified. If a minimal set of equations is required, then all measurement pairs can be reduced to one of the members. It is advisable, however, to work with an over-specified set of measurements to reduce the sensitivity to measurement errors if all the coefficients are desired. It is a distinct advantage to specify equation pairs if a particular complex valued coefficient is to be isolated. The above technique does not pre-suppose that the scattered fields are completely polarized.

If one further assumes that the scattered fields are completely polarized, then the inversion problem reduces to that for non-statistical targets. Various measurement schemes have been reviewed for this case by Huynen [21]. One of these schemes is based on field amplitude and phase measurements of a pair of orthogonal returns from each of the two orthogonal illuminating polarizations. Another scheme involves amplitude measurements at different polarizations. The latter technique yields a set of target invariant parameters which must be transformed to a scattering matrix. Intensity measurements as described above will, of course, also work. The set of measurements may be solved subject to the constraints

$$
\begin{aligned}
|\langle S_{vv} S_{hh}^{*} \rangle| &= \sqrt{\langle |S_{vv}|^2 \rangle \langle |S_{hh}|^2 \rangle} \\
|\langle S_{vv} S_{vh}^{*} \rangle| &= \sqrt{\langle |S_{vv}|^2 \rangle \langle |S_{vh}|^2 \rangle} \qquad (6\text{-}11) \\
|\langle S_{hv} S_{hh}^{*} \rangle| &= \sqrt{\langle |S_{hv}|^2 \rangle \langle |S_{hh}|^2 \rangle}
\end{aligned}
$$

for additional accuracy. Non-linear regression techniques as described in reference [45] or [46] may be employed to solve the system of measurements subject to these constraints.

In retrospect one can also use correlation and cross-correlation techniques to isolate some of the non-coherent scattering coefficients. For example to measure $\langle S_{vv} S_{hv}^{*} \rangle$, e_{vt} is transmitted. During reception both e_{vs} and e_{hs} are cross-correlated without and with 90° phase shift injected into one of the channels to isolate the real and imaginary parts, respectively.

Either correlation techniques or intensity techniques as proposed will suffer from poor realizations of the desired antenna properties. Since intensity measurements are commonly made, this investigation will restrict its attention to the intensity technique.

7.0 PRACTICAL CONSIDERATIONS IN RETRIEVING THE SCATTERING COEFFICIENTS

7.1 Introduction

In attempting to retrieve the scattering coefficients by the method developed in Chapter 6, one is immediately confronted with the fact that the ideal antenna polarization states specified in each measurement are seldom achieved in practice. To determine the sensitivity of the measurement to deviations from these ideal states, computer simulations were conducted. Measurements were simulated on the basis of the complete scatterometer equation as developed in Chapter 4 and a scattering characteristic similar to that of the sea under low wind conditions. The scattering coefficients were expressed with respect to the surface polarizations; and, consequently, all simulated power returns involve transforming the pattern information to the surface polarization states to compute accurate power returns. Measurements were computed based on known deviations from the ideal antenna polarization requirements and were inverted on the basis of the ideal antenna specifications. The sensitivity in retrieving each coefficient was thus established, namely, by comparing the actual coefficient with the estimated coefficient.

The computer simulation was designed not only to determine the sensitivity of the measurement to non-ideal antenna polarization states, but was designed to establish the beamwidth limitation to realize the delta function approximation for the integrand in the scatterometer equation. It was also designed to determine whether the distinction between surface polarizations and antenna polarization is important; and if so, under what conditions it is important.

Within the latter portion of this chapter special consideration is given to the sampling requirements when measuring an antenna pattern. The simulations described above were based on idealized functional representations for antenna patterns. In reality these ideal symmetric representations are seldom achieved (See Figures 6.2 and 6.3, for examples of non-symmetric patterns). As a consequence, to accurately specify the scatterometer integrand recourse to pattern measurements is necessary. The latter section of this chapter develops the theory which specifies the density of points at which the pattern must be measured to uniquely represent the pattern. This section of the chapter is important in numerically evaluating the inversion parameters in the scatterometer equation.

7.2 Description of the Scatterometer Simulation Program

The reader will recall that the inversion technique developed in Chapter 6 was derived without regard to the distinction between surface and antenna polarizations. As a consequence to compute the return power accurately from scattering coefficients defined with respect to the surface polarizations, the scatterometer simulation program was specifically designed to compute the return power on the basis of Equation (4-50) of Chapter 4 rather than Equation (4-29), i.e., with the pattern transformation included. For an antenna pattern and a view angle selected externally to the program, the exact return power is computed for all fifteen measurements described in Chapter 6.

The inversion of the resulting measurements is performed in two ways. In the first method, called the approximate method, the inversion is performed without regard to the distinction between antenna and surface polarizations. It is (erroneously) assumed, as in Chapter 6, that the scattering coefficients are expressed in the antenna coordinate system. Equation (6-19) served as the inversion model. Since the return power was computed on the basis of the difference between surface and antenna polarization and the inversion was performed without regard to the difference, the distinction between surface and antenna polarizations could be evaluated. The second method, called the exact method, does not ignore the difference between antenna and surface polarizations. The inversion is based on antenna weights that are computed by transforming the pattern polarization states to the surface polarization states for each of the fifteen measurements. The transformation, in general, "excites" additional scattering coefficients above those recognized in the approximate method (See, for example, Equation (4-49).)

A delta function approximation was also employed in the matrix inversion model. The model was based on an approximation of Equation (4-47) and takes the form

$$W_{tr} = \lambda^2 G_t G_r W_t/(4\pi z)^2 \Big\{ \langle|S_{vv}|^2\rangle \int I_1 \cos\Theta^2 d\Omega +$$

$$\langle|S_{hh}|^2\rangle \int I_2 \cos\Theta^2 d\Omega + \langle|S_{vh}|^2\rangle \int I_3 \cos\Theta^2 d\Omega + \ldots$$

$$2\mathrm{Re}\langle S_{vv}S^*_{hh}\rangle \int I_4 \cos\Theta^2 d\Omega \;-\; 2\mathrm{Im}\langle S_{vv}S^*_{hh}\rangle \int I_5 \cos\Theta^2 d\Omega \;+$$

$$2\mathrm{Re}\langle S_{vv}S^*_{vh}\rangle \int I_6 \cos\Theta^2 d\Omega \;-\; 2\mathrm{Im}\langle S_{vv}S^*_{vh}\rangle \int I_7 \cos\Theta^2 d\Omega \;+$$

$$2\mathrm{Re}\langle S_{hv}S^*_{hh}\rangle \int I_8 \cos\Theta^2 d\Omega \;-\; \mathrm{Im}\langle S_{hv}S^*_{hh}\rangle \int I_9 \cos\Theta^2 d\Omega \Big\} \tag{7-1}$$

where the Is are defined in Equations (4-50). The resulting fifteen equations are employed in a least squares estimation technique to recover the scattering coefficients. The matrix technique was developed to test whether the fifteen measurements were sufficient to invert for the coefficients when the difference in polarizations is recognized.

In addition to specifying the choice of antenna view angle, the program user may, through the use of the input control card, introduce cross pattern amplitude bias and relative phase bias into those measurements employing vertically or horizontally polarized transmissions or receptions. The return power is accurately computed for all fifteen measurements with the biases included. The inversions, both approximate and exact methods, are performed, however, without regard to the biases, i.e., they are based on ideal antenna states. The sensitivity of the inversions to pattern deviations from ideal conditions could thus be studied.

Cross pattern amplitude and phase biases have precise meanings for vertically and horizontally polarized transmissions or receptions. However, for those measurements requiring simulationeous vertically polarized and horizontally polarized patterns (eg., LC, RC, linear $\pm$ 45°*), it was more meaningful to conduct Monte Carlo studies on amplitude and phase. This technique requires many simulations to be conducted. Each simulation is based on a different set of deviations in amplitude and/or in phase. First and second order error statistics are accumulated from all the experiments conducted in this fashion. In the measurements requiring simultaneous cross patterns, it is evident from Chapter 6 that balanced patterns are required, i.e.,

* Assuming the antenna is not simply rotated.

$g_v = g_h = 1/2g$. So it was appropriate to specify the pattern amplitude perturbation in the Monte Carlo studies as a deviation from a balanced condition. For each experiment the amplitude and phase are randomly perturbed within bounds specified by the user. The deviations are based on samples from a uniform distribution so that the perturbed gain and phase satisfy

$$\begin{aligned} g_h' &= 1/2g_h + A\rho_g \\ g_v' &= 1 - g_h' \\ \beta' &= \beta + B\rho_\beta \end{aligned} \tag{7-2}$$

where $A < 1/2$, $0 < \beta < \pi$ and ρ_g and ρ_β are random samples from a population distributed uniformly over $[-1, 1]$. $1/2g_h$ and β are the ideal gain and phase requirements. Both approximate and exact inversions are performed for each experiment. The error statistics are formed independently for each. The above studies are initiated by specifying 2A and 2B on the input control card.

This program allows the selection of one of four symmetric antenna patterns. For any selection it is assumed that both dominant and cross patterns have identical functional forms. The relative phase between the patterns (if both exist) was assumed stationary. When amplitude error is introduced into any one of the fifteen measurements, the deviation is applied so that the normalized gains satisfy $g_v(0) + g_h(0) = 1$ on the boresight axis. The specific pattern options are given by the following functions:

$$\begin{aligned} p_1 &= (\sin x/x)^2 \\ p_2 &= (J_1(x)/x)^2 \\ p_3 &= \left(\frac{3}{x^2}\left(\frac{\sin x}{x} - \cos x\right)\right)^2 \\ p_4 &= \frac{J_2(x)}{x^2} \end{aligned} \tag{7-3}$$

where

$$x = ka \sin\theta'$$
$$a = \text{aperture radius}$$
$$k = 2\pi/\lambda$$

The above pattern functions correspond to one-way patterns having respective side lobe levels of -13.2, -17.6, -20.6 and -24.6 dB. In addition to providing a choice in pattern functions, the program requires an input parameter denoted as ka to control the beamwidth. The beamwidth for the respective patterns are related to ka by the following expressions:

$$
\begin{aligned}
\Delta\theta_1 &= 0.88\,\pi/ka \\
\Delta\theta_2 &= 1.02\,\pi/ka \\
\Delta\theta_3 &= 1.15\,\pi/ka \\
\Delta\theta_4 &= 1.27\,\pi/ka
\end{aligned}
\tag{7-4}
$$

For a fuller understanding of the pattern functions the reader is referred to pages 9.14-9.21 of reference [5].

The scattering characteristics on which the simulations were conducted are illustrated in Figure 7.1. The coefficients except for the real and imaginary parts of $< S_{vv} S_{hv}^* >$ are based on theoretical results reported in reference [10]. The magnitude of $< S_{vv} S_{hh}^* >$ was set at the geometric mean of $<|S_{vv}|^2>$ and $<|S_{hh}|^2>$ in accordance with the results of Chapter 5. The phase characteristic of $< S_{vv} S_{hh}^* >$ was assigned to be that for small perturbation theory for a sea water temperature of 293°. The characteristics are similar to that of the sea under low wind conditions. In accordance with small perturbation theory the coefficients $< S_{vv} S_{hv}^* >$ and $< S_{vh} S_{hh}^* >$ are extremely small. For the sake of the simulations weak but identical characteristics were arbitrarily assigned to the real and imaginary parts of these coefficients. All characteristics were assumed isotropic.

For a complete description of the scatterometer simulation program the reader is referred to Appendix D.

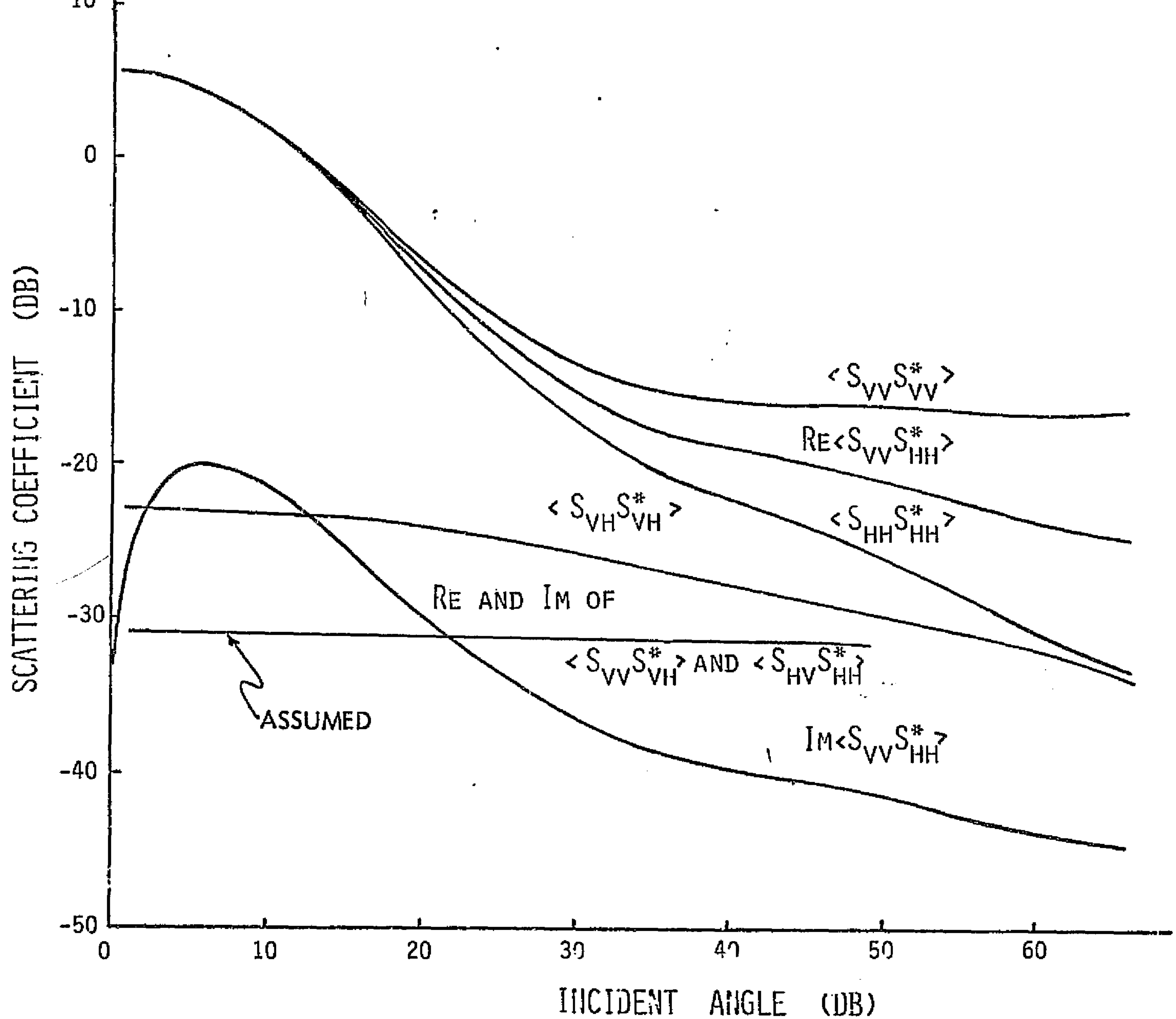

FIGURE 7.1 SCATTERING CHARACTERISTICS EMPLOYED IN THE SIMULATION

7.3 Resolution Requirement

7.3.1 General

Angular resolution in scatterometry has been achieved either by employing a narrow beam or by doppler filtering or by a combination of both. Angular resolution is clearly required to search the scattering characteristic. It is also required to realize the delta function approximation in the inversion technique. It has been common practice to specify the resolution on the basis of some notion of the scattering characteristic. However, when the difference between surface and antenna polarizations is an important consideration, a resolution guideline can also be established to assure that the antenna polarization coincides with the surface polarization over the significant portion of the beam. An expression is developed showing the percent power incident on the surface in the orthogonal surface polarization for an antenna whose polarization is pure with respect to the antenna frame. The results can be interpreted in terms of resolution (beamwidth).

Resolution requirements are also established for the assumed scattering characteristics by employing the simulation program. The result expresses the measurement accuracy achieved by the delta function approximation with ideal antenna polarization specifications.

7.3.2 Polarization Decomposition of the Incident Beam

Suppose a scatterometer transmits a horizontally polarized wave $E_{\phi'}$ when pointed in direction θ_o. The total power incident on the surface is given by

$$P = \frac{1}{2Z_o} \int |E_{\phi'}|^2 \, d\Omega \qquad (7\text{-}5)$$

When $E_{\phi'}$ is decomposed into orthogonal surface components, the above expressions can be written by

$$P = \frac{1}{2Z_o} \int |E_{\phi'}|^2 \left[|i_\theta \cdot i_{\phi'}|^2 + |i_\phi \cdot i_{\phi'}|^2 \right] d\Omega \qquad (7\text{-}6)$$

The percent power appearing in the orthogonal surface polarization is given by

$$\left(\frac{P_\theta}{P}\right)\% = 100 \int \frac{|E_{\phi'}|^2 \, |i_\theta \cdot i_{\phi'}|^2}{P} \, d\Omega \qquad (7\text{-}7)$$

or

$$\left(\frac{P_\theta}{P}\right)\% = 100\left[1 - \int \frac{|E_\phi|^2 \;|i_\phi \cdot i_{\phi'}|^2}{P}\, d\Omega\right] \tag{7-8}$$

The latter expression is simpler to evaluate numerically.

The above expression was evaluated as a function of view-angle for various beamwidths. A Jinc pattern function was employed in the computation. The results of the evaluation are shown in the graphs of Figure 7.2. The polarization mis-match as anticipated from Chapter 5 is greatest at nadir regardless of beamwidth. It is evident that small beamwidths are able to probe closer to nadir without introducing significant orthogonally polarized components. The permissable level of orthogonal polarization will be treated in a subsequent section. Although the above results were based on a horizontally polarized incident wave, a similar result could have been computed for a vertically polarized incident wave.

If one chooses to avoid transforming the pattern polarization states to the surface and accurate measurements of the surface scattering coefficient are desired near nadir, then the graphs of Figure 7.2 are helpful in choosing the proper beamwidth. If the experiment requires that the cross polarized content be less than, say, -20 dB, then the 1% ordinant will specify how close one can probe nadir with various beamwidths.

An alternative to the above procedure is to employ the exact inversion model based on the differences between antenna and surface polarizations. The delta function accuracy of this technique for small angles is developed in the succeeding section.

7.3.3 An Evaluation of the Delta Function Approximation

To determine the beamwidth (resolution) requirement to realize the delta function approximation, scatterometer simulations were conducted in the vicinity of nadir where angular resolution is required to search the rapidly varying scattering characteristics. The ability of the delta function approximation to retrieve each scattering coefficient was established at incident angles of 0°, 4° and 8°. Beamwidths from 1 degree to 12 degrees were considered. The results are illustrated in the graphs of Figures 7.3 and Figures 7.5 through 7.8 for both the approximate and exact methods.

The performance of the delta function approximation at nadir is shown in Figure 7.3 for the approximate method. It is evident that there is little difficulty in retrieving $\langle S_{vv}S_{vv}^*\rangle$, $\langle S_{hh}S_{hh}^*\rangle$ and Re $\langle S_{vv}S_{hh}^*\rangle$ except for beamwidths in excess of 10 degrees. The degradation at large beamwidths is, of course, the result of

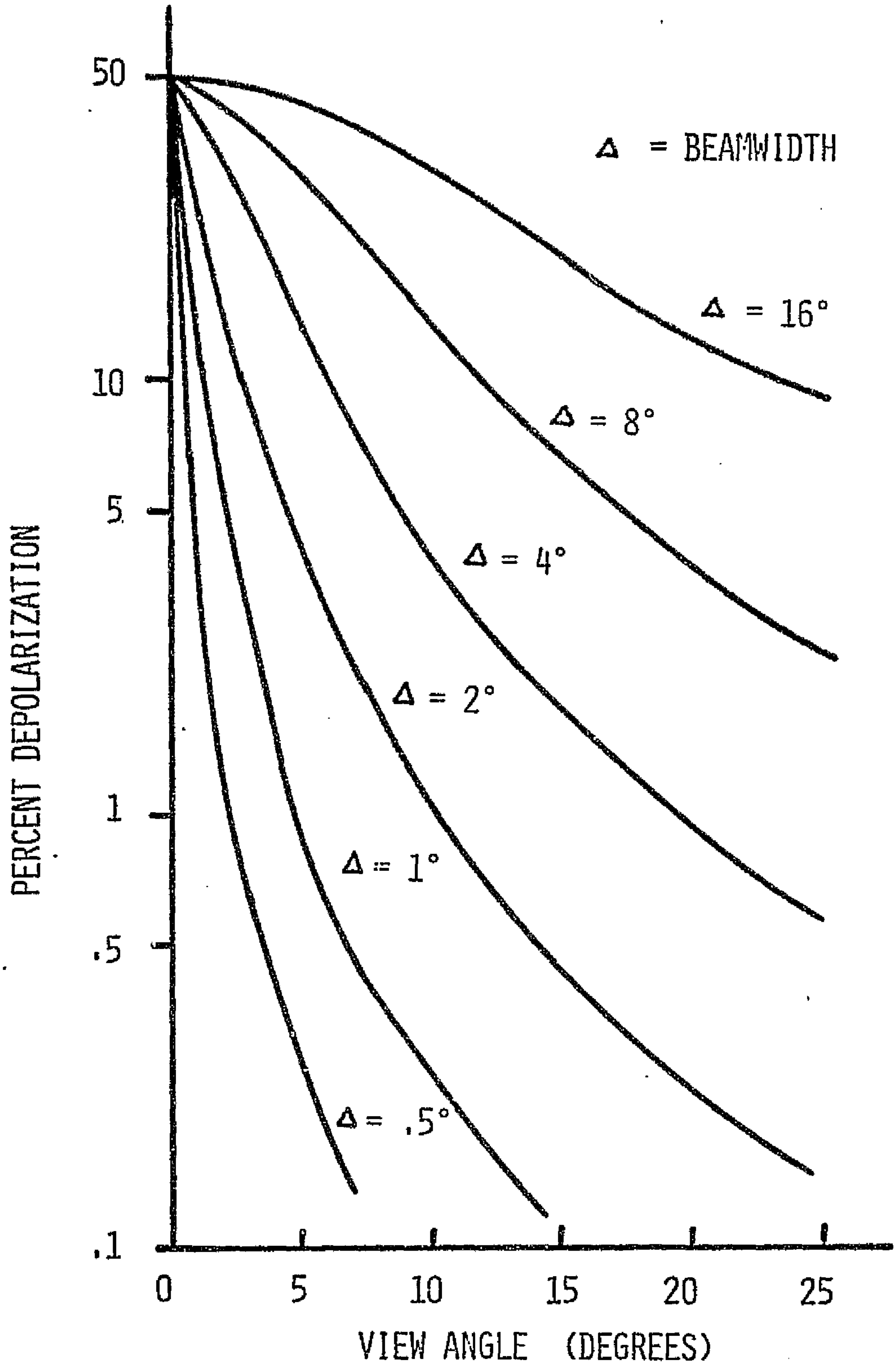

FIGURE 7.2 DEPOLARIZATION OF THE INCIEDNT BEAM AS INDUCED BY THE DIFFERENCE BETWEEN THE ANTENNA AND SURFACE POLARIZATIONS

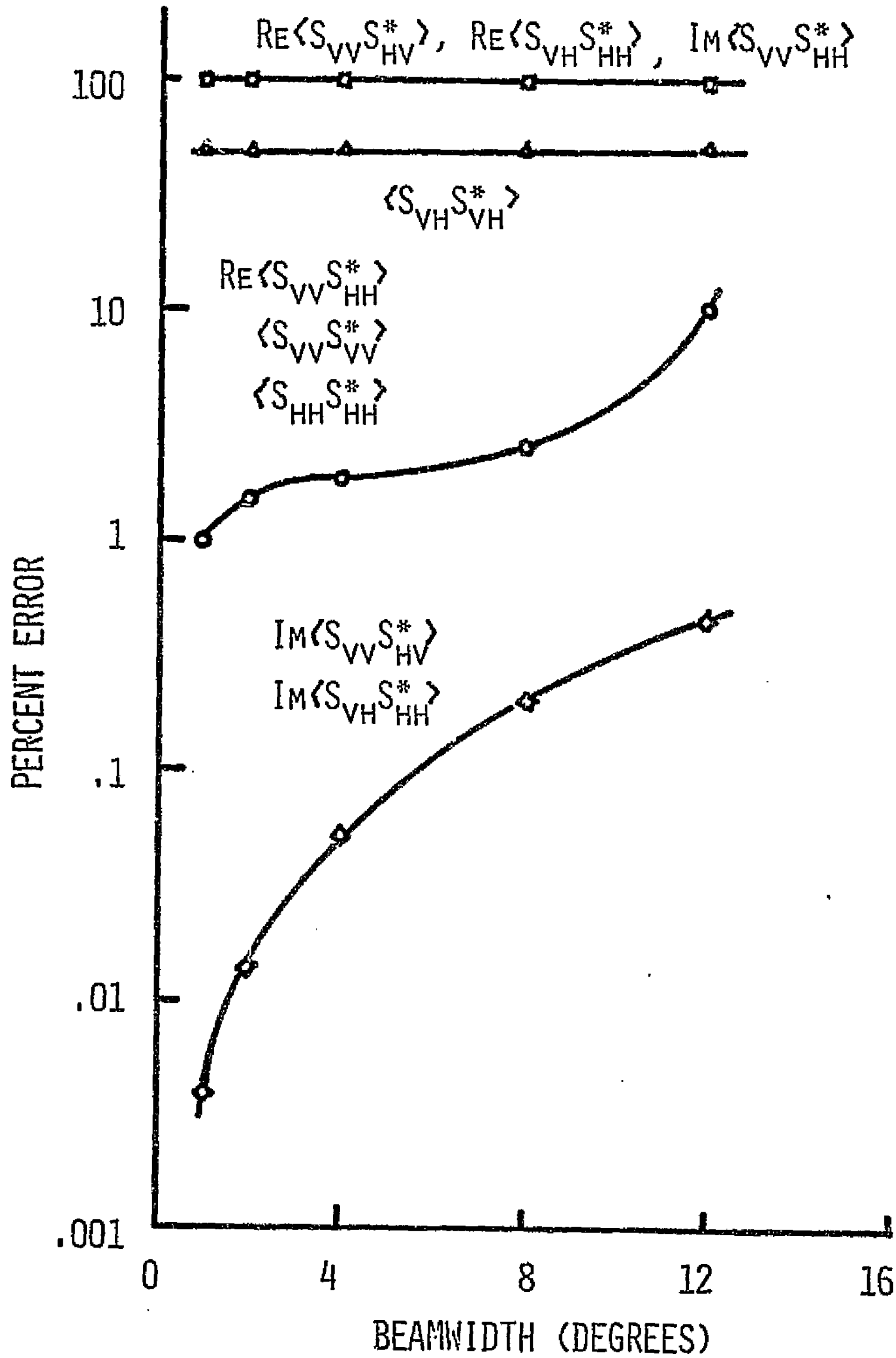

FIGURE 7.3 ACCURACY OF THE DELTA FUNCTION APPROXIMATION FOR THE APPROXIMATE INVERSION MODEL FOR $\theta = 0°$

the antenna beamwidth interacting with the scattering surface "beamwidth". The beamwidth interaction problem is clearly evident in the error characteristic of Im $< S_{vv} S_{hh}^* >$. Since this coefficient has a notch character at nadir, it is impossible for any non-zero beamwidth antenna to retrieve this parameter.

Unusual error performances are apparent in retrieving $<|S_{vh}|^2>$, Re $< S_{vv} S_{hv}^* >$ and Re $< S_{vh} S_{hh}^* >$. A constant 50% error occurs for $<|S_{vh}|^2>$ regardless of beamwidth; whereas a 100% error occurs for the latter two parameters. An explanation for the error in $<|S_{vh}|^2>$ can be constructed solely on the basis of the difference between antenna and surface polarizations. A similar explanation is thought to apply to the other two parameters, although no quantitative argument could be constructed. The error in $<|S_{vh}|^2>$ can be best understood when the antenna and surface polarizations are projected on the surface. The surface polarizations will project as a polar grid whereas the antenna polarizations will project roughly as a rectangular grid as illustrated in Figure 7.4. From these diagrams it is understood that when a vertically polarized spherical wave is incident on the surface, half the power appears in the surface vertical polarization and the other half in the surface horizontal polarization. As shown in the accompanying decomposition diagram both incident components are depolarized by the surface and upon their return to the antenna each depolarized component is transformed (T) back to the antenna polarizations. Upon transforming back to the antenna polarizations, one half of each depolarized component is transformed into the antenna horizontally polarized state. As a result, the inversion based on the antenna polarizations is 50% low. This result indicates that it is futile to recover $<|S_{vh}|^2>$ as defined with respect to surface polarizations with a recovery technique based on the antenna polarizations.

It is also informative to examine the power structure for a cross-polarized measurement. The third row of Table 7.1 shows how the return power is distributed among the scattering coefficients for a cross-polarized measurement. A sizeable contribution arises from the polarized coefficients (columns 1 and 2); however, the sum of those components is fortunately cancelled by the contribution from Re $<S_{vv} S_{hh}^*>$ (column 4). The cancellation is assured by the isotropic character assumed for the surface.

For the same incident angle no results can be reported for the exact method. For the nadir angle the observation matrix is singular. The singularity is plainly evident in the observation matrix as shown in Table 7.2. The reader will observe that the

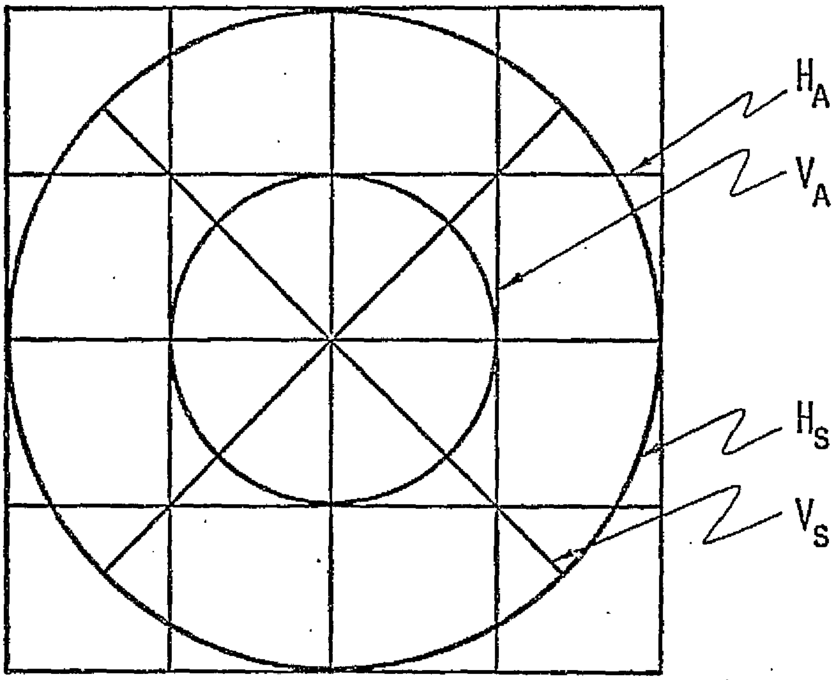

A) PROJECTION OF AND ANTENNA AND SURFACE POLARIZATIONS

$$V_a \rightarrow \tfrac{1}{2}H_s \rightarrow \tfrac{1}{2}\langle|S_{hv}|^2\rangle H_s \rightarrow \begin{cases} \tfrac{1}{4}\langle|S_{hv}|^2\rangle H_s = V_a \\ \tfrac{1}{4}\langle|S_{hv}|^2\rangle H_s = H_a \end{cases}$$

$$V_a \rightarrow \tfrac{1}{2}V_s \rightarrow \tfrac{1}{2}\langle|S_{vh}|^2\rangle V_s \rightarrow \begin{cases} \tfrac{1}{4}\langle|S_{vh}|^2\rangle V_s = V_a \\ \tfrac{1}{4}\langle|S_{vh}|^2\rangle V_s = H_a \end{cases}$$

B) DECOMPOSITION DIAGRAM

FIGURE 7.4 COMPARISION OF ANTENNA AND SURFACE POLARIZATIONS AT NADIR WITH DECOMPOSITION DIAGRAM TO EXPLAIN CROSS POLARIZED MEASUREMENTS

POWER MATRIX

MEAS/COEF	VV	HH	VH	VVHHR	VVHHI	VVVHR	VVVHI	HVHHR	HVHHI	POWER
1	0.6829E 00	0.6829E 00	0.1398E-02	0.4553E 00	0.	0.	0.	0.	0.	0.1822E 01
2	0.6829E 00	0.6829E 00	0.1398E-02	0.4553E 00	0.	0.	0.	0.	0.	0.1822E 01
3	0.2276E 00	0.2276E 00	0.1398E-02	-0.4553E 00	0.	0.	0.	0.	0.	0.1398E-02
4	0.4553E 00	0.4553E 00	0.2328E-09	0.9105E 00	-0.6595E-19	-0.5857E-17	0.	-0.5857E-17	0.	0.1821E 01
5	0.2276E 00	0.2276E 00	0.1398E-02	-0.4553E 00	0.1309E-16	0.	-0.4376E-12	0.	-0.4376E-12	0.1398E-02
6	0.3415E 00	0.3415E 00	0.6988E-03	0.2276E 00	-0.6596E-08	0.	0.	0.	0.	0.9112E 00
7	0.3415E 00	0.3415E 00	0.6988E-03	0.2276E 00	0.6596E-08	0.	0.	0.	0.	0.9112E 00
8	0.4553E 00	0.4553E 00	0.1398E-02	0.	0.	-0.2979E-08	0.	-0.2924E-08	0.	0.911[illegible] 00
9	0.4553E 00	0.4553E 00	0.1398E-02	0.	0.	0.2979E-08	-0.4376E-12	0.2924E-08	-0.4376E-12	0.9119E 00
10	0.4553E 00	0.4553E 00	0.1398E-02	0.	0.	-0.2941E-17	0.2205E-03	-0.2887E-17	0.2205E-03	0.9124E 00
11	0.4553E 00	0.4553E 00	0.1398E-02	0.	0.	-0.2969E-17	-0.2205E-03	-0.2916E-17	-0.2205E-03	0.9115E 00
12	0.4553E 00	0.4553E 00	0.1398E-02	0.	0.	-0.2924E-08	0.	-0.2979E-08	0.	0.9119E 00
13	0.4553E 00	0.4553E 00	0.1398E-02	0.	0.	0.2924E-08	-0.4376E-12	0.2979E-08	-0.4376E-12	0.9119E 00
14	0.4553E 00	0.4553E 00	0.1398E-02	0.	0.	-0.2887E-17	0.2205E-03	-0.2941E-17	0.2205E-03	0.9124E 00
15	0.4553E 00	0.4553E 00	0.1398E-02	0.	0.	-0.2916E-17	-0.2205E-03	-0.2969E-17	-0.2205E-03	0.9115E 00

TABLE 7.1 POWER COMPOSITION MATRIX FOR A NADIR MEASUREMENT

MEAS/COEF	VV	HH	VH	VVHHR	VVHHI	VVVHR	VVVHI	HVHHR	HVHHI
1	0.1654E-01	0.1654E-01	0.2205E-01	0.1103E-01	0.	0.	0.	0.	0.
2	0.1654E-01	0.1654E-01	0.2205E-01	0.1103E-01	0.	0.	0.	0.	0.
3	0.5513E-02	0.5513E-02	0.2205E-01	-0.1103E-01	0.	0.	0.	0.	0.
4	0.1103E-01	0.1103E-01	0.3725E-08	0.2205E-01	-0.2968E-17	-0.5856E-15	0.	-0.5[illegible]E-15	0.
5	0.5513E-02	0.5513E-02	0.2205E-01	-0.1103E-01	0.5891E-15	0.	-0.4376E-10	0.	-0.4376E-10
6	0.8270E-02	0.8270E-02	0.1103E-01	0.5513E-02	-0.2969E-06	0.	0.	0.	0.
7	0.8270E-02	0.8270E-02	0.1103E-01	0.5513E-02	0.2969E-06	0.	0.	0.	0.
8	0.1103E-01	0.1103E-01	0.2205E-01	0.	0.	-0.2978E-06	0.	-0.2924E-06	0.
9	0.1103E-01	0.1103E-01	0.2205E-01	0.	0.	0.2978E-06	-0.4376E-10	0.2924E-06	-0.4376E-10
10	0.1103E-01	0.1103E-01	0.2205E-01	0.	0.	-0.2940E-15	0.2205E-01	-0.2886E-15	0.2205E-01
11	0.1103E-01	0.1103E-01	0.2205E-01	0.	0.	-0.2971E-15	-0.2205E-01	-0.2915E-15	-0.2205E-01
12	0.1103E-01	0.1103E-01	0.2205E-01	0.	0.	-0.2924E-06	0.	-0.2978E-06	0.
13	0.1103E-01	0.1103E-01	0.2205E-01	0.	0.	0.2924E-06	-0.4376E-10	0.2978E-06	-0.4376E-10
14	0.1103E-01	0.1103E-01	0.2205E-01	0.	0.	-0.2886E-15	0.2205E-01	-0.2940E-15	0.2205E-01
15	0.1103E-01	0.1103E-01	0.2205E-01	0.	0.	-0.2915E-15	-0.2205E-01	-0.2971E-15	-0.2205E-01

TABLE 7.2 OBSERVATION MATRIX BASED ON SURFACE POLARIZATIONS

ORIGINAL PAGE IS
OF POOR QUALITY

following pairs of observations are identical: 1 and 2, 3 and 5, 6 and 7, 8 and 12, 9 and 13, 10 and 14 and 11 and 15. The rank of the matrix is consequently 8. For isotropic scenes the singularity may be removed by solving the system of measurements subject to the constraints: $<|S_{vv}|^2> = <|S_{hh}|^2>$, $<S_{vv}S_{hv}^*> = <S_{vh}S_{hh}^*>$, and $<S_{vv}S_{hh}^*> = \sqrt{<|S_{vv}|^2><|S_{hh}|^2>}$. As a result of the constraint there are only five independent parameters. This result was anticipated from the "Gedanken Experimente" referenced in Chapter 3.

In general, retrieval of the scattering coefficients at nadir is a difficult task, it is merely coincidence that the approximate method yielded as many accurate estimates as it did. If a scene is anisotropic or if it has a peculiar character where $|<S_{vv}S_{hh}^*>|^2 < <|S_{vv}|^2><|S_{hh}|^2>$, then there is no assurance that either method will work. See the fourth column of Table 7.1 where it is evident that $\mathrm{Re}<S_{vv}S_{hh}^*>$ plays an important role in forming the polarized measurements. Careful investigations at nadir will require very narrow beams to search nadir asymptotically if the coefficients are to be reported with respect to the surface polarizations.

The accuracies of the delta function approximation for the approximate and exact models at a view angle of 4° are shown, Figures 7.5 and 7.6, respectively. From Figure 7.6 it is apparent that the approximate method can be employed with reasonable accuracy (0.5 dB) to retrieve all coefficients if the beamwidth is less than 3°. A beamwidth as much as 10° can be tolerated for the recovery is restricted to the polarized coefficients. The exact inversion method will permit beamwidths up to 9° in retrieving all the scattering coefficients. Similar results are apparent in the error characteristics for a view angle of 8° (See Figures 7.7 and 7.8).

7.4 Antenna Requirements for the Accurate Recovery of the Scattering Coefficients

7.4.1 General

A number of simulations were conducted at various incident angles with and without biases and also with and without random perturbations introduced into the measurement. These simulations served as a training set to identify the particular scattering coefficient or coefficients which primarily contributed to the error characteristic for each scattering coefficient. Invariably the best single parameter to which the error could be attributed was the magnitude of $<S_{vv}S_{hh}^*>$. The magnitude of this parameter conveys a notion of the size of $<|S_{vv}|^2>$ and $<|S_{hh}|^2>$ as well. These three coefficients generally interacted to introduce an error in the measurement when

C, 2

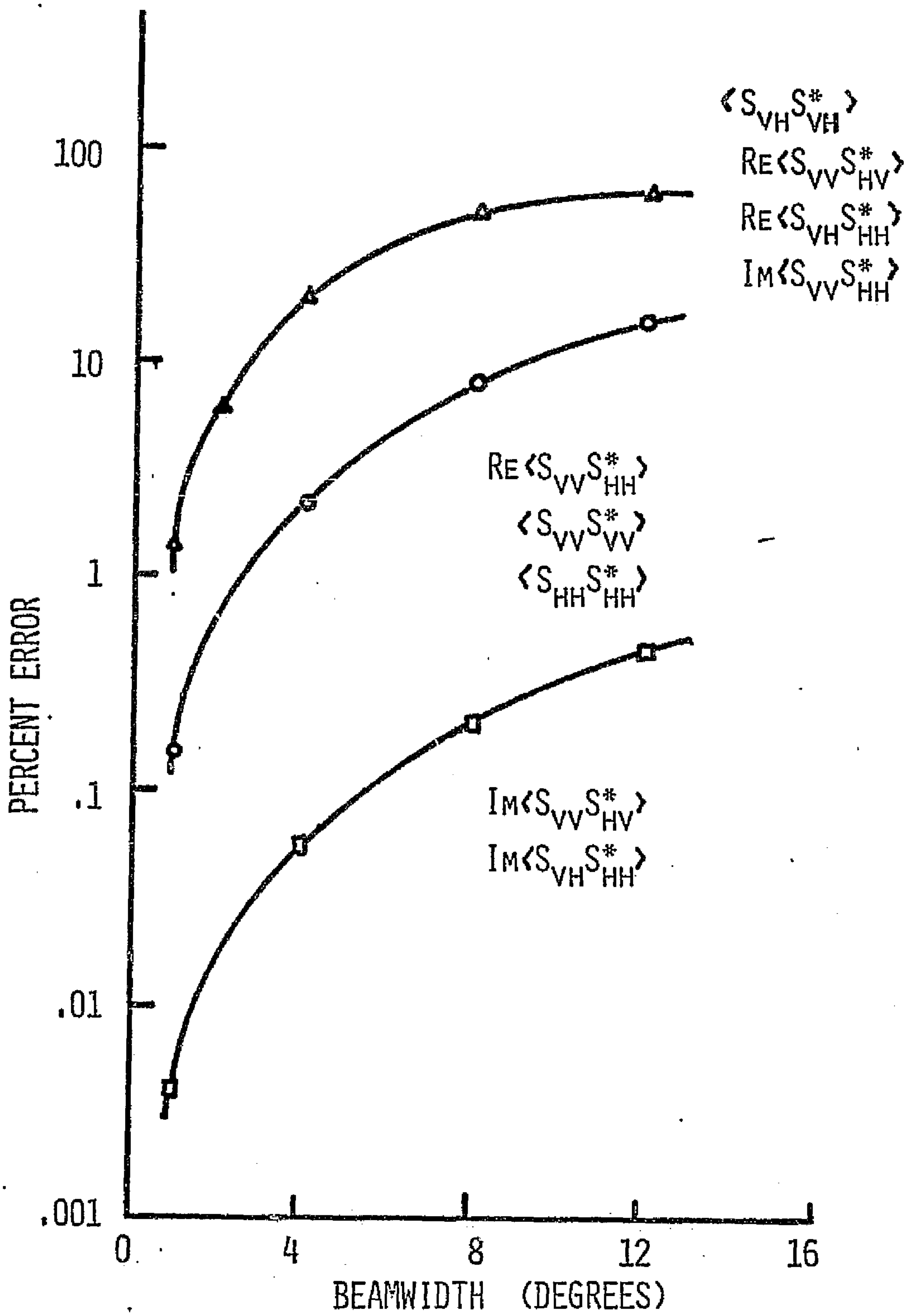

FIGURE 7.5 ACCURACY OF THE DELTA FUNCTION APPROXIMATION FOR THE APPROXIMATE INVERSION MODEL FOR $\theta = 4°$

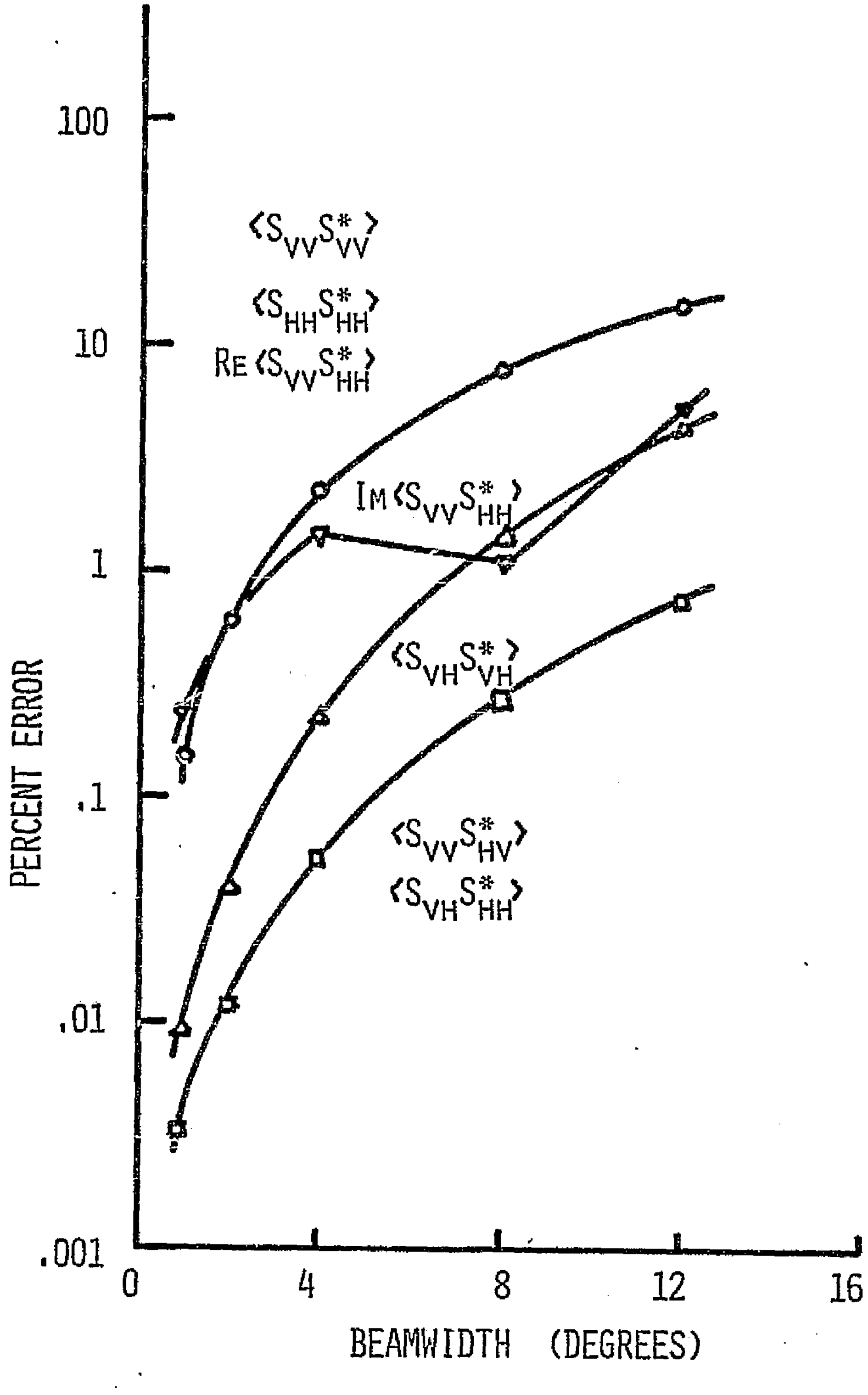

FIGURE 7.6 ACCURACY OF THE DELTA FUNCTION APPROXIMATION FOR THE EXACT INVERSION MODEL FOR $\theta = 4°$

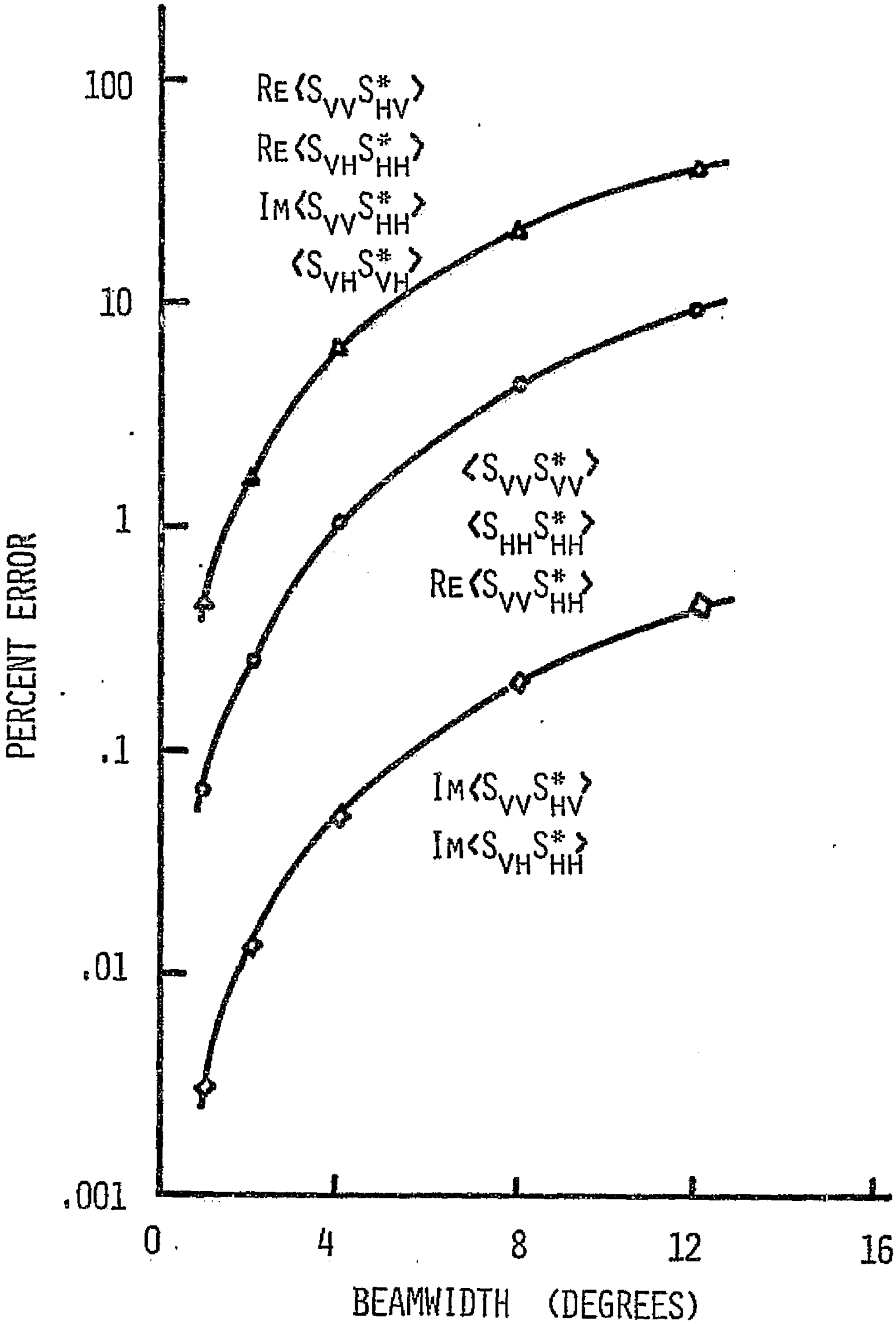

FIGURE 7.7 ACCURACY OF THE DELTA FUNCTION APPROXIMATION FOR THE APPROXIMATE INVERSION FOR $\theta = 8°$

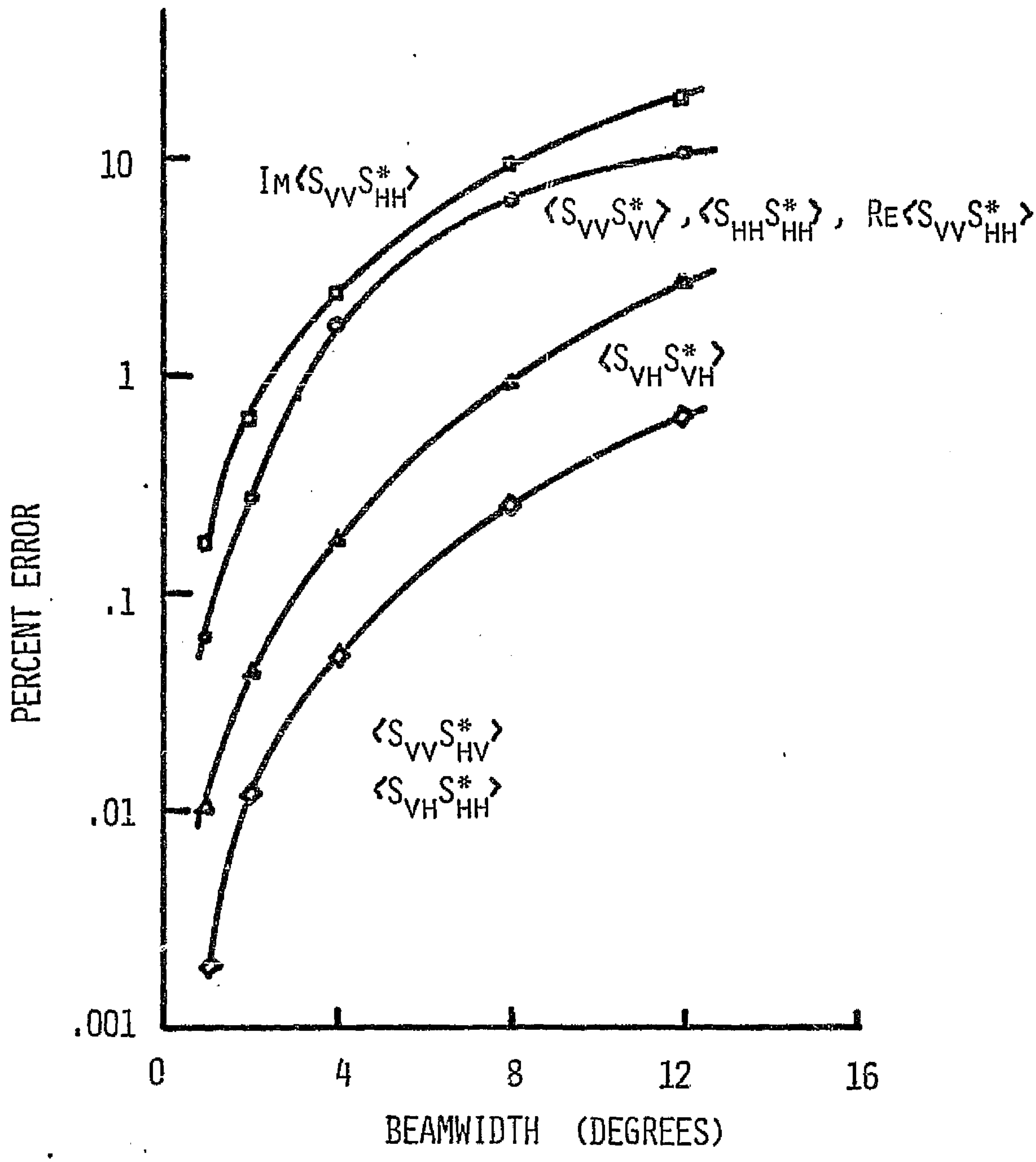

FIGURE 7.8 ACCURACY OF THE DELTA FUNCTION APPROXIMATION FOR THE EXACT INVERSION MODEL FOR $\theta = 8°$

the antenna transmission and reception properties deviated from the ideal state specified in Chapter 6.

The training set also made it apparent that the error characteristics were primarily governed by the level of the cross polarized leakage for those measurements involving linearily polarized transmission or reception. The level of the leakage is expressed in terms of one-way depression relative to the dominant pattern. The relative phase between the dominant and leakage patterns was treated as an independent error parameter. A bias error study was, therefore, applied to the retrieval of $\langle S_{vv} S_{hh}^* \rangle$, $\langle |S_{hh}|^2 \rangle$, $\langle S_{vv} S_{hv}^* \rangle$ and $\langle S_{vh} S_{hh}^* \rangle$. Although the latter two coefficients involve balanced cross patterns during reception, studies showed that the error performance was largely insensitive to small deviations from a balanced condition or small deviations from the required phase condition in comparison to leakage appearing in the linearily polarized transmission. Now in the case of $\langle S_{vv} S_{hh}^* \rangle$, it is more meaningful to consider Monte Carlo studies since both transmissions and receptions involve balanced cross patterns.

All simulations were conducted for a one degree beam having a $(2 J_1 (x)/x)^2$ pattern. The resulting error characteristics apply equally as well to approximate or exact inversion methods. When translating the performance to small incident angles where the antenna and surface polarizations differ significantly across the beam, then one must assume that the inversions had been performed by the exact method. The graphs of Figure 7.2 serve as a guide as to when the matrix method must be used. Simulations with the other pattern functions yielded similar results and so are not reported.

7.4.2 Error Characteristics

The error characteristics for the recovery of $\langle S_{vv} S_{vv}^* \rangle$ are shown in Figures 7.9 and 7.10. The results are shown for two phase conditions in which $\beta_t = \beta_r = 0^\circ$ and $\beta_t = \beta_r = 90^\circ$, respectively. These two conditions result in extremal error characteristics in which the maximum error results from one phase condition and a minimum error from the other condition. The extremes are induced by a sign change in the contribution from $\mathrm{Re}\langle S_{vv} S_{hh}^* \rangle$, a dominant parameter. As shown by Figure 7.9 there is no difficulty in retrieving the dominant scattering coefficient $\langle |S_{vv}|^2 \rangle$ except for a cross polarized pattern less than 10 dB beneath the vertical polarized pattern and a large separation between $\langle |S_{vv}|^2 \rangle$ and $\langle |S_{hh}|^2 \rangle$. The weakened dominant pattern results in less return power from $\langle |S_{vv}|^2 \rangle$. A further reduction occurs when $\langle |S_{hh}|^2 \rangle$ and $\langle S_{vv} S_{hh}^* \rangle$ are significantly weaker than $\langle |S_{vv}|^2 \rangle$. A similar result occurs when $\beta_t = \beta_r = 90^\circ$ (Figure 7.10). The error is slightly larger because the coefficient

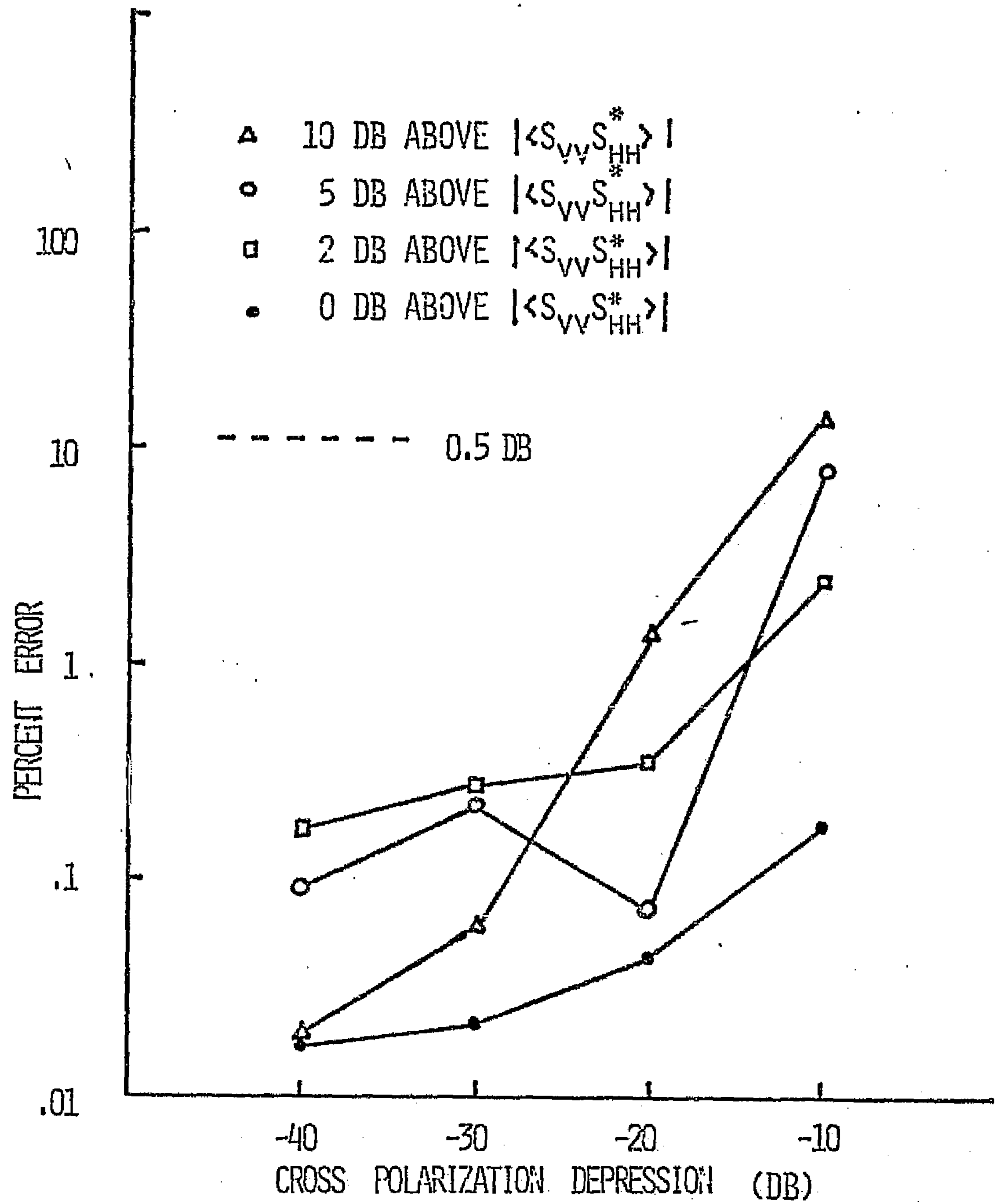

FIGURE 7.9 ERROR CHARACTERISTICS OF $\langle|S_{VV}|^2\rangle$ FOR VARIOUS ANTENNA CROSS POLARIZATION ISOLATIONS WITH PHASE CONDITION $\beta_T = \beta_R = 0°$

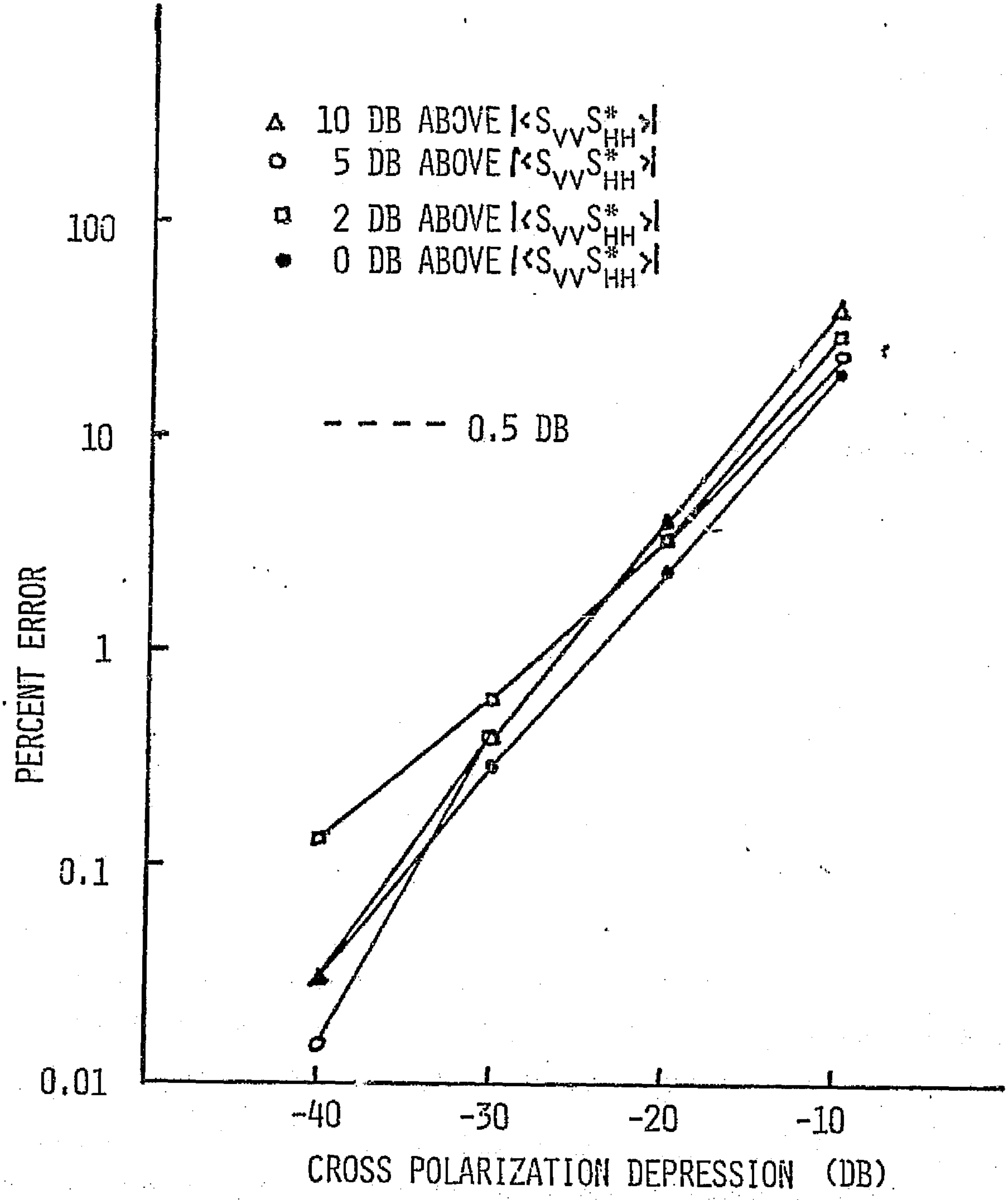

FIGURE 7.10 ERROR CHARACTERISTICS OF $\langle|S_{VV}|^2\rangle$ FOR VARIOUS ANTENNA CROSS POLARIZATION ISOLATIONS WITH A PHASE CONDITION OF $\beta_T = \beta_R = 90°$

Re $<S_{vv}S_{hh}^*>$ causes a "negative" power contribution, resulting in an even smaller resultant power. Recall that $<S_{vv}S_{hh}^*>$ responds to the product pattern $\sqrt{g_v g_h}$ and its sign is controlled by the sum $\beta_t + \beta_r$ (See Equation 4-29).

The retrieval performance, when attempting measurements of $<|S_{hh}|^2>$, is illustrated in Figures 7.11 and 7.12 for pattern phase conditions corresponding to $\beta_t = \beta_r = 0^o$ and $\beta_t = \beta_r = 90^o$, respectively. Since $<|S_{hh}|^2>$ is generally less than or equal to $<|S_{vv}|^2>$, one can anticipate a poorer error characteristic. For the case where $\beta_t = \beta_r = 0^o$, the ability to recover $<|S_{hh}|^2>$ is shown to be strongly dependent on its separation from $|<S_{vv}S_{hh}^*>|$. Positive power contributions are made by both $<|S_{vv}|^2>$ and $<S_{vv}S_{hh}^*>$. The resultant power in this case is excessive. When $\beta_t = \beta = 90^o$, the contributions by $<S_{vv}S_{hh}^*>$ is negative and partially cancels the $<S_{vv}S_{vv}^*>$ contribution. As a consequence, one may suspect that the latter phase condition yields a slightly better error characteristic. Comparison of Figures 7.11 and 7.12 demonstrates that this is the case. From either graph it is observed that when $<|S_{hh}|^2>$ is 10 dB lower than $|<S_{vv}S_{hh}^*>|$, the antenna cross polarization level must be less than -30 dB for a error less than 0.5 dB. When the separation is 5 dB, the antenna cross polarization level must be better than -20 dB. The latter is probably representative of the sea for angles of incidence up to 70^o.

The error characteristics for retrieving $<|S_{vh}|^2>$ for the same two relative phase conditions are shown in Figures 7.13 and 7.14. From Figure 7.13 it is apparent that the weakness of the scattering coefficient in the presence of cross-leakage makes it very difficult to isolate. The ability to measure $<|S_{vh}|^2>$ is shown to depend strongly on its depression from the polarized scattering coefficients as conveyed parametrically by $|<S_{vv}S_{hh}^*>|$. Figure 7.13 represents a worst case situation in which all the dominant coefficients to include Re $<S_{vv}S_{hh}^*>$ make positive contributions to the return power. This situation is consequently useful for formulating a criteria for accurate measurement of $<|S_{vh}|^2>$. It has been common practice to judge the ability of an antenna to measure cross-polarized coefficients by its one-way and in some cases by its two-way isolation in comparison to the separation between the polarized and cross-polarized coefficients. The graphs of Figure 7.13 show explicit the antenna requirement. If a 0.5 dB accuracy is desired and if $<|S_{vh}|^2>$ lies X dB beneath $|<S_{vv}S_{hh}^*>|$, then approximately X + 16 dB one-way isolation is required. The above result indicates that one must not only consider the polarized coefficients in making a judgement on an antenna but a complex valued coefficient must also be considered.

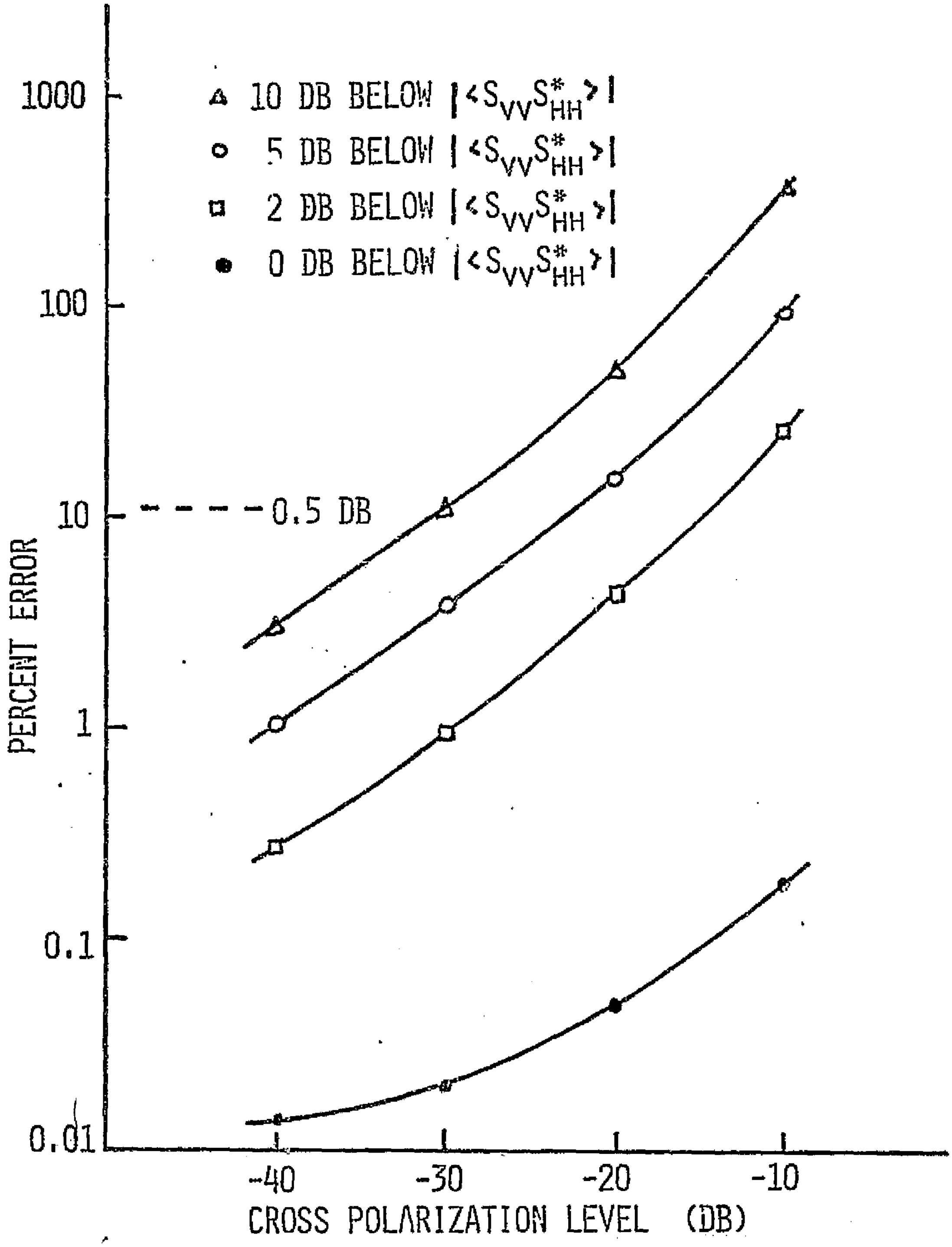

FIGURE 7.11 ERROR CHARACTERISTICS FOR $\langle|S_{HH}|^2\rangle$ AT VARIOUS LEVELS OF PATTERN CROSS POLARIZATION FOR AN ANTENNA PHASE CONDITION $\beta_T = \beta_R = 0°$

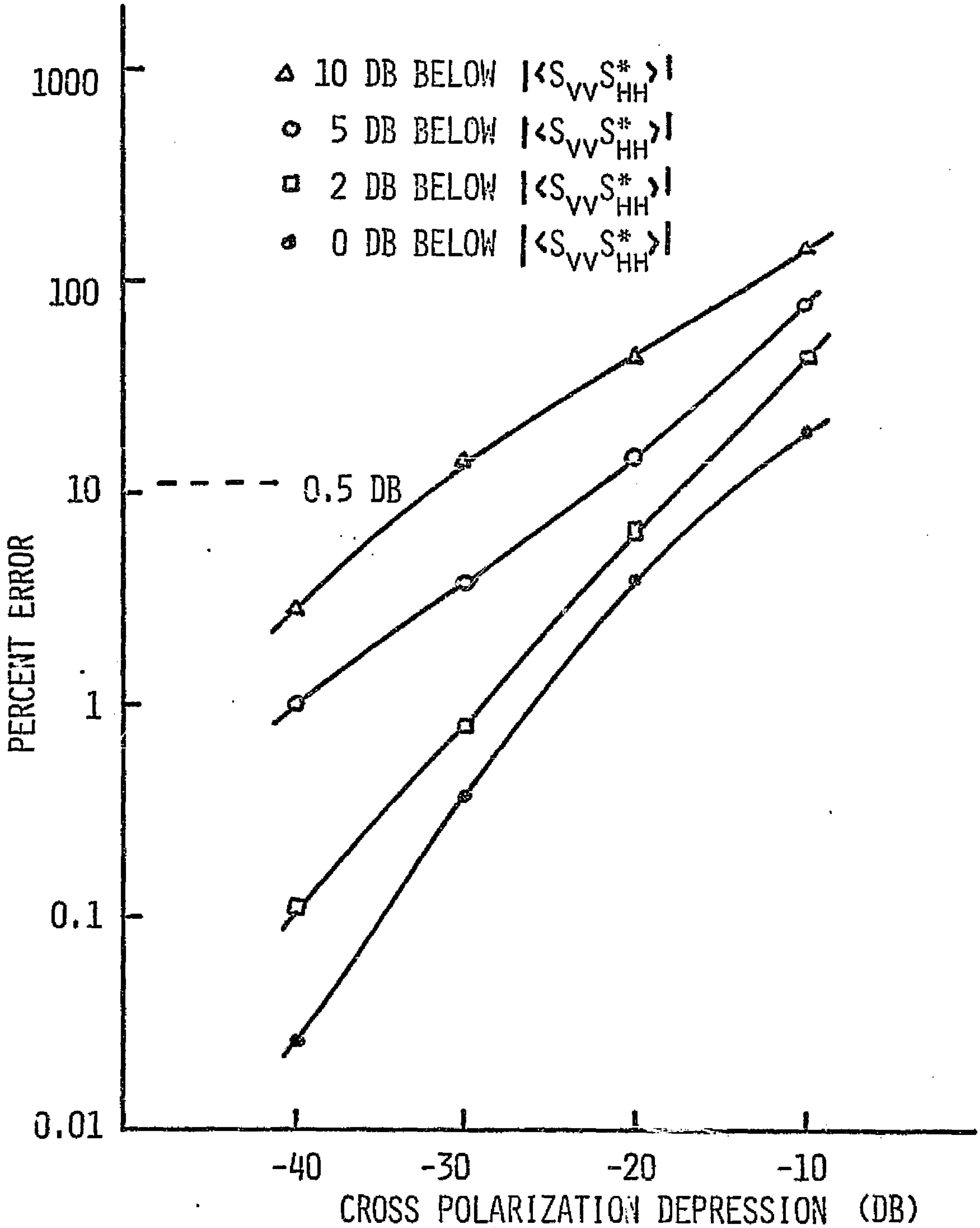

FIGURE 7.12 ERROR CHARACTERISTICS FOR $\langle|S_{HH}|^2\rangle$ AT VARIOUS LEVELS OF PATTERN CROSS POLARIZATION FOR AN ANTENNA PHASE CONDITION $\beta_T = \beta_R = 90°$

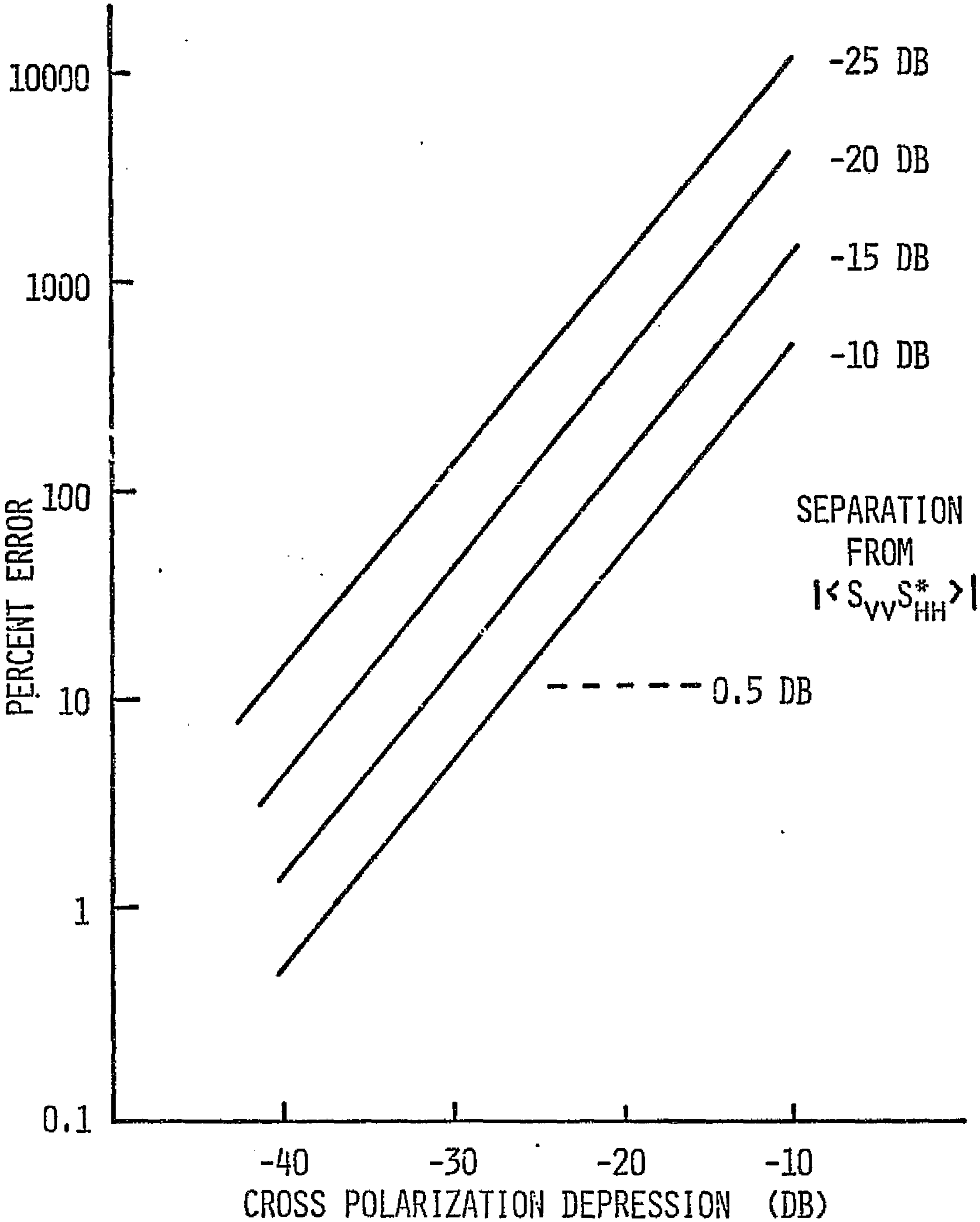

FIGURE 7.13 ERROR CHARACTERISTICS FOR $\langle |S_{VH}|^2 \rangle$ AT VARIOUS LEVELS OF PATTERN CROSS POLARIZATION FOR AN ANTENNA PHASE CONDITION $\beta_T = \beta_R = 0°$

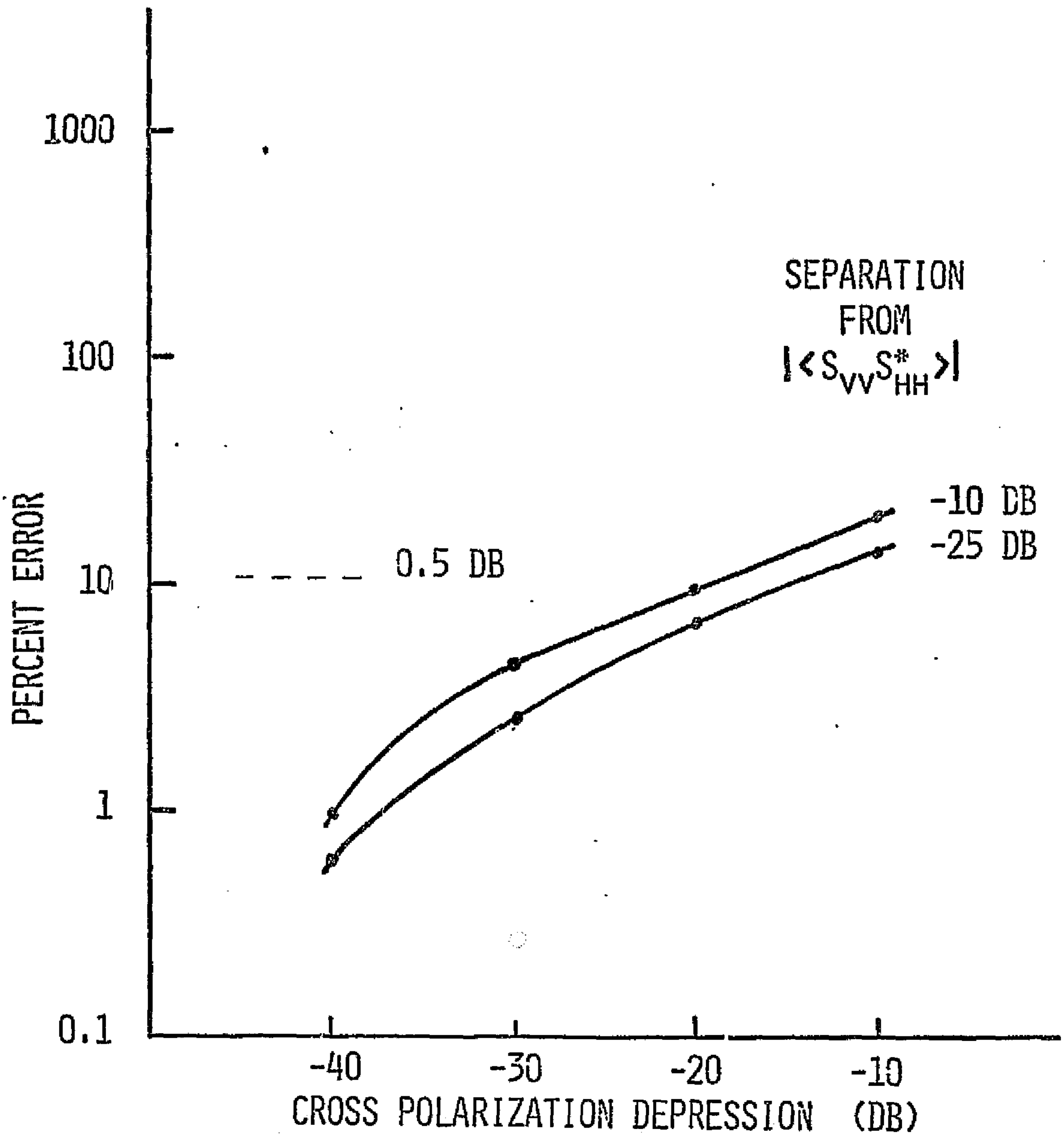

FIGURE 7.14 ERROR CHARACTERISTICS FOR $\langle|S_{VH}|^2\rangle$ AT VARIOUS LEVELS OF PATTERN CROSS POLARIZATION FOR AN ANTENNA PHASE CONDITION $\beta_T = \beta_R = 90°$

It is apparent from the graphs of Figure 7.14 that if the phase of the leakage pattern can be adjusted to 90^o during transmission and reception, the level of leakage is almost immaterial. In this case contributions by $<|S_{vv}|^2>$ and $<|S_{hh}|^2>$ are almost entirely cancelled by the contribution from Re $< S_{vv}S_{hh}^*>$. These results show that if the phase of the cross leakage can be adjusted for $\beta_t = \beta_r = 90^o$, the stringent requirements on the cross pattern amplitude can be relaxed.

The error characteristics for Re $< S_{vv}S_{hh}^*>$ and Im $< S_{vv}S_{hh}^* >$ are shown in Figure 7.15. Monte Carlo studies were performed to construct this characteristic. The random deviations in amplitude (from balance) and in phase were uniformly distributed. Maximum deviations are indicated on the graphs. It is apparent that the real part of $< S_{vv}S_{hh}^* >$ is easy to recover. Phase perturbations have little effect on the accuracy. The recovery of the imaginary part appears to be more difficult; but this is mainly a result of its weak response in comparison to $<|S_{vv}|^2>$ and $<|S_{hh}|^2>$.

The error characteristics for the cross-correlation coefficients $< S_{vv}S_{hv}^*>$ and $<S_{vh}S_{hh}^*>$ are all shown in the graphs of Figure 7.16. Both extremal phase conditions are superimposed on the same plot. The graphs show that the real parts of the coefficients are difficult to retrieve if $\beta_t = \beta_r = 0$. Similarly, the imaginary parts are difficult to retrieve if $\beta_t = \beta_r = 90^o$. On the otherhand, the imaginary part and the real parts are easily recovered if $\beta_t = \beta_r = 0^o$ and $\beta_t = \beta_r = 90^o$, respectively. The graphs also indicate that the ability to retrieve the coefficients is dependent upon the separation of the coefficients from the real or imaginary part of $<S_{vv}S_{hh}^* >$. It is again evident if the correct phase property is employed that a reasonable accuracy can be anticipated.

7.4.3 Alternatives

When the ideal antenna states as specified in Ch er 6 cannot be approximated reasonably and if as a consequence significant error is introduced into the measurements, the experimenter has recourse to specifying the complete antenna polarization states he is able to achieve. As long as he approaches the desired states and performs an adequate number of measurements, he can be reasonably assured that inversions based on the complete scatterometer equation will yield improvements in the estimates of the coefficients. The inversion model should be tested to determine whether his system of measurements is well conditioned. At least nine measurements must be performed unless one has prior knowledge that some of the coefficients are negligible. In this technique one must reconcile with making at least nine measurements; whereas if the beamwidth constraint

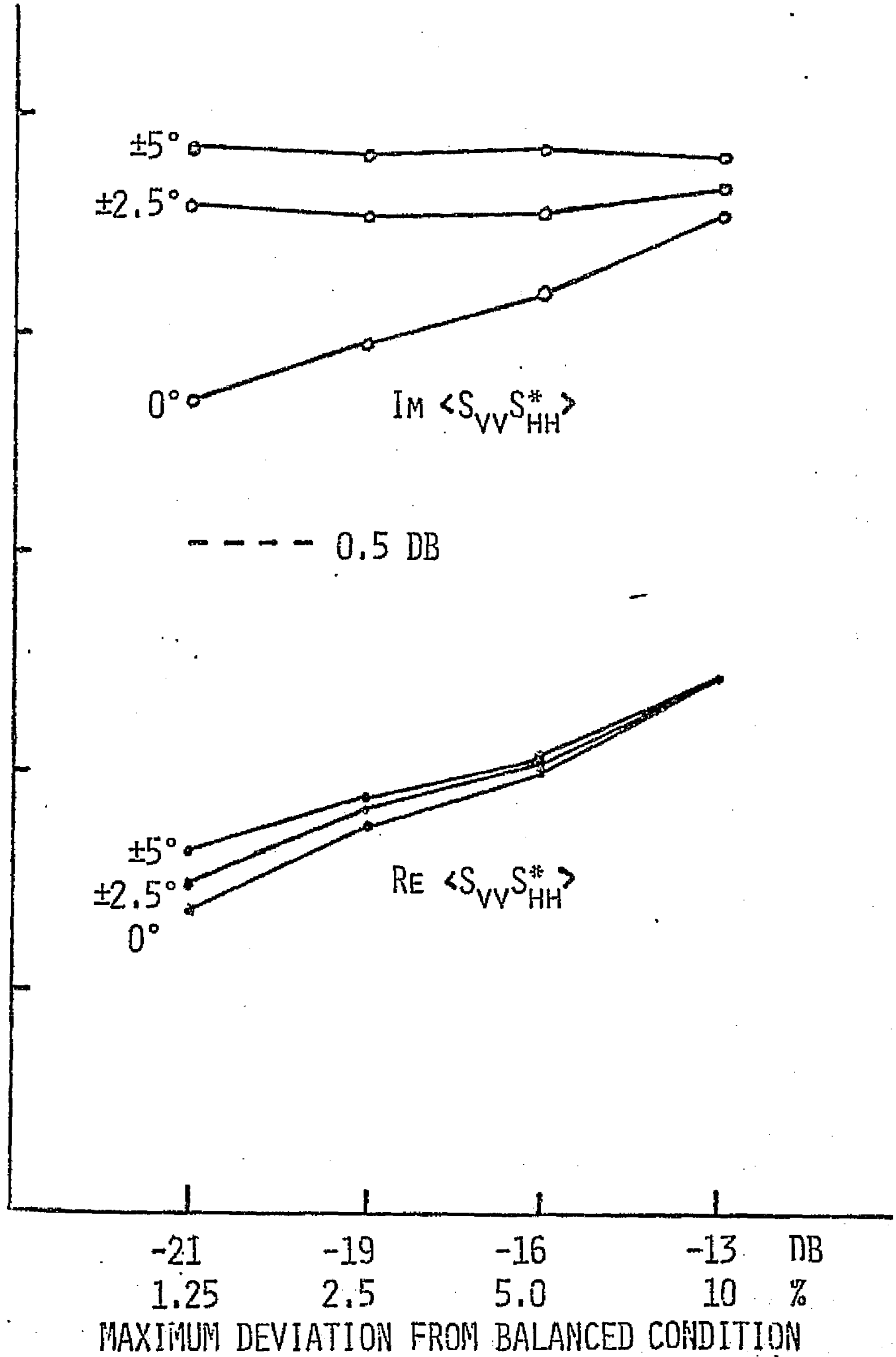

FIGURE 7.15 ERROR CHARACTERISTICS FOR $\langle S_{VV}S^*_{HH}\rangle$ AS DEPENDENT ON UNCERTAINTY IN PATTERN BALANCE AND PHASE

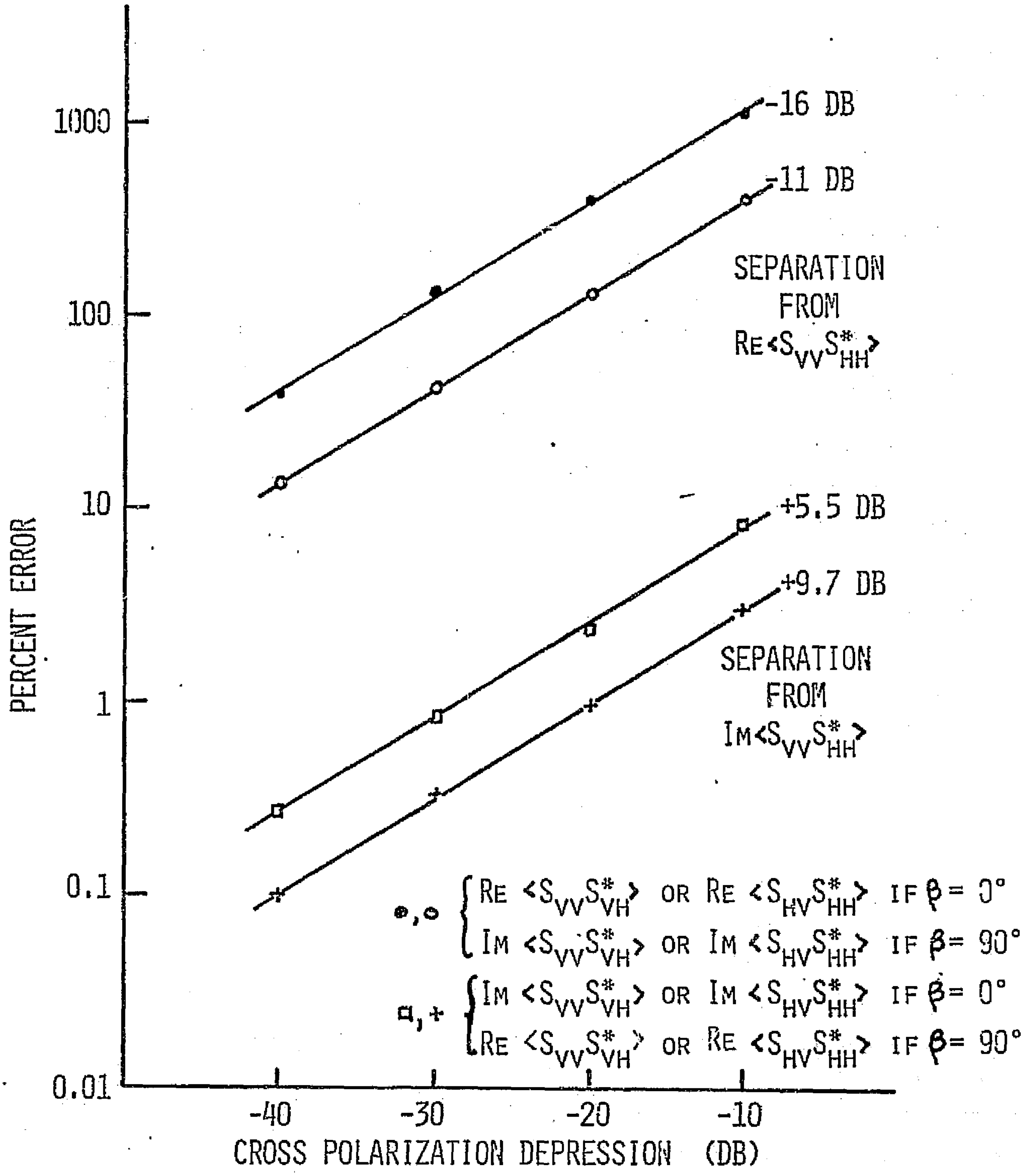

FIGURE 7.16 ERROR CHARACTERISTICS FOR THE CROSS CORRELATIONS <$S_{VV}S^*_{VH}$> AND <$S_{HV}S^*_{HH}$> AS A FUNCTION OF PATTERN CROSS POLARIZATION LEVEL

is met, a single scattering parameter can be recovered with at most two measurements if the antenna specification can be realized.

7.5 Evaluation of the Inversion Parameters

7.5.1 Introduction

Essential to accurate inversion of scatterometric measurements is the knowledge of the actual antenna pattern. To form the integral weights for each scattering coefficient, the pattern and phase functions must be numerically integrated over the main beam and perhaps the first side lobes. Since pattern information is seldom available in functional form, one is dependent on measurements. In measuring the pattern, the question arises as to what sampling density is required to adequately specify the pattern. The sample requirement is derived on the basis of simple aperture theory. The results of the theory are applied to the SKYLAB S-193 antenna to illustrate the sampling requirement.

7.5.2 Derivation of the Pattern Spectrum

It is well known that the far field E of an aperture type antenna is related to the aperture illumination function, $A(x,y)$, through an inverse Fourier transform relationship [19]

$$E\,(r, \theta, \phi) = K_o \iint_{-\infty}^{\infty} A(x,y)\, \exp\,[j(k_x x + k_y y)]\; dx\, dy \tag{7-9}$$

where

$$\begin{aligned} K_o &= (j/\lambda r) \exp(-jkr) \\ k_x &= k \sin\theta \cos\phi \\ k_y &= k \sin\theta \sin\phi \\ k &= 2\pi/\lambda \end{aligned} \tag{7-10}$$

The relationship is considered valid for spherical polar angles θ satisfying $\cos\theta \geq 0.9$. A is assumed to be a real function* so that the main beam of the antenna is located about the positive z axis. Now it is convenient to rewrite the above expression in the form

$$E\,(r, f_\xi, f_\eta) = K_1 \iint A(\xi,\eta)\, \exp\; j\, 2\pi\, (f_\xi \xi + f_\eta \eta)\;\; d\xi\, d\eta \tag{7-11}$$

---

* A uniform phase distribution across the aperture.

where

$$
\begin{aligned}
f_\xi &= \sin\theta \cos\phi \\
f_\eta &= \sin\theta \sin\phi \\
\xi &= x/\lambda \\
\eta &= y/\lambda \\
K_1 &= (j\lambda/r)\exp(-jkr)
\end{aligned}
\qquad (7\text{-}12)
$$

The far field power pattern P is given by

$$P(f_\xi, f_\eta) = K_2 EE^* \qquad (7\text{-}13)$$

where K_2 is a suitable constant. The Fourier spectrum of P is given by

$$\mathcal{F}[P] = K_2 \mathcal{F}[EE^*] \qquad (7\text{-}14)$$

or

$$= K_2\ A * A \qquad (7\text{-}15)$$

where $*$ is the autocorrelation operator. Specifically

$$\mathcal{F}[P] = K_2 \iint A(\xi,\eta)\ A(\xi+\alpha, \eta+\beta)\ d\xi\ d\eta \qquad (7\text{-}16)$$

and implies that the spectrum of the power pattern is proportional to the autocorrelation of the aperture distribution and is therefore band limited for finite apertures.

For circularly symmetric aperture distribution a similar theory could have been derived if the initial expression had been transformed to the Bessel-Fourier integral. However, seldom are aperture distribution circularly symmetric, as a consequence, we have a more general result.

7.5.3 Sampling Requirement

Now suppose that an aperture has maximum length x_o and maximum height y_o. From the above result and the illustration in Figure 7.17, it is clear that the spectrum of P is restricted to the product domain $(x_o/\lambda, -x_o/\lambda) \times (y_o/\lambda, -y_o/\lambda)$. By the sampling theorem, the pattern can be specified uniquely if samples are taken at

$$(f_\xi, f_\eta) = \left(\frac{m\lambda}{2x_o}, \frac{n\lambda}{2y_o}\right) \qquad (7\text{-}17)$$

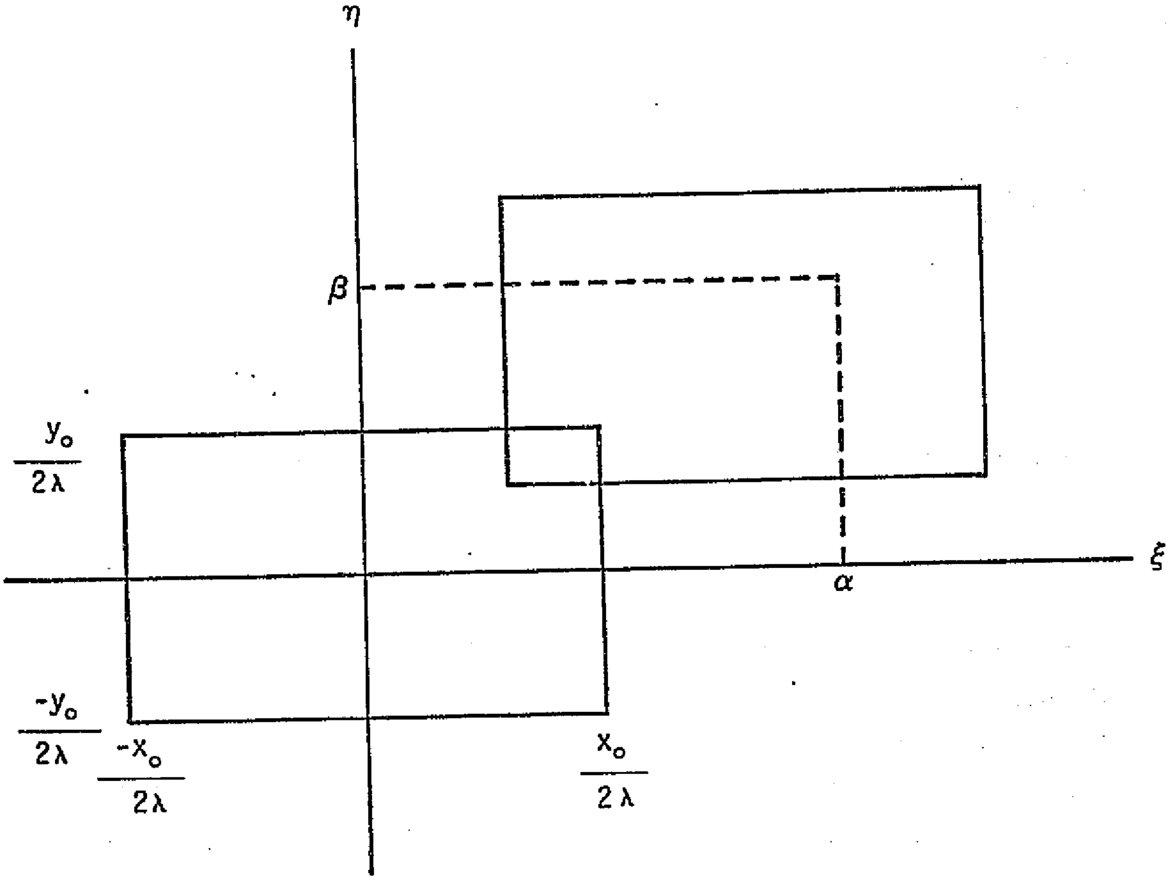

FIGURE 7.17 THE DOMAIN OF INTEGRATION FOR THE AUTOCORRELATION FUNCTION

where m, n ε .... -2,-1,0,1,2,... . The above result can be written in terms of θ and ϕ by means of (Equation 7-14). Specifically

$$\sin\theta \cos\phi = \frac{m\lambda}{2x_o} \quad (7\text{-}18)$$

and

$$\sin\theta \sin\phi = \frac{n\lambda}{2y_o} \quad (7\text{-}19)$$

As can be easily shown the above relationships require that the antenna pattern be sampled at points (θ_{mn}, ϕ_{mn}) satisfying

$$\theta_{mn} = \sin^{-1}\left[\frac{\lambda}{2}\left(\frac{m^2}{x_o^2} + \frac{n^2}{y_o^2}\right)^{\frac{1}{2}}\right] \quad (7\text{-}20)$$

$$\phi_{mn} = \tan^{-1}\frac{n}{m}\,\frac{x_o}{y_o} \quad (7\text{-}21)$$

In the principal planes the above sampling requirements reduce to

$$\theta_{mo} = \sin^{-1}\frac{m\lambda}{2x_o} \quad (7\text{-}22)$$

in the "x" plane and

$$\theta_{on} = \sin^{-1}\frac{n\lambda}{2y_o} \quad (7\text{-}23)$$

in the "y" plane. Between the planes in the pattern must be sampled in accord with Equations (7-22) and (7-23).

7.5.4 Illustration

To develop an understanding of the sample requirement, Equations (7-20) and (7-21) were evaluated for an aperture having a maximum dimension of 1.12 meters in the x as well as the y dimension and illuminated at 13.9 GHz. The sampling points for one quadrant out to approximately seven degrees in theta is illustrated in Figure 7.18. Sampling in the remaining quadrants is performed in an identical fashion. It is noted that the sampling array forms a square matrix in polar coordinates where theta is represented as the polar radius and phi as the polar angle.

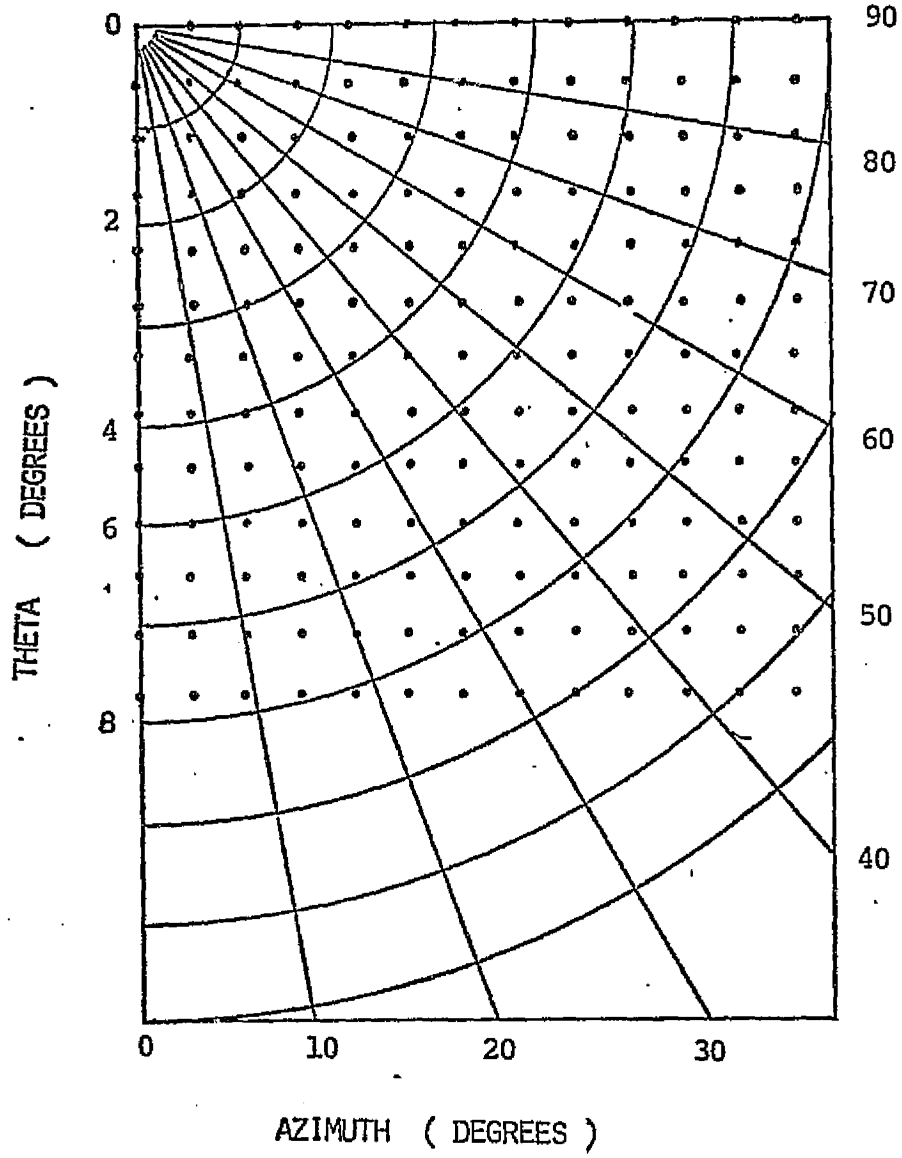

FIGURE 7.18 SAMPLING POINTS FOR A SQUARE APERTURE 1.1 METERS BY 1.1 METERS OPERATING AT A WAVELENGTH OF 2.16 CENTIMETERS

The above results are representative of the sampling requirement for the S-193 antenna [12]. Although, since the physical aperture was under-illuminated, the above result is a very conservative sampling density. A description of a program which computes the sampling points when given the aperture dimensions appears in Appendix E.

8.0 CONCLUSIONS AND RECOMMENDATIONS

8.1 General

The scatterometer equation was derived for scenes whose mean plane is flat and for an antenna having an arbitrary polarization. Ten scattering coefficients were identified for scenes not satisfying reciprocity and six were identified for scenes satisfying reciprocity. Some of the scattering coefficients were demonstrated to be complex valued and were shown to impart a relative phase between the vertically and horizontally polarized scattered components. As a result of the complex valued coefficients, the definition of a scattering coefficient had to be generalized. A new descriptive notation for the coefficients was suggested.

As a consequence of linearily scanning the scene to obtain a spatial average, it was demonstrated that the scattering coefficients must satisfy Schwartz' inequality

$$|< S_{ij}S^*_{kl}>|^2 \leqq \quad <|S_{ij}|^2> <|S_{kl}|^2> \qquad (8-1)$$

where i, j, k or l = v or h. This naturally implies that equality is assured for the polarized and cross-polarized coefficients. However, equality should, in general, not be anticipated for the cross-correlation scattering coefficients. It is this feature which distinguishes coherent and non-coherent scattering coefficients. As a result of this inequality, scatterometer returns can be partially polarized. Furthermore, the inequality also implies that one cannot employ the properties of the (coherent) scattering matrix to describe non-coherent measurements. For a coherent target five independent parameters (from the scattering matrix) are required to describe its scattering coefficients. However, a non-coherent scene requires as many as nine independent parameters.

The scatterometer equation under the reciprocity assumption was extended to account for the difference between antenna and surface polarizations. It was illustrated that the difference in polarizations was significant only a. nall view angles for narrow beam radars. The effect of misalignment can be minimized by reducing the beamwidth as one approaches nadir as illustrated in Figure (7.2). Minimizing the misalignment is important if an experimenter wishes to compare his measurements with theoretical predictions which are invariably reported with respect to the surface polarizations. It is shown, for example, that a cross polarized measurement at nadir

cannot be interpreted as an attempt to retrieve $<|S_{vh}|^2>$ as defined with respect to the surface polarizations. In view of the difficulty in interpreting measurements at small angles with respect to the surface polarizations, it is recommended that the nadir region be probed in an asymptotic sense with a very narrow beam antenna when scattering parameters are to be reported with respect to the surface polarizations. When a scene has an anisotropic behavior at small incident angles, it is particularly advantageous to report parameters in this fashion.

A measurement and inversion technique was proposed to measure all nine scattering parameters. The technique was formulated without regard to the distinction between antenna and surface polarizations. Since the difference between the polarizations is negligible for narrow beam radars at all but the small view angles, the formulation without alteration is valid there. In addition, it was shown that the system of measurements (antenna polarization states) is sufficient to retrieve all the parameters at small incident angles under an isotropic surface assumption if the inversion is based on the extended formulation, i.e., accounting for the difference between antenna and surface polarizations.

The computer simulations based on the above technique demonstrated that the dominant scattering parameters could be recovered with modest realizations of the antenna polarization requirements. However, retrieval of the weaker scattering parameters, as shown by the simulations, requires more careful adherence to the antenna polarization requirements. Cross polarized leakage in the case of linearily polarized transmissions or receptions causes the antenna to couple to the dominant scattering parameters. The leakage results not only in coupling to the real valued coefficients but also to the complex valued coefficients. The degree of coupling depends strongly on the relative phase of the leakage as well as on its amplitude. For scattering characteristics similar to that of the sea (where $<S_{vv}S_{hv}^*>$ and $<S_{vh}S_{hh}^*>$ are considered weak), strong undesirable contributions can be anticipated from $<|S_{vv}|^2>$, $<|S_{hh}|^2>$, and $<S_{vv}S_{hh}^*>$, as demonstrated by the simulations. For a scene having randomly oriented linear re-radiators such as vegetation one can anticipate not only strong contributions from the above coefficients but also from $<S_{vv}S_{hv}^*>$, $<S_{vv}S_{vh}^*>$, $<S_{vh}S_{hh}^*>$ and $<S_{hv}S_{hh}^*>$. All four scattering coefficients have been cited to emphasize that the scattering processes are different although under the reciprocity assumption there are only two independent coefficients.

It is evident from the simulations that when only the amplitude of the orthogonal leakage is known and not its phase, stringent specifications on the amplitude

are required to achieve, say, an accuracy of 0.5 dB for the weaker coefficients. This is illustrated when $<|S_{vh}|^2>$ is to be recovered from scenes having weak cross-correlation coefficients $<S_{vv}S_{hv}{}^*>$ and $<S_{vh}S_{hh}{}^*>$. When it is suspected that $<|S_{vh}|^2>$ is X dB beneath the geometric mean of $<|S_{vv}|^2>$ and $<|S_{hh}|^2>$, then the permissible level in the cross leakage is $-(X+16)$ dB. On the otherhand if the phase of the leakage can be adjusted so that it is at or near 90° (or it is known to be near 90°) during transmission and reception, then the amplitude specification can be relaxed as demonstrated by Figure 7.14. For scenes in which Re $<S_{vv}S_{hv}{}^*>$ and Re $<S_{hv}S_{hh}{}^*>$ are dominant, this same phase condition can minimize contributions by these terms in the case of cross-polarized measurements. This may be concluded by an examination of Equation (4-29).

Although the assumed scattering characteristics reflected a wide latitude of conditions, the error characteristics generated here are by no means exhaustive. The retrieval accuracy to some degree is dependent on the assumed scattering characteristics. For example, $<S_{vv}S_{vv}{}^*>$ and $<S_{vh}S_{hh}{}^*>$ were assumed weak and their error characteristics reflected this weakness. It is recommended that simulations similar to those reported in this effort be conducted whenever significantly different scattering behaviors are encountered. The antenna specifications can be established on the basis of these simulations. One may employ the program described in Appendix D in which case subroutine SIGMA must be replaced with a subroutine that will compute the scattering parameters of interest.

It is evident from these efforts that there is a fine opportunity to extend the three standard measurements to nine measurements. When the distinction between polarizations is not important,* any combinations of measurements can be selected to isolate particular coefficients. It is intriguing to consider certain combinations of measurements to observe soil moisture, crop maturity, etc. From small perturbation theory there is evidence that the cross-correlation coefficients may contain additional information on the dielectric property of the scene when compared with the auto-correlation coefficients. The comparison of like and cross-correlated coefficients may be the key to distinguishing dielectric effects, say in agrarian scenes, from volume roughness effects.

---

* This can always be achieved at all view angles except nadir if the beam is sufficiently small.

The above results also have an impact on emission theory and radiometer measurements. It is clear that the backscatter coefficients employed within this effort can be extended to the bi-static case. As a consequence, we may address emission theory from the aspects of bi-static coefficients as Peake [24] did. Generalizing Kirchoff's radiation law, Peake has shown that the definition of emissivity, when assigned standard surface polarizations, may be related to the bistatic differential scattering coefficients in the following way

$$\varepsilon_p = 1 - \int (<|S_{pp}|^2> + <|S_{pq}|^2>) \, d\Omega \qquad p \neq q \tag{8-2}$$

where the integration is performed over all incident angles. The corresponding brightness temperatures were given as

$$T_p = \varepsilon_p T_s \tag{8-3}$$

where T_s is the physical temperature of the emitting surface. Peake's formulation for brightness ignores the possibility of correlation between emitted components. When correlation exists between the components, the concept of brightness temperature must be extended as shown by Ko [47]. Ko had shown that an emission of total brightness (intensity) B_o and with a normalized coherency matrix ρ can be regarded as a unique superposition of two coherent oppositely polarized emissions, i.e.,

$$B_o \begin{bmatrix} \rho_{11} & \rho_{12} \\ \rho_{21} & \rho_{22} \end{bmatrix} = B_1 \begin{bmatrix} \rho'_{11} & \rho'_{12} \\ \rho'_{21} & \rho'_{22} \end{bmatrix} + B_2 \begin{bmatrix} \rho''_{11} & \rho''_{12} \\ \rho''_{21} & \rho''_{22} \end{bmatrix} \tag{8-4}$$

where

$$\begin{aligned} \rho'_{11} &= \rho''_{22} \\ \rho'_{12} &= -\rho''_{21} \\ \rho'_{21} &= -\rho''_{12} \\ \rho'_{22} &= \rho''_{11} \\ \rho'_{11} + \rho'_{22} &= 1 \\ \rho''_{11} + \rho''_{22} &= 1 \end{aligned} \tag{8-5}$$

Temperatures are assigned to the brightness according to the Rayleigh-Jeans law

$$T_i = B_i \lambda^2/k \tag{8-6}$$

Arbitrary measurement of this emitted field, say, with any two orthogonal polarizations will not necessarily result in any unique temperatures. The correlation between emitted components plays an important role in defining the brightness temperatures. Within the context of bi-static theory, the cross-correlation coefficients $\langle S_{vv} S_{hh}^* \rangle$, $\langle S_{vv} S_{vh}^* \rangle$, $\langle S_{hv} S_{hh}^* \rangle$, $\langle S_{vv} S_{hv}^* \rangle$ and $\langle S_{vh} S_{hh}^* \rangle$ establish this correlation. For some surfaces, the first three coefficients are not important unless the emissions within the radiating body are correlated. Under this circumstance the correlation is governed by $\langle S_{vv} S_{hv}^* \rangle$ and $\langle S_{vh} S_{hh}^* \rangle$, i.e., by the correlations which the emitting surface induces. These cross-correlations for the sea are assumed negligibly small. The brightness temperatures are, therefore, given by the vertically and horizontally polarized emissions and the corresponding decomposition into coherency matrices is given by

$$B_0 \begin{bmatrix} \rho_{11} & \rho_{12} \\ \rho_{21} & \rho_{22} \end{bmatrix} = kT_v/\lambda^2 \begin{bmatrix} 1 & 0 \\ 0 & 0 \end{bmatrix} + kT_h/\lambda^2 \begin{bmatrix} 0 & 0 \\ 0 & 1 \end{bmatrix}. \tag{8-7}$$

For an agrarian scene the above simple decomposition may not occur at all, since multiple reflections are likely to induce correlations into the emissions internal to the radiating boundary and because $\langle S_{vv} S_{hv}^* \rangle$ and $\langle S_{vh} S_{hh}^* \rangle$ are not negligible. Therefore the brightness temperature concept must be altered for agrarian scenes.

8.2 Final Remarks

The above observations as well as the developments in the earlier chapters indicate the importance of having derived the complete scatterometer equation and in particular having derived it in the framework of coherency theory. The interaction of the transmitted fields with the scattering surface was expressed as a transformation of a coherence matrix (Equation (4-41)). Interpretation of the scattered fields from its coherence matrix imparted meaning to the cross-correlation scattering coefficients. The complete scattering action of the surface, when interpreted in the context of emission theory also enables one to interpret the coherency properties of microwave emissions. The reception of scattered or emitted fields is also expressed as the product of two coherence matrices.

Although a fuller interpretational basis lies in coherency theory, practical application of the theory has led to a technique for measuring all six scattering coefficients. The measuring technique was evaluated for practical antennas. As a result of this evaluation it becomes apparent that measurement standards or standardized reporting procedures or both should be instituted. There is also a clear need to distinguish scattering parameters reported with respect to the antenna polarizations from those reported with respect to the surface polarizations. The measurement of weak scattering coefficients requires stringent realization of the antenna polarization requirements. The documentation of the antenna transmission and reception property must be complete, to include amplitude and phase properties, to validate a measurement. Until such a procedure is followed it could be erroneous to report, for example, "cross-polarized" measurements as cross-polarized scattering coefficients. To assist the experimenter it is also clear that a program should be initiated to develop a scatterometer antenna which is capable of meeting the antenna specifications for most if not all the scattering parameters for a variety of scenes.

REFERENCES

1. Ko, H. C., "Coherence Theory of Radio-Astronomical Measurements", IEEE Trans. on Ant. and Prop., vol. AP-15, no. 1, pp. 10-20, January, 1967.

2. Claassen, J. P. and A. K. Fung, "The Recovery of Apparent Temperature Distributions of Flat Scenes from Antenna Temperature Measurements", IEEE Trans. on Ant. and Prop., vol. AP-22, no. 3, pp. 433-442, May, 1974.

3. Peake, W. H., "Radar Return and Radiometric Emission from the Sea", Semi-Annual Report 3266-1, Ohio State University, Octover, 1972.

4. Grody, N. C., "Antenna Temperature for a Scanning Microwave Radiometer", IEEE Trans. on Ant. and Prop., vol. AP-23, no. 1, pp. 141-144, January, 1975.

5. Moore, R. K., "Ground Echo", Chapter 25, Radar Handbook, McGraw Hill, New York, 1970.

6. Williams, C. S., J. A. Cooper and J. R. Huynen, "Antenna-Polarization and Terrain-Depolarization Effects on Pulse-Radar Return from Extended Areas at the Near Vertical", Proceedings of the IEEE, vol. 58, no. 9, pp. 1322-1328, September, 1970.

7. Special Issue on Radar Reflectivity, Proceedings of the IEEE, vol. 53, no. 8, August, 1965.

8. Hagfor, Tor, "A Study of the Depolarization of Linear Radar Echoes", Radio Science, vol. 2, no. 5, pp. 445-465, May, 1967.

9. Collin, R. E., "The Receiving Antenna", Chapter 4, Antenna Theory, McGraw Hill Book Co., New York, 1972.

10. Axline, R. A. and R. Mater, "Theoretical and Experimental Study of Wave Scattering from Composite Rough Surfaces", University of Kansas Center for Research, Inc., RSL Technical Report 234-2, Contract DAAK02-73-C-0106, May, 1974.

11. Ulaby, F. T., "Radar Response to Vegetation", IEEE Trans. on Ant. and Prop., vol. AP-23, no. 1, pp. 36-45, January, 1975.

12. Moore, R. K., J. P. Claassen, A. C. Cook, D. L. Fayman, J. C. Holtzman, A. Sobti, W. E. Spencer, F. T. Ulaby, J. D. Young, W. J. Pierson, V. J. Cardone, J. Hayes, W. Spring, R. J. Kern and N. M. Hatcher, "Simultaneous Active and Passive Microwave Response of the Earth — The SKYLAB RADSCAT Experiment", 9th International Symposium on Remote Sensing of the Environment, Ann Arbor, Michigan, April, 1974.

13. Schelkunoff, S. A., Electromagnetic Waves, D. Van Nostrand, New York, N. Y., pp. 332-335, 1943.

14. Sinclair, G., "The Transmission and Reception of Elliptically Polarized Waves", Proceedings of the IRE, vol. 38, no. 2, pp. 148-151, February, 1950.

15. Clayton, L. and S. Hollis, "Antenna Polarization Analysis by Amplitude Measurements of Multiple Components", Microwave Journal, vol. 8, no. 1, pp. 1-6, January, 1965.

16. Schelkunoff, S. A., Electromagnetic Waves", D. Van Nostrand, New York, N. Y., p. 479, 1943.

17. Sinclair, G., "Modification of the Radar Range Equation for Arbitrary Targets and Arbitrary Polarization", Report 309-19, Antenna Laboratory, The Ohio State University Research Foundation, Columbus, Ohio, U. S. Army Contract 36-039 SC 33634, September, 1948.

18. Kennaugh, E. M., "Polarization Properties of Radar Reflections", Report 389-12, Antenna Laboratory, The Ohio State University Research Foundation, Columbus, AD2494, March, 1952.

19. Silver, S., Microwave Antenna Theory and Design, McGraw Hill, p. 177, 1949.

20. Copeland, J. P., "Radar Target Classification by Polarization Properties", Proceedings of the IRE, vol. 48, no. 7, pp. 1290-1296, July, 1960.

21. Huynen, J. R., "Measurement of the Target Scattering Matrix", Proceedings of the IEEE, vol. 53, no. 8, pp. 936-946, August, 1965.

22. Blacksmith, P., R. E. Hiatt, and R. B. Mack, "Introduction to Radar Cross Section Measurements", Proceedings of the IEEE, vol. 53, no. 8, pp. 901-920, August, 1965.

23. Kell, R. E. and R. A. Ross, "Radar Cross Section of Targets", Chapter 27, Radar Handbook, McGraw Hill, New York, 1970.

24. Peake, W. H., "Interaction of Electromagnetic Waves with Some Natural Surfaces", IRE Transaction of Ant. and Prop., (Special Supplement), vol. AP-7, pp. 5324-5329, December, 1959.

25. Ko, H. C., "On the Reception of Quasi-Monochromatic Partially Polarized Radio Waves", Proceedings of the IRE, vol. 50, no. 9, pp. 1950-1957, September, 1962.

26. Gabor, D., "Theory of Communication", Journal of the IEE (London), vol. 93, Part 3, pp. 429-457, November, 1946.

References (Continued)

27. Wiener, N., "Coherence Matrices and Quantum Theory", Journal of Mathematics and Physics, vol. 7, pp. 109-125, 1927-28.

28. Perrin, F., "Polarization of Light Scattered by Isotropic Opalescent Media", Journal of Chemistry and Physics, vol. 10, pp. 415-427, July, 1942.

29. Wolf, E., "Coherence Properties of Partially Polarized Electromagnetic Radiation", Il Nuovo Cimento, vol. 8, no. 6, pp. 2732-2753, September, 1959.

30. Born, M. and E. Wolf, Principle of Optics, Second Edition, The Macmillan Co., New York, N. Y., Chapter 10, 1964.

31. Renau, J., P. K. Cheo and H. G. Cooper, "Polarization of Linearily Polarized E. M. Waves Backscattered from Rough Metals and Inhomogeneous Dielectrics", Journal of the Opt. Soc. of America, vol. 57, pp. 459-465, April, 1967.

32. Rice, S. O., "Reflection of Electromagnetic Waves from Slightly Rough Surfaces", Communications in Pure and Applied Mathematics, vol. 4, pp. 361-378, February, 1951.

33. Peake, W. H., "Theory of Radar Return from Terrain", IRE Convention Record, vol. 7, p. 27, June, 1959.

34. Fung, A. K., "Mechanisms of Polarized and Depolarized Scattering from a Rough Dielectric Surface", Journal of the Franklin Institute, vol. 285, no. 2, pp. 125-133, February, 1968.

35. Valenzuela, G. R., "Backscattering of Electromagnetic Waves from a Tilted Slightly Rough Surface", Radio Science, vol. 3, no. 11, pp. 1057-1066, November, 1968.

36. Fung, A. K., "On Depolarization of Electromagnetic Waves Backscattered from a Rough Surface", Planetary Space Science, vol. 14, pp. 563-568, 1966.

37. Fung, A. K. and H. L. Chan, "Backscattering from a Two-Scale Rough Surface with Application to Radar Sea Return", NASA Contractor Report CR-2327, The University of Kansas Center for Research, Inc., November, 1973.

38. Hanley, W., "Analysis of the S-193 Scatterometer/Radiometer for SKYLAB", CRES TR 190-3 (Ph.D Thesis), September 1972, Supported by NASA Contract NAS 9-10261.

39. Chu, T. S. and R. G. Kouyoumjian, "An Analysis of Polarization Variation and Its Application to Circularly-Polarized Radiators", IRE Transactions on Ant. and Prop., vol. AP-10, no. 2, pp. 188-192, March, 1962.

40. Minnett, H. C. and B. MacA. Thomas, "A Method of Synthesizing Radiation Patterns with Axial Symmetry, IRE Trans. on Ant. and Prop., vol. AP-14, no. 5, pp. 654-656, September, 1966.

41. Rumsey, V. H., "Horn Antennas with Univorm Power Patterns Around Their Axis", IRE Trans. on Ant. and Prop., vol. AP-14, no. 5, pp. 656-658, September, 1968.

42. Turrin, R. H., "Dual Mode Small Aperture Antennas", IRE Trans. on Ant. and Prop. (Commun), vol. AP-15, no. 2, pp. 307-308, March, 1967.

43. Potter, P. D., "A New Horn Antenna with Suppressed Side Lobes and Equal Beamwidths", Microwave Journal, vol. 6, pp. 71-78, June, 1963.

44. Chu, T. S. and R. H. Turrin, "Depolarization Properties of Off-Set Reflector Antenna", IEEE Trans. on Ant. and Prop., vol. AP-21, no. 3, pp. 339-345, May, 1973.

45. Dixon, W. J. (Editor), BMD — Biomedical Computer Programs, University of California Press, pp. 387-396, Berkeley, 1973.

46. Law, V. J. and R. V. Bailey, "A Method for the Determination of Approximate System Transfer Functions", Chemical Engineering Science, vol. 18, pp. 189-202, 1963.

47. Ko, H. C. "Antenna Temperature and the Temperature of Electromagnetic Radiation", IEEE Trans. on Ant. and Prop., vol. AP-12, no. 1, pp. 126-127, January, 1964.

48. Klerer, M. and G. A. Korn, Digital Computer User's Handbook, Chapter 2.5 — Numerical Integration by A. H. Stroud, McGraw Hill, 1971.

APPENDIX A

Correlation and Cross-Correlation Products from Kirchhoff Theory

1.0 INTRODUCTION

The scattering and coherency properties of a finitely conducting random surface satisfying the Kirchhoff approximation are investigated within this appendix. The expressions for the polarized scattered fields in the plane of incidence are specifically derived for both vertically polarized and horizontally polarized incident plane waves. The scattered fields are derived under the assumption that the surface slopes are small. (Only zero order and first order slope terms are retained within the derivation). The resulting expression is specialized to the backscatter case to derive the self-correlation and cross-correlation scattering coefficients. The angular coherency of the scattered fields about the backscatter direction is also considered.

2.0 THEORY

2.1 General

For a plane wave $\bar{E}_o$ incident with direction $\bar{n}_i$ on a gently undulating finitely conducting bounded surface Fung [36] has shown that the far field scattered in direction $\bar{n}_s$ is given by

$$\bar{E}_s = K\bar{n}_s \times \iint \left[\bar{n}\times\bar{E} - \eta\bar{n}_s \times (\bar{n}\times\bar{H}) \right] e^{jk(\bar{n}_s-\bar{n}_i)\cdot\bar{\rho}}\, dS \qquad \text{(A-1)}$$

where

$$K = \frac{-jke^{-jkR}}{4\pi R} \qquad \text{(A-2)}$$

R = distance from the surface to the far field point

$\vec{\rho}$ = position vector from an origin local to the surface to a point on that surface

$$\bar{n}\times\bar{E} = \left[(1+R_n)(\bar{a}\cdot\bar{t}_i)(\bar{n}\times\bar{t}_i) - (1-R_v)(\bar{n}\cdot\bar{n}_i)(\bar{a}\cdot\bar{d}_i)\bar{t}_i \right] |\bar{E}_o| \quad \text{(A-3)}$$

$$\bar{n}\times\bar{H} = \left[-(1+R_v)(\bar{a}\cdot\bar{d}_i)(\bar{n}\times\bar{t}_i) - (1-R_n)(\bar{a}\cdot\bar{t}_i)\bar{t}_i \right] |\bar{E}_o| \quad \text{(A-4)}$$

$$E = E\,\bar{a}\,e^{j(\omega t - \bar{k}_i\cdot\bar{\rho})} \quad \text{(A-5)}$$

$$\bar{k}_i = k\bar{n}_i$$

$$k = 2\pi/\lambda$$

$$\bar{t}_i = \frac{\bar{n}_i \times \bar{n}}{|\bar{n}_i \times \bar{n}|}$$

$$\bar{d}_i = \bar{n}_i \times \bar{t}_i$$

η = intrinsic impedance

$R_{v,h}$ = Fresnel coefficient for horizontal (vertical) polarization

The geometry associated with the scattering problem is illustrated in Figure A-1. $\{\bar{n}_i, \bar{t}_i, \bar{d}_i\}$ forms an orthogonal triad of vectors at each point of the random surface. The plane of incidence coincides with the y - z plane. Now expanding the terms

Figure A-1. Scattering Geometry

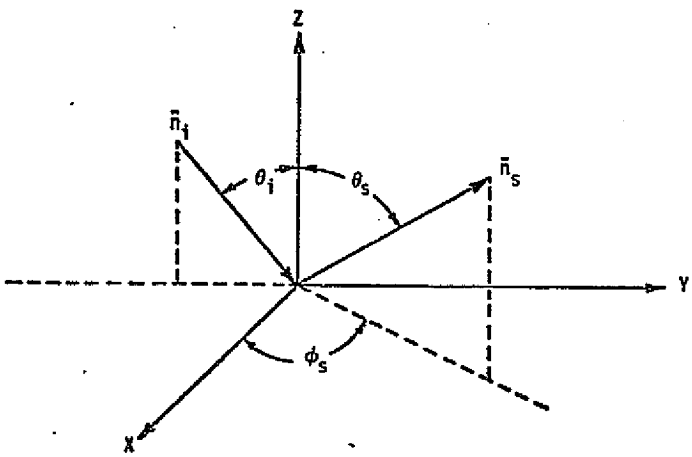

within the integrand we have

$$\bar{n}_s\times(\bar{n}\times\bar{E}) = |\bar{E}_o| \Big\{ (1+R_h)(\bar{a}\cdot\bar{t}_i) \left[(\bar{n}_s\cdot\bar{t}_i)\bar{n} - (\bar{n}_s\cdot\bar{n})\bar{t}_i \right] - (1-R_v)(\bar{n}\cdot\bar{n}_i)(\bar{a}\cdot\bar{d}_i)(\bar{n}_s\times\bar{t}_i) \Big\} \quad \text{(A-6)}$$

and

$$-\eta\bar{n}_s x(\bar{n}_s x(\bar{n} x \bar{H})) = |E_0| \Big\{ (1+R_v)(\bar{a}\cdot\bar{d}_i)\Big[(\bar{n}_s\cdot\bar{t}_i)\bar{n}_s x\bar{n} - (\bar{n}_s\cdot\bar{n})\bar{n}_s x\bar{t}_i\Big] - (\bar{n}\cdot\bar{n}_i)(1-R_h)(\bar{a}\cdot\bar{t}_i)\bar{t}_i \Big\} \qquad \text{(A-7)}$$

where a radial component was dropped under the far-field assumption. Now restrict observations to the plane of incidence so that

$$\bar{n}_s = \sin\theta_s \sin\phi_s \,\bar{i}_y + \cos\theta_s \,\bar{i}_z \qquad \text{(A-8)}$$

with $\phi_s = \pi/2$ or $-\pi/2$, depending whether the forward or back scatter quadrant is, respectively, chosen. Denote

$$\bar{n}_i = \sin\theta_i \bar{i}_y - \cos\theta_i \bar{i}_z \qquad \text{(A-9)}$$

where θ_i is the incident angle. Now it is easily shown that [36]

$$\bar{t}_i = \Big[(\sin\theta_i - \cos\theta_i Z_y)\bar{i}_x + \cos\theta_i Z_x \bar{i}_y + \sin\theta_i Z_x \bar{i}_z\Big]/D_1 \qquad \text{(A-10)}$$

and

$$\bar{d}_i = \Big[Z_x\bar{i}_x + \cos\theta_i(\cos\theta_i Z_y - \sin\theta_i)\bar{i}_y + \sin\theta_i(\cos\theta_i Z_y - \sin\theta_i)\bar{i}_z\Big]/D_1 \qquad \text{(A-11)}$$

where

$$D_1^2 = Z_x^2 + (\sin\theta_i - \cos\theta_i Z_y)^2 \qquad \text{(A-12)}$$

$$Z = Z(x,y)$$

$$Z_{x,y} = \frac{\partial Z}{\partial x,y}$$

Then

$$\bar{n}_s\cdot\bar{t}_i = (\sin\theta_s\sin\phi_s\cos\theta_i + \cos\theta_s\sin\theta_i)Z_x / D_1$$

$$\bar{n}\cdot\bar{n}_i = -(\sin\theta_i Z_y + \cos\theta_i)/D_2$$

$$\bar{n}_s\cdot\bar{n} = (\cos\theta_s - \sin\theta_s\sin\phi_s Z_y)/D_2 \qquad \text{(A-13)}$$

$$\bar{n}_s x\bar{t}_i = \Big[(\sin\theta_s\sin\phi_s\sin\theta_i - \cos\theta_s\cos\theta_i)Z_x\bar{i}_x + \cos\theta_s(\sin\theta_i - \cos\theta_i Z_y)\bar{i}_y - \sin\theta_s\sin\phi_s(\sin\theta_i - \cos\theta_i Z_y)\bar{i}_z\Big]/D_1$$

$$\bar{n}_s x\bar{n} = \Big[(\sin\theta_s\sin\theta_s + \cos\theta_s Z_y)\bar{i}_x - \cos\theta_s Z_x\bar{i}_y + \sin\theta_s\sin\phi_s Z_x\bar{i}_z\Big]/D_1$$

where

$$D_2^2 = 1+Z_x^2 + Z_y^2 \qquad \text{(A-14)}$$

2.2 Horizontally Polarized Incident Wave

Suppose $a = \bar{i}_x$, i.e., the incident wave is horizontally polarized. Then

$$\bar{a}\cdot\bar{t}_i = -(\sin\theta_i - \cos\theta_i Z_y)/ D_1^{1/2} \qquad \text{(A-15)}$$

and

$$\bar{a}\cdot\bar{d}_1 = -Z_x/ D_1^{1/2} \qquad \text{(A-16)}$$

The horizontally polarized field scattered in the plane of incidence may be shown to be given by

$$\bar{E}_s\cdot\bar{i}_{\phi_s} = K \iint I_{hh}\exp[ik(\bar{n}_s-\bar{n}_i)\cdot\bar{\rho}]\,dxdy \qquad \text{(A-17)}$$

where

$$\bar{i}_{\phi_s} = -\sin\phi_s\bar{i}_x \qquad \text{(A-18)}$$

$$I_{hh} = \sin\phi_s\left[-(1+R_h)(\cos\theta_s - \sin\theta_s\sin\phi_s Z_y) + (1-R_h)(\cos\theta_i + \sin\theta_i Z_y)\right]|E_o| \qquad \text{(A-19)}$$

Only terms to first order in Z_x and Z_y have been retained. To the same order it may be shown that the depolarized component is zero, i.e.,

$$\bar{E}_s\cdot\bar{i}_\theta = 0 \qquad \text{(A-20)}$$

2.3 Vertically Polarized Incident Wave

Suppose $\bar{a} = -\cos\theta_i\bar{i}_y - \sin\theta_i\bar{i}_z$, i.e., a vertically polarized wave is incident on the x - y plane. Then

$$\bar{a}\cdot\bar{t}_i = -Z_x/D_1 \qquad \text{(A-21)}$$

and

$$\bar{a}\cdot\bar{d}_i = (\sin\theta_i - \cos\theta_i Z_y)/D_1 \qquad \text{(A-22)}$$

The vertically polarized scattered field may be shown to be given by

$$\bar{E}_s \cdot \bar{i}_{\theta s} = K \iint I_{vv} \exp[jk(\bar{n}_s - \bar{n}_i)\cdot\bar{\rho}] ds \qquad \text{(A-23)}$$

where

$$\bar{i}_{\theta s} = \cos\theta_s \sin\phi_s \bar{i}_y - \sin\theta_s \bar{i}_z \qquad \text{(A-24)}$$

$$I_{vv} = \sin\phi_s \left[-(1+R_v)(\cos\theta_s - \sin\theta_s \sin\phi_s Z_y) + (1-R_v)(\cos\theta_i + \sin\theta_i Z_y)\right] |\vec{E}_o| \qquad \text{(A-25)}$$

Only terms to first order in Z_x and Z_y have been retained in I_{vv}. To the same order it may be shown that the depolarized component is zero, i.e.,

$$\vec{E}_s \cdot \vec{i}_\phi = 0 \qquad \text{(A-26)}$$

2.4 Linear Approximations for the Reflection Coefficients

It is necessary to understand that the reflection coefficients are functions of the local incident angle and are therefore functions of the local slopes, Z_x and Z_y. For small slopes we may approximate R_h and R_v linearily by

$$R_{h,v}(Z_x,Z_y) = R_{h,v}(0,0) + \frac{\partial R_{h,v}(0,0)}{\partial Z_x} Z_x + \frac{\partial R_{h,v}(0,0)}{\partial Z_y} Z_y \qquad \text{(A-27)}$$

Now the relation between the local incident angle θ' and the local slopes is

$$\cos\theta' = -\bar{n}_i \cdot \bar{n} \qquad \text{(A-28)}$$

or

$$= [Z_y \sin\theta_i + \cos\theta_i]/D_2 \qquad \text{(A-29)}$$

The derivatives within the linearily approximated reflection coefficients can then by the chain rule be written

$$\frac{\partial R_{v,h}}{\partial Z_{x,y}} = \frac{\partial R_{v,h}}{\partial \theta'} \frac{\partial \theta'}{\partial Z_{x,y}} \qquad \text{(A-30)}$$

An evaluation of the derivatives yields

$$\left.\frac{\partial R_h}{\partial \theta'}\right|_{Z_x=Z_y=0} = \frac{2\sin\theta_i R_h(\theta_i)}{\sqrt{\epsilon_r - \sin^2\theta_i}}$$

$$\left.\frac{\partial R_v}{\partial \theta'}\right|_{Z_x=Z_y=0} = \frac{-2\epsilon_r \sin\theta_i R_v(\theta_i)}{\sqrt{\epsilon_r-\sin^2\theta_i}\,(\epsilon_r\cos^2\theta_i-\sin^2\theta_i)}$$

$$\left.\frac{\partial \theta'}{\partial Z_x}\right|_{Z_x=Z_y=0} = 0 \qquad \text{(A-31)}$$

$$\left.\frac{\partial \theta'}{\partial Z_y}\right|_{Z_x=Z_y=0} = -1$$

It has been recognized in the above expressions that $\theta' = \theta_i$ when $Z_x = Z_y = 0$. We finally have the approximate expressions

$$R_v(Z_x,Z_y) \cong R_v(\theta_i) + \frac{2\epsilon_r \sin\theta_i R_v(\theta_i) Z_y}{\sqrt{\epsilon_r-\sin^2\theta_i}\,(\epsilon_r\cos^2\theta_i-\sin^2\theta_i)} \qquad \text{(A-32)}$$

and

$$R_h(Z_x,Z_y) \cong R_h(\theta_i) - \frac{2\sin\theta_i R_h(\theta_i)\, Z_y}{\sqrt{\epsilon_r-\sin^2\theta_i}} \qquad \text{(A-33)}$$

2.5 Partial Evaluation of the Field Integrals

The evaluation of the polarized field expressions requires that integrals of the type

$$\text{Intg} = \iint Z_y \exp[jk(\bar{n}_s-\bar{n}_i)\cdot\bar{\rho}]\,dx\,dy \qquad \text{(A-34)}$$

be considered. By employing an integration by parts technique, specifically by letting

$$dv = \exp[jk(\cos\theta_s+\cos\theta_i)Z]Z_y\,dy \qquad \text{(A-35)}$$

and

$$u = \exp[jk(\sin\theta_s\sin\phi_s-\sin\theta_i)y] \qquad \text{(A-36)}$$

we get

$$\text{Intg} = \int vu\Big|_{\text{boundary}} dx - \iint \frac{s}{c} \exp[jk(\bar{n}_s-\bar{n}_i)\cdot\bar{\rho}] \qquad \text{(A-37)}$$

where

$$\frac{s}{c} = \frac{\sin\theta_s \sin\phi_s - \sin\theta_i}{\cos\theta_s + \cos\theta_i} \qquad \text{(A-38)}$$

The first term is identified as the edge effect and may be neglected.

When the above results are incorporated in the field integrals we can write a unifying expression

$$E_j(\theta_s, \theta_s) = -K B_j \; I(\bar{n}_s, \bar{n}_i) \; E_0 \qquad \text{(A-39)}$$

where

$$I = \iint \exp[jk(\bar{n}_s - \bar{n}_i)\cdot\bar{\rho}] \; dxdy$$

$$B_j = \sin\phi_s \left\{ (1+R_j - \frac{s}{c}\frac{\partial R_j}{\partial Z_y})\cos\theta_s - (1-R_j + \frac{s}{c}\frac{\partial R_j}{\partial Z_y})\cos\theta_i - [(1+R_j)\sin\theta_s\sin\phi_s + (1-R_j)\sin\theta_i]\frac{s}{c} \right\} \qquad \text{(A-40)}$$

E_j (j = v or h) denotes the like polarized field component when a jth polarized wave of amplitude E_o illuminates the surface. The reflection coefficient and its derivative are evaluated at the incident angle.

3.0 THE BACKSCATTER COEFFICIENTS

Now specialize to the backscatter case. Specifically, let $\theta_s = \theta_i$ and $\theta_s = -\pi/2$. Then

$$E_j(\theta_i, -\frac{\pi}{2}) = K B_j' I(-\bar{n}_i, \bar{n}_i) E_0 \qquad \text{(A-41)}$$

where

$$B_j' = B_j(\theta_s = \theta_i, \; \Phi = -\Pi/2) \qquad \text{(A-42)}$$

The differential scattering coefficient employed in this effort is given by

$$\langle S_{jj} S_{kk}^* \rangle = \frac{\langle E_j E_k^* \rangle R^2}{|E_o|^2 \; A\cos\theta_i} \qquad \text{(A-43)}$$

where A is the illuminated area. Consider the ratio of the intensities

$$\frac{<E_j E_k^*>}{|E_o|^2} = |K|^2 B_j B_k <II^*> \tag{A-44}$$

where

$$<II^*> = \iiiint \exp[-j2k_y(y_1-y_2)]<\exp[j2k_z(Z_1-Z_2)]>dx_1dx_2dx_2dy_2$$

$$k_y = k\sin\theta_i \tag{A-45}$$

$$k_z = k\cos\theta_i \tag{A-46}$$

Suppose that Z_1 and Z_2 are joint gaussian variables with zero mean, variance σ^2 and correlation $\Lambda(x_1, x_2, y_1, y_2)$. Then it is easily shown from the characteristic function properties of gaussian variables that

$$<\exp[j2k_z(Z_1-Z_2)]> = \exp[-4k_z^2\sigma^2(1-\Lambda)] \tag{A-47}$$

Now transform the resulting integral to the center of mass coordinates. Let

$$\begin{aligned} u &= x_1-x_2 \\ v &= y_1-y_2 \\ x_2 &= x_2 \\ y_2 &= y_2 \end{aligned} \tag{A-48}$$

The integral then can be written as

$$<II^*> = \iiiint \exp[-j2k_yv]\ \exp[-4k_z^2\sigma^2(1-\Lambda)]\ dudvdx_2dy_2 \tag{A-49}$$

Further transform the integral to cylindrical coordinates where

$$\begin{aligned} u &= \rho\cos\xi \\ v &= \rho\sin\xi \\ x_2 &= \rho'\cos\zeta \\ y_2 &= \rho'\sin\zeta \end{aligned} \tag{A-50}$$

If it is further assumed that the surface is statistically stationary and isotropic, then

$$\langle II^* \rangle = \iiiint G(\rho)G(\rho') \exp[-j2k_z \sin\xi\rho] \exp[-4k_z^2\sigma^2(1-\Lambda(\rho))]\,\rho\, d\rho d\xi \rho' d\rho' d\zeta \quad \text{(A-51)}$$

where $G(\rho)$ is a gate function describing the limits of the illuminated area. Specifically

$$G(\rho) = \begin{cases} 1 & \text{if } \rho \leq A/\pi \\ 0 & \text{if } \rho \geq A/\pi \end{cases} \quad \text{(A-52)}$$

where A is the area of illumination in the mean plane of the surface. Now recall that

$$\int_0^{2\pi} \exp(\pm j\alpha \sin\xi)d\xi = 2\pi J_0(\alpha) \quad \text{(A-53)}$$

The integral will then reduce to

$$\langle II^* \rangle = 2\pi A \int_0^{\infty} G(\rho)\exp[-4k_z^2\sigma^2(1-\Lambda(\rho))]\, J_0(2k\sin\theta_i\rho)\rho d\rho \quad \text{(A-54)}$$

An asymptotic evaluation of the above integral for large $k_z^2\sigma^2$ yields

$$\langle II^* \rangle = \frac{\pi A e^{-\tan^2\theta_i/2m^2}}{2k^2m^2\cos^2\theta_i} \quad \text{(A-55)}$$

where $\sigma^2/\ \rho''(0)$ has been identified as the slope variance m^2.

Combining the above results it is clear that

$$\langle S_{jj} S_{kk}^* \rangle = \frac{B_j' B_k^{*\prime}\, e^{-\tan^2\theta_i/2m^2}}{32\pi m^2\cos^3\theta_i} \quad \text{(A-56)}$$

where j, k = v or h.

4.0 THE ANGULAR COHERENCY OF THE SCATTERED FIELDS

At this point consider the mutual coherence function

$$\mathcal{E}_{ij}(\theta_1, \theta_2, \phi_s) = \langle E_i(\theta_1, \phi_s) E_j^*(\theta_2, \phi_s) \rangle \quad \text{(A-57)}$$

where $i(j) = v$ or h. The coherence function denotes the cross-correlation between two field components scattered in the plane of incidence at scattering angles θ_1 and θ_2 with a common range R. The expectation is an ensemble average over all random surfaces satisfying the Kirchhoff approximation. Now in view of (A-39) the coherence function can be written in the form

$$\mathcal{E}_{ij} = |E_0 K|^2 C_{ij} \iiiint \langle \exp[jk(\bar{n}_1-\bar{n}_i)\cdot\bar{\rho}_1 - (\bar{n}_2-\bar{n}_i)\cdot\bar{\rho}_2] \rangle dx_1 dy_1 dx_2 dy_2 \quad \text{(A-58)}$$

where

$$C_{jk} = B_j B_k^* \quad \text{(A-59)}$$

Now transform the center of mass coordinate system where

$$\begin{aligned} u &= x_1 - x_2 \\ v &= y_1 - y_2 \end{aligned} \quad \text{(A-60)}$$

Also let $\theta_1 = \theta_i$ and $\theta_2 = \theta_i + \Delta\theta$ where $\Delta\theta$ is a small deviation from the backscatter direction. We have

$$(\bar{n}_1-\bar{n}_i)\cdot\bar{\rho}_1 = -2(\sin\theta_i y_1 + \cos\theta_i Z_1) \quad \text{(A-61)}$$

$$(\bar{n}_2-\bar{n}_i)\cdot\bar{\rho}_2 = (-2\sin\theta_i + \Delta\theta\cos\theta_i)y_2 + (2\cos\theta_i - \Delta\theta\sin\theta_i)Z_2$$

Now for a gaussian random surface having a surface height characteristic with zero mean, variance σ^2 and correlation function Λ, the expectation within the integral becomes

$$\langle \quad \rangle = \exp[-j2k_y v + jk_z\Delta\theta y_2]\exp[-k_y^2\sigma^2\Delta\theta^2/2]\exp[-4k_z^2\sigma^2(1-\Lambda)] \quad \text{(A-62)}$$

The integral then can be written as

$$\text{Intg} = \exp[-k_y^2\sigma^2\Delta\theta^2/2]\iiiint \exp[-j2k_y v + jk_z\Delta\theta y_2]\cdot \exp[4k_z^2\sigma^2(1-\Lambda)]\, du\,dv\,dx_2\,dy_2 \quad \text{(A-63)}$$

Now transform the integral expression to cylindrical coordinates by letting

$$\begin{aligned} u &= \rho\cos\xi \\ v &= \rho\sin\xi \\ x_2 &= \rho'\cos\xi \\ y_2 &= \rho'\sin\xi \end{aligned} \tag{A-64}$$

Then

$$\mathcal{E}_{jk}(\Theta_1,\Theta_2) = |K|^2 C_{jk}\, |E_o|^2 \exp(-k_y^2\sigma^2\Delta\Theta^2/2)\,\mathrm{Intg} \tag{A-65}$$

where

$$\mathrm{Intg} = \iiiint G(\rho)G(\rho')\exp[-j2k_y\sin\xi\rho]\exp[jk_z\Delta\theta\sin\zeta\rho'] \exp[2k_z{}^2\sigma^2(1-\Lambda(\rho))]\,\rho d\rho d\xi\rho' d\rho d\zeta \tag{A-66}$$

and where it has been assumed that z is stationary and isotropic. $G(\rho)$ is a gate function defining the region of uniform illumination on the mean plane. Using Equation A-53 twice, we can write the integral as

$$\mathrm{Intg} = (2\pi)^2 I_1 I_2 \tag{A-67}$$

where

$$\begin{aligned} I_1 &= \int G(\rho)J_o(2k_y\rho)\,\exp[4k_z{}^2\sigma^2(1-\Lambda)]\rho\, d\rho \\ I_2 &= \int G(\rho')J_o(k_z\,\Delta\theta\,\rho')\rho' d\rho' \end{aligned} \tag{A-68}$$

For a circularly illuminated area of radius R_o the latter integral can be evaluated to get

$$I_2 = R_o^2\,\mathrm{Jinc}(k_z R_o \Delta\theta) \tag{A-69}$$

where $\mathrm{Jinc}(x) = J_1(x)/x$. As a consequence, for a circular region of area A we have

$$\mathcal{E}_{jk} = 4\,A\,|K|^2 C_{jk}\exp(-k_y^2\sigma^2\Delta\Theta^2/2)\,\mathrm{Jinx}(k_z R_o\Delta\Theta)\,I_1|E_o|^2 \tag{A-70}$$

Now normalize the mutual coherence function in the following fashion

$$\Gamma_{jk} = \mathcal{E}_{jk}\, 4\pi R_o^2/(|E_o|^2 A \cos\Theta_i) \tag{A-71}$$

Now recognize that for small $\Delta\Theta$

$$\Gamma_{jk} \cong 2\exp(-k_y^2\sigma^2\Delta\theta^2/2)\,\mathrm{Jinc}(x)\,4\pi\langle S_{jj}S_{kk}^*\rangle$$

where $x = k_z R_o \Delta\Theta$. (See equations A-43 and A-54). The degree of coherence or correlation is consequently related to the mutual coherency function by

$$D = \Gamma_{jk}/(4\pi\langle S_{jj}S_{kk}^*\rangle) \tag{A-72}$$

or

$$= 2\exp(-k_y^2\sigma^2\Delta\theta^2/2)\,\mathrm{Jinc}(k_z R_o \Delta\theta)$$

Consider the character of the degree of coherency. Except for extremely large $k\sigma$ values the exponential term contributes negligibly to D at small incident angles. The decorrelation is consequently largely governed by the Bessel function for small incident angles. D vanishes at the zeroes of Jinc. The first zero occurs where

$$\Delta\Theta k R_o \cos\Theta = 3.832 \tag{A-73}$$

The corresponding angular separation is given by

$$\Delta\Theta = 3.832/kR_o\cos\Theta \tag{A-74}$$

Suppose $k = 291$ ($f = 13.9$ GHz), $R_o = 10$ meters and $\theta = 25^\circ$; then decorrelation occurs when $\Delta\theta = 0.00146$ radians or at .08 degrees. It is concluded that radar returns decorrelate rapidly with changes in view angles.

At large incident angle (grazing angles) the exponential factor will predominate. This result is physically reasonable since the surface roughness predominates the view; whereas at small angles the area of illumination as conveyed in Jinc is the dominant factor.

APPENDIX B

The Scatterometer Equation Within the Context of a Scattering Theory

1.0 INTRODUCTION

The scatterometer equation is once again derived within the context of a specific scattering theory. The structure and meaning of the formulation, as a consequence, readily becomes apparent. Specifically, the angular correlation assumption is shown to be equivalent to the non-coherent property of scattering; the relation between scattering operator and the scattering coefficient is clarified also.

1.1 Derivation and Discussion

Silver [19] has shown that the far field radiated in the direction $\bar{n}_s$ from a bounded closed surface S having surface excitation $\bar{E}$ and $\bar{H}$ is given by

$$\bar{E}_s = \frac{-jk}{4\pi R} e^{-jkR} \bar{n}_s \times \iint_S \left[\bar{n} \times \bar{E} - \eta \bar{n}_s \times (\bar{n} \times \bar{H}) \right] e^{jk\bar{\rho}\cdot\bar{n}_s} \, ds \tag{B-1}$$

where

R = distance from the surface to the far field point

$\bar{\rho}$ = position vector from an origin local to the surface to a point on the surface

$\bar{n}$ = surface unit normal

$k = 2\pi/\lambda$

η = intrinsic impedance

The geometrical entries of the above expression are illustrated in Figure B-1. Suppose that the surface is smoothly undulating and perfectly conducting. Then under the Kirchhoff approximation the tangent surface fields are given by

$$\bar{n} \times \bar{E} = 0 \tag{B-2}$$

and

$$\bar{n} \times \bar{H} = 2\, \bar{n} \times \bar{H}_t \tag{B-3}$$

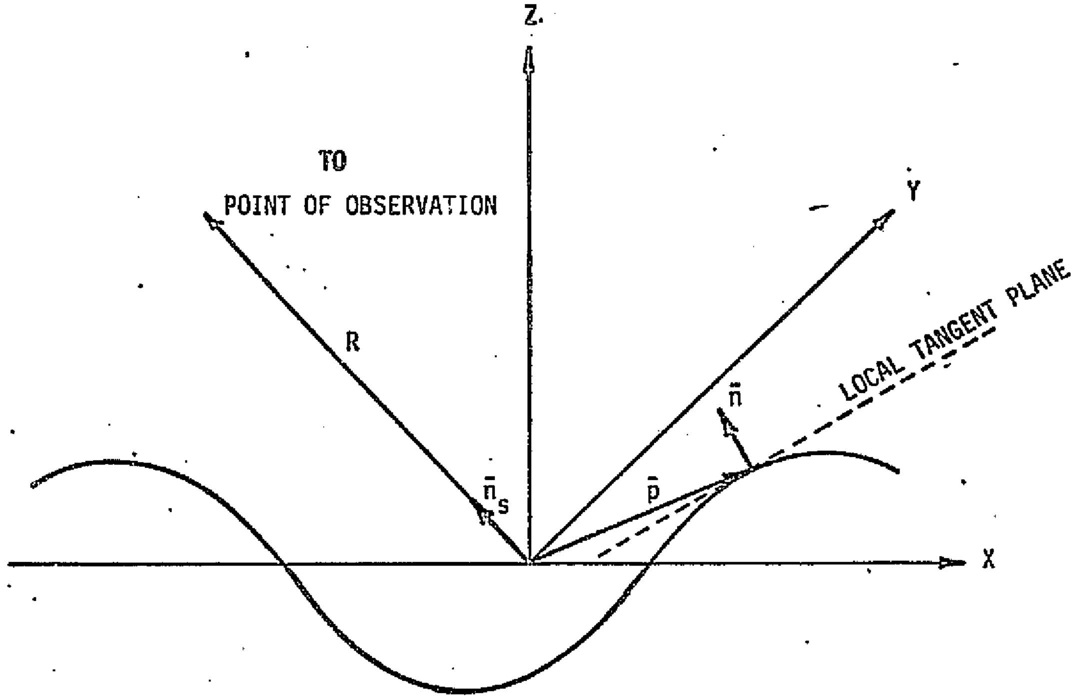

FIGURE B-1 GEOMETRY FOR SCATTERING INTEGRAL

where $\bar{H}_t$ is transmitted field incident on the surface. The scattered field, therefore, simplifies to

$$\bar{E}_s = \frac{jk\eta}{2\pi R} e^{-jkR} \bar{n}_s \times \iint \bar{n}_s \times (\bar{n} \times \bar{H}_t) e^{jk\bar{p}\cdot\bar{n}_s} ds \qquad \text{(B-4)}$$

Now when specializing to the backscatter case we can write

$$\bar{n}_s \times (\bar{n}_s \times (\bar{n} \times \bar{H}_t)) = - (\bar{n}_s \cdot \bar{n}) \bar{n}_s \times \bar{H}_t \qquad \text{(B-5)}$$

so that

$$\bar{E}_s = \frac{-jke^{-jkR}}{2\pi R} \iint (\bar{n}_s \cdot \bar{n}) \bar{E}_t e^{jk\bar{p}\cdot\bar{n}_s} ds \qquad \text{(B-6)}$$

where for the backscatter case

$$\bar{E}_t = \eta \bar{n}_s \times \bar{H}_t \qquad \text{(B-7)}$$

In beginning with the far field expression we have in effect anticipated the use of a non-coherent assumption since in scatterometry one would not necessarily be in the far field if the entire scattering aperture were coherent.

Now the spherical incident field is denoted as

$$\bar{E}_t = -j K \bar{L}_t e^{j(\omega t - kR)} \qquad \text{(B-8)}$$

where

$K = \omega\mu_o i_t/4\pi R$ (B-9)

i_t = antenna input current

$\bar{L}_t$ = complex effective height vector of the antenna

The range R is measured from the antenna as illustrated in Figure B-1. The spherical wave can be approximated by segments of plane waves each illuminating a patch of the surface. In addition, the incident field amplitude components as conveyed by $\bar{L}_t$ may be considered constant on a given patch. Suppose the entire illuminated surface is segmented into N patches. Then the incident field on the mth patch may be approximated by

$$\bar{E}_{tm} = -j K_m \bar{L}_{tm} e^{j(\omega t - kR_m + k \bar{p}_m\cdot\bar{n}_{sm})} \qquad \text{(B-10)}$$

where

R_m = range to the centroid of the mth patch

$\bar{\rho}_m$ = position vector from the centroid to a surface point in the mth patch

$\bar{n}_{sm}$ = unit vector in the backscatter direction for the mth patch

$K_m = \omega\mu_o i_t / 4 R_m$

Now from Equation (B-6) we note that the backscattered field for the mth patch is given by

$$\bar{E}_{sm} = \frac{k K_m e^{-j\,2kR_m}}{2\pi R_m} \bar{L}_{tm} \iint_{S_m} (\bar{n} \cdot \bar{n}_{sm})\, e^{j\,2k\,\bar{\rho}\cdot\bar{n}_{sm}}\, ds \qquad \text{(B-11)}$$

The integration is performed on the surface within patch m.

Now define the scattered field per differential steradian subtended about the antenna as

$$\vec{\mathcal{E}}_{sm} = \frac{\vec{E}_{sm} R_m^2}{\Delta A_m \cos\theta_m} \qquad \text{(B-12)}$$

where ΔA_m is the area of the mth patch in the mean plane of the surface and θ_m is the incident angle on the mth patch. The scattering operator employed within Chapter 4 may be identified with the above expression, viz.,

$$\mathcal{S}_{vv}(\theta_m, \phi_m) = \lim_{\Delta A_m \to 0} \frac{\vec{\mathcal{E}}_{sm} \cdot \bar{i}_{\theta m}\, 4\pi R}{-j\, K_m\, l_{vtm}\, e^{-jkR_m}} \qquad \text{(B-13)}$$

$$\mathcal{S}_{hh}(\theta_m, \phi_m) = \lim_{\Delta A_m \to 0} \frac{\vec{\mathcal{E}}_{sm} \cdot \bar{i}_{\phi m}\, 4\pi R}{-j\, K_m\, l_{htm}\, e^{-jkR_m}}$$

where

$$l_{vtm} = \vec{L}_t \cdot \bar{i}_{\theta m}$$

$$l_{htm} = \vec{L}_t \cdot \bar{i}_{\phi m} \qquad \text{(B-14)}$$

The inner products above isolate the vertically and horizontally polarized components as defined with respect to surface. It is appropriate to denote $\mathcal{S}_{pp}$ as an operator since it must recognize the phase of the incident field relative to the centroid of the patch. Whether these differential scattering operators exist is not important to the development within the appendix. However, within the main text they are assumed to exist at least in approximate form.

Within the context of this theory $\mathcal{S}_{vh} = \mathcal{S}_{hv} = 0$. This is simply a statement of a well known result that a smoothly undulating perfectly conducting surface does not depolarize the incident field. In general, the latter operators are not zero. The above incremental field is defined so that the total field at the antenna is given by

$$\bar{E}_a = \sum_{m=1}^{N} \bar{\mathcal{E}}_{sm} \quad \Delta\Omega_m \tag{B-15}$$

or in the continuum limit

$$\bar{E}_a = \int \vec{\mathcal{E}}_s \quad d\Omega \tag{B-16}$$

It must be recognized that the antenna does not respond to the total field, a quantity often computed by the theorist. Instead the antenna responds so that the open circuit voltage induced into the antenna terminals by the mth patch is given by

$$\Delta V_{oc} = \bar{\mathcal{E}}_{sm} \cdot \bar{L}_{rm} \, \Delta\Omega_m \tag{B-17}$$

where $\bar{L}_{rm}$ is the complex effective height vector in the direction of the mth patch during reception. The total induced voltage is clearly approximated by

$$V_{oc} = \sum_{m=1}^{N} \bar{\mathcal{E}}_{sm} \cdot \bar{L}_{rm} \, \Delta\Omega_m \tag{B-18}$$

The average power available under matched conditions at the antenna terminals is given by the ensemble average

$$W_r = \frac{1}{8R_r} \quad < |V_{oc}|^2 > \tag{B-19}$$

or

$$W_r = \frac{1}{8R_r} \sum_{m=1}^{N} \sum_{n=1}^{N} < \bar{\mathcal{E}}_{sm} \cdot \bar{L}_{rm} \; \vec{\mathcal{E}}_{sn}^{*} \cdot \bar{L}_{rn}^{*} > \quad \Delta\Omega_m \, \Delta\Omega_n \tag{B-20}$$

where R_r is the radiation resistance of the antenna during reception.
Now the scattered fields and effective heights can be decomposed into polarization components coinciding with the surface polarizations, viz.,

$$\vec{\mathcal{E}}_{sm} = \mathcal{E}_{smv} \, \bar{i}_{\theta m} + \mathcal{E}_{smh} \, \bar{i}_{\phi m} \tag{B-21}$$

and

$$\bar{L}_{rm} = l_{vrm} \, \bar{i}_{\theta m} + l_{hrm} \, \bar{i}_{\phi m} \tag{B-22}$$

The expectation can then be written in the form

$$< \vec{\mathcal{E}}_{sm} \cdot \bar{L}_{rm} \, \vec{\mathcal{E}}^{*}_{sm} \cdot \bar{L}^{*}_{rn} > \; = \; < (\mathcal{E}_{vsm} \, l_{vrm} + \mathcal{E}_{hsn} \, l_{hrn}) (\mathcal{E}^{*}_{vsn} \, l^{*}_{vrn} + \mathcal{E}^{*}_{hsn} \, l^{*}_{hsn}) > \tag{B-23}$$

or

$$= \mathrm{tr}\, M_{rmn} \, M^{\dagger}_{smn} \tag{B-24}$$

where

$$M_{smn} = \begin{bmatrix} < \mathcal{E}_{vsm} \, \mathcal{E}^{*}_{vsn} > & < \mathcal{E}_{vsm} \, \mathcal{E}^{*}_{hsn} > \\ < \mathcal{E}_{hsm} \, \mathcal{E}^{*}_{vsn} > & < \mathcal{E}_{hsm} \, \mathcal{E}^{*}_{hsn} > \end{bmatrix} \tag{B-25}$$

and

$$M_{rmn} = \begin{bmatrix} l_{vrm} \, l^{*}_{vrn} & l_{vrm} \, l^{*}_{hrn} \\ l_{hrm} \, l^{*}_{vrn} & l_{hrm} \, l^{*}_{hrn} \end{bmatrix} \tag{B-26}$$

are identified as mutual coherence matrices. The mutual coherence matrix for the scattered field is composed of elements correlating fields arriving from patches m and n or equivalently from different angular directions (θ_m, ϕ_m) and (θ_n, θ_n). Now within Appendix A it is shown it is reasonable to assume, on pragmatic grounds, that returns arriving at different view angles from the same patch are uncorrelated. The assumption is exact in the geometric-optics limit. It is even more reasonable to assume here that fields arriving from different angles are uncorrelated since they arise from different patches. As a consequence the mutual coherence matrices have the special property

$$M_{sjk} = N_{sjj} \delta_{jk} \tag{B-27}$$

for every jk. δ_{jk} is the Kronecker delta and

$$N_{sjj} = \begin{bmatrix} < |\mathcal{E}_{vsj}|^2 > & < \mathcal{E}_{vsj} \, \mathcal{E}^{*}_{hsj} > \\ < \mathcal{E}_{hsj} \, \mathcal{E}^{*}_{vsj} > & < |\mathcal{E}_{hsj}|^2 > \end{bmatrix} \tag{B-28}$$

The non-coherent assumption, consequently, allows us to write the received power in the form

$$W_r = \frac{1}{8R_r} \; \mathrm{tr} \sum_{j=1}^{N} \Big(\sum_{k=1}^{N} M_{rjk} \, \delta_{jk} \, \Delta\Omega_k \Big) \, N^{\dagger}_{sjj} \, \Delta\Omega_j \tag{B-29}$$

or

$$= \frac{1}{8R_r} \sum \mathrm{tr}\, C_{rj} \left(N^{\dagger}_{sjj} \;\; \Delta\Omega_j \right) \Delta\Omega_j \tag{B-30}$$

where

$$C_{rj} = M_{rjj} \tag{B-31}$$

is the coherency matrix for the receiving antenna in direction (θ_j, ϕ_j). Now expanding $N_{sjj}\, \Delta\Omega_j$, we have

$$N_{sjj}\, \Delta\Omega_j = \frac{4\, k^2 |K_j|^2 R_j^2}{(4\pi)^2\, \Delta A_j \cos\theta_j} \begin{bmatrix} B_{jvv} & B_{jvh} \\ B_{jhv} & B_{jhh} \end{bmatrix} \tag{B-32}$$

where

$$B_{jpq} = 1_{ptj}\, 1^*_{qtj} \iint_{S_j} < (\bar{n} \cdot \bar{n}_{sj})(\bar{n}' \cdot \bar{n}_{sj})\, e^{-j2k[\bar{\rho}\cdot\bar{n}_{sj} - \bar{\rho}'\cdot\bar{n}_{sj}]} > dS\, dS' \tag{B-33}$$

From the above expression we note that the incident field complex amplitude components 1_{vt} and 1_{ht} have been separated from the scattering integrals. The relative phase between incident amplitude components is retained in the products $1_{ptj} 1_{qtj}^*$. Now the non-coherent differential scattering coefficients per unit steradian for the jth patch is defined as

$$< S_{pp}\, S^*_{qq} > = \frac{4k^2}{(4\pi)^2} \iint_{S_j} < (\bar{n}\cdot\bar{n}_{sj})(\bar{n}'\cdot\bar{n}_{sj})\, e^{j2k[\bar{\rho}\cdot\bar{n}_{sj} - \bar{\rho}'\cdot\bar{n}_{sj}]} > dS\, dS' \tag{B-34}$$

(See Equation (A-43), Appendix A). As a consequence we can write the coherency matrix for the scattered fields based on intensities per unit steradian in notation similar to that of Equation (4-16) of Chapter 4. We have

$$C_{sj} = N_{sjj}\, \Delta\Omega_j \tag{B-35}$$

or

$$= |K_j|^2 \begin{bmatrix} <|S_{vv}|^2> |1_{vtj}|^2 & < S_{vv}\, S^*_{hh} > 1_{vtj}\, 1^*_{htj} \\ < S^*_{vv}\, S_{hh}> 1^*_{vtj}\, 1_{htj} & <|S_{hh}|^2> |1_{htj}|^2 \end{bmatrix} \tag{B-36}$$

We have shown above that the elements of the coherency matrix change units after the non-coherent assumption has been applied to the double summation. The return power can now be written as

$$W = \frac{1}{8R_r} \sum_{j=1}^{N} \mathrm{tr}\, C_{rj}\, C_{sj}^{\dagger}\, \Delta\Omega_j \tag{B-37}$$

or upon taking the limit of the sum as $\Delta\Omega_k \to 0$, we get an integral approximation

$$W = \frac{1}{8R_r} \int \mathrm{tr}\, C_r\, C_s^{\dagger}\, d\Omega \tag{B-38}$$

where the above equation has a form identical to that of Equation (4-13) of Chapter 4 when $\beta_{vh} = 0$.

APPENDIX C

Correlation and Cross-Correlation

Scattering Properties of a Slightly Rough Surface

1.0 THEORETICAL DEVELOPMENT

For a plane wave incident with angle θ_i in the x - z plane on slightly rough surface, satisfying the requirement

$$(k\,\sigma\cos\theta_i)^2 \ll 1 \tag{C-1}$$

where σ^2 = surface height variance and $k = 2\pi/\lambda$, the solution for the scattered fields is expressed in a perturbation expansion of spatial Fourier components [32] [33] [34] [35]. The Fourier components are interpreted as an angular spectrum of plane waves. Suppose, the spectral components are denoted as $A_p^v\,(k_x, k_y)$ where

$$k_x = k\sin\theta_s\cos\phi_s$$

$$k_y = k\sin\theta_s\sin\phi_s \tag{C-2}$$

$$p = x, y, z$$

Figure C-1. Scattering Geometry

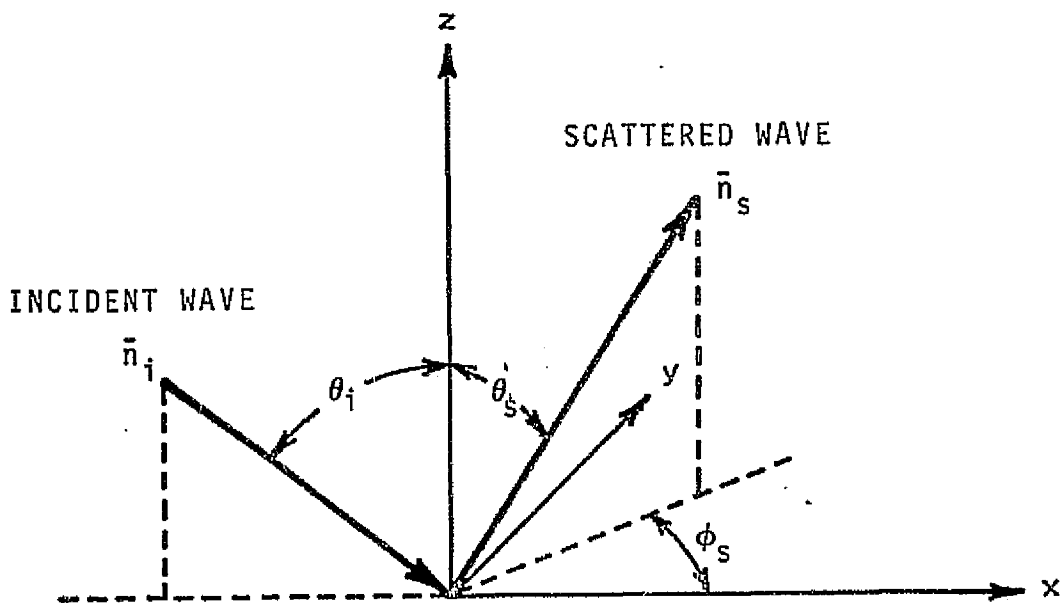

when a vertically polarized plane wave illuminates the surface and as $A^h_p(x,y,z)$ when a horizontally polarized plane illuminates the surface. (See Figure C-1). For either case the electric field E_p^q at point (x,y,z) is given by an inverse Fourier transform relationship

$$E_p^r = \frac{1}{(2\pi)^2}\iint A_p^r\,(k_x\,,\,k_y)\,e^{j(k_x x + k_y y - k_z z)}\,dk_x dk_y \tag{C-3}$$

where $k_z^2 = k^2 - k_x^2 - k_y^2$. The superscripts denote the incident polarization whereas the subscripts denote the scattered cartesian components (E_x^r, E_y^r, E_z^r). If we suppose that a highly directional antenna points in the direction (θ_s, ϕ_s) with beam-volume $\Delta\theta\Delta\phi$, then only certain spectral components near

$$\begin{aligned} k_x &= k\sin\theta_s\cos\phi_s \\ k_y &= k\sin\theta_s\sin\phi_s \\ k_z &= k\cos\theta_s \end{aligned} \tag{C-4}$$

will be observed. The angular spectral space surrounding (θ_s, ϕ_s) with angular volume $\sin\theta_s\Delta\theta\Delta\phi$ is given by

$$\Delta k_x\,\Delta k_y = |J|\,\Delta\theta\,\Delta\phi \tag{C-5}$$

where

$$|J| = \begin{vmatrix} \dfrac{\partial k_x}{\partial\theta_s} & \dfrac{\partial k_y}{\partial\theta_s} \\ \dfrac{\partial k_x}{\partial\phi_s} & \dfrac{\partial k_y}{\partial\phi_s} \end{vmatrix} = k^2\sin\theta_s\,\cos\theta_s \tag{C-6}$$

Now the cross-correlation of electric field components <u>observed</u> within the antenna beamwidth is given by

$$<\Delta E_p^r\,\Delta E_q^{s*}> \cong \frac{1}{(2\pi)^4}\iiiint_{\Delta\times\Delta} <A_p^r A_q^{s*}>\,e^{j(k_x x + k_y y)}\,e^{-j(\kappa_x x + \kappa_y y)}\,dk_x dk_y d\kappa_x d\kappa_y \tag{C-7}$$

where

$\Delta x \Delta = (\Delta k_x \Delta k_y) \times (\Delta k_x \Delta k_y)$ denotes the cartesian domain of integration. The solution for the spectral components are given by the form [35]

$$A_p^{\,r}(k_x,k_y) = A_{op}^{\,r}(\bar{k},\bar{k}')Z(k_x+k\sin\theta_o,\, k_y) \qquad \text{(C-8)}$$

for the first order solutions and by the forms

$$\begin{aligned} B^r_{x,y}\,(k_x,k_y) = {} & B^r_{o\,x,y}\iint A^r_{x,y}\, Z(k_x-\alpha, k_y-\beta)\,d\alpha\, d\beta\; + \\ & B^r_{1_{x,y}}\iint f_1(\bar{k},\bar{k}')\, Z(\alpha+k\sin\theta,\beta)\, Z(k_x-\alpha,\, k_y-\beta)\,d\alpha\, d\beta\; + \\ & B^r_{2_{x,y}}\iint f_2(\bar{k},\bar{k}')\, Z(\alpha+k\sin\theta,\beta)\, Z(k_x-\alpha,\, k_y-\beta)\,d\alpha\, d\beta\; + \\ & B_{3_{x,y}}\iint A^r_{y,x}\; Z(k_x-\alpha,\, k_y-\beta)\,d\alpha\, d\beta \end{aligned} \qquad \text{(C-9)}$$

and

$$B_z^{\,r}\,(k_x,k_y) = \frac{k_x}{k_z}\, B_x^{\,r} + \frac{k_y}{k_z}\, B_y^{\,r} \qquad \text{(C-10)}$$

for the second order fields. $Z(k_x, k_y)$ is a random variable describing the Fourier spectral heights of the rough surface and $k_z = \sqrt{k^2 - k_x^2 - k_y^2}$. The coefficients A^r_{op}, $B^r_{ox,y}$ $B^r_{2x,y}$ and $B^r_{3x,y}$ are determinstic functions depending on the propagation constants in the upper and lower media. For the purposes of this appendix it is sufficient to observe that the first order fields are dependent on $Z(k_x, k_y)$ whereas the second order fields are dependent on $Z(\alpha+k\sin\theta_o, \beta)\, Z(k_x-\alpha, k_y-\beta)$. The functional form of the A and B coefficients is at this point immaterial.

2.0 CORRELATION PRODUCTS FROM THE FIRST ORDER FIELDS — CASE I

Now consider a typical correlation product from the first order solutions. We have from the integrand of (C-5)

$$A_p(k_x,k_y)\, A_p^*(\kappa_x,\kappa_y) = A^r_{op}(\bar{k},\bar{k}')\, A^{s\,*}_{op}(\bar{\kappa},\bar{\kappa}') \langle Z(k_x+k\sin\theta_o,\, k_y)Z^*(\kappa_x+k\sin\theta_o,\, \kappa_y)\rangle \qquad \text{(C-11)}$$

The expectation can be written as

$$<Z(u\ ,v\ )Z^*(u',v')> \quad = \quad \iiiint <z(x\ ,y\ )z(x',y')> \cdot e^{-j(ux + vy)}\, e^{j(u'x'+v'y')}\, dx\, dy\, dx'dy' \qquad \text{(C-12)}$$

where z and Z are Fourier transform pairs. If the random process is stationary, then

$$<z(x\ ,y\ )\ z(x',v')> \ = \ R(x-x',\ v-y') \qquad \text{(C-13)}$$

where R is the auto-correlation function of the surface heights. Now transform the variable to the center of mass coordinates, i.e., let $\tau_x = x - x'$, $\tau_y = y - y'$, $x' = x$ and $y' = y'$. Then

$$<Z(u\ ,v\ )Z^*(u',v')> \ = \ \iiiint R(\tau_x,\ \tau_y)e^{-j(\tau_x u\ +\ \tau_y v)}\, d\tau_x d\tau_y\ e^{j[(u'-u)x'\ +\ (v'-v)y']}\, dx'dy'$$

or

$$= \ \iint W(u,v)\ e^{-j\left[(u-u')x'\ +\ (v-v')y'\right]}\, dx'dy' \qquad \text{(C-14)}$$

where W(u,v) is the spectral density of the surface heights. Finally we recognize that

$$<Z(u\ ,v\ )Z^*(u',v')> \ = \ (2\pi)^2\ W(u\ ,v\ )\ \delta(u-u',v-v') \qquad \text{(C-15)}$$

When the above results is substituted into the correlation integral we get

$$<\Delta E_p^r\ \Delta E_q^{*s}> \ = \frac{1}{(2\pi)^2} \iint_{\Delta\times\Delta} A_{op}^r\ A_{oq}^{*s}\ W(k_x + k\sin\theta_o,\ k_y)dk_x\ dk_y \qquad \text{(C-16)}$$

When Δ is sufficiently small, the incremental complex intensity may be approximated by

$$<\Delta E_p^r\ \Delta E_q^{*s}> \ = \ \frac{A_{op}^r\ A_{oq}^{*s}}{(2\pi)^2}\, W(k_x + k\sin\theta_o,\ k_y)\Delta k_x \Delta k_y \qquad \text{(C-17)}$$

The cross-correlation per unit steradian is therefore given by

$$\frac{<\Delta E_p^r\ \Delta E_q^{*s}>}{\sin\theta_s \Delta\theta_s \Delta\phi_s} \ = \ \frac{k^2\cos\theta_s A_{op}^r\ A_{oq}^{*s}}{(2\pi)^2}\ W(k_x + k\sin\theta,\ k_y) \qquad \text{(C-18)}$$

where (C-5) has been used. The total cross-correlation in direction (θ_s, ϕ_s) is given by

$$<E_p^r E_q^{s*}> = \frac{k^2\cos^2\theta_s A_{op}^r A_{oq}^{s*} W(k_x + k\sin\theta_o, k_y)}{(2\pi)^2} \frac{\Delta A}{R^2} \quad \text{(C-19)}$$

where ΔA is the illuminated area in the x - y plane and R is the range to the element of area.

To consider the horizontally and vertically polarized backscattered components we must realize that the horizontal polarized component is related to the cartesian components by

$$A_h^r(k_x,k_y) = -A_x^r(k_x,k_y)\sin\phi_s + A_y^r(k_x,k_y)\cos\phi_s \quad \text{(C-20)}$$

and the vertical component by

$$A_v^r(k_x, k_y) = A_x^r(k_x,k_y)\cos\theta_s\cos\phi_s + A_y^r(k_x, k_y)\cos\theta_s\sin\phi_s - A_z^r(k_x,k_y)\sin\theta_s \quad \text{(C-21)}$$

When we specialize to the backscatter direction $(\theta_s = \theta_o, \phi_s = \pi)$, we see that

$$A_h^r(k_x,k_y) = -A_y^r(k_x,k_y) \quad \text{(C-22)}$$

and

$$A_v^r(k_x,k_y) = A_x^r(k_x,k_y)\cos\theta_o - A_z^r(k_x,k_y)\sin\theta_o \quad \text{(C-23)}$$

with $k_x = k\sin\theta_o$, $k_y = 0$, $k_z = k\cos\theta_o$. It is well known that the first order backscatter fields do not involve depolarized components [34]. From reference [35] we now identify

$$A_h^h\ (k_x,k_y) \ = \ -j2k\cos\theta_o R_h\ Z(2k\sin\theta_o,0) \tag{C-24}$$

and

$$A_v^v\ (k_x,k_y) \ = \ -j2k\cos\theta_o T_v[\ \epsilon_r(1+\sin^2\theta_o) - \sin^2\theta_o]Z(2k\sin\theta_o,0) \tag{C-25}$$

where

R_h = Fresnel reflection coefficient for horizontal polarization

T_v = Fresnel transmission coefficient for vertical polarization

ε_r = relative (complex) dielectric constant.

and where a unit amplitude incident wave has been assumed. Therefore the correlation components in the backscatter direction become

$$<E_v^v\ E_v^{v*}> \ = \ \frac{4k^4\cos^4\theta_o}{(2\pi)^2}\left|T_v\left[\epsilon_r(1+\sin^2\theta_o) - \sin^2\theta_o\right]\right|^2\ W(2k\sin\theta_o,\ 0)\frac{\Delta A}{R^2} \tag{C-26}$$

$$<E_v^v\ E_h^{h*}> \ = \ \frac{4k^4\cos^4\theta_o}{(2\pi)^2}\ T_v\left[\epsilon_r(1+\sin^2\theta_o) - \sin^2\theta_o\right]R_h^*\ W(2k\sin\theta_o,\ 0)\ \frac{\Delta A}{R^2} \tag{C-27}$$

$$<E_h^h\ E_h^{h*}> \ = \ \frac{4k^4\cos^4\theta_o}{(2\pi)^2}\ |R_h|^2\ \ W(2k\sin\theta_o,\ 0)\frac{\Delta A}{R^2} \tag{C-28}$$

The corresponding generalized differential scattering coefficient per unit intensity per steradian is given by

$$<S_{pp}^r\ S_{qq}^{*s}> \ = \ <E_p^r\ E_q^{s*}>\frac{R^2}{\Delta A\cos\theta_o} \tag{C-29}$$

(See the generalized definition of the scattering coefficients in Chapter 4). So

$$<|S_{vv}|^2> \ = \ \frac{k^4}{\pi^2}\ \cos^3\theta_o\ |T_v[\ \epsilon_r(1+\sin^2\theta_o)-\sin^2\theta_o]|^2\ \ W(2k\sin\theta_o,\ 0) \tag{C-30}$$

$$<S_{vv}S_{hh}^{*}> = \frac{k^4\cos^3\theta}{\pi^2}\left[T_v\left[\epsilon_r(1+\sin^2\theta_o) - \sin^2\theta_o\right]\right]R_h^{*}\, W(2k\sin\theta_o, 0) \qquad \text{(C-31)}$$

$$<|S_{hh}|^2> = \frac{k^4\cos^3\theta}{\pi^2}|R_h|^2 \quad W(2k\sin\theta_o, 0) \qquad \text{(C-32)}$$

3.0 CORRELATION BETWEEN FIRST AND SECOND ORDER FIELDS — CASE II

To develop the correlations between first and second order fields it is sufficient to note that the correlations involve expectations of the type $< Z(k_x,k_y) Z^*(\alpha,\beta) Z^*(K_x - \alpha, K_y - \beta)$ and of type $Z(k_x,k_y) Z^*(\alpha+k\sin\theta,\beta) Z^*(K_x-\alpha, K_y-\beta)$. These expectations involve independent gaussian random variables with zero mean and consequently vanish. The first and second order fields are therefore uncorrelated. It is concluded that $<S_{vv}S_{vh}^*> = 0$ and $<S_{hv}S_{hh}^*> = 0$ at the lowest order.

APPENDIX D

Scatterometer Simulation Program (SCATSIM)

1.0 INTRODUCTION

The theory and operation of the scatterometer simulation program is described within this appendix. The following section shows how the scatterometer equation of Chapter 4 was implemented with ideal and non-ideal antenna parameters. The computation of the inversion models with and without recognition of the difference between surface and antenna polarizations is also described. Finally the operation of the program is treated by means of a flow chart. A source listing and a sample output is also presented. Additional program documentation is provided by comments within the program.

2.0 THEORY

2.1 Simulation of the Scatterometer Equation

Since the scattering characteristics were based on surface polarizations, Equations (6-47), (6-49) and (6-50a) through (6-50i) were implemented for use on the computer. The equation was simulated using identical functional forms for the vertically and horizontally polarized patterns (if they are both present during a transmission or reception). Recall that the normalized patterns are given by

$$g_{v,h} = \frac{|1_{v,h}(\theta',\phi')|^2}{|1_v(0,0)|^2 + |1_h(0,0)|^2} \qquad \text{(D-1)}$$

where $(\theta', \phi') = (0, 0)$ is the boresight point. As a consequence, we require

$$g_v(0,0) + g_h(0,0) = 1 \qquad \text{(D-2)}$$

Now if g denotes the functional form for the pattern and has the property $g(0,0) = 1$ and if g_h is assigned the value ag where $a \leq 1$, then we require that $g_v = (1-a)g$. The scatterometer equation under the above assumption can be written as

$$W(\theta_o) = \frac{\lambda^2 G_t G_r}{(4\pi z)^2} \int I_{tr}(g \cos\theta)^2 \, d\Omega \qquad \text{(D-3)}$$

where

$$\begin{aligned} I_{tr} = \; & I_1 \langle |S_{vv}|^2 \rangle + I_2 \langle |S_{hh}|^2 \rangle + I_3 \langle |S_{vh}|^2 \rangle + \\ & 2I_4 \operatorname{Re}\langle S_{vv} S_{hh}^* \rangle - 2I_5 \operatorname{Im}\langle S_{vv} S_{hh}^* \rangle + 2I_6 \operatorname{Re}\langle S_{vv} S_{hv}^* \rangle - \\ & 2I_7 \operatorname{Im}\langle S_{vv} S_{hv}^* \rangle + 2I_8 \operatorname{Re}\langle S_{vh} S_{hh}^* \rangle - 2I_9 \operatorname{Im}\langle S_{vh} S_{hh}^* \rangle \end{aligned} \qquad \text{(D-4)}$$

where

$$\begin{aligned} I_1 = \; & (1-a_r)(1-a_t)\cos^4\psi + a_r a_t \sin^4\psi + ((1-a_r)a_t + \\ & (1-a_t)a_r + 4c_t c_r)\sin^2\psi\cos^2\psi \end{aligned} \qquad \text{(D-5)}$$

$$\begin{aligned} I_2 = \; & a_t a_r \cos^4\psi + (1-a_t)(1-a_r)\sin^4\psi + ((1-a_r)a_t + \\ & (1-a_t)a_r + 4c_t c_r)\sin^2\psi\cos^2\psi \end{aligned} \qquad \text{(D-6)}$$

$$\begin{aligned} I_3 = \; & ((1-a_t)a_r + (1-a_r)a_t - 2c_t c_r)(\cos^4\psi + \sin^4\psi) + \\ & 2((1-a_r)(1-a_t) + a_t a_r - 6c_t c_r + (2a_r-1)(2a_t-1)) \cdot \\ & \sin^2\psi\cos^2\psi + 2s_t s_r \end{aligned} \qquad \text{(D-7)}$$

$$I_4 = c_t c_r(\cos^4\psi + \sin^4\psi) + ((2a_r-1)(2a_t-1) - 2c_t c_r)\cdot \sin^2\psi\cos^2\psi - s_r s_t \tag{D-8}$$

$$I_5 = (c_r s_t + c_t s_r)(\cos^2\psi - \sin^2\psi) \tag{D-9}$$

$$I_6 = ((1-a_r)c_t + (1-a_t)c_r)\cos^4\psi - (a_r c_t + a_t c_r) \sin^4\psi + 3((2a_r-1)c_t + (2a_t-1)c_r)\sin^2\psi \cos^2\psi \tag{D-10}$$

$$I_7 = ((1-a_r)s_t + (1-a_t)s_t)\cos^2\psi + (a_r s_t + a_t s_r)\sin^2\psi \tag{D-11}$$

$$I_8 = (a_t c_r + a_r c_t)\cos^4\psi - ((1-a_r)c_t + (1-a_t)c_r) \sin^4\psi - 3((2a_r-1)c_t + (2a_t-1)c_r)\cos^2\psi\sin^2\psi \tag{D-12}$$

$$I_9 = (a_t s_r + a_r s_t)\cos^2\psi + ((1-a_r)s_t + (1-a_t)s_r) \sin^2\psi \tag{D-13}$$

$$\begin{aligned} c_t &= \sqrt{a_t(1-a_t)}\ \cos\beta_t \\ c_r &= \sqrt{a_r(1-a_r)}\ \cos\beta_t \\ s_t &= \sqrt{a_t(1-a_t)}\ \sin\beta_t \\ s_r &= \sqrt{a_r(1-a_r)}\ \sin\beta_r \end{aligned} \tag{D-14}$$

The integration is performed in the surface coordinate system (See Figure 4.1). In the above expression all odd powers in $\sin\psi$ have been pragmatically dropped. These factors are odd functions of $\emptyset$ and will not contribute to the integral (See Equation 4-33).

Now since the scattering characteristic was assumed isotropic, the return power can be approximated by

$$
\begin{aligned}
W(\theta_\circ) = \frac{\lambda^2 G_t G_r}{(4\pi z)^2} \sum_{\omega=1}^{N} & <|s_{vv}|^2>_\omega \int_{\Omega_\omega} I_1 (g \cos\theta)^2 \, d\Omega \\
& + <|s_{hh}|^2>_\omega \int_{\Omega_\omega} I_2 (g \cos\theta)^2 \, d\Omega \\
& + <|s_{vh}|^2>_\omega \int_{\Omega_\omega} I_3 (g \cos\theta)^2 \, d \\
& + 2 \operatorname{Re}<|s_{vv} s_{hh}^*>_\omega \int_{\Omega_\omega} I_4 (g \cos\theta)^2 \, d\Omega \\
& - 2 \operatorname{Im}<|s_{vv} s_{hh}^*>_\omega \int_{\Omega_\omega} I_5 (g \cos\theta)^2 \, d\Omega \\
& + 2 \operatorname{Re} <s_{vv} s_{hv}^*>_\omega \int_{\Omega_\omega} I_6 (g \cos\theta)^2 \, d\Omega \\
& - 2 \operatorname{Im} <s_{vv} s_{hv}^*>_\omega \int_{\Omega_\omega} I_7 (g \cos\theta)^2 \, d\Omega \\
& + 2 \operatorname{Re} <s_{vh} s_{hh}^*>_\omega \int_{\Omega_\omega} I_8 (g \cos\theta)^2 \, d\Omega \\
& - 2 \operatorname{Im} <s_{vh} s_{hh}>_\omega \int_{\Omega_\omega} I_9 (g \cos\theta)^2 \, d\Omega
\end{aligned} \tag{D-15}
$$

and where $\{\Omega_\omega , \omega = 1,2,\ldots,N\}$ is a set of half degree annuli centered about the sub-observation point. $< >_\omega$ denotes an evaluation of the scattering coefficient on the Ω_ω annulus. Function subroutine SIGMA contains the functional representations for all nine scattering coefficients. The integrations are performed, of course, only over those annuli where the pattern function g is significant. The above approximation reduces the computation to integrals of the following kinds:

$$J_1(\omega) = \int_{\Omega_\omega} g^2 \cos^2\theta \cos^4\psi \, d\Omega \qquad J_3(\omega) = \int_{\Omega_\omega} g^2 \cos^2\theta \sin^2\psi \cos^2\psi \, d\Omega$$

$$J_2(\omega) = \int_{\Omega_\omega} g^2 \cos^2\theta \sin^4\psi \, d\Omega \qquad J_4(\omega) = \int_{\Omega_\omega} g^2 \cos^2\theta \sin^2\psi \, d\Omega.$$

$$J_5(\omega) = \int_{\Omega_\omega} g^2 \cos^2\theta \cos^2\psi \, d\Omega \qquad J_6(\omega) = \int_{\Omega_\omega} g^2 \cos^2\theta \, d\Omega \tag{D-16}$$

These integrals are evaluated in subroutine DINTEG using a two-dimensional Gaussian-Legendre quadrature technique [48]. For a selected antenna pattern and a selected view angle the return power is computed in accord with the above expression. The antenna gains G_t and G_r are formed in a separate computation. These factors are based on an evaluation of the expression

$$G_t = G_r = \frac{2}{\int g \sin\theta' \, d\theta'} \tag{D-17}$$

The evaluation of the above integral is performed in subroutine SOLID, which employs a single dimension Gaussian-Legendre quadrature. The numerical evaluation of the pattern functions is provided by subroutine LAMBDA. All of the above integrations are executed from the mainline of SCATSIM.

Since the relative phases β_t and β_r were assumed stationary over the main beam and first side lobe, the return power could be evaluated for various combinations of a_r, a_t, β_t and β_r without re-evaluating the double integrals. As a consequence, an arbitrary pattern condition within the above constraints ($g_v = (1-a)g$ and $g_h = ag$) could be established. The combination of relative amplitudes and phases for the fifteen prescribed measurements are shown in Table D.1. Subroutine ANTENNA, when addressed with zero arguments, generates those prescribed values. When amplitude and phase biases and/or perturbations are entered as arguments, subroutine ANTENNA will apply biases of the prescribed value to all measurements in which a_r or a_t is zero or unity. Random perturbations are applied to the remaining cases if the perturbation arguments are non-zero. In this fashion either measurements based on 15 ideal or 15 deviated antenna conditions can be generated. The actual coefficients required in the integrand factors $\{I_i, i = 1, 9\}$ are computed in subroutine COEF. COEF fills a 15 x 9 x 6 array with the appropriate values so that the return power can be computed for each of the 15 measurements. Let C_{ijk} denote the array. The i subscript designates the measurement number, the j subscript identifies one of the nine scattering coefficients within the integrand, and the k subscript identifies one of the six kinds of integrands ($J_k(\omega)$). See Table D.2 for the entries in C_{ijk}. Let γ_i, $i = 1,9$ denote the nine scattering coefficients and

TABLE D.1

MEASUREMENT NO.	COEF	α_t	β_t	α_r	β_r
1	$<\|S_{vv}\|^2>$	0	—	0	—
2	$<\|S_{hh}\|^2>$	1	—	1	—
3	$<\|S_{vh}\|^2>$	0	—	1	—
4	$Re<S_{vv}S_{hh}^*>$	0.5	-90°	0.5	90°
5	$Re<S_{vv}S_{hh}^*>$	0.5	0°	0.5	180°
6	$Im<S_{vv}S_{hh}^*>$	0.5	45°	0.5	-135°
7	$Im<S_{vv}S_{hh}^*>$	0.5	-45°	0.5	135°
8	$Re<S_{vv}S_{hv}^*>$	0	—	0.5	0°
9	$Re<S_{vv}S_{hv}^*>$	0	—	0.5	180°
10	$Im<S_{vv}S_{hv}^*>$	0	—	0.5	90°
11	$Im<S_{vv}S_{hv}^*>$	0	—	0.5	-90°
12	$Re<S_{vh}S_{hh}^*>$	1	—	0.5	0°
13	$Re<S_{vh}S_{hh}^*>$	1	—	0.5	180°
14	$Im<S_{vh}S_{hh}^*>$	1	—	0.5	90°
15	$Im<S_{vh}S_{hh}^*>$	1	—	0.5	-90°

TABLE D-2

THE COEFFICIENT MATRIX C_{ijk}

ROW/COL.	1	2	3	4	5	6
1	$(1-a_t)(1-a_r)$	$a_r a_t$	$(1-a_r)a_t + (1-a_t)a_r + 4c_t c_r$	0	0	0
2	$a_r a_t$	$(1-a_t)(1-a_r)$	$(1-a_r)a_t + (1-a_t)a_r + 4c_t c_r$	0	0	0
3	$(1-a_t)a_r + (1-a_r)a_t - 2c_t c_r$	$(1-a_t)a_r + (1-a_r)a_t - 2c_t c_r$	$(1-a_r)(1-a_t) + a_t a_r + (2a_r-1)(2a_t-1) - 6c_t c_r$	0	0	$2s_t s_r$
4	$2c_t c_r$	$2c_t c_r$	$2[(2a_r-1)(2a_t-1) - 2c_t c_r]$	0	0	$-2s_t c_r$
5	0	0	0	$-2(c_r s_t + c_t s_r)$	$2(c_r s_t + c_t s_r)$	0
6	$2[(1-a_r)c_t + (1-a_t)c_r]$	$-2[a_r c_t + a_t c_r]$	$6[(2a_r-1)c_t + (2a_t-1)c_r]$	0	0	0
7	0	0	0	$-2[(1-a_r)s_t + (1-a_t)s_r]$	$-2[a_r s_t + a_t s_r]$	0
8	$2[a_t c_r + a_r c_t]$	$-2[(1-a_r)c_t + (1-a_t)c_r]$	$-6[(2a_r-1)c_t + (2a_t-1)c_r]$	0	0	0
9	0	0	0	$-2(a_t s_r + a_r s_t)$	$-2[(1-a_r)s_t + (1-a_t)s_r]$	0

NOTE: The different planes of C_{ijk}, $i = 1,2,\ldots,15$, are formed by substituting values for a_t, β_t, a_r and β_r from Table D.2.

let $\gamma_i(\omega)$ denote its evaluation on the Ω_ω annulus. Furthermore let

$$K_{kl} = \sum_{\omega=1}^{N} \gamma_l(\omega)\; J_k(\omega) \tag{D-18}$$

where $J_k(\omega)$ denotes the evaluation of J_k on the Ω_ω annulus. Then the return power is given by

$$W_i(\theta_o) = \left[\frac{\lambda^2 G_t G_r}{(4\pi z)^2}\right] \operatorname{tr}\left[\sum_{k=1}^{6} C_{ijk}\; K_{kl}\right]_{jl} \tag{D-19}$$

Subroutine EXACT performs the above computation for $i = 1,2,\ldots.15$. For each measurement (i) the contribution by each γ_j is isolated by EXACT and stored in its second argument. The power matrix is clearly given by

$$P_{ij} = \frac{\lambda^2 G_t G_r}{(4\pi z)^2} \sum_{k=1}^{6} C_{ijk} K_{kj} \tag{D-20}$$

The structure of the return can thus be examined.

Another routine, called IDEAL, also estimates the return power but without regard to the distinction between surface and antenna polarizations. The computation follows the above scheme, however, it recognizes that $\psi = 0$. In this case all the necessary information is carried in $J_6(\omega)$. Again IDEAL isolates the power contributions by each scattering coefficient and consequently forms a power matrix also.

2.^ The Inversion Models

The above formulation of the return power was designed so that the exact or approximate inversion model parameters could be isolated from intermediate steps. Either model assumes that the measurement can be approximated by

$$\sum_{j=1}^{4} M_{ij}\;\gamma_j(\theta_o) = W_i(\theta_o) \tag{D-21}$$

where M_{ij} is a 15 x 9 matrix. Each row of M corresponds to one of the fifteen measurements. When the distinction between surface and antenna polarizations is required, the elements of M_{ij} are simply filled by forming

$$M_{ij} = \sum_{k=1}^{6} C_{ijk} \sum_{\omega=1}^{N} J_k(\omega) \qquad \text{(D-22)}$$

M_{ij} is constructed in subroutine EXACT. Once M_{ij} has been constructed the inverse model is computed by forming the normal equations $M_{ij} M_{ik}$ and computing its inverse (HEMINV in the mainline). The inversion for this model is performed in subroutine MATRIX. Within MATRIX a least squares solution is executed, viz.,

$$\gamma_i'(\theta_o) = (M^{\dagger}M)^{-1}_{ij} \sum_{k=1}^{15} M^{\dagger}_{jk} \, W_k(\theta_o) \qquad \text{(D-23)}$$

This subroutine also accumulates the first and second order error statistics during a Monte Carlo study. A call to a secondary entry MATSHOW will display the statistical results.

Similarly when the distinction between polarization frames is not required, an approximate inversion model may be formed from Equation D-22 above by simply setting $\psi = 0$ in each $J_K(\omega)$ (See Equation D-16). Symbolically we have

$$M_{ij} = \sum_{k=1}^{6} C_{ijk} \sum_{\omega=1}^{N} J_k(\omega, \psi=0) \qquad \text{(D-24)}$$

The integrals need not be re-evaluated since all the desired information is contained in $J_6(\omega)$. Particularly $J_1(\omega, \psi = 0) = J_5(\omega, \psi = 0) = J_6(\omega)$. The remaining J are identically zero. These special properties were recognized and accordingly a routine (IDEAL) was prepared to evaluate the elements of M_{ij} for this case. The inversion of this model is performed as suggested in Chapter 6. Recall that the $<|S_{vv}|^2>$, $<|S_{hh}|^2>$ and $<|S_{vh}|^2>$ are each computed from a single observation (a row of M). The remaining coefficients are computed by differencing pairs of equations (rows). The inversion for this model is performed in subroutine DIFFER. Again first and second order error statistics are accumulated. They are displayed by calling the secondary entry DIFSHOW.

The reader should note that routines EXACT and IDEAL play dual roles. Either can form their respective inversion models or they can compute the return powers for the fifteen kinds of measurements. Only EXACT computes the exact return power since the scattering coefficients are defined with respect to the surface polarizations. The option to use IDEAL to compute return power exists to compare the two polarization frames.

2.3 Documentation for SCATSIM

A macro-flow chart of program SCATSIM is shown in Figures D.1 through D.4. The program is organized into roughly four functions. Each figure covers one of the program functions. Figure D.1 documents the part of the program which reads the instruction card and initializes various parameters for use in the actual simulations. This portion of the program, once validating the instruction, prepares various descriptive antenna parameters such as beamwidth and gain. These parameters and the input parameters are displayed to document the case study. The second zero in the pattern function is employed to establish the domain of integration. The domain is broken into N half degree annuli. On each annulus $J_k(\omega)$, $k = 1,2,\ldots 6$ and $\omega = 1,2,\ldots,N$ is computed. Once $J_k(\omega)$ are formed, $K_{k1}, \sum_{\omega=1}^{N} J_k(\omega)$ and $\sum_{\omega=1}^{N} J_k(\omega, \psi=0)$ are computed and scaled for the antenna gain effect.

Following the above initialization, the program simulates the fifteen measurements under ideal antenna specifications. The structure of this program portion is illustrated in Figure D.2. Subroutine ANTENNA is called with zero arguments to prepare an ideal antenna parameter set $\{\alpha_t, \beta_t, \alpha_r, \beta_r\}_i$, $i = 1,2,\ldots,15$. Subroutine IDEAL forms the approximate (ideal) inversion model and a power matrix which ignores the distinction between surface and antenna polarizations. Both the inversion model and the power matrix are displayed. The inversion model is stored for subsequent use by DIFFER. Subroutine COEF forms C_{ijk} from the ideal antenna parameter set. In turn, EXACT then uses C_{ijk} to compute the exact inversion model, M_{ij}. It is again called to form the exact power matrix. The normal equations are prepared from the model and then is inverted by HEMINV. If the system is singular, a flag (ISING) is set true. All matrix inversions are subsequently by-passed by an appropriate test. The exact inversion model and the inverse of the normal equations are stored for subsequent use by MATRIX. Once the return power is computed, both difference and matrix inversions are performed and the statistical (accuracies) results are shown for the ideal antenna.

If the bias parameter ABIAS is non-zero, a bias error study is performed. This portion of the program is illustrated in Figure D.3. The processing follows, for the most part, that performed in characterization of the ideal antenna; however, the two bias parameters ABIAS and BBIAS are employed in the arguments of ANTENNA to introduce pattern deviations from the ideal case. The inversions are performed using the ideal antenna models.

If the perturbation parameter AMAX is non-zero a Monte-Carlo study is performed.

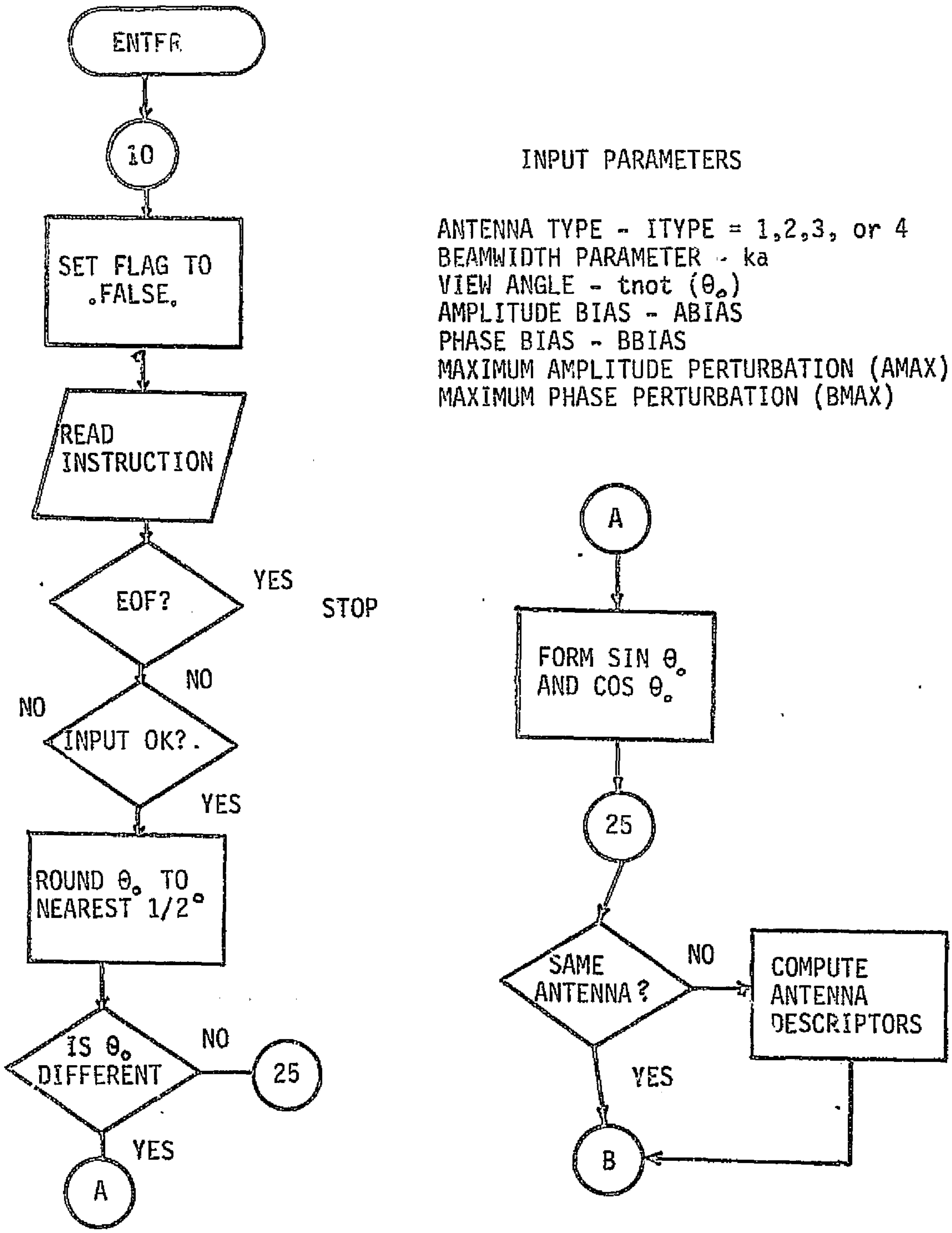

Figure D.1a — MACRO-FLOW CHART FOR SCATSIM — PROGRAM INITIALIZATION AND ANTENNA PARAMETERIZATIONS

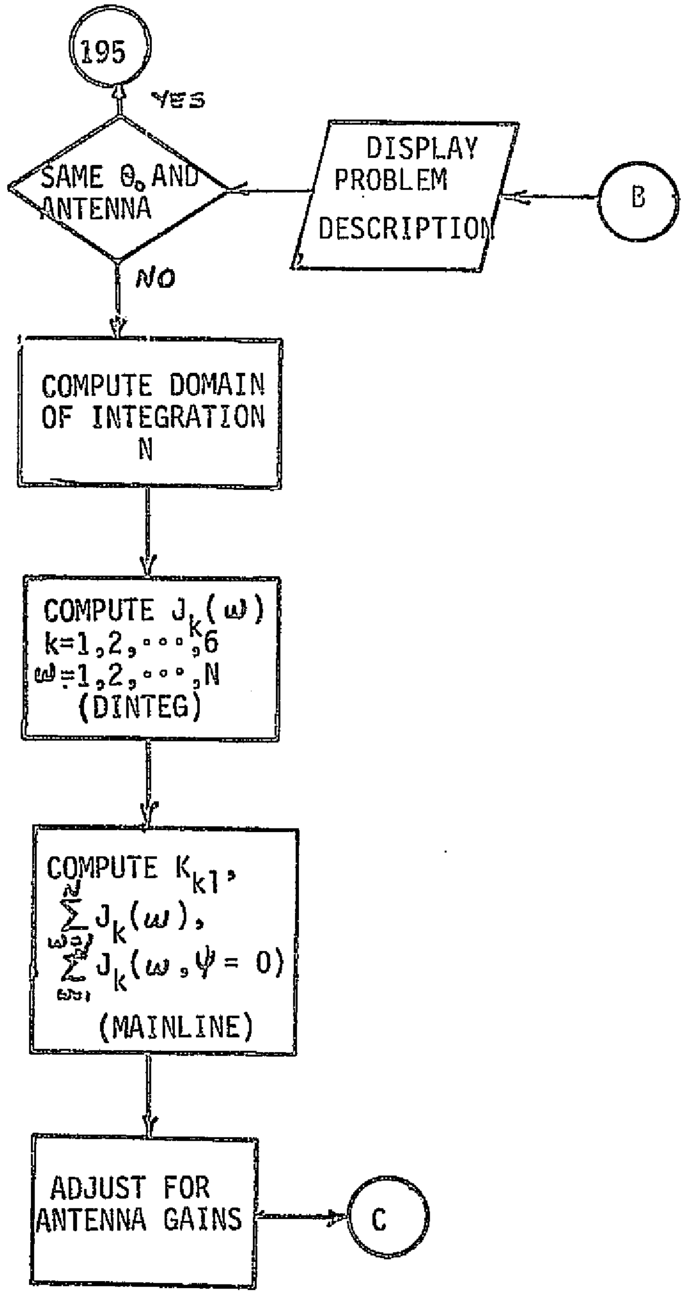

Figure D.1b — MACRO-FLOW CHART FOR SCATSIM —
PROGRAM INITIALIZATION AND ANTENNA PARAMETERIZATIONS

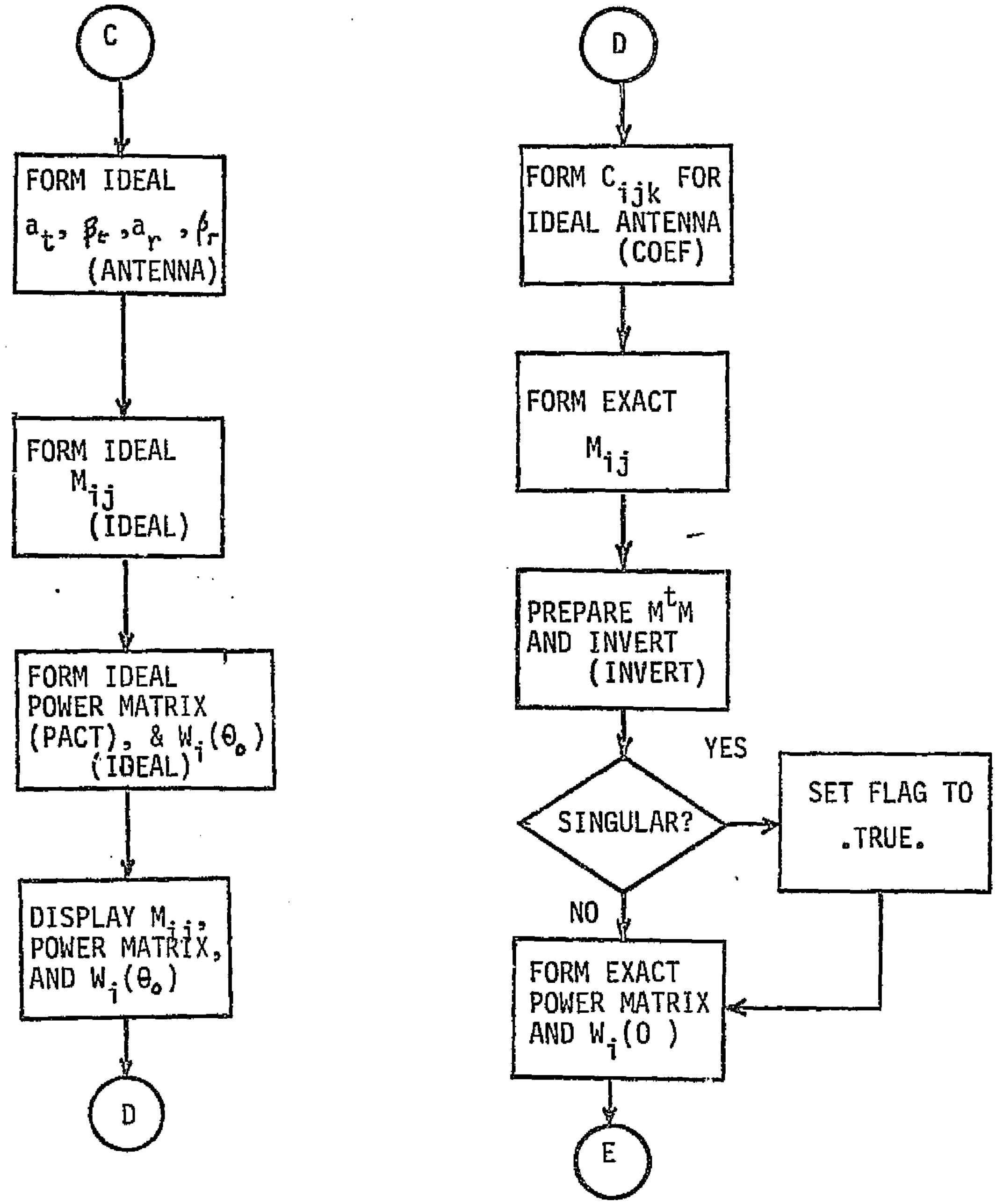

Figure D.2a — MACRO-FLOW CHART OF SCATSIM — COMPUTATION OF THE IDEAL ANTENNA RESPONSE

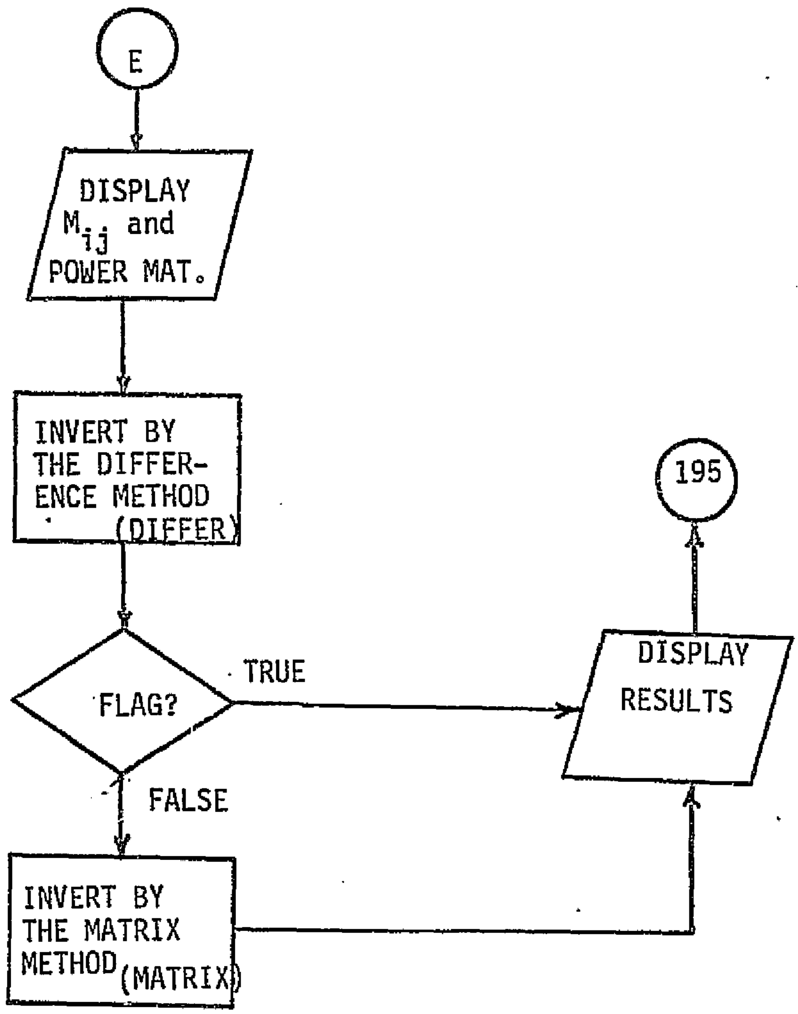

Figure D.2b — MACRO-FLOW CHART OF SCATSIM — COMPUTATION OF THE IDEAL ANTENNA RESPONSE

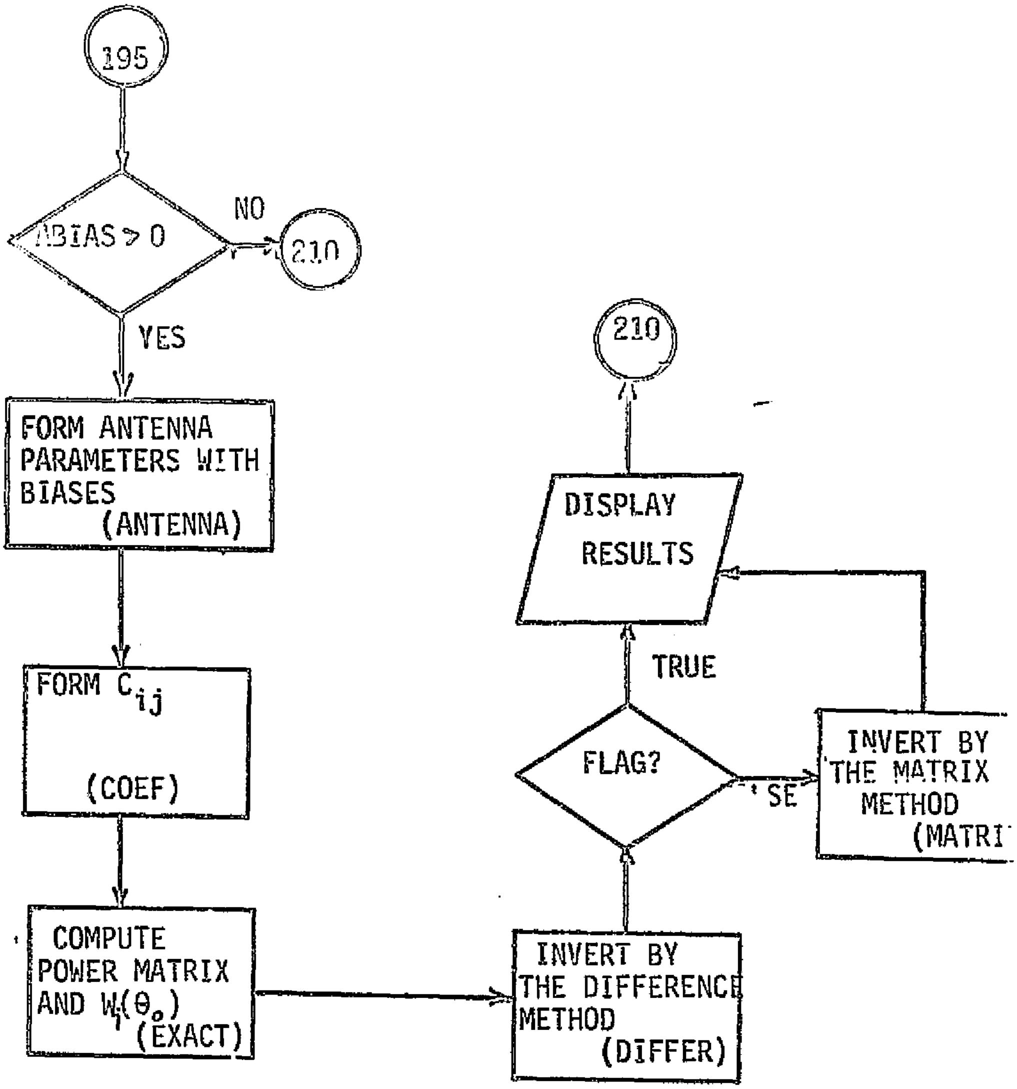

Figure D.3 — MACRO FLOW CHART FOR SCATSIM — COMPUTATION OF THE BIAS RESPONSE

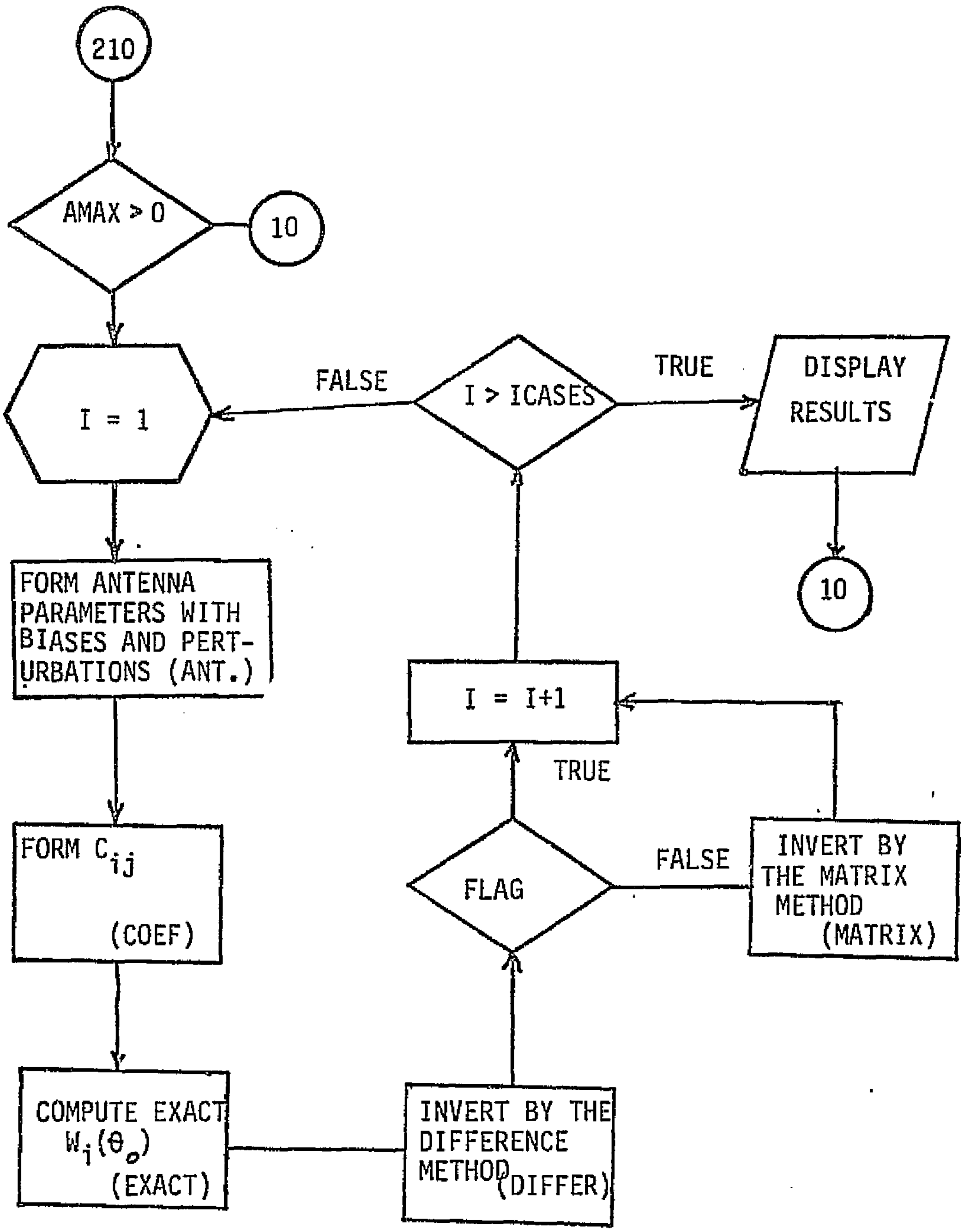

Figure D.4 — MACRO FLOW CHART FOR SCATSIM — COMPUTATION OF THE MONTE CARLO STUDY

The documentation for this portion of the program is illustrated in Figure D.4. The course of this portion of the program is identical to the bias study except that many cases are examined. The number of cases is specified on the instruction card. For each case the antenna parameter set is perturbed randomly within subroutine ANTENNA.

2.4 Program Listing and Sample Output

The source listing of SCATSIM is shown in Figures D.5 through D.18. Sufficient comments have been inserted to identify variables with the theory and to track the operation of the program. A sample output is shown in Figures D.19a through D.19f.

```
      CHAIN      SCAT SIMULATION PROGRAM                                00000070
      C                                                                 00000080
      C            THIS PROGRAM ENABLES THE USER TO STUDY THE PERFOR-   00000090
      C          MANCE OF HIS SCATTEROMETER ANTENNA WHEN IT POSSESSES   00000100
      C          LEAKAGE PROBLEMS FROM THE ORTHOGONAL POLARIZATION OR   00000110
      C          WHEN ITS POLARIZATION PROPERTIES AREN'T KNOWN WITH     00000120
      C          CERTAINTY.  THE PROGRAM PRE-SUPPOSES THAT THE USER     00000130
      C          WILL ATTEMPT ANYONE OF THE FIFTEEN MEASUREMENTS AS     00000140
      C          DESCRIBED IN THE REPORT BY J.P. CLAASSEN ENTITLED      00000150
      C                                                                 00000160
      C          (CR      ).  THE USER HAS FOUR CHOICES OF ANTENNA      00000170
      C          PATTERNS AS SPECIFIED BY ITYPE =1,2,3 OR 4.  THE       00000180
      C          TYPES CORRESPOND TO THE LAMBDA PATTERNS OF TYPE        00000190
      C          P=-1/2,0,1/2,1 AS DESCRIBED IN THE RADAR HANDBOOK,     00000200
      C          CHP. 9  .  THE BEAM WIDTH OF THE CHOSEN PATTERN IS     00000210
      C          GOVERNORED BY THE INPUT PARAMETER KA.  THE BEAMWIDTH   00000220
      C          IS RELATED TO KA IN STATEMENT NO.     OF THE PROGRAM   00000230
      C          THE VIEW ANGLE AT WHICH THE USER WISHES TO CONDUCT     00000240
      C          HIS STUDY IS SPECIFIED IN TNOT.  THE OUTCOME OF THE    00000250
      C          SIMULATION IS BASED ON A SCATTERING CHARACTER-         00000260
      C          ISTIC SIMILAR TO THAT OF THE SEA.  BY REPLACING        00000270
      C          SUBROUTINE SIGMA, THE USER MAY INTRODUCE ANOTHER       00000280
      C          CHARACTERISTIC.  NOTE THAT THE ROUTINE MUST COMPUTE    00000290
      C          THE SCATTERING COEF PER UNIT STERADIAN.  BIAS          00000300
      C          LEAKAGE BY THE ORTHOGONAL POLARIZATION IS INTRODUCED   00000310
      C          BY THE USE OF THE INPUT PARAMETER ABIAS.               00000320
      C          THE PHASE OF THIS LEAKAGE IS DEFINED RELATIVE          00000330
      C          TO VERTICAL POLARIZATION AND IS CONTROLLED WITH        00000340
      C          INPUT PARAMETER BBIAS.  TO CONDUCT MONTE-CARLO STUDIES 00000350
      C          OF THE OUTCOME OF THE SCAT MEASUREMENTS WHEN SMALL UN- 00000360
      C          CERTAINTIES IN THE AMPLITUDE AND PHASE PROPERTIES OF   00000370
      C          THE ANTENNA EXIST, INPUT PARMETERS AMAX AND BMAX       00000380
      C          MAY BE SPECIFIED TO BE OTHER THAN ZERO.  WHEN AMAX=0   00000390
      C          AND BMAX=0, IT IS ASSUMED THAT NO SUCH STUDY IS DE-    00000400
      C          SIRED.  THE CONTRAINTS ON THE BIAS AND RANDOM PARA-    00000410
      C          METERS ARE DESCRIBED IN SUBROUTINE ANTENNA.            00000420
      C          WHEN BIASES ARE NON-ZERO THE MONTE CARLO               00000430
      C          STUDIES ARE CONDUCTED WITH BIASES INSERTED.            00000440
      C                                                                 00000450
      C             PDE = INTEGRAL(PATTERN*COS(THETA))**2               00000460
      C             PSC(I) = INTEGRAL((PATTERN*COS(THETA))**2*SIGMA(I)) 00000470
      C             PDBS = IDEAL OBSERVATION MATRIX                     00000480
      C             PACT = ACTUAL OBSERVATION MATRIX WITH PERTURBATIONS 00000490
      C             PINV = INVERSE OF THE NORMAL EQUATIONS FORMED       00000500
      C             FROM PDBS                                           00000510
      C             SC = ACTUAL SCATTERING COEFFICIENTS AT TNOT         00000520
      C             TNOT = VIEW ANGLE                                   00000530
      C             ITYPE = ANTENNA TYPE                                00000540
      C             KA = ANTENNA NORMALIZED RADIUS                      00000550
      C             AT = RELATIVE GAIN OF HORIZONTAL PATTERN            00000560
      C             DURING XMISSION                                     00000570
      C             AR = RELATIVE GAIN OF HORIZONTAL PATTERN            00000580
```

Figure D.5a — FORTRAN LISTING FOR THE SCATTEROMETER SIMULATION PROGRAM — MAINLINE

ORIGINAL PAGE IS OF POOR QUALITY

```
C                  DURING RECEPTION                                      00000590
C                  BT = PHASE RELATIVE TO V PATTERN DURING TRANS         00000600
C                  BR = PHASE RELATIVE TO V PATTERN DURING RECP          00000610
C                  ABIAS = PATTERN AMPLITUDE BIAS                        00000620
C                  BBIAS = PATTERN PHASE BIAS                            00000630
C                  AMAX = MAX PATTERN PERTURBATION                       00000640
C                  BMAX = MAX PHASE PERTURBATION                         00000650
C                                                                        00000660
      COMMON /ONE/  H(15), PODSI(15,9), PODSE(15,9), PINV(9,9), SC(9),   00000670
     & LABEL(10), AT(15), AR(15), BT(15), BR(15), SINTN, COSTN,          00000680
     & KA, ITYPE                                                         00000690
      DIMENSION THETA(150), SNDO(4), ANT(4), WIDTH(4), PACT(15,10),      00000700
     & PSCE(6,9),PSCI(9),C(9,6,15),PBE(6,9),PDI(9),PAT(6),Q(6)           00000710
      EXTERNAL LAMBDA                                                    00000720
      REAL KA,LAMBDA,KAO                                                 00000730
      LOGICAL JUMP1,JUMP2,ISING                                          00000740
C          DATA STATEMENTS                                               00000750
      DATA KAO,THOTO,ITYPEO /2*-1.0,-1/                                  00000760
      DATA WIDTH /0.88, 1.02, 1.15, 1.27/                                00000770
      DATA ANT /-0.5,1.0,1.5,2.0/                                        00000780
      DATA SNDO/6.283,7.016,7.725,8.416/                                 00000790
      DATA PI/3.14159265/,DELTA/4.36332313E-03/,DEG/0.0174532925/        00000800
C                                                                        00000810
      CALL SETDIM(PINV,9,9)                                              00000820
C                                                                        00000830
C          INPUT ANTENNA TYPE, NORMALIZED RADIUS,                        00000840
C          VIEW ANGLE, AMPL BIAS, PHASE BIAS, MAX AMPL                   00000850
C          PERTURBATION, MAX PHASE PERTURBATION,                         00000860
C          SAMPLE SIZE IN MONTE CARLO STUDY.                             00000870
C                                                                        00000880
   10 READ (5,1000,END=230) ITYPE,KA,TNOT,ABIAS,BPHASE,                  00000890
     & AMAX,BPHASE,ICASES                                                00000900
 1000 FORMAT(I2,6F8.5,I5)                                                00000910
      IF(ITYPE .GT. 4 .OR. ITYPE .LT. 1) CALL ABORT(2HTY)                00000920
      IF(.NOT.(AMAX .LT. 0.0 .OR. ABIAS .LT. 0.0 .OR.                    00000930
     & (ABIAS+AMAX) .GT. 1.0)) GO TO 20                                  00000940
      WRITE(6,2000) ABIAS,AMAX                                           00000950
 2000 FORMAT(1H1,1X,'PERTURBATIONS TOO LARGE',5X,                        00000960
     & 'ABIAS='F10.5,3X,'AMAX='F10.5)                                    00000970
      GO TO 10                                                           00000980
C                                                                        00000990
C           ROUND ANT LOOK ANGLE TO NEAREST HALF DEGREE.                 00001000
C                                                                        00001010
   20 JUMP1 = KAO .EQ. KA .AND. ITYPEO .EQ. ITYPE                        00001020
      TNOT  =  IFIX((TNOT + 0.25) * 2.0) / 2.0                           00001030
      JUMP2 = THOTO .EQ. TNOT                                            00001040
      ISING = .FALSE.                                                    00001050
      IF(JUMP2) GO TO 25                                                 00001060
      TNOTR =  TNOT * DEG                                                00001070
      COSTN =  COS( TNOTR )                                              00001080
      SINTN =  SIN( TNOTR )                                              00001090
   25 WRITE (6,3000) TNC.                                                00001100
```

ORIGINAL PAGE IS OF POOR QUALITY

Figure D.5b — FORTRAN LISTING FOR THE SCATTEROMETER SIMULATION PROGRAM — MAINLINE

```
 3000 FORMAT(1H1//' SCAT STUDY FOR VIEW ANGLE OF',
     & F5.1,' DEGREES'//)
C
C              COMPUTE THETA(MAX ).
C
      IF(JUMP1) GO TO 30
      SINTM =  SNCO(ITYPE) / KA
      COSTM =  SQRT( 1.0 - SINTM * SINTM )
      THAX = ATAN( SINTM,COSTM )/DEG
      THAX = IFIX((THAX+0.25) * 2.0 ) / 2.0
C
C              COMPUTE ANTENNA PARAMETERS.
C
      CALL SOLID( LAMBDA,ITYPE,KA,1.0,COSTM,10,4,S)
      GAIN = 2.0 / S
      FACTOR =  GAIN*GAIN / ( 4.0 * PI * KA )**2
      GDB  = 10.0 * ALOG10( GAIN )
      BEAM = WIDTH(ITYPE)*PI/(KA*DEG)
   30 CBIAS = 10.*ALOG10(ABIAS+1.0E-28)
      CRAND = 10.*ALOG10(AMAX+1.0E-28)
      WRITE(6,4000) ANT(ITYPE),KA,BEAM,GDB,CBIAS,BPHASE,CRAND,RPHASE
 4000 FORMAT(//,20X,'ANTENNA PARAMETERS'/
     & 1X,'TYPE'7X,'KA',6X,'WIDTH',5X,'GAIN',5X,'CROSS',6X,'RELA'/
     & 20X,'(DEG)',5X,'(DB)',6X,'(DB)',6X,'PHASE',5X,'AMAX',7X,'BMAX'/
     & F4.1,1X,7F10.2//)
      BBIAS = BPHASE*DEG
      BMAX = RPHASE*DEG
C
C              CHECK WHETHER SAME ANTENNA AND ANGLE
C
      IF(JUMP1 .AND. JUMP2) GO TO 195
      WRITE(6,5000)
 5000 FORMAT(//1X,'STRIP',2X,'THETA',33X,'HEIGHTS',25X,
     & 'PRECISION'//)
C
C              COMPUTE NUMBER OF SAMPLING ANNULI.
C
C
C              A) RIGHT OF BORESIGHT.
C
      INCR = 2.0 * THAX
C
C              B) LEFT OF BORESIGHT.
C
      IF ( THOT - THAX )35,40,40
   35 INCL  =  2.0 * THOT
      GO TO 50
   40 INCL  =  INCR
C
C               TOTAL NUMBER OF ANNULI.
C
   50 ITOTAL =  INCR + INCL + 1
```

Figure D.5c — FORTRAN LISTING FOR THE SCATTEROMETER SIMULATION PROGRAM — MAINLINE

```
C
C                COMPUTE MIDPOINTS OF SAMPLING STRIPS.
C
         IF ( INCL .EQ. 0 )  GO TO 70
         ITEMP =  INCL + 1
         DO  60  I = 1,INCL
                 THETA(I)  =  TNOT - ( ITEMP - I ) / 2.0
      60 CONTINUE
      70 DO  80  I = 1,INCR+1
                 THETA(INCL + I)  =  TNOT + ( I - 1 ) / 2.0
      80 CONTINUE
C
C                CLEAR ACCUMULATORS
C
         DO 85 I=1,9
                 FSCI(I) = 0.0
                 PBI(I) = 0.0
         DO 85 J=1,6
                 PBE(J,I)=0.0
                 FSCE(J,I)=0.0
     85  CONTINUE
         DO 150 II = 1,ITOTAL
                 I   =  II
C
C                 A)  LIMITS ON COS(THETA)
C
                 THETAR = THETA(I)*DEG
                 X2 = COS(THETAR-DELTA)
                 IF (THETAR .LT. 0.0001)  X2 = 1.0
                 X1 = COS(THETAR+DELTA)
C
C                 B)  LIMITS ON PHI.
C
                 DENOM = SIN(THETAR)*SINTN
                 IF (DENOM .LT. 0.00001) GO TO 90
                 COSPHI =  ( COSTM - COS(THETAR)*COSTN )/DENOM
                 IF ( COSPHI .GT. -1.0 )  GO TO 100
      90         PHI  = PI
         GO TO 110
     100         PHI  = ATAN2( SQRT( ABS(1.0-COSPHI*COSPHI) ) ,
     &            COSPHI )
C
C                C) SET NO. OF INTEGRATION DOMAINS
C
     110         INCY  =  PHI / DEG + 1
                 IF(INCY .GT. 31) INCY = 31
C
C                C)  INITIALIZE CONVERGENCE TESTING PARAMETERS.
C
         DO 114 J = 1,6
                 Q(J)  =  0.0
     114 CONTINUE
```

Figure D.5d — FORTRAN LISTING FOR THE SCATTEROMETER SIMULATION PROGRAM — MAINLINE

```
C
C              E)  INTEGRATE WITH PRECISION J.
C
        DO 120  J = 4,8
                JJ  =  J
C
C              F)  COMPUTE HEIGHT ON ITH ANNULUS.
C
                CALL FXOPT(67,1,1,0)
                CALL DINTEG( PAT,X2,X1,PHI,-PHI,INCY,JJ,JJ )
                CALL FXOPT(67,1,0,0)
C
C              G)  TEST FOR CONVERGENCE.
C
        DO 116 K = 1,6
                IF(PAT(K) .LT. 1.0E-28) GO TO 116
                IF ( ABS(PAT(K)-Q(K)) / PAT(K) .LT. 1.E-5 ) GO TO 116
                GO TO 118
  116   CONTINUE
                GO TO 130
  118   DO 120 K = 1,6
                Q(K) = PAT(K)
  120   CONTINUE
C
C              H)  CONVERGENCE ADMITTED
C
  130           WRITE (6,6000) (I,THETA(I),PAT,JJ)
  6000          FORMAT(I4,F5.1,6E11.3,I5)
C               I) SYNTHESIZE PARAMETERS TO COMPUTE EXACT RETURN AND
C               OBSERVATION MATRIX
        DO 150 J=1,9
                JJ=J
                SCATC = SIGMA(JJ,THETA(I))
        DO 140 K=1,6
                PSCE(K,J)=PSCE(K,J)+PAT(K)*SCATC
                PBE(K,J)=PBE(K,J)+PAT(K)
  140   CONTINUE
                PSCI(J) = PSCI(J)+PAT(6)*SCATC
                PBI(J) = PBI(J)+PAT(6)
  150   CONTINUE
C       WRITE(6,5100) FACTOR,PBI,PSCI
C 5100  FORMAT(1H1,10E12.4/9E12.4//)
C       CALL MATOUT(PBE,6,9,6,9,3HPBE,3HRAW)
C       CALL MATOUT(PSCE,6,9,6,9,4HPSCE,3HRAW)
C               I)  COMPUTE REFERENCE SCAT. COEF.
        DO 160 I = 1,9
                II = I
                SC(I) = SIGMA(II,TNCT)
C               J)  SCALE FOR ANTENNA GAIN
                PBI(I) = PBI(I)*FACTOR
                PSCI(I) = PSCI(I)*FACTOR
        DO 160 J = 1,6
```

Figure D.5e — FORTRAN LISTING FOR THE SCATTEROMETER SIMULATION PROGRAM — MAINLINE

```
                  PSCE(J,I) = PSCE(J,I)*FACTOR
                  PBE(J,I) = PBE(J,I)*FACTOR
   160      CONTINUE
C           WRITE(6,5100)  FACTOR,PBI,PSCI
C           CALL MATOUT(PBE,6,9,6,9,3HPBE,3HSCA)
C           CALL MATOUT(PSCE,6,9,6,9,4HPSCE,3HSCA)
C                 FORM IDEAL PENCIL BEAM WEIGHTS AND POWER MATRIX
            WRITE(6,7000)
  7000      FORMAT(1H1,'IDEAL ANTENNA WEIGHTS AND POWER MATRIX')
            CALL ANTENNA(0.0,0.0,0.0,0.0)
            CALL IDEAL(PBI,POBSI)
            CALL IDEAL(PSCI,PACT)
C                 APPEND POWER VECTOR TO PACT FOR DISPLAY
            DO 170 I = 1,15
            PACT(I,10) = W(I)
   170      CONTINUE
            CALL MATOUT(POBSI,15,9,15,9,5HDELTA,6HWEIGHT)
            CALL MATOUT(PACT,15,10,15,10,5HPOWER,6HMATRIX)
C                 FORM EXACT PENCIL WEIGHTS AND POWER MATRIX
            WRITE(6,7500)
  7500      FORMAT(1H1,'EXACT ANTENNA WEIGHTS AND POWER RETURNS')
C           WRITE(6,7100)  (AT(I),BT(I),AR(I),BR(I),I=1,15)
C 7100      FORMAT(//15(4E12.4/))
            CALL COFF(C)
C           WRITE(6,6100)  (((C(I,J,K),J=1,6),I=1,9),K=1,15)
C 6100      FORMAT(//9(6E12.4/))
            CALL EXACT(PBE,POBSE,C,W)
            CALL MATOUT(POBSE,15,9,15,9,5HDELTA,6HWEIGHT)
C                 PREPARE NORMAL EQNS.
            DO 180 I = 1,9
            DO 180 J = 1,I
                  PINV(I,J) = 0.0
            DO 175 K = 1,15
                  PINV(I,J) = PINV(I,J)+POBSE(K,I)*POBSE(K,J)
   175      CONTINUE
                  PINV(J,I) = PINV(I,J)
   180      CONTINUE
C                 COMPUTE AND DISPLAY INVERSION MATRIX
            CALL MEMINV(PINV,9,PBI,&240)
C                 FORM EXACT POWER MATRIX
   185      CALL EXACT(PSCE,PACT,C,W)
C                 APPEND POWER VECTOR TO PACT FOR DISPLAY
            DO 190 I = 1,15
            PACT(I,10) = W(I)
   190      CONTINUE
            CALL MATOUT(PACT,15,10,15,10,5HPOWER,6HMATRIX)
C                 COMPUTE SCATTERING COEFFICIENTS
C                 A) BY THE DIFFERENCE METHOD.
            WRITE(6,6500)
  6500      FORMAT(1H1)
            CALL DIFFER
            CALL DIFSHOW
```

Figure D.5f — FORTRAN LISTINGS FOR THE SCATTEROMETER SIMULATION PROGRAM — MAINLINE

ORIGINAL PAGE IS OF POOR QUALITY

```
      C               B) BY THE MATRIX METHOD
            IF(ISING) GO TO 195
            CALL MATRIX
            CALL MATSHOW
       195  THOTO = THOT
            KAO = KA
            ITYPEO = ITYPE
      C               CHECK IF CASE WITH BIAS IS DESIRED
            IF(.NOT.(ABIAS .GT. 0.0)) GO TO 210
            WRITE(6,8000) CBIAS,BPHASE
      8000  FORMAT(1H1,' ANTENNA WITH BIASES ONLY'//
          & 1X,'AMPL BIAS=',F6.1,' DB',5X,'PHASE BIAS=',F6.2,' DEG'//)
            CALL ANTENNA(0.0,ABIAS,0.0,BBIAS)
            CALL COEF(C)
            CALL EXACT(PSCE,PACT,C,H)
      C               APPEND POWER VECTOR TO PACT FOR DISPLAY
            DO 200 I = 1,15
            PACT(I,10) = H(I)
       200  CONTINUE
            CALL MATOUT(PACT,15,10,15,10,5HPOWER,6HMATRIX)
      C               A) BY THE DIFFERENCE METHOD
            CALL DIFFER
            CALL DIFSHOW
      C               B) BY THE MATRIX METHOD
            IF(ISING) GO TO 210
            CALL MATRIX
            CALL MATSHOW
      C               CHECK IF MONTE CARLO STUDY DESIR..
       210  IF(.NOT.(AMAX .GT. 0.0)) GO TO 10
            WRITE(6,9000) CBIAS,BPHASE,CRAND,RPHASE
      9000  FORMAT(1H1//' MONTE CARLO STUDY'//
          & 1X,'AMPL BIAS=',F6.1,' DB',5X,'PHASE BIAS=',F6.1,' DEG',
          & 5X,' RANDOM AMPL=',F6.1,' DB',5X,'RANDOM PHASE=',5X,
          & F6.1,' DEG'//)
      C               PERFORM MONTE CAR.. S...Y
            DO 220 I=1,ICASES
            CALL ANTENNA(AMAX,ABIAS,BMA.. ..IAS)
            CALL COEF(C)
            CALL EXACT(PSCE,PACT,C,H)
            CALL DIFFER
            IF(ISING) GO TO 220
            CALL MATRIX
       220  CONTINUE
      C               SHOW RESULTS OF STUDY
            CALL DIFSHOW
            IF(ISING) GO TO 10
            CALL MATSHOW
            GO TO 10
       230  STOP
       240  WRITE(6,9500)
      9500  FORMAT(/1X,10(1H*),'MATRIX SINGULAR',10(1H*)//)
            ISING = .TRUE.
            GO TO 185
            END
```

Figure D.5g — FORTRAN LISTING FOR THE SCATTEROMETER SIMULATION PROGRAM — MAINLINE

```
      CANTENNA       SUBROUTINE ANTENNA                                        00003730
            SUBROUTINE ANTENNA(AMAX,ABIAS,BMAX,BBIAS)                          00003740
      C                                                                        00003750
      C                 THIS SUBROUTINE SYNTHESIZES THE RELATIVE AMPLITUDES    00003760
      C                AND PHASES OF THE TWO ORTHOGONALLY POLARIZED ANTENNA    00003770
      C                PATTERNS DURING TRANSMISSSION T AND RECEPTION R FOR     00003780
      C                THE FIFTEEN STANDARD MEASUREMENTS.  THE INPUT AR-       00003790
      C                GUMENTS PERMIT THE PRECISE ANTENNA REQUIREMENTS FOR     00003800
      C                EACH OF THE FIFTEEN MEASUREMENT CONDITIONS TO BE        00003810
      C                PERTURBED WITH BIASES EITHER FIXED OR RANDOM OR BOTH    00003820
      C                                                                        00003830
      C                AMAX=MAXIMUM RANDOM PERTURBATION INTRODUCED INTO THE    00003840
      C                HORZONTALLY POLARIZED PATTERN                           00003850
      C                                                                        00003860
      C                ABIAS=BIAS INTRODUCED INTO THE HORIZONTALLY POLA-       00003870
      C                RIZED PATTERN                                           00003880
      C                                                                        00003890
      C                BMAX=MAXIMUM RANDOM PERTURBATION INTRODUCED INTO THE    00003900
      C                RELATIVE PHASE BETWEEN ORTHOGONALLY POLARIZED           00003910
      C                PATTERNS                                                00003920
      C                                                                        00003930
      C                BBIAS=BIAS INTRODUCED INTO THE RELATIVE PHASE           00003940
      C                BETWEEN ORTHOGONALLY POLARIZED PATTERN                  00003950
      C                                                                        00003960
      C                IF THE INPUT ARGUMENTS ARE SET TO ZERO, PRECISE         00003970
      C                ANTENNA REQUIREMENTS ARE ESTABLISHED IN THE OUTPUT      00003980
      C                VECTORS:                                                00003990
      C                                                                        00004000
      C                AT(R)=RELATIVE AMPLITUDE OF THE HORIZONTALLY POLA-      00004010
      C                RIZED PATTERN DURING TRANSMISSION(RECEPTION)            00004020
      C                                                                        00004030
      C                BT(R)=RELATIVE PHASE BETWEEN ORTHOZONAL POLARIZATION    00004040
      C                DURING TRANSMISSION(RECEPTION)                          00004050
      C                                                                        00004060
      C                OTHERWISE, PERTURBATIONS ARE INTRODUCED IN ACCORD       00004070
      C                WITH ALGORITHMS BELOW.  BIASES ARE EFFECTIVE ONLY       00004080
      C                WHEN POLARIZED TRANSMISSIONS OR RECEPTIONS ARE MADE     00004090
      C                IN THE FIFTEEN MEASUREMENTS.  IT IS ASSUMED THAT        00004100
      C                LEAKAGE OR DE-POLARIZATION IS THE CAUSE OF THE          00004110
      C                BIASES.  THE USER MUST ABSERVE THAT                     00004120
      C                                                                        00004130
      C                1)AMAX .GT. 0.                                          00004140
      C                                                                        00004150
      C                2)ABIAS .GT. 0.                                         00004160
      C                                                                        00004170
      C                3)AMAX+ABIAS .LE. 1.0                                   00004180
      C                4)-PI .GT. BBIAS .LE. PI                                00004190
      C                5)-PI .GT. BMAX .LE. PI                                 00004200
      C                                                                        00004210
      C                THE RANDOM PERTURBATIONS ARE DISTRIBUTED UNIFORMLY      00004220
      C                OVER(0,AMAX/2)                                          00004230
      C                IF AT OR AR IS ZERO IN THE UNPERTURBED CASE, AND        00004240
```

Figure D.6a — FORTRAN LISTING FOR THE SCATTEROMETER SIMULATION PROGRAM — SUBROUTINE ANTENNA

```
      C              OVER(1-AMAX/2,1)                                   00004250
      C              IF AT OR AR IS ONE IN THE UNPERTURBED CASE, AND    00004260
      C              OVER(.5-AMAX/2,.5+AMAX/2)                          00004270
      C              IF AT OR AR IS .5 IN THE UNPERTURBED CASE.  RANDOM 00004280
      C              PHASES ARE DISTRIBUTED UNIFORMILY OVER             00004290
      C              (BT(R)-BMAX/2,BT(R)+BMAX/2)                        00004300
      C                                                                 00004310
            COMMON /CHE/  W(15), POBSI(15,9), POBSE(15,9), PINV(9,9), SC(9),  00004320
           & LABEL(10), AT(15), AR(15), BT(15), BR(15), SIMTN, COSTN,   00004330
           & KA, ITYPE                                                  00004340
            DATA IST /33333333333/                                      00004350
            DATA PIO4,PIO2,TPIO4,PI /0.785398163,1.57079633,2.35619449, 00004360
           & 3.14159265/                                                00004370
      C              ARITHMETIC ASSIGNMENT STATEMENTS(AAS)              00004380
            AERR2(I)=(0.5-RCM(I))*AMAX                                  00004390
            BERR2(I)=(0.5-RCM(I))*BMAX                                  00004400
      C                                                                 00004410
      C                              VV                                 00004420
      C                                                                 00004430
            AT(1)=ABIAS                                                 00004440
            AR(1)=ABIAS                                                 00004450
            BT(1)=BBIAS                                                 00004460
            BR(1)=BBIAS                                                 00004470
      C                              HH                                 00004480
            AT(2)=1.0-ABIAS                                             00004490
            AR(2)=1.0-ABIAS                                             00004500
            BT(2)=BBIAS                                                 00004510
            BR(2)=BBIAS                                                 00004520
      C                              VH                                 00004530
            AT(3)=ABIAS                                                 00004540
            AR(3)=1.0-ABIAS                                             00004550
            BT(3)=BBIAS                                                 00004560
            BR(3)=BBIAS                                                 00004570
      C              VVHHR                                              00004580
            AT(4)=0.5+AERR2(IST)                                        00004590
            AR(4)=0.5+AERR2(IST)                                        00004600
            BT(4)=PIO2+BERR2(IST)                                       00004610
            BR(4)=-PIO2+BERR2(IST)                                      00004620
            AT(5)=0.5+AERR2(IST)                                        00004630
            AR(5)=0.5+AERR2(IST)                                        00004640
            BT(5)=BERR2(IST)                                            00004650
            BR(5)=PI+BERR2(IST)                                         00004660
      C                              VVHHI                              00004670
            AT(6)=0.5+AERR2(IST)                                        00004680
            AR(6)=0.5+AERR2(IST)                                        00004690
            BT(6)=PIO4+BERR2(IST)                                       00004700
            BR(6)=-TPIO4+BERR2(IST)                                     00004710
            AT(7)=0.5+AERR2(IST)                                        00004720
            AR(7)=0.5+AERR2(IST)                                        00004730
            BT(7)=-PIO4+BERR2(IST)                                      00004740
            BR(7)=TPIO4+BERR2(IST)                                      00004750
      C                              VVVHR                              00004760
```

Figure D.6b — FORTRAN LISTING FOR THE
SCATTEROMETER SIMULATION PROGRAM — SUBROUTINE ANTENNA

```
      AT(8)=ABIAS                                                       00004770
      AR(8)=0.5+AERR2(IST)                                              00004780
      BT(8)=BBIAS                                                       00004790
      BR(8)=BERR2(IST)                                                  00004800
      AT(9)=ABIAS                                                       00004810
      AR(9)=0.5+AERR2(IST)                                              00004820
      BT(9)=BBIAS                                                       00004830
      BR(9)=PI+BERR2(IST)                                               00004840
C                         VVVHI                                         00004850
      AT(10)=ABIAS                                                      00004860
      AR(10)=0.5+AERR2(IST)                                             00004870
      BT(10)=BBIAS                                                      00004880
      BR(10)=-PIO2+BERR2(IST)                                           00004890
      AT(11)=ABIAS                                                      00004900
      AR(11)=0.5+AERR2(IST)                                             00004910
      BT(11)=BBIAS                                                      00004920
      BR(11)=PIO2+BERR2(IST)                                            00004930
C                         HVHHR                                         00004940
      AT(12)=1.0-ABIAS                                                  00004950
      AR(12)=0.5+AERR2(IST)                                             00004960
      BT(12)=BBIAS                                                      00004970
      BR(12)=BERR2(IST)                                                 00004980
      AT(13)=1.0-ABIAS                                                  00004990
      AR(13)=0.5+AERR2(IST)                                             00005000
      BT(13)=BBIAS                                                      00005010
      BR(13)=PI+BERR2(IST)                                              00005020
C                         HVHHI                                         00005030
      AT(14)=1.0-ABIAS                                                  00005040
      AR(14)=0.5+AERR2(IST)                                             00005050
      BT(14)=BBIAS                                                      00005060
      BR(14)=-PIO2+BERR2(IST)                                           00005070
      AT(15)=1.0-ABIAS                                                  00005080
      AR(15)=0.5+AERR2(IST)                                             00005090
      BT(15)=BBIAS                                                      00005100
      BR(15)=PIO2+BERR2(IST)                                            00005110
      RETURN                                                            00005120
      END                                                               00005130
```

Figure D.6c — FORTRAN LISTING FOR THE SCATTEROMETER SIMULATION PROGRAM — SUBROUTINE ANTENNA

ORIGINAL PAGE IS OF POOR QUALITY

```
CCOEF          SUBROUTINE COEF
      SUBROUTINE COEF(C)
      COMMON /CNE/  W(15), POBSI(15,9), POBSE(15,9), PINV(9,9), SC(9),
     & LABEL(10), AT(15), AR(15), BT(15), BR(15), SINTN, COSTN,
     & KA, ITYPE
      DIMENSION C(5,6,15)
C             THIS ROUTINE PREPARES THE ANTENNA PATTERN
C             FACTORS FROM THE ANTENNA GAINS AND PHASES SET
C             BY SUBROUTINE ANTENNA
C
      DO 10 I=1,15
      AT1=1.0-AT(I)
      SA=2.0*SQRT(AT(I)*AT1)
      CBT=SA*COS(BT(I))
      SBT=SA*SIN(BT(I))
      AR1=1.0-AR(I)
      SA = 2.0*SQRT(AR(I)*AR1)
      SBR=SA*SIN(BR(I))
      CBR=SA*COS(BR(I))
      CBTCBR=CBT*CBR
      C(4,1,I) = CBTCBR/2.0
      AR2=2.0*AR(I)-1.0
      AT2=2.0*AT(I)-1.0
      AT2AR2 = AT2*AR2
C
C             SIGMA-VV
C
      C(1,1,I)=AR1*AT1
      C(1,2,I)=AR(I)*AT(I)
      C(1,3,I)=AR1*AT(I)+AT1*AR(I)+CBTCBR
C
C             SIGMA-HH
C
      C(2,1,I)=C(1,2,I)
      C(2,2,I)=C(1,1,I)
      C(2,3,I)=C(1,3,I)
C
C             SIGMA-VH
C
      C(3,1,I)=C(1,3,I)-C(4,1,I)
      C(3,2,I)=C(3,1,I)
              CALL FXOPT(67,1,1,0)
      C(3,3,I)=2.0*(C(1,1,I)+C(1,2,I)-1.5*CBTCBR+AT2AR2)
              CALL FXOPT(67,1,0,0)
      C(3,6,I)=SBT*SBR/2.0
C
C             REAL SIGMA VVHH
C
C
C     C(4,1,I)=CBTCBR/2.0
      C(4,2,I)=C(4,1,I)
      C(4,3,I)=2.0*AT2AR2-CBTCBR
      C(4,6,I)=-C(3,6,I)
```


Figure D.7a — FORTRAN LISTING FOR THE SCATTEROMETER SIMULATION PROGRAM — SUBROUTINE COEF

```
      C
      C            IMAGINARY SIGMA VVHH
      C
            C(5,4,I) = (CBT*SBR+CBR*SBT)/2.0
            C(5,5,I)=-C(5,4,I)
      C
      C            REAL SIGMA VVHV
      C
            C(6,1,I)=AR1*CBT+AT1*CBR
            C(8,1,I)=AT(I)*CBR+AR(I)*CBT
            C(6,2,I) = -C(8,1,I)
            C(6,3,I) = 3.0*(AR2*CBT+AT2*CBR)
      C
      C            IMAGINARY SIGMA VVHV
      C
            C(7,4,I)=-(AR(I)*SBT+AT(I)*SBR)
            C(7,5,I)=-(AR1*SBT+AT1*SBR)
      C
      C            REAL SIGMA VHHH
      C
      C     C(8,1,I)=AT(I)*CBR+AR(I)*CBT
            C(8,2,I)=-C(6,1,I)
            C(8,3;I)=-C(6,3,I)
      C
      C            IMAGINARY SIGMA VHHH
      C
            C(9,4,I)=C(7,5,I)
            C(9,5,I)=C(7,4,I)
       10   CONTINUE
            PETURN
            END
```

Figure D.7b– FORTRAN LISTING FOR THE SCATTEROMETER SIMULATION PROGRAM – SUBROUTINE COEF

```
      CMATOUT        SUBROUTINE MATOUT                                    00005970
      C                                                                   00005980
      C              ROUTINE DISPLAYS MATRIX A BY ROWS AND                00005990
      C              COLUMNS OF 10.  MATRIX NAME APPEARS IN WORD LABEL    00006000
      C                                                                   00006010
            SUBROUTINE MATOUT (A,IRDIM,ICDIM,IRSIZE,ICSIZE,NAME1,NAME2)   00006020
            COMMON /CNE/  W(15), POSI(15,9), PCBSE(15,9), PINV(9,9), SC(9), 00006030
           & LABEL(10), AT(15), AR(15), BT(15), BR(15), SINTN, COSTN,     00006040
           & KA, ITYPE                                                    00006050
            DIMENSION A(IRDIM,ICDIM)                                      00006060
      C                                                                   00006070
            DO 10 I=1,ICSIZE,10                                           00006080
               N = I+9                                                    00006090
               IF (N .GT. ICSIZE) N=ICSIZE                                00006100
               WRITE (6,1000) NAME1,NAME2, (LABEL(K), K=I,N)              00006110
       1000    FORMAT (//40X,A6,1X,A6//1X,'MEAS/COEF',2X,A5,9(6X,A6)//)   00006120
            DO 10 J=1,IRSIZE                                              00006130
               WRITE (6,2000) J,(A(J,K), K=I,N)                           00006140
       2000    FORMAT (I4,3X,10E12.4)                                     00006150
       10   CONTINUE                                                      00006160
            RETURN                                                        00006170
            END                                                           00006180
```

Figure D.8 — FORTRAN LISTING FOR THE SCATTEROMETER SIMULATION PROGRAM — SUBROUTINE MATOUT

```
T8144 01   02-15-75   23.095          SUBROUTINE EXACT                                   LABEL EXACT   PAGE    1
      CEXACT          SUBROUTINE EXACT
      C
            SUBROUTINE EXACT(PIN,POT,C,W)
      C
      C                 THIS ROUTINE COMPUTES THE SCATTEROMETER POWER
      C                 COMPONENTS FOR THE FIFTEEN STANDARD MEASUREM-
      C                 MENTS. EACH COMPONENT WITHIN A MEASUREMENT
      C                 IS ASSOCIATED WITH ONE OF THE NINE SCATTERING COEFFI-
      C                 CIENTS. TYPICALLY, THE INPUT ARGUMENT PIN CONTAINS
      C                 THE PATTERN-SURFACE WEIGHTS. WHEREAS, THE
      C                 OUTPUT PARAMETER POT CONTAINS THE POWER COMPONENTS.
      C                 IF PIN CONTAINS ONLY PATTERN WEIGHTS,
      C                 THE OBSERVATION MATRIX WILL BE CONSTRUCTED
      C                 IN POT. THE SUM OF THE COMPONENTS IS
      C                 FORMED IN W, THE TOTAL RETURN POWER.
      C
            DIMENSION PIN(6,1), W(1), POT(15,1), C(9,6,15)
      C                 FOR EACH MEASUREMENT...
            DO 10 I=1,15
      C                 FORM THE POWER COMPONENTS
            DO 10 J=1,9
            POT(I,J)=0.0
      C                 BY ISOLATING THE TRACE ELEMENTS
            DO 10 K=1,6
            POT(I,J)=POT(I,J)+C(J,K,I)*PIN(K,J)
       10   CONTINUE
      C                 SUM THE ELEMENT IN THE TRACE
            DO 20 I=1,15
            W(I)=0.0
      C                 TO GET THE TOTAL POWER
            DO 20 J=1,9
            W(I)=W(I)+POT(I,J)
       20   CONTINUE
            RETURN
            END
```

Figure D.9 — FORTRAN LISTING FOR THE SCATTEROMETER SIMULATION PROGRAM — SUBROUTINE EXACT

ORIGINAL PAGE IS OF POOR QUALITY

```
CMATRIX                     SUBROUTINE MATRIX
      SUBROUTINE MATRIX
C              THIS ROUTINE ESTIMATES THE MEASURED
C              SCAT COEFICIENTS BY THE MATRIX METHOD.
C              SINCE THE SYSTEM IS OVER SPECIFIED A LEAST
C              SQUARES TECHNIQUE IS EMPLOYED TO INVERT THE
C              MEASUREMENTS.  THE ESTIMATES ARE COMPARED
C              WITH THE EXACT COEFICIENTS.
C
      COMMON /ONE/ W(15), POBSI(15,9), POBSE(15,9), PINV(9,9), SC(9),
     & LABEL(10), AT(15), AR(15), BT(15), BP(15), SINTN, COSTN,
     & KA, ITYPE
      DIMENSION HP(9),SUM(9),RMS(9),PSUM(9),PRMS(9)
C              FORM TRANSFORMED POWER MEASUREMENTS
      IOBS = IOBS+1
      DO 10 I = 1,9
              HP(I) = 0.0
      DO 10 J = 1,15
              HP(I) = HP(I) + POBSE(J,I)*W(J)
   10 CONTINUE
      DO 30 I  = 1,9
              W(I) = 0.0
      DO 20 J = 1,9
              W(I) = W(I) + PINV(I,J)*HP(J)
   20 CONTINUE
              ERR = W(I) - SC(I)
              SUM(I) = SUM(I) + ERR
              RMS(I) = RMS(I) + ERR*ERR
   30 CONTINUE
      RETURN
C              SECONDARY ENTRY
      ENTRY MATSHOW
      DO 40 I = 1,9
              SUM(I) = SUM(I)/IOBS
              PSUM(I) = 100.0*SUM(I)/SC(I)
              IF(IOBS .LT. 2) GO TO 35
              RMS(I) = SQRT(ABS(RMS(I)/IOBS-SUM(I)*SUM(I)))
              PRMS(I) = 100.0*RMS(I)/SC(I)
   35         CONTINUE
   40 CONTINUE
      WRITE(6,1000) IOBS,(LABEL(I),SC(I),SUM(I),RMS(I),
     & PSUM(I),PRMS(I),I = 1,9)
 1000 FORMAT(//1X,'STATISTICS FOR THE MATRIX ',
     & 'METHOD BASED ON',I4,' OBSERVATIONS'//
     & 1X,'SCAT COEF',3X,'VALUE',8X,'MEAN',9X,'RMS',
     & 7X,'%MEAN',8X,'%RMS'//
     & (2X,A6,2X,3E12.3,2F12.3))
C              CLEAR SUMMING VARIABLES
      DO 50 I = 1,9
              SUM(I) = 0.0
              RMS(I) = 0.0
   50 CONTINUE
      IOBS = 0
      RETURN
      END
```

Figure D.10 — FORTRAN LISTING FOR THE SCATTEROMETER SIMULATION PROGRAM — SUBROUTINE MATRIX

```
CDINTEG         SUBROUTINE DINTEG
          SUBROUTINE DINTEG (SUM,X2P,X1P,Y2P,Y1P,MNY,NNP,MMP)
C
C
C                THIS ROUTINE EMPLOYS A QUASSIAN LEGENDRE QUADRATURE
C                (INTEGRATION) PROCEDURE.  INTEGRATION OVER X-Y SEGMENTS
C                ARE PERFORMED AFTER TRANSLATION TO (-1,1)X(-1,1).
C                X2P,X1P = UPPER AND LOWER LIMITS ON X
C                Y2P,Y1P = UPPER AND LOWER LIMITS ON Y
C                MY = SEGMENTS IN  Y
C                NP,MP = DEGREE OF PRECISION IN X AND Y, RESPECTIVELY
C
          COMMON /ONE/ W(15), POSSI(15,9), POBSE(15,9), PINV(9,9), SC(9),
        & LABEL(10), AT(15), AR(15), BT(15), BR(15), SINTN, COSTN,
        & KA, ITYPE
          DIMENSION SUM(6)
          DIMENSION SAMPLE(8,8),COEF(8,8),SX(8),SY(8),C(8,8)
          REAL LAMBDA,KA
          DATA ((SAMPLE(I,J),J=1,8),I=2,8)/-0.577350269,0.577350269,
        & 0.0,0.0,0.0,0.0,0.0,0.0,
        & -0.774596669,0.0,0.774596669,0.0,0.0,0.0,0.0,0.0,
        & -0.861136312,-0.339981044,0.339981044,0.861136312,
        & 0.0,0.0,0.0,0.0,
        & -0.906179846,-0.538469310,0.0,0.538469310,0.906179846,
        & 0.0,0.0,0.0,
        & -0.932469514,-0.661209386,-0.238619186,0.238619186,0.661209396,
        & 0.932469514,0.0,0.0,
        & -0.949107912,-0.741531185,-0.405845151,0.0,0.405845151,
        & 0.741531185 ,0.949107912,0.0,
        & -.960289856,-.796666477,-.525532410,-.183434642,.183434642,
        & 0.525532410,0.796666477,0.960289856/
          DATA ((COEF(I,J),J=1,8),I=2,8)/1.0,1.0,0.0,0.0,0.0,0.0,0.0,0.0,
        & 0.555555556 ,0.888888889 ,0.555555556 ,0.0,0.0,0.0,0.0,0.0,
        & 0.347854851,0.652145155 ,0.652145155 ,0.347854851,0.0,0.0,0.0,
        & 0.0,
        & 0.236926885,0.478628670,0.568888889,0.478628670,
        & 0.236926885,0.0,0.0,0.0,
        & 0.171324492,0.360761573,0.467913935,0.467913935,0.360761573,
        & 0.171324492,0.0,0.0,
        & 0.129484966,0.279705391,0.381830051,0.417959184,
        & 0.381830051,0.279705391,0.129484966,0.0,
        & 0.101228536,0.222381034,0.313706646,0.362683783,0.362683783,
        & 0.313706646,0.222381034,0.101228536/
C
C                CLEAR SUMMING VARIABLES
C
          DO 10 I=1,6
          SUM(I)=0.0
   10     CONTINUE
C
C                RE-ASSIGN INPUT ARGUMENTS
C
```


Figure D.11a — FORTRAN LISTING FOR THE SCATTEROMETER SIMULATION PROGRAM — SUBROUTINE DINTEG

```
      NY = NNY
      NP = NNP
      MP = MMP
C
C              COMPUTE LENGTH OF CELL SIDES
C
      XM = (X2P+X1P)*0.5
      DELX = X2P-X1P
      HDELX = DELX*0.5
      DELY = (Y2P-Y1P)/FLOAT(NY)
      HDELY = DELY*0.5
      RJACOB = HDELX*HDELY
C
C              FORM SAMPLE FACTOR FOR X
C
      DO 20 I = 1,NP
      SX(I) = SAMPLE(NP,I)*HDELX+XM
   20 CONTINUE
C
C              FORM SAMPLE FACTOR FOR Y
C
      DO 30 I = 1,MP
      SY(I) = SAMPLE(MP,I)*HDELY
   30 CONTINUE
C
C              FORM GAUSSIAN WEIGHTS
C
      DO 50 I = 1,NP
      DO 40 J=1,MP
      C(I,J) = COEF(NP,I)*COEF(MP,J)
   40 CONTINUE
   50 CONTINUE
C
C              INTEGRATE IN STRIP OF DELX
C
      DO 90 I = 1,NP
      COSX = SX(I)
      SINX = SQRT(1.0-COSX*COSX)
C
C              INTEGRATE ALONG Y
C
      YM = Y1P - HDELY
      DO 80 M = 1,NY
      YM = YM + DELY
      DO 70 J = 1,MP
      PHI = SY(J)+YM
      CALL SINCOS(PHI, SINPHI, COSPHI)
      FACTOR= SINX*SINTN*COSPHI+COSX*COSTN
      ARG=KA*SQRT(1.0-FACTOR**2)
      PHIP=ATAN2(SINX*SINPHI, FACTOR)
      CALL SINCOS (PHIP, SINPHP, COSPHP)
      COSPSI=COSPHI*COSPHP+SINPHI*SINPHP*SINTN
```

Figure D.11b — FORTRAN LISTING FOR THE SCATTEROMETER SIMULATION PROGRAM — SUBROUTINE DINTEG

```
      SINPSI=COSX*(SINPHI*COSPHP-COSPHI*SINPHP*SINTN)+              00008130
     & SINX*COSTN*SINPHP                                            00008140
      P=C(I,J)*COSX*LAMBDA(ITYPE,ARG)**2                            00008150
      SUM(6)=SUM(6)+P                                               00008160
      SUM(5)=SUM(5)+P*COSPSI**2                                     00008170
      SUM(4)=SUM(4)+P*SINPSI**2                                     00008180
      SUM(3)=SUM(3)+P*(COSPSI**2)*(SINPSI**2)                       00008190
      SUM(2)=SUM(2)+P*(SINPSI**2)**2                                00008200
      SUM(1)=SUM(1)+P*(COSPSI**2)**2                                00008210
C                                                                   00008220
C             FORM PARTIAL SUMS                                     00008230
C                                                                   00008240
   60 CONTINUE                                                      00008250
   70 CONTINUE                                                      00008260
   80 CONTINUE                                                      00008270
   90 CONTINUE                                                      00008280
C                                                                   00008290
C             APPLY JACOBIAN                                        00008300
C                                                                   00008310
      DO 100 I = 1,6                                                00008320
      SUM(I) = RJACOB*SUM(I)                                        00008330
  100 CONTINUE                                                      00008340
      RETURN                                                        00008350
      END                                                           00008360
```


Figure D.11c — FORTRAN LISTING FOR THE SCATTEROMETER SIMULATION PROGRAM — SUBROUTINE DINTEG

ORIGINAL PAGE IS OF POOR QUALITY

```
      DIFFER                        SUBROUTINE DIFFER                   00008370
            SUBROUTINE DIFFER                                           00008380
      C              THIS ROUTINE ESTIMATES THE MEASURED SCATTERING     00008390
      C              COEFFICIENTS BY THE SO-CALLED DIFFERENCE           00008400
      C              METHOD. THE ESTIMATES ARE COMPARED WITH THE ACTUAL 00008410
      C              COEFFICIENTS AND THE STATISTICS ARE ACCUMULATED.   00008420
      C                                                                 00008430
            COMMON /ONE/ W(15), POBSI(15,9), POBSE(15,9), PINV(9,9), SC(9),   00008440
           & LABEL(10), AT(15), AR(15), BT(15), BR(15), SINTN, COSTN,  00008450
           & KA, ITYPE                                                  00008460
            DIMENSION SUM(9),RMS(9),PSUM(9),PRMS(9)                     00008470
            DATA LABEL/'VV    ','HH    ','VH    ','VVHHR ','VVHHI ',   00008480
           & 'VVVHR ','VVVHI ','HVHHR ','HVHHI ','POWER '/             00008490
            IOBS = IOBS+1                                               00008500
      C              COMPARE MEASURED AGAINST EXACT                     00008510
            DO 10 I = 1,3                                               00008520
                     ERR = W(I)/POBSI(I,I)-SC(I)                        00008530
                     SUM(I) = SUM(I) +ERR                               00008540
                     RMS(I) = RMS(I)+ERR*ERR                            00008550
         10 CONTINUE                                                    00008560
            DO 20 I = 4,9                                               00008570
                     II = 2*I-4                                         00008580
                     ERR = (W(II)-W(II+1))/2.0/POBSI(II,I)-SC(I)        00008590
                     SUM(I) = SUM(I)+ERR                                00008600
                     RMS(I) = RMS(I)+ERR*ERR                            00008610
         20 CONTINUE                                                    00008620
            RETURN                                                      00008630
            ENTRY DIFSHOW                                               00008640
      C              SECONDARY ENTRY                                    00008650
            DO 30 I = 1,9                                               00008660
                     SUM(I) = SUM(I)/IOBS                               00008670
                     PSUM(I) = 100.0*SUM(I)/SC(I)                       00008680
                     IF(IOBS .LT. 2) GO TO 25                           00008690
                     RMS(I) = SQRT(ABS(RMS(I)/IOBS-SUM(I)*SUM(I)))      00008700
                     PRMS(I) = 100.0*RMS(I)/SC(I)                       00008710
         25          CONTINUE                                           00008720
         30 CONTINUE                                                    00008730
            WRITE(6,1000) IOBS,(LABEL(I),SC(I),SUM(I),RMS(I),           00008740
           & PSUM(I),PRMS(I),I = 1,9)                                   00008750
       1000 FORMAT(//1X,'STATISTICS FOR THE DIFFERENCE ',               00008760
           & 'METHOD BASED ON',I4,' OBSERVATIONS'//                     00008770
           & 1X,'SCAT COEF',3X,'VALUE',8X,'MEAN',9X,'RMS',              00008780
           & 7X,'%MEAN',6X,'%RMS'//                                     00008790
           & (2X,A6,2X,3E12.3,2F12.3))                                  00008800
      C              CLEAR SUMMING VARIABLES                            00008810
            DO 40 I = 1,9                                               00008820
                     SUM(I) = 0.0                                       00008830
                     RMS(I) = 0.0                                       00008840
         40 CONTINUE                                                    00008850
            IOBS = 0                                                    00008860
            RETURN                                                      00008870
            END                                                         00008880
```

Figure D.12 — FORTRAN LISTING FOR THE SCATTEROMETER SIMULATION PROGRAM — SUBROUTINE DIFFER

```
      CIDEAL          SUBROUTINE IDEAL                                  00008890
            SUBROUTINE IDEAL(PIN,POT)                                   00008900
      C              THIS ROUTINE PREPARES AN ANTENNA OBSERVATION MATRIX 00008910
      C              AND ITS ROW SUMS FOR THE ANTENNA AS PREVIOUSLY     00008920
      C              SPECIFIED BY SUBROUTINE ANTENNA                    00008930
      C                                                                 00008940
            COMMON /ONE/ H(15), POBSI(15,9), POBSE(15,9), PINV(9,9), SC(9), 00008950
           & LABEL(10), AT(15), AR(15), BT(15), BR(15), SINTN, COSTN,   00008960
           & KA, ITYPE                                                  00008970
            DIMENSION PIN(9),POT(15,1)                                  00008980
      C         PIN=VECTOR CONTAINING PATTERN OR PATTERN AND SCATTER    00008990
      C              COEFFICIENT EFFECT 1=VV,2=HH,3=VH,4=VVHHR,5=VVHHI  00009000
      C              6=VVVHR,7=VVVHI,8=HVHHR,9=HVHHI                    00009010
      C         POT=VECTOR CONTAINING MEASUREMENT COMPONENTS            00009020
      C          H =SUM OF ROW ELEMENTS IN POT                          00009030
      C              INITIAL SOME PARAMETERS                            00009040
            DO 10 I=1,15                                                00009050
                     CAT=1.0-AT(I)                                      00009060
                     CAR=1.0-AR(I)                                      00009070
                     SRT=2.0*SQRT(CAT*AT(I))                            00009080
                     SRR=2.0*SQRT(CAR*AR(I))                            00009090
                     SR=SRT*SRR/2.0                                     00009100
                     COSBR=COS(BR(I))                                   00009110
                     COSBT=COS(BT(I))                                   00009120
                     SINBR=SIN(BR(I))                                   00009130
                     SINBT=SIN(BT(I))                                   00009140
      C              COMPUTE THE NINE CONTRIBUTIONS                     00009150
                     POT(I,1)=CAT*CAR*PIN(1)                            00009160
                     POT(I,2)=AT(I)*AR(I)*PIN(2)                        00009170
                     POT(I,3)=(AT(I)*CAR+AR(I)*CAT+                     00009180
           &         SR*COS(BR(I)-BT(I)))*PIN(3)                        00009190
                     POT(I,4)=SR*COS(BR(I)+BT(I))*PIN(4)                00009200
                     POT(I,5)=-SR*SIN(BR(I)+BT(I))*PIN(5)               00009210
                     POT(I,6)=(CAR*SRT*COSBT+CAT*SRR*COSBR)*PIN(6)      00009220
                     POT(I,7)=-(CAR*SRT*SINBT+CAT*SRR*SINBR)*PIN(7)     00009230
                     POT(I,8)=(AR(I)*SRT*COSBT+AT(I)*SRR*COSBR)*PIN(8)  00009240
                     POT(I,9)=-(AR(I)*SRT*SINBT+AT(I)*SRR*SINBR)*PIN(9) 00009250
      C              COMPUTE THE TOTAL OBSERVATIONS                     00009260
         10 CONTINUE                                                    00009270
            DO 20 I=1,15                                                00009280
                     H(I)=0.0                                           00009290
            DO 20 J=1,9                                                 00009300
                     H(I)=H(I)+POT(I,J)                                 00009310
         20 CONTINUE                                                    00009320
            RETURN                                                      00009330
            END                                                         00009340
```

Figure D.13 — FORTRAN LISTING FOR THE SCATTEROMETER SIMULATION PROGRAM — SUBROUTINE IDEAL

```
      CSIGMA          SUBROUTINE SIGMA                                  00009350
            FUNCTION SIGMA(I,B)                                         00009360
            DIMENSION C(4,8)                                            00009370
            DATA TEN, DEG /10.0, 0.0174532925/                          00009380
            DATA ((C(I,J),J=1,8),I=1,4)/                                00009390
          & -0.16268E-02,  0.41799E-01, -0.39750E 00,  0.16080E 01,     00009400
          & -0.17226E 01, -0.41559E 01,  0.13382E 01,  0.16117E 02,     00009410
          & -0.22604E-02,  0.59789E-01, -0.59855E 00,  0.27116E 01,     00009420
          & -0.47098E 01, -0.11435E 01,  0.50802E 00,  0.16106E 02,     00009430
          &  0.0        ,  0.0        , -0.48897E-02,  0.75403E-01,     00009440
          & -0.38450E 00,  0.39101E 00, -0.47384E 00, -0.11964E 02,     00009450
          &  0.91338E-05, -0.39295E-03,  0.62964E-02, -0.48574E-01,     00009460
          &  0.19450E 00, -0.41108E 00,  0.51675E 00,  0.28714E-02/     00009470
      C                                                                 00009480
      C             THIS ROUTINE COMPUTES SCATTERING COEFFICIENTS       00009490
      C             OF FIVE KINDS, I=1,2,3,4,5, CORRESPONDING TO        00009500
      C             VV,HH,VH,RE(VVHH),IMAG(VVHH).  THE REMAINING        00009510
      C             COEFFICIENTS ARE ASSUMED ZERO.                      00009520
      C                                                                 00009530
            A = B/TEN                                                   00009540
            GO TO(10,10,10,20,20,40,40,40,40), I                        00009550
       10   IF(I .LT. 3 .AND. B .LT. 12.0) I=1                          00009560
            SIGMA = ((((((C(I,1)*A+C(I,2))*A+C(I,3))*A+C(I,4))*A+       00009570
          & C(I,5))*A+C(I,6))*A+C(I,7))*A+C(I,8))/TEN                   00009580
            SIGMA = TEN**SIGMA                                          00009590
            RETURN                                                      00009600
       20   ARG = ((((((C(4,1)*A+C(4,2))*A+C(4,3))*A+                   00009610
          & C(4,4))*A+C(4,5))*A+C(4,6))*A+C(4,7))*A+C(4,8))*DEG         00009620
            SIGMA = ((((((C(1,1)*A+C(1,2))*A+C(1,3))*A+C(1,4))*A+       00009630
          & C(1,5))*A+C(1,6))*A+C(1,7))*A+C(1,8))/TEN                   00009640
            IF(B .LT. 12.0) GO TO 25                                    00009650
            SIGMA = ((((((C(2,1)*A+C(2,2))*A+C(2,3))*A+C(2,4))*A+       00009660
          & C(2,5))*A+C(2,6))*A+C(2,7))*A+C(2,8))/TEN/2.0+SIGMA/2.0     00009670
       25   IF(I .GT. 4) GO TO 30                                       00009680
            SIGMA = (TEN**SIGMA)*(COS(ARG))                             00009690
            RETURN                                                      00009700
       30   SIGMA = (TEN**SIGMA)*(SIN(ARG))                             00009710
            RETURN                                                      00009720
       40   SIGMA = 1.0E-02 - 1.836734E-04*A*A                          00009730
            RETURN                                                      00009740
            END                                                         00009750
```

Figure D.14 — FORTRAN LISTING FOR THE
SCATTEROMETER SIMULATION PROGRAM — SUBROUTINE SIGMA

C-3

ORIGINAL PAGE IS
OF POOR QUALITY


```
CSOLID           SUBROUTINE SOLID
      SUBROUTINE SOLID (FCT,HA,WNA,X2P,X1P,NNX,NNP,SUM)
C
C              THIS ROUTINE EMPLOYS A QUASSIAN LEGENDRE QUADRATURE
C              (INTEGRATION) PROCEDURE;  INTEGRATION OVER X SEGMENTS
C              ARE PERFORMED AFTER TRANSLATION TO (-1,1)X(-1,1).
C              X2P,X1P = UPPER AND LOWER LIMITS ON X
C              NNX = SEGMENTS IN  X
C              NNP = DEGREE OF PRECISION IN X
C
      DIMENSION SAMPLE(8,8),COEF(8,8),SX(8),C(8)
      DATA ((SAMPLE(I,J),J=1,8),I=2,8)/-0.577350269,0.577350269,
     & 0.0,0.0,0.0,0.0,0.0,0.0,
     & -0.774596669,0.0,0.774596669,0.0,0.0,0.0,0.0,0.0,
     & -0.861136312,-0.339981044,0.339981044,0.861136312,
     & 0.0,0.0,0.0,0.0,
     & -0.906179846,-0.538469310,0.0,0.538469310,0.906179846,
     & 0.0,0.0,0.0,
     & -0.932469514,-0.661209386,-0.238619186,0.238619186,0.661209386,
     & 0.932469514,0.0,0.0,
     & -0.949107912,-0.741531185,-0.405845151,0.0,0.405845151,
     & 0.741531185 ,0.949107912,0.0,
     & -0.960289856,-0.796666477,-0.525532410,-0.183434642,0.183434642,
     & 0.525532410,0.796666477,0.960289856/
      DATA ((COEF(I,J),J=1,8),I=2,8) /1.0, 1.0, 0.0,0.0,0.0, 0.0,0.0,0.0,
     & 0.0,
     & 0.555555556 ,0.888888889 ,0.555555556 ,0.0,0.0,0.0,0.0,0.0,
     & 0.347854851,0.652145155 ,0.652145155 ,0.347854851,0.0,0.0,0.0,
     & 0.0,
     & 0.236926885,0.478628670,0.568888889,0.478628670,
     & 0.236926885,0.,0.0, 0.0,
     & 0.171324492,0.360761573,0.467913935,0.467913935,0.360761573,
     & 0.171324492,0.0,0.0,
     & 0.129484966,0.279705391,0.381830051,0.417959184,
     & 0.381830051,0.279705391,0.129484966,0.0,
     & 0.101228536,0.222381034,0.313706646,0.362683783,0.362683783,
     & 0.313706646,0.222381034,0.101228536/
C
C              CLEAR SUMMING VARIABLE
C
      SUM = 0.0
C
C              RE-ASSIGN INPUT ARGUMENTS
C
      WN = WNA
      H = HA
      NX = NNX
      NP = NNP
C
C              COMPUTE LENGTH OF CELL SIDES
C
      DELX = (X2P-X1P)/FLOAT(NX)
```

Figure D.15a — FORTRAN LISTING FOR THE SCATTEROMETER SIMULATION PROGRAM — SUBROUTINE SOLID

```
      HDELX = DELX*0.5
C
C           FORM SAMPLE FACTOR FOR X
C
      DO 20 I = 1,NP
      SX(I) = SAMPLE(NP,I)*HDELX
      C(I) = COEF(NP,I)
   20 CONTINUE
C
C           INTEGRATE IN STRIPS OF DELX
C
      XH = X1P - HDELX
      DO 40 N = 1,NX
      XH = XH + DELX
C
C           TRANSFORM TO CELL (-1,1)
C
      DO 30 I = 1,NP
      X = SX(I)+XH
      WNSIN = WN*SQRT(1.0-X*X)
C
C           FORM PARTIAL SUMS
C
      SUM = SUM+FCT(H,WNSIN)*C(I)
   30 CONTINUE
   40 CONTINUE
      SUM = 0.5*DELX*SUM
      RETURN
      END
```


Figure D.15b — FORTRAN LISTING FOR THE SCATTEROMETER SIMULATION PROGRAM — SUBROUTINE SOLID

```
      CLAMBDA         SUBROUTINE LAMBDA                                              00007690
            REAL FUNCTION LAMBDA(H,U)                                                00007700
      C                                                                              00007710
      C                 H IS AN INTERGER WITH VALUE 1,2,3, OR 4                      00007720
      C                   DEPENDING ON ANTENNA TYPE.                                 00007730
      C                                                                              00007740
      C                                                                              00007750
            GO TO ( 100,200,300,400 ),H                                              00007760
      C                                                                              00007770
      C                 H = 1 MEANS ANTENNA TYPE = -1/2.                             00007780
      C                                                                              00007790
        100 IF ( ABS(U) .LT. 1.E-27 ) GO TO 600                                      00007800
            LAMBDA = ( SIN(U) / U )**2                                               00007810
            RETURN                                                                   00007820
      C                                                                              00007830
      C                 H = 2 MEANS ANTENNA TYPE = 1.                                00007840
      C                                                                              00007850
        200 LAMBDA = (2.0 *  BJ1XOX(U))**2                                           00007860
            RETURN                                                                   00007870
      C                                                                              00007880
      C                 H = 3 MEANS ANTENNA TYPE = 3/2.                              00007890
      C                                                                              00007900
        300 IF ( ABS(U) .LT. 1.E-27 ) GO TO 600                                      00007910
            LAMBDA = ( 3.0 / ( U * U ) * (( SIN(U)/ U ) - COS(U) ))**2               00007920
            RETURN                                                                   00007930
      C                                                                              00007940
      C                 H = 4 MEANS ANTENNA TYPE = 2.                                00007950
      C                                                                              00007960
        400 IF ( ABS(U) .LT. 1.E-27 ) GO TO 600                                      00007970
            LAMBDA = ( 8.0/(U*U) * ( 2.0 * BJ1XOX(U) - BJZERO(U)))**2                00007980
            RETURN                                                                   00007990
        600 LAMBDA = 1.0                                                             00008000
            RETURN                                                                   00008010
            END                                                                      00008020
```

Figure D.16 — FORTRAN LISTING FOR THE SCATTEROMETER SIMULATION PROGRAM — SUBROUTINE LAMBDA

ORIGINAL PAGE IS OF POOR QUALITY

```
77671 01  01-26-75   16.391            SUBROUTINE BJZERO                                          LABEL BJZERO  PAGE    1
      CBJZERO         SUBROUTINE BJZERO
            REAL FUNCTION BJZERO(X)
      C
      C               COMPUTES THE BESSEL FUNCTION OF INTEGER ORDER ZERO.
      C               USES A POLYNOMIAL METHOD.
      C
            REAL X,T1,T2
      C
      C               CHECK TO SEE WHICH APPROXIMATION IS NEEDED.
      C               0<X<3
            IF ( X .GT. 3.0 ) GO TO 100
      C
            T1 = .333333333 * X
            T1 = T1*T1
            BJZERO = (((((.0002100 * T1 - .0039444)*T1 + .0444479)*T1
           & -.3163866)*T1 + 1.2656208)*T1 - 2.2499997)*T1 + 1.0
            RETURN
      C
      C               X > 3.0
      C
        100 T1 = 3.0 / X
            BJZERO = (((((.00014476*T1 -.00072805)*T1 + .00137237)*T1 -
           & .00009512)*T1 -.00552740)*T1 - .00000077)*T1 + .79788456
      C
            T2 = ((((((.00013558*T1-.00029333)*T1+.00054125)*T1+.00262573)
           & *T1-.00003954)*T1-.00003954)*T1-.04166397)*T1-.78539816+X
            BJZERO = BJZERO * COS(T2) / SQRT(X)
            RETURN
            END
```

Figure D.17 — FORTRAN LISTING FOR THE SCATTEROMETER SIMULATION PROGRAM — SUBROUTINE BJZERO

```
CBJ1XOX          SUBROUTINE BJ1XOX
      FUNCTION BJ1XOX(X)
      IF(X .GT. 3.0) GO TO 10
C
C              0 .GE. X .LE. 3
C
      Y = .333333333*X
      Y = Y*Y
      BJ1XOX = (((((.00001109*Y-0.00031761)*Y+.00443319)*Y-
     & .03954289)*Y+.21093573)*Y-.56249985)*Y+.5
      RETURN
C
C              X .GT. 3
C
   10 Y = 3.0/X
      BJ1XOX = (((((-.00020033*Y+.00113653)*Y-.00249511)*Y+
     & .00017105)*Y+.01659667)*Y+.00000156)*Y+.79788456
      BJ1XOX = BJ1XOX/(X*SQRT(X))
      Z = (((((-.00029166*Y+.00079824)*Y+.00074348)*Y-
     & .00637879)*Y+.00005650)*Y+.12499612)*Y-2.35619449+X
      BJ1XOX = BJ1XOX*COS(Z)
      RETURN
      END
```


Figure D.18 — FORTRAN LISTING FOR THE SCATTEROMETER SIMULATION PROGRAM — SUBROUTINE BJ1XOX

ORIGINAL PAGE IS OF POOR QUALITY

SCAT STUDY FOR VIEW ANGLE OF 10.0 DEGREES

TYPE	KA	ANTENNA PARAMETERS WIDTH (DEG)	GAIN (DB)	CROSS (DB)	RELA PHASE	AMAX	BMAX
1.0	180.00	1.02	45.51	-40.00	0.	-10.00	0.

STRIP	THETA	HEIGHTS						PRECISION
1	8.0	0.846E-08	0.691E-13	0.154E-10	0.154E-10	0.847E-08	0.849E-08	7
2	8.5	0.654E-07	0.419E-11	0.385E-09	0.389E-09	0.659E-07	0.662E-07	6
3	9.0	0.636E-06	0.162E-10	0.112E-08	0.114E-08	0.637E-06	0.638E-06	8
4	9.5	0.341E-04	0.686E-10	0.291E-07	0.292E-07	0.341E-04	0.341E-04	8
5	10.0	0.104E-03	0.240E-09	0.910E-07	0.912E-07	0.104E-03	0.104E-03	6
6	10.5	0.354E-04	0.741E-10	0.280E-07	0.280E-07	0.354E-04	0.354E-04	8
7	11.0	0.687E-06	0.121E-10	0.102E-08	0.103E-08	0.688E-06	0.690E-06	8
8	11.5	0.755E-07	0.273E-11	0.332E-09	0.334E-09	0.758E-07	0.762E-07	6
9	12.0	0.101E-07	0.390E-13	0.126E-10	0.126E-10	0.101E-07	0.101E-07	6

Figure D.19a — SAMPLE OUTPUT FOR SCATTEROMETER SIMULATION PROGRAM

IDEAL ANTENNA HEIGHTS AND POWER MATRIX

DELTA HEIGHT

MEAS/COEF	VV	HH	VH	VVHHR	VVHHI	VVVHR	VVVHI	HVHHR	HVHHI
1	0.4343E-01	0.	0.	0.	0.	0.	0.	0.	0.
2	0.	0.4343E-01	0.	0.	0.	0.	0.	0.	0.
3	0.	0.	0.4343E-01	0.	0.	0.	0.	0.	0.
4	0.1096E-01	0.1096E-01	0.1793E-10	0.2172E-01	0.	0.4309E-10	0.	0.4309E-10	0.
5	0.1096E-01	0.1096E-01	0.1793E-10	-0.2172E-01	-0.4309E-10	0.	-0.4309E-10	0.	-0.4309E-10
6	0.1096E-01	0.1096E-01	0.1793E-10	0.2144E-10	0.2172E-01	0.	0.	0.	0.
7	0.1096E-01	0.1006E-01	0.1793E-10	-0.3019E-09	-0.2172E-01	0.	0.	0.	0.
8	0.2172E-01	0.	0.2172E-01	0.	0.	0.4343E-01	0.	0.	0.
9	0.2172E-01	0.	0.2172E-01	0.	0.	-0.4343E-01	-0.8610E-10	0.	0.
10	0.2172E-01	0.	0.2172E-01	0.	0.	0.4287E-10	0.4343E-01	0.	0.
11	0.2172E-01	0.	0.2172E-01	0.	0.	0.4331E-10	-0.4343E-01	0.	0.
12	0.	0.2172E-01	0.2172E-01	0.	0.	0.	0.	0.4343E-01	0.
13	0.	0.2172E-01	0.2172E-01	0.	0.	0.	0.	-0.4343E-01	-0.8610E-10
14	0.	0.2172E-01	0.2172E-01	0.	0.	0.	0.	0.4287E-10	0.4343E-01
15	0.	0.2172E-01	0.2172E-0[illegible]	0.	0.	0.	0.	0.4331E-10	-0.4343E-01

POWER MATRIX

MEAS/COEF	VV	HH	VH	VVHHR	VVHHI	VVVHR	VVVHI	HVHHR	HVHHI	POWER
1	0.8331E 00	0.	0.	0.	0.	0.	0.	0.	0.	0.8331E 00
2	0.	0.8331E 00	0.	0.	0.	0.	0.	0.	0.	0.8331E 00
3	0.	0.	0.2521E-02	0.	0.	0.	0.	0.	0.	0.2521E-02
4	0.2083E 00	0.2083E 00	0.1041E-11	0.4165E 00	0.	0.4230E-12	0.	0.4230E-12	0.	0.8331E 00
5	0.2083E 00	0.2083E 00	0.1041E-11	-0.4165E 00	-0.3753E-11	0.	-0.4230E-12	0.	-0.4230E-12	0.42[illegible]E-05
6	0.2083E 00	0.2083E 00	0.1041E-11	0.4112E-09	0.1891E-02	0.	0.	0.	0.	0.4194E 00
7	0.2083E 00	0.2083E 00	0.1041E-11	-0.5791E-08	-0.1891E-02	0.	0.	0.	0.	0.4146E 00
8	0.4165E 00	0.	0.1261E-02	0.	0.	0.4263E-03	0.	0.	0.	0.41[illegible] 00
9	0.4165E 00	0.	0.1261E-02	0.	0.	-0.4263E-03	-0.8460E-12	0.	0.	0.4174E 00
10	0.4165E 00	0.	0.1261E-02	0.	0.	0.4209E-12	0.4263E-03	0.	0.	0.4182E 00
11	0.4165E 00	0.	0.1261E-02	0.	0.	0.4251E-12	-0.4263E-03	0.	0.	0.4174E 00
12	0.	0.4165E 00	0.1261E-02	0.	0.	0.	0.	0.4263E-03	0.	0.4182E 00
13	0.	0.4165E 00	0.1261E-02	0.	0.	0.	0.	-0.4263E-03	-0.8460E-12	0.4174E 00
14	0.	0.4165E 00	0.1261E-02	0.	0.	0.	0.	0.4209E-12	0.4263E-03	0.4182E 00
15	0.	0.4165E 00	0.1261E-02	0.	0.	0.	0.	0.4251E-12	-0.4263E-03	0.4174E 00

Figure D.19b — SAMPLE OUTPUT FOR SCATTEROMETER SIMULATION PROGRAM

ORIGINAL PAGE IS OF POOR QUALITY

EXACT ANTENNA WEIGHTS AND POWER RETURNS

DELTA WEIGHT

MEAS/COEF	VV	HH	VH	VVHHR	VVHHI	VVVHR	VVVHI	HVHHR	HVHHI
1	0.4336E-01	0.1095E-06	0.1494E-03	0.7472E-04	0.	0.	0.	0.	0.
2	0.1095E-06	0.4336E-01	0.1494E-03	0.7472E-04	0.	0.	0.	0.	0.
3	0.3736E-04	0.3736E-04	0.4328E-01	-0.7472E-04	0.	0.	0.	0.	0.
4	0.1086E-01	0.1086E-01	-0.9313E-09	0.2172E-01	0.2168E-12	0.4302E-10	0.	0.4302E-10	0.
5	0.1042E-01	0.1042E-01	0.1494E-03	-0.2164E-01	-0.4302E-10	0.	-0.4309E-10	0.	-0.4309E-10
6	0.1084E-01	0.1084E-01	0.7472E-04	0.3736E-04	0.2168E-01	0.	0.	0.	0.
7	0.1084E-01	0.1084E-01	0.7472E-04	0.3736E-04	-0.2168E-01	0.	0.	0.	0.
8	0.2170E-01	0.1873E-04	0.2172E-01	0.	0.	0.4324E-01	0.	0.1120E-03	0.
9	0.2170E-01	0.1873E-04	0.2172E-01	0.	0.	-0.4324E-01	-0.8611E-10	-0.1120E-03	-0.7435E-13
10	0.2170E-01	0.1873E-04	0.2172E-01	0.	0.	0.4269E-10	0.4339E-01	0.1105E-12	0.3747E-04
11	0.2170E-01	0.1873E-04	0.2172E-01	0.	0.	0.4312E-10	-0.4339E-01	0.1117E-12	-0.3747E-04
12	0.1873E-04	0.2170E-01	0.2172E-01	0.	0.	0.1120E-03	0.	0.4324E-01	0.
13	0.1873E-04	0.2170E-01	0.2172E-01	0.	0.	-0.1120E-03	-0.7435E-13	-0.4324E-01	-0.8611E-10
14	0.1873E-04	0.2170E-01	0.2172E-01	0.	0.	0.1105E-12	0.3747E-04	0.4269E-10	0.4339E-01
15	0.1873E-04	0.2170E-01	0.2172E-01	0.	0.	0.1117E-12	-0.3747E-04	0.4312E-10	-0.4339E-01

POWER MATRIX

MEAS/COEF	VV	HH	VH	VVHHR	VVHHI	VVVHR	VVVHI	HVHHR	HVHHI	POWER
1	0.8316E 00	0.2113E-05	0.8677E-05	0.1436E-02	0.	0.	0.	0.	0.	0.8331E 00
2	0.2113E-05	0.8316E 00	0.8677E-05	0.1436E-02	0.	0.	0.	0.	0.	0.8331E 00
3	0.7179E-03	0.7176E-03	0.2513E-02	-0.1436E-02	0.	0.	0.	0.	0.	0.2513E-02
4	0.2093E 00	0.2093E 00	-0.4366E-10	0.4165E 00	0.1808E-13	0.4223E-12	0.	0.4223E-12	0.	0.8331E 00
5	0.2075E 00	0.2075E 00	0.8677E-05	-0.4151E 00	-0.3746E-11	0.	-0.4230E-12	0.	-0.4230E-12	0.1295E-04
6	0.2079E 00	0.2074E 00	0.4338E-05	0.7178E-03	0.1888E-02	0.	0.	0.	0.	0.4184E 00
7	0.2079E 00	0.2079E 00	0.4338E-05	0.7178E-03	-0.1888E-02	0.	0.	0.	0.	0.4146E 00
8	0.4162E 00	0.3599E-03	0.1261E-02	0.	0.	0.4245E-03	0.	0.1099E-05	0.	0.4192E 00
9	0.4162E 00	0.3599E-03	0.1261E-02	0.	0.	-0.4245E-03	-0.8453E-12	-0.1099E-05	-0.7299E-15	0.4174E 00
10	0.4162E 00	0.3599E-03	0.1261E-02	0.	0.	0.4190E-12	0.4259E-03	0.1085E-14	0.3678E-06	0.4182E 00
11	0.4162E 00	0.3599E-03	0.1261E-02	0.	0.	0.4233E-12	-0.4259E-03	0.1096E-14	-0.3678E-06	0.4174E 00
12	0.3599E-03	0.4162E 00	0.1261E-02	0.	0.	0.1099E-05	0.	0.4245E-03	0.	0.4182E 00
13	0.3599E-03	0.4162E 00	0.1261E-02	0.	0.	-0.1099E-05	-0.7299E-15	-0.4245E-03	-0.8453E-12	0.4174E 00
14	0.3599E-03	0.4162E 00	0.1261E-02	0.	0.	0.1085E-14	0.3678E-06	0.4190E-12	0.4259E-03	0.4182E 00
15	0.3599E-03	0.4162E 00	0.1261E-02	0.	0.	0.1096E-14	-0.3678E-06	0.4233E-12	-0.4259E-03	0.4174E 00

Figure D.19c — SAMPLE OUTPUT FOR SCATTEROMETER SIMULATION PROGRAM

STATISTICS FOR THE DIFFERENCE METHOD BASED ON 1 OBSERVATIONS.

SCAT COEF	VALUE	MEAN	RMS	%MEAN	%RMS
VV	0.192E 02	0.276E-02	0.762E-05	0.014	0.
HH	0.192E 02	0.276E-02	0.762E-05	0.014	0.
VH	0.581E-01	-0.207E-03	0.429E-07	-0.357	0.
VVHHR	0.192E 02	0.236E-02	0.558E-05	0.012	0.
VVHHI	0.872E-01	-0.216E-03	0.468E-07	-0.248	0.
VVVHR	0.982E-02	-0.173E-04	0.299E-09	-0.176	0.
VVVHI	0.982E-02	-0.309E-06	0.956E-13	-0.003	0.
HVHHR	0.982E-02	-0.173E-04	0.299E-09	-0.176	0.
HVHHI	0.982E-02	-0.309E-06	0.956E-13	-0.003	0.

STATISTICS FOR THE MATRIX METHOD BASED ON 1 OBSERVATIONS

SCAT COEF	VALUE	MEAN	RMS	%MEAN	%RMS
VV	0.192E 02	0.256E-02	0.656E-05	0.013	0.
HH	0.192E 02	0.256E-02	0.657E-05	0.013	0.
VH	0.581E-01	-0.786E-05	0.618E-10	-0.014	0.
VVHHR	0.192E 02	0.256E-02	0.656E-05	0.013	0.
VVHHI	0.872E-01	-0.662E-04	0.438E-08	-0.076	0.
VVVHR	0.982E-02	-0.330E-06	0.109E-12	-0.003	0.
VVVHI	0.982E-02	-0.294E-06	0.865E-13	-0.003	0.
HVHHR	0.982E-02	-0.359E-06	0.129E-12	-0.004	0.
HVHHI	0.982E-02	-0.317E-06	0.101E-12	-0.003	0.

Figure D.19d — SAMPLE OUTPUT FOR SCATTEROMETER SIMULATION PROGRAM

ORIGINAL PAGE IS OF POOR QUALITY

MONTE CARLO STUDY

APPL BIAS= -40.0 DB   PHASE BIAS= 0. DEG   RANDOM AMPL= -10.0 DB   RANDOM PHASE= 0. DEG

STATISTICS FOR THE DIFFERENCE METHOD BASED ON 150 OBSERVATIONS

SCAT COEF	VALUE	MEAN	RMS	%MEAN	%RMS
VV	0.192E 02	0.317E-02	0.113E-05	0.017	0.000
HH	0.192E 02	0.318E-02	0.119E-05	0.017	0.000
VH	0.581E-01	0.785E-02	0.306E-05	13.530	0.005
VVHHR	0.192E 02	-0.676E-01	0.553E-01	-0.352	0.288
VVHHI	0.872E-01	-0.235E-02	0.444E-01	-2.701	51.418
VVVHR	0.982E-02	0.171E 00	0.362E 00	1739.784	3691.119
VVVHI	0.982E-02	0.344E-01	0.399E 00	350.817	4062.628
HVHHR	0.982E-02	0.162E 00	0.377E 00	1653.317	3839.045
HVHHI	0.982E-02	-0.828E-02	0.359E 00	-84.299	3654.711

STATISTICS FOR THE MATRIX METHOD BASED ON 150 OBSERVATIONS

SCAT COEF	VALUE	MEAN	RMS	%MEAN	%RMS
VV	0.192E 02	-0.192E-01	0.222E 00	-0.100	1.155
HH	0.192E 02	0.156E-01	0.222E 00	0.081	1.156
VH	0.581E-01	-0.865E-02	0.226E 00	-14.889	389.728
VVHHR	0.192E 02	-0.675E-01	0.554E-01	-0.352	0.289
VVHHI	0.872E-01	-0.221E-02	0.449E-01	-2.533	51.506
VVVHR	0.982E-02	0.171E 00	0.364E 00	1743.189	3704.870
VVVHI	0.982E-02	0.345E-01	0.399E 00	351.193	4066.049
HVHHR	0.982E-02	0.163E 00	0.378E 00	1656.123	3853.521
HVHHI	0.982E-02	-0.831E-02	0.359E 00	-84.675	3657.770

Figure D.19e — SAMPLE OUTPUT FOR SCATTEROMETER SIMULATION PROGRAM

ANTENNA WITH BIASES ONLY

APPL BIAS= -40.0 DB   PHASE BIAS= 0. DEG

POWER MATRIX

MEAS/COEF	VV	HH	VH	VVHHR	VVHHI	VVVHR	VVVHI	HVHHR	HVHHI	POWER
1	0.8315E 00	0.2551E-05	0.9678E-05	0.1601E-02	0.	0.1698E-04	0.	0.4565E-07	0.	0.8331E 00
2	0.2551E-05	0.8315E 00	0.9678E-05	0.1601E-02	0.	0.4566E-07	0.	0.1698E-04	0.	0.8331E 00
3	0.8011E-03	0.8011E-03	0.2513E-02	-0.1269E-02	0.	0.8511E-05	0.	0.8511E-05	0.	0.2863E-02
4	0.2083E 00	0.2083E 00	-0.4366E-10	0.4165E 00	0.1800E-13	0.4223E-12	0.	0.4223E-12	0.	0.8331E 00
5	0.2075E 00	0.2075E 00	0.8677E-05	-0.4151E 00	-0.3746E-11	0.	-0.4230E-12	0.	-0.4230E-12	0.1295E-04
6	0.2073E 00	0.2079E 00	0.4338E-05	0.7178E-03	0.1888E-02	0.	0.	0.	0.	0.4184E 00
7	0.2073E 00	0.2079E 00	0.4338E-05	0.7178E-03	-0.1888E-02	0.	0.	0.	0.	0.4146E 00
8	0.4161E 00	0.4159E-03	0.1286E-02	0.8301E-02	0.	0.4287E-03	0.	0.5397E-05	0.	0.4266E 00
9	0.4161E 00	0.3872E-03	0.1236E-02	-0.8301E-02	-0.7492E-13	-0.4282E-03	-0.8452E-12	0.3114E-05	-0.8143E-15	0.4090E 00
10	0.4161E 00	0.4015E-03	0.1261E-02	0.8195E-11	0.3776E-04	0.4256E-05	0.4259E-03	0.4256E-05	0.4104E-06	0.4183E 00
11	0.4161E 00	0.4015E-03	0.1261E-02	0.8278E-11	-0.3776E-04	0.4256E-05	-0.4259E-03	0.4256E-05	-0.4104E-06	0.4173E 00
12	0.4159E-03	0.4161E 00	0.1286E-02	0.8301E-02	0.	0.5397E-05	0.	0.4287E-03	0.	0.4266E 00
13	0.3872E-03	0.4161E 00	0.1236E-02	-0.8301E-02	-0.7493E-13	0.3114E-05	-0.8143E-15	-0.4282E-03	-0.8452E-12	0.4090E 00
14	0.4015E-03	0.4161E 00	0.1261E-02	0.8195E-11	0.3776E-04	0.4256E-05	0.4104E-06	0.4256E-05	0.4259E-03	0.4183E 00
15	0.4015E-03	0.4161E 00	0.1261E-02	0.8278E-11	-0.3776E-04	0.4256E-05	-0.4104E-06	0.4256E-05	-0.4259E-03	0.4173E 00

STATISTICS FOR THE DIFFERENCE METHOD BASED ON 1 OBSERVATIONS

SCAT COEF	VALUE	MEAN	RMS	%MEAN	%RMS
VV	0.192E 02	0.317E-02	0.101E-04	0.017	0.
HH	0.192E 02	0.318E-02	[illegible]91E-04	0.017	0.
VH	0.581E-01	0.786E-02	0.[illegible]17E-04	13.530	0.
VVHHR	0.192E 02	0.236E-02	0.594E-05	0.012	0.
VVHHI	0.872E-01	-0.216E-03	0.464E-07	-0.248	0.
VVVHR	0.982E-02	0.192E 00	0.370E-01	1959.587	0.
VVVHI	0.982E-02	0.86 E-03	0.755E-06	8.852	0.
HVHHR	0.982E-02	0.192E 00	0.370E-01	1959.604	0.
HVHHI	0.982E-02	0.869E-03	0.755E-06	8.852	0.

STATISTICS FOR THE MATRIX METHOD BASED ON 1 OBSERVATIONS

SCAT COEF	VALUE	MEAN	RMS	%MEAN	%RMS
VV	0.192E 02	0.139E-02	0.190E-05	0.007	0.
HH	0.192E 02	0.138E-02	0.190E-05	0.007	0.
VH	0.581E-01	0.374E-02	0.140E-04	6.432	0.
VVHHR	0.192E 02	0.259E-02	0.664E-05	0.013	0.
VVHHI	0.872E-01	-0.662E-04	0.438E-08	-0.076	0.
VVVHR	0.982E-02	0.193E 00	0.371E-01	1963.148	0.
VVVHI	0.982E-02	0.869E-03	0.755E-06	8.852	0.
HVHHR	0.982E-02	0.193E 00	0.371E-01	1963.164	0.
HVHHI	0.982E-02	0.869E-03	0.755E-06	8.852	0.

Figure D.19f — SAMPLE OUTPUT FOR SCATTEROMETER SIMULATION PROGRAM

APPENDIX E
Routine WHERE

1.0 PROGRAM DESCRIPTION

Fortran program WHERE was developed to compute the sampling points for apertures having maximum dimensions x_o and y_o across the x and y axis, respectively. The program will compute and list (θ_{mn}, ϕ_{mn}) for $m \geq 0$ and $n \geq 0$ out to values of m and n restricted by

$$0.9 \leq \cos\theta \leq 1.0 \qquad \text{(E-1)}$$

If the value of m or n exceeds 48 the value is restricted to 48 to limit the storage and printed output to a reasonable amount. The listing of the program is shown in Figure E-1.

2.0 EXAMPLE RUN

The maximum aperture dimensions (x_o, y_o) and operating wavelength (λ) form the program input requirement. These must be dimensionally in the same units. An input data card containing these parameters must be prepared in accord with the read statement and its accompanying format statement.

An example output of the program is illustrated in Table E.1 for an aperture having a maximum dimension of 1.1760 meters and illuminated at a .02158 meter wavelength.

```
CNHERE
C
C                ROUTINE WHERE
C
C                ANTENNA PATTERN SAMPLING POINTS ARE SPECIFIED FOR
C                A RECTANGULAR APERTURE OF WIDTH XNOT AND LENGTH YNOT.
C                THE THEORY IS BASED ON CRES TR 294-1 BY J. P. CLAASSEN.
C                WAVELENGTH (LAMBDA) AND APERTURE DIMENSIONS MUST BE
C                SPECIFIED IN SAME UNITS.
C
         DIMENSION KK(48), TH(48,48), PHI(48,48)
         REAL LAMBDA
         DATA THMAX, DEG/0.4509, 0.01745329257
C
C                SPECIFIED APERTURE DIMENSIONS AND WAVELENTH
C                (DIMENSIONS ORDERED IN RIGHT-HANDED COORDINATE
C                SYSTEM X-Y-Z)
C
         READ (5,1000) XNOT,YNOT,LAMBDA
  1000   FORMAT (3F10.5)
         WRITE (66,1500) XNOT, YNOT, LAMBDA
  1500   FORMAT(3X,'X='F10.4,3X,'Y='F10.4,3X,'LAMBDA='F10.4)
C
C                ESTABLISH VALID DOMAIN OF SAMPLING
C                NOT TO EXCEED A 48*48 MATRIX
C
         MMAX = 2.0*SIN(THMAX)*XNOT/LAMBDA
         IF (MMAX .GT. 48) MMAX=48
         NMAX = 2.0*SIN(THMAX)*YNOT/LAMBDA
         IF (NMAX .GT. 48) NMAX=48
C
C                DETERMINE SAMPLING POINTS
C
         HLAM = LAMBDA/2.0
         DO 10 I=1,MMAX
              RM = I-1
         DO 10 J=1,NMAX
              RN = J-1
C
C                FORM SIN(THETA(I,J))
C
              SINTH = HLAM*SQRT((RM/XNOT)**2+(RN/YNOT)**2))
              IF (SINTH .GE. 1.0) GO TO 10
              TH(I,J) = ATAN(SINTH/SQRT(1.0-SINTH*SINTH))/DEG
              IF (I .EQ. 1 .AND. J .EQ. 1) GO TO 5
              PHI(I,J) = ATAN2(RN*XNOT,RM*YNOT)/DEG
              GO TO 10
    5         PHI(I,J) = 0.0
   10    CONTINUE
C
C                DISPLAY SAMPLING POINTS
C
         DO 20 I=1,NMAX,8
              N = I+7
              IF (N .GT. NMAX) N=NMAX
         DO 15 K = I,N
              KK(K) = K-1
   15    CONTINUE
              WRITE (6,2000) XNOT, YNOT, LAMBDA, (KK(K),K=I,N)
  2000        FORMAT (1H1,45X,'SAMPLING MATRIX (THETA, PHI)',
     *        /40X,'FOR APERTURE',F10.5,' BY',F10.5,' AND WAVELENGTH',
     *        F10.5,/4X,'M/N',I8,7I15//)
         DO 20 J=1,MMAX
              M = J-1
              WRITE (6,3000) M,(TH(J,K),PHI(J,K),K=I,N)
  3000        FORMAT (I5,8(3X,1H(,F4.1,2H, ,F4.1,1H)))
   20    CONTINUE
         STOP
         END
```

FIGURE E-1. FORTRAN LISTING OF PROGRAM WHERE.

ORIGINAL PAGE IS
OF POOR QUALITY